Regulation of the Ability to Generate Transit Amplifying Progenitors

by

Cyrina M. Ostgaard

A dissertation submitted in partial fulfillment
of the requirements for the degree of
Doctor of Philosophy
(Cell and Developmental Biology)
in the University of Michigan
2025

Doctoral Committee:

Professor Emeritus Doug Engel ,Chair
Professor Cheng-Yu Lee
Professor Tom Kerppola
Professor Marina Pasca di Magliano

Cyrina M. Ostgaard
cyrinao@umich.edu

ORCID iD: 0000-0003-1852-0824

© Cyrina M. Ostgaard, 2025

Dedication

To my parents whose endless love and support made this possible. I hope you are proud of how far I've come.

Acknowledgements

This has been one intense journey, and I wouldn't have made it this far without the support of number of people. First, I would like to thank my thesis committee who has trusted in my progress over these last couple of years and helped me get to this point. Next, I would like to thank my lab members. Science is a collaborative process, and their help has been indispensable to this work. Special thanks goes out to Arjun who was instrumental in developing Cut&Run approaches in the lab and whose bioinformatics expertise made it possible to take this work to new heights. I would also like to thank Hide who has endured my endless questions and has taught me countless protocols in the lab. Beyond the lab, I need to thank my friends who've been there for me every step of the way. Especially Fatima and Kenny who I met in my first year of grad school. They are the friends a girl could ask for and have been a well needed support in staying sane throughout this entire process.

Two of the most important people in my life who I haven't been able to see much over the past years of grad school are my sisters. Aryanna and Gabi are the weirdest yet most avid supporters I have. They understand me like only family can. They are the two people I have that will be proud of how far I've come. From the first in my family to get a bachelor's degree to the first to get a PhD, they know just how trying this journey has been.

My cat Nova may not be able to read this, but she deserves all the love and appreciation as the brightest point in my life and the only company I had during the pandemic. She is always there for pets and my persistent little writing buddy. Lastly, my advisor Cheng-Yu deserves the most appreciation. He believed in me when I didn't always believe in myself. He saw me through this far and knows just how much I've come into my own as a scientist. Without his support I wouldn't have made it this far. He made overcoming a pandemic, multiple deaths in the family, and getting through a PhD when it felt like the world was falling apart possible.

I'm thankful for so much other supports that are too numerous to list and it is a point of immense pride that I can put this document out into the world.

Table of Contents

Dedication ii

Acknowledgements iii

List of Tables viii

List of Figures ix

Abstract xi

Chapter 1 : Introduction 1

Increased high-potential transit-amplifying progenitors correlates with increased brain surface area 1

Drosophila larval brain neural stem cells as an *in vivo* paradigm for investigating generation of specific TAP subtypes 7

Type 1 NB (T1NB) 10

Type 2 NB (T2NB) 12

Regulation of NB identity 17

Trithorax (Trx) 17

Tailless (Tll) 19

Buttonhead (Btd) 20

Precise regulation of gene expression in T2NBs 21

Zelda (Zld) 22

Fruitless (Fru) 23

Investigating stem cell capability to generate high vs low potential TAPs using fly NBs 26

References 27

Chapter 2 A Double-Assurance Mechanism Restrains Generation of High Potential Transit-Amplifying Progenitors During Neurogenesis 35

Summary 35

Introduction 36

Transcriptional states regulate NB capability to generate INPs 40

Ase limits the capability to generate INPs in T1NBs 47

Elevated Ase expression promotes T2NBs to generate GMCs via bypassing INPs 51

Ase functions through Prospero to promote generation of GMCs by T2NBs 56

Prospero reprograms immature INPs to bypass an INP state and adopt a GMC fate 62

Reprogramming tumor NB progeny fate bypasses differentiation blockades and halts tumor growth 66

Discussion 71

References 78

Material and Methods 84

Appendices 105

Chapter 3 Regulation of T2NB Functional Identity and Lineage Progression 183

Summary 183

Introduction 183

Tll and Trx are necessary to maintain T2NB functional identity 185

Tll is likely acting to repress gene function in T2NBs 190

Identification of genes that promote T2NB lineage progression 195

Ase alone is not responsible for loss of INPs upon loss of Tll or Trx 200

Identifying the role of Vsx2 and Hmx in T2NB lineages 202

Approach to visualize enhancer activity 205

Identification of Btd targets 209
Discussion 214
References 216
Material and Methods 219
Chapter 4 Future Directions and Conclusions 240
References 246

List of Tables

Table 1.1 Genes expression profile differences in Trx, Btd, and Tll mutant T2 NBs compared to wild-type T1 and T2 NBs. 20

Table 2.1 Key Resources for Chapter 2 84

Table 2.2 Enhancers and genes corresponding to Fig 2.1B..... 105

Table 2.3 Pan Neural enhancers annotated with activity patterns identified from Fig 2.1C..... 141

Table 2.4 T2 lin enhancers annotated with activity patterns identified from Fig 2.1C.. 159

Table 2.5 T2 NB enhancers annotated with activity patterns identified from Fig 2.1C 170

Table 2.5 Pan NB enhancers annotated with activity patterns identified from Fig 2.1C..... 171

Table 2.7 Random non-promoter enhancers patterns from Janelia Flyight. 172

Table 2.8 Expression pattern in CB validated using GFP reporters, antibodies, or published data for TFs identified in Fig. 2.3A as T1NB or T1NB and INP enriched 176

Table 2.9 Expression pattern in CB validated using GFP reporters, antibodies, or published data for candidate Ase target TFs identified in Figure 2.7..... 178

Table 2.10 Coordinates and sequences for newly made enhancer reporters 180

Table 3.1 Key Resources for Chapter 3 219

Table 3.2 Pnt intron sequence used for enhancer reporter construction..... 235

List of Figures

Figure 1.1 Gyrencephalic vs Lissencephalic Brains 2

Figure 1.2 Model of human vs mouse cortical RGC lineage progression 5

Figure 1.3 Asymmetric division to generate NB progeny 9

Figure 1.4 T1 and T2NB lineages have well defined hierarchy 11

Figure 1.5 9D11 enhancer for *erm* is kept poised for rapid activation 14

Figure 1.6 Erm and Ham likely act to prevent reactivation of a Notch target subset in INPs. 16

Figure 1.7 T1 and T2NB lineages express separate sets of lineage specific transcription factors 17

Figure 1.8 Fru and Zld modulate NB related gene activity 25

Figure 2.1 Cell-type-specific enhancers associated with genes essential for INP formation are poised in T1NBs 42

Figure 2.2 Identification of active neurogenic enhancers in fly larval brain NBs 46

Figure. 2.3 Ase limits the capability of T1NBs to generate INPs induced by Btd 49

Figure 2.4 Elevated Ase expression promotes T2NBs to generate GMCs via bypassing INPs 53

Figure 2.5 Elevated Ase expression promotes T2NBs to generate GMCs and bypass INPs 56

Figure 2.6 Pros mediates Ase-induced bypass of INP generation in the T2NB lineage 58

Figure 2.7 Ase functions through Pros to promote generation of GMCs by T2NBs 61

Figure 2.8 Pros reprograms immature INPs to bypass an INP state and adopt a GMC fate 65

Figure 2.9 Reprogramming tumor NBs to generate GMCs halts tumor growth driven by defective INPs 67

Figure 2.10 Elevating Ase expression suppresses premalignant NBs formation in *brat*,*patr-1*-hypomorphic brains 70

Figure 2.11 The capability to generate INPs is inherent to both NB types but activated exclusively in T2NBs 73

Figure 3.1 Tll likely functions downstream of Trx to maintain T2NB cell identity 188

Figure 3.2 Tll likely functions as a repressor to promote T2NB functional identity 191

Figure 3.3 Experimental design to identify Tll targets 194

Figure 3.4 Identification of genes that promote T2NB lineage progression 198

Figure 3.5 Ase knockdown does not restore generation of INPs upon loss of Tll or Trx 201

Figure 3.6 Identifying the role of Hmx and Vsx2 in T2NB lineages 204

Figure 3.7 Method to improve enhancer activity detection 208

Figure 3.8 Candidate Btd targets could not recapitulate Btd function 210

Figure 3.9 Experimental design to identify Btd targets 213

Abstract

During development, neural stem cells produce multiple types of transit amplifying progenitors (TAPs) to generate a large number of differentiated cells. Understanding the mechanisms that regulate the ability to generate different types of TAPs, defined by proliferative capacity, can improve our understanding of how normal brain development occurs. Study has been limited in vertebrates because the lineage relationship between stem cells progeny produced cannot be clearly defined.

Gene function is highly conserved between fruit flies, *Drosophila*, and humans. Similar to humans, neural stem cells in flies (neuroblasts; NBs) divide asymmetrically to generate low and high potential TAPs (ganglion mother cells (GMC) and intermediate neural progenitors (INPs) respectively). Two NB subtypes exist in the fly larval brain with well-defined lineages. Type 1 NBs (T1NB) invariably generate a GMC that divides once to generate two differentiated progeny. Type 2 NBs (T2NBs) increase output of differentiated progeny by producing an INP with each division that divides 5-6 times, generating one GMC per division. Understanding the mechanisms that control NB capacity to generate INPs can provide insight into how neural stem cells in humans can produce different TAP subtypes.

My thesis work contributes to understanding how NBs generate progeny with altered proliferative potential. Although it was previously reported that T1 and T2NBs are interconvertible, insight into how progeny output is specifically altered is limited. There is

a lack of insight into how chromatin state affects generation of INPs vs GMCs. Chromatin at immature INP specific enhancers for genes needed for INP formation can be inaccessible to transcription factor (TF) binding limiting NBs from generating INPs. Chromatin at these enhancers could be accessible but inactivity of these enhancers is maintained to limit INP generation.. I took an unbiased approach to identify what genes specify INP function and defined chromatin state at cell-type specific enhancers that drive expression. The chromatin at the enhancers of genes essential for specifying INP function is accessible in T2NBs and T1NBs even though T1NBs never generate INPs. This indicates that the capacity to generate INPs is shared between T1 and T2NBs and can be readily activated or suppressed.

If both NB subtypes are capable of generating INPs, why do they generate different TAP subtypes? The gene *tailless (tll*) gene is highly expressed in T2NBs, and *tll* function is necessary and sufficient for T2NB-specific gene expression and INP generation. Additionally, Buttonhead (Btd) is necessary and sufficient to promote INP generation without affecting T2NB-specific marker expression patterns. This is consistent with the chromatin at cell-type-specific enhancers of these genes being accessible in T1NBs. Furthermore, transcriptome analysis reveals that immature INPs and GMCs are the highly similar cell types and are interconvertible upon altering expression of lineage-specific transcription factors. These data led me to conclude that activity of T2NB-

specific TFs builds upon T1NB-specific TF activity to drive INP generation in T2NBs, and the default state is GMC production in NBs.

My thesis work has leveraged the well-established NB lineages to define neurogenic enhancers genome-wide and established a framework for how NB lineage-specific TFs function together to regulate generation of INPs or GMCs. I have also identified putative Tll and Btd targets. Future molecular and functional characterization of these targets should provide critical insight into the gene regulatory network that control NB capacity to generate progeny with distinct potential during neurogenesis.

Chapter 1 : Introduction

Increased high-potential transit-amplifying progenitors correlates with increased brain surface area

The size and complexity of the cerebral cortex is increased disproportionately compared to other regions of the central nervous system during mammalian brain evolution.(Finlay & Darlington, 1995; Florio & Huttner, 2014) Gyrencephalic species like carnivores and primates, have a very large and folded cortex where folds (outward bending; gyri) and fissures (inward bending; sulci) form in distinct patterns (Figure 1.1). (Borrell & Reillo, 2012; Lewitus et al., 2013; Lewitus et al., 2014; Llinares-Benadero & Borrell, 2019; Rakic, 2009) The formation of a folded brain morphology is necessary to accommodate increased neuronal production combined with production of diverse neuron types with varying morphologies, including the development of more complex dendritic projections and neuropile.(De Juan Romero & Borrell, 2015; Florio & Huttner, 2014; Geschwind & Rakic, 2013; Rakic, 2009) Human brains display a 1000-fold increase in surface area to accommodate drastically increased neuron numbers but only a 2-fold increase in thickness as compared to a mouse brain that shows a smooth brain morphology (lissencephalic mammal) (Figure 1.1).(Rakic, 2009) Human patients exhibiting developmental defects resulting in less folded brain structure, such as in cases of lissencephaly or microcephaly, suffer from profound cognitive impairments and demonstrate issues with seizures.(Faheem et al., 2015; Hu et al., 2014; Jayaraman et

al., 2018; Tanaka & Gleeson, 2000) The evolutionary expansion and increased complexity of cerebral cortex is largely driven by the formation of new neural progenitor cells which have increased neurogenic potential and the ability to produce a large number of new projection neuron subtypes in a short timeframe. Understanding what regulates the output of these neural progenitors can provide important insights into brain development.

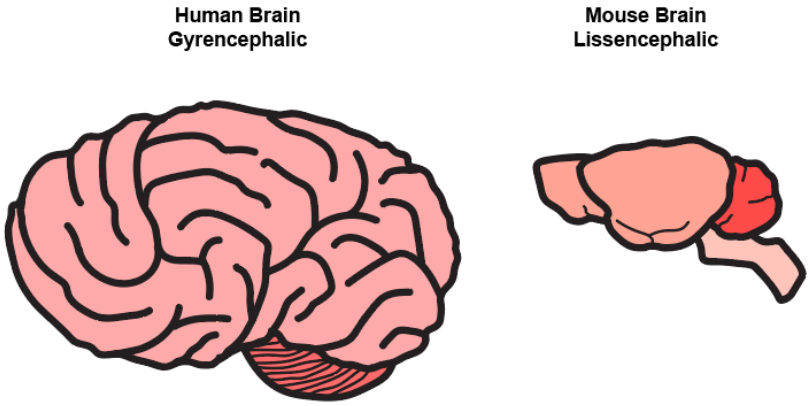


Figure 1.1 Gyrencephalic vs Lissencephalic Brains

Depiction of a gyrencephalic (folded) human brain structure, compared to a lissencephalic (smooth) mouse brain structure.

At the onset of vertebrate neurogenesis, neuroepithelial cells that line the ventricle of developing cerebral cortex will transform into apical radial glia cells (aRGCs). These aRGCs can undergo multiple modes of division (1) symmetric proliferative division to generate more aRGCs, (2) symmetric neurogenic division to produce two neurons, (3) asymmetric neurogenic division to produce one aRGC and a neuron, (4) asymmetric proliferative division to generate one aRGC and a transit amplifying progenitor (TAP).(Taverna et al., 2014) Most TAPs migrate to the basal side of the ventricular zone (VZ) and form a secondary neurogenic region: the subventricular

zone (SVZ) (Figure 1.2).(De Juan Romero & Borrell, 2015; Fernández et al., 2016) In the mouse cerebral cortex, TAPs are the main basal progenitor cell type and divide symmetrically to generate two neurons (Figure 1.2).(Attardo et al., 2008; Haubensak et al., 2004; Kowalczyk et al., 2009; Noctor et al., 2004) TAPs will also rarely undergo proliferative divisions to amplify the generation of neurons.(Kowalczyk et al., 2009; Sessa et al., 2008) The development of a gyrencephalic cortex requires rapid generation of a large number of neurons and dispersion of these neurons towards the cortical place.(Borrell & Reillo, 2012; Llinares Benadero & Borrell, 2019; Martínez-Martínez et al., 2019). This correlates with a significant expansion of the SVZ, which becomes subdivided into inner and outer SVZ (ISVZ and OSVZ, respectively) which is abundantly populated by TAPs and basal radial glia cells (bRGCs) (Figure 1.2). (Betizeau et al., 2013; Fietz et al., 2010; Hansen et al., 2010; Reillo & Borrell, 2012; Reillo et al., 2011) (Smart et al., 2002) Analyses in ferrets (a gyrencephalic species) demonstrate that bRGCs are derived from aRGCs during a brief period of embryonic development, and these bRGCs will self-amplify to expand the SVZ region further. (Franco et al., 2012) Although bRGCs are also present in rodents with a smooth cortex (mouse, rat) the abundancy is much lower than in gyrencephalic species.(Martínez-Cerdeño et al., 2012; Wang et al., 2011) Multiple varieties of bRGCs with differential morphologies have been found in primates and carnivores.(Betizeau et al., 2013; Borrell & Reillo, 2012; Pilz et al., 2013; Reillo et al., 2011) Two key aspects of bRGCs are essential for expansion and fold formation of the gyrencephalic cortex: an increased capability to generate neurons and a basal process extending toward the cortical surface.(Betizeau et al., 2013; Fietz et al., 2010; Hansen et al., 2010; Reillo et al., 2011)

This basal process drives the tangential migration of the neurons proceeding towards the cortical surface, in turn leading to the expansion in surface area and folding of the cerebral cortex (Figure 1.2). In addition to self-amplification, recent advances indicate that subsets of bRGCs can generate tri-potent TAPs that divide multiple times to further amplify the output of neurons.(Pebworth et al., 2021; Wang et al., 2025) These tri-potent TAPs have been implicated as the cell-of-origin for glioblastoma. As such, better understanding of what regulates radial glial capability to generate TAP subtypes could provide important insight into normal brain development and how brain tumors form.

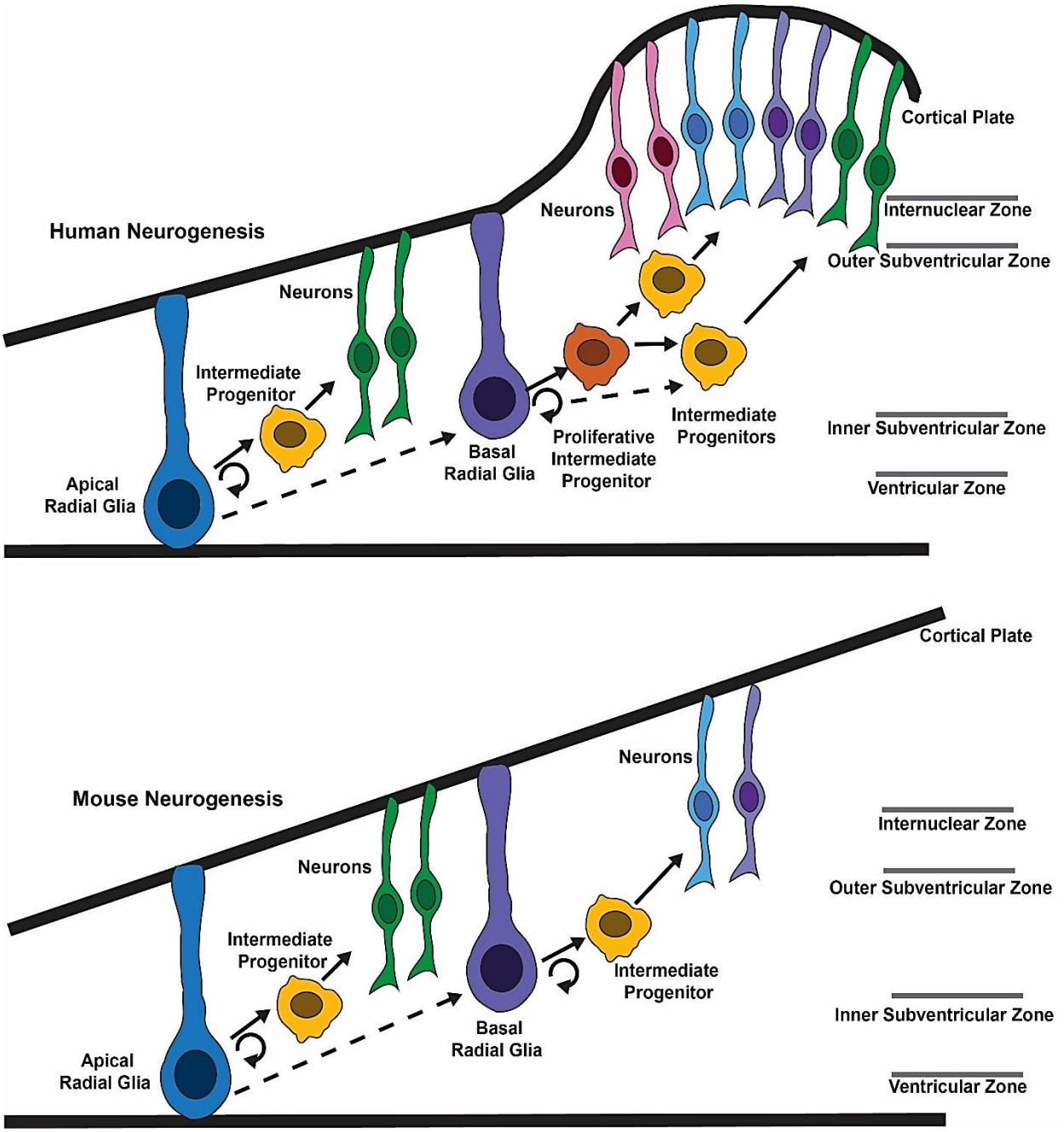


Figure 1.2 Model of human vs mouse cortical RGC lineage progression

In both human and mice, apical radial glia can asymmetrically divide to produce a TAP (intermediate progenitor) that will divide once to generate two neurons. Basal radial glia, which are derived from apical radial glia, can also asymmetrically divide to generate a TAP that will terminally divide to produce two neurons. In contrast to mice neurogenesis, in human cortical neurogenesis it is thought that a subset of basal radial glia can generate proliferative TAPs that will divide multiple times and will rapidly expand the pool of basal TAPs and the generation of subsuquent neurons. This rapid

and tangential dispersion of neurons is thought to paly a role in promoting the formation of folds in the cortical plate.

Several factors are essential for mechanistic insight into the control of radial glial capability to generate specific TAP subtypes. These factors include well-defined cell type progression in radial glial lineages that generate distinct TAP subtypes, characterized transcription factors that determine identity of TAPs to be generated and what epigenetic regulators are that drive TAP generation, and lastly what the enhancers are that promote cell-type-specific expression of key transcription factors. Even with genomic techniques advancing and more complex brain organoid development, cell type hierarchy in radial glial lineages that normally generate TAP subtypes is still poorly understood. Currently, transcription factors that determine radial glial capability to generate TAP subtypes or the associated epigenetic regulators are still unknown. As such, defining cell-type-specific enhancers associated with genes essential for TAP subtype formation is currently impossible. These limitations restrict our ability to answer the following questions: How is the capability of radial glia to produce higher potential TAPs regulated? Is the ability to produce higher potential TAPs inherent only to specific bRGC types or do all RGCs possess the capacity to generate these progeny. Can higher potential TAPs be interconverted to lower potential TAPs or vice versa? Lastly, can tumor cells derived from higher potential TAPs that fail to differentiate be reprogrammed to suppress tumorigenesis by inducing generation of low potential TAPs instead and bypass differentiation defective lineage trajectory?

Drosophila larval brain neural stem cells as an *in vivo* paradigm for investigating generation of specific TAP subtypes

The fruit fly *Drosophila* larval brain has well-defined hierarchies for neural stem cell (neuroblast; NB) lineages that generate an identical TAP subtype throughout their lifetime.(Bello et al., 2008; Boone & Doe, 2008; Bowman et al., 2008) These lineages provide an *in vivo* system for studying regulation of NB capability to generate TAPs with distinct developmental and proliferative potential at a single-cell resolution. All NBs undergo asymmetric divisions to regenerate and to produce a TAP. The cortex of a mitotic NB is highly polarized, and discrete protein complexes are assembled in the apical and basal cortical domains.(Boone & Doe, 2008; Bowman et al., 2008; Wu et al., 2008) In telophase, the apical protein complexes remain in the cortex of the NB, whereas the basal protein complexes segregate into the cortex of NB progeny destined to differentiate into a TAP (Figure 1.3). Genetic and live imaging studies indicate that the apical protein complexes serve to promote basal protein localization into the NB progeny, where they will downregulate NB gene expression to promote the onset of differentiation. The scaffolding protein Miranda asymmetrically localizes at the basal cortex of mitotic NBs and segregates into the cortex of future TAP (Figure 1.3).(Ikeshima-Kataoka et al., 1997; Shen et al., 1997; Lee, Andersen, et al., 2006; Lee, Robinson, et al., 2006; Rolls et al., 2003) Miranda functions to partition its interacting proteins Brain tumor (Brat) and Prospero (Pros) exclusively into differentiating NB progeny.(Hirata et al., 1995; Knoblich et al., 1995; Lee, Wilkinson, et al., 2006; Spana & Doe, 1995) Numb, a conserved antagonist of Notch signaling, asymmetrically partitions into the cortex of future TAP independently of Miranda (Figure 1.3).(Frise et al., 1996; Guo et al., 1996; Lee, Andersen, et al., 2006; Wang et al., 2006) When cortical aPKC is

not properly localized, asymmetric segregation of basal proteins is perturbed which leads to defects in differentiation in the NB progeny causing reversion to NBs.(Lee, Robinson, et al., 2006; Rolls et al., 2003) Similarly, loss of *brat*, *pros* or *numb* function during asymmetric NB division results in differentiation defects in NB progeny results in supernumerary NB formation at the expense of neuron generation.(Bello et al., 2006; Betschinger et al., 2006; Lee, Andersen, et al., 2006; Lee, Robinson, et al., 2006; Lee, Wilkinson, et al., 2006; Wang et al., 2007; Wang et al., 2006) Restoring *brat* function can rescue the supernumerary NB phenotype by reinstating neuronal generation in *brat*-mutant brains.(Komori, Xiao, McCartney, et al., 2014) Similarly, restoring *numb* function can rescue the supernumerary NB phenotype in *numb*-mutant brains.(Lee, Andersen, et al., 2006; Wang et al., 2007; Wang et al., 2006; Wirtz-Peitz et al., 2008) As such, brains that show unrestrained cortical aPKC kinase activity or loss of basal protein activity in NBs can provide a physiologically relevant source of enriched NB-specific nuclear lysate for genomic analyses of gene functions.(Carney et al., 2012; Janssens et al., 2014; Komori, Xiao, McCartney, et al., 2014; Larson et al., 2021; Ostgaard et al., 2025; Quinto-Rives et al., 2020; Rajan et al., 2023)

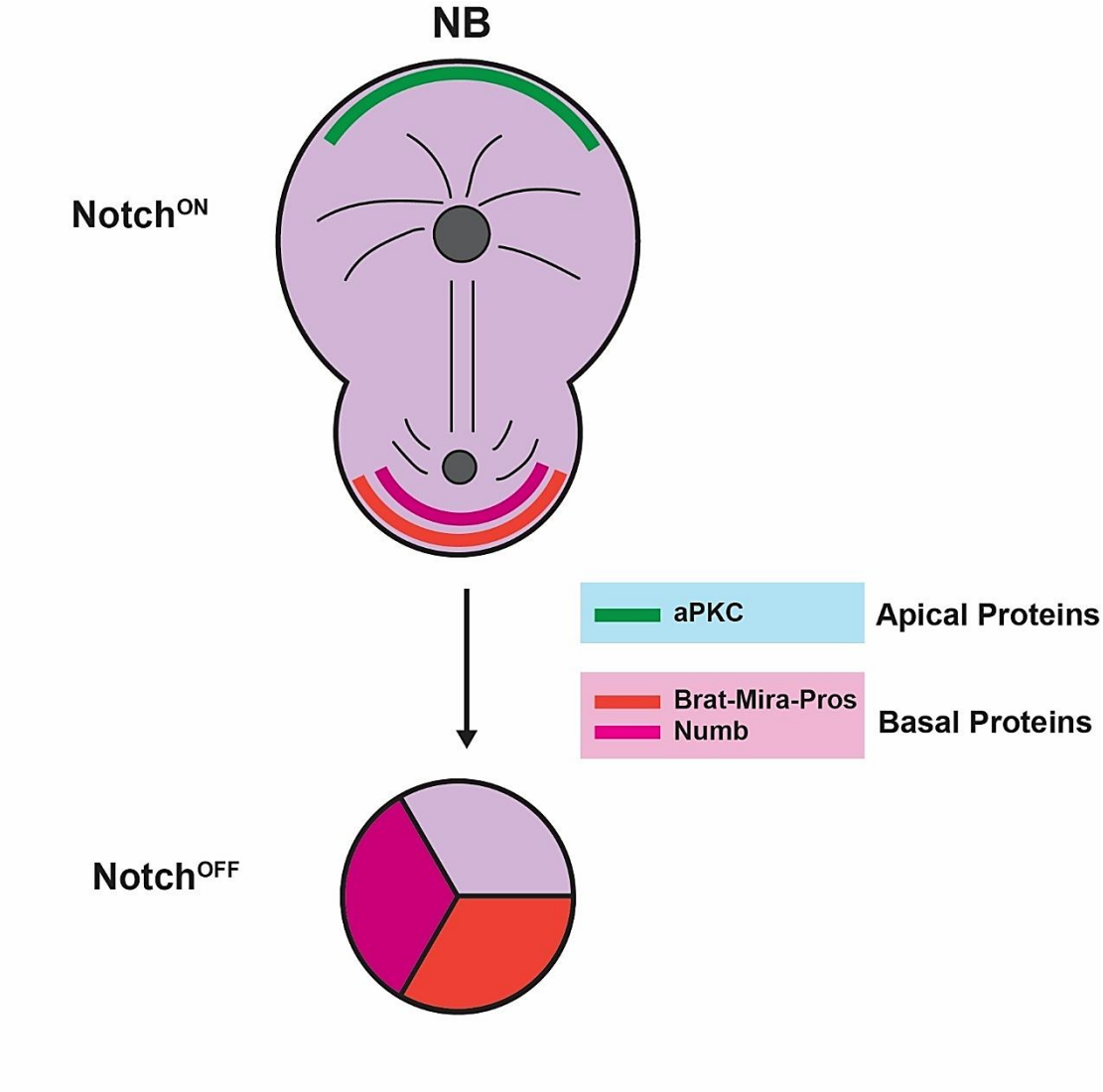


Figure 1.3 Asymmetric division to generate NB progeny

During NB division, aPKC complex will work to maintain apical polarity. Numb and Brat-Mira-Pros are basally segregated during division into the newly born progeny. Brat binds to mRNA transcripts of Notch effector gene transcripts to promote degradation while Pros promotes cell cycle exit. Numb antagonizes Notch activity.

Larvae lacking basal protein activity in NBs can develop to adulthood and present with an adult brain tumor phenotype that appears similar to differentiation defects seen in larval NB progeny. As seen in *brat*-mutant larvae, thousands of supernumerary NBs in the brain, but the vast majority of these NBs undergo terminal neuronal differentiation to exit from the cell cycle during pupal development. (Genovese

et al., 2019; Narbonne-Reveau et al., 2016) A small subset supernumerary NBs formed during early larval development in *brat*-mutant brains maintain expression of the early temporal identity gene *chinmo* and bypass programmed cell cycle exit during metamorphosis. These NBs become immortalized and continually propagate to drive tumor formation in adult fly brains. (Genovese et al., 2019; Narbonne-Reveau et al., 2016; Ostgaard et al., 2025) These tumor NBs also maintain T2NB marker expression pattern and likely function similar to larval T2NBs and can serve as an *in vivo* paradigm for testing the effects of reprogramming NB capacity to generate distinct TAP subtypes in altering tumor growth.

Type 1 NB (T1NB)

Two classes of central brain NB lineages (Type 1 and Type 2) can be found in larval brains and are unambiguously identified based on expression of the Achaete-scute complex member and transcription factor Asense (Ase) (Figure 1.4) .(Bello et al., 2008; Boone & Doe, 2008; Bowman et al., 2008) Asymmetric division of a T1NB leads to generation of TAPs with low developmental and proliferative potential called ganglion mother cells (GMCs)(Figure 1.4). A GMC divides only once to produce two post-mitotic neurons. Notch signaling is active in NBs and becomes rapidly downregulated in GMCs by basal proteins Numb and Pros (Figure 1.3). Numb likely prevents activation of Notch downstream-effector gene transcription in GMCs, and loss of *numb* function leads to supernumerary T1NB formation.(Wirtz-Peitz et al., 2008) Pros promotes GMC specification and defects in asymmetric Pros segregation also leads to supernumerary T1NB formation. Although Brat also asymmetrically segregates into GMCs, loss of *brat* function has no effect on GMC specification suggesting parallel mechanisms exist. Ase

has been long proposed to serve as the key gene to maintain the T1NB identity. (Álvarez, 2018; Bahrampour et al., 2017; Bayraktar et al., 2010; Bello et al., 2008; Boone & Doe, 2008; Bowman et al., 2008; Chen & Konstantinides, 2022; Walsh & Doe, 2017) This is in contrast to the observation that postembryonic loss of Ase has no apparent phenotype. (Bowman et al., 2008) This suggests that Ase is not necessary to maintain T1NB identity or for the generation of GMCs and likely serves mainly as a reliable marker for identifying T1NBs.

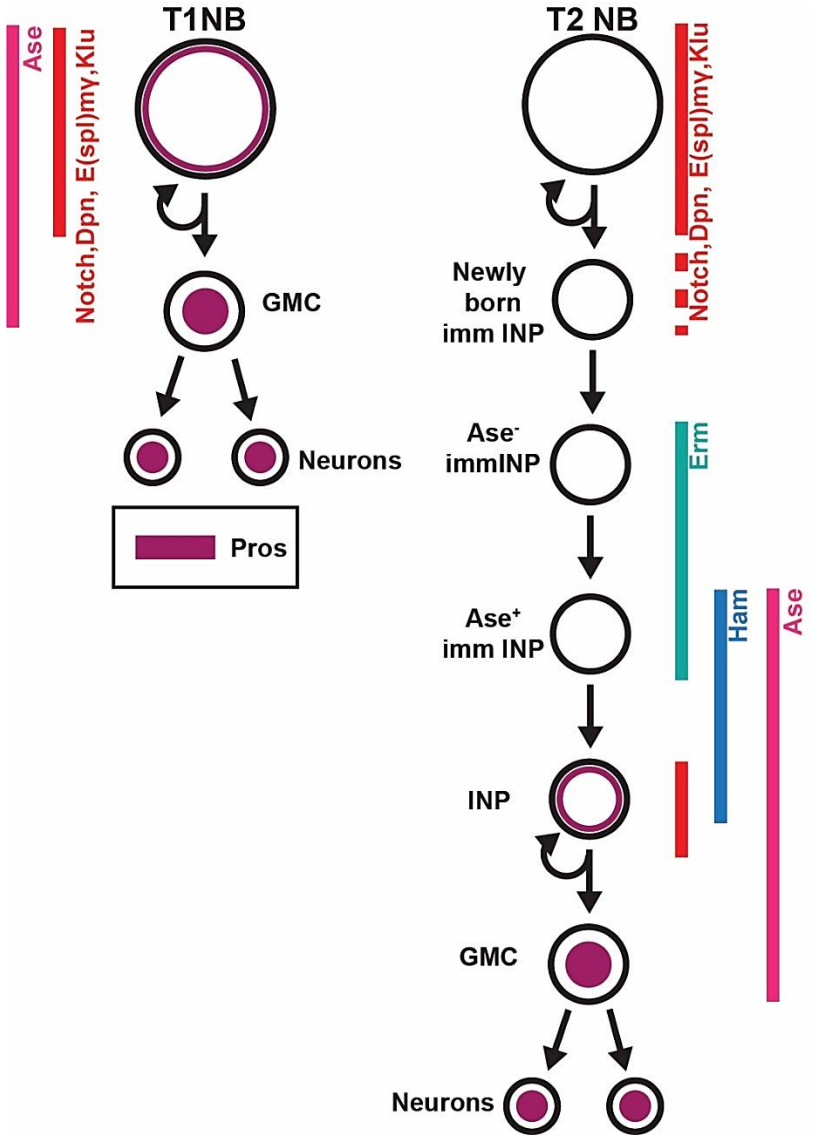


Figure 1.4 T1 and T2NB lineages have well defined hierarchy

T1NBs normally generate an $Ase^{+}Pros^{+}$ GMC. T2NBs generate immature INPs that will mature through various stages marked by Erm, Ase, and Ham before acquiring INP identity and divide multiple times to produce GMCs. Notch activity and expression of Notch downstream effectors Dpn, E(spl)mγ, and Klu are found in both T1 and T2 NBs..

Type 2 NB (T2NB)

T2NBs lack Ase expression and generate progeny that differentiate into TAPs characterized by high developmental and proliferative potential called intermediate neural progenitor (INP) (Figure 1.4). (Bello et al., 2008; Boone & Doe, 2008; Bowman et al., 2008). A newborn T2NB progeny (newborn immature INP) must downregulate the activity of Notch downstream-effector genes including *deadpan* (*dpn*), *enhancer of splitz mγ* (*E(spl)mγ*) and *klumpfuss* (*klu*) at all levels to initiate differentiation into an INP (Komori et al., 2018; Reichardt et al., 2018). Asymmetric segregation of the basal proteins Numb and Brat promote downregulation of Notch signaling activity at the transcriptional and translational levels respectively. (Komori et al., 2018) In parallel, the competitive antagonist protein Insensible sequesters Dpn and E(spl)mγ in inactive heterodimers to alleviate continual repression of their target genes (Komori et al., 2018). Coordinated downregulation of *dpn*, *E(spl)mγ* and *klu* activity at all levels ensures rapid and robust termination of their protein functions in newborn immature INP, which allows for timely activation of the master regulator of differentiation *earmuff* (*erm*). Erm activation marks the transition from newborn immature INPs to Ase^{-} immature INPs (Figure 1.4). (Janssens et al., 2017) Several hours after Erm activation, Ase^{-} immature INPs transition to Ase^{+} immature INPs by upregulating the expression of Ase and transcription factor Hamlet (Ham). (Eroglu et al., 2014; Quinto-Rives et al., 2020) Regulation of enhancer activity that drives cell-type-specific activation of *erm* and *ham*

expression in immature INPs might provide insight into control of NB capability to generate INPs.

Erm expression becomes rapidly activated in newborn immature INPs to ensure a properly timed transition from an undifferentiated NB state into the onset of INP differentiation and to restrict the developmental and proliferative potential in INPs. Erm protein is undetectable in T2NBs and newborn immature INPs but is detected in all remaining immature INPs (Figure 1.5).(Janssens et al., 2014) Without Erm, INPs revert back to T2NBs. (Weng et al., 2010) When Erm is ectopically activated in NBs, premature differentiation occurs.(Janssens et al., 2014) An enhancer (9D11) was identified for *erm* that is necessary and sufficient for Erm function in immature INPs differentiation.(Janssens et al., 2014; Weng et al., 2010; Hildebrandt et al.,2021) Live-cell imaging of a GFP reporter controlled by the 9D11 enhancer confirms enhancer activation less than 90-minutes after the completion of asymmetric T2NB division Figure 1.5).(Janssens et al., 2017) The 9D11 enhancer contains consensus sequences bound by Notch downstream-effector transcriptional repressors Klu, Dpn and E(spl) as well as Pnt. Klu and Dpn/E(spl) bind their predicted binding sites in the *erm* enhancer *in vitro*, and mutating Klu- or Dpn/E(spl)-binding sites leads to premature activation of enhancer activity in T2NBs. Dpn, Klu and E(spl)mγ most likely functions together with Histone deacetylase 1 (Hdac1) to continually deacetylate histone proteins on the 9D11 enhancer and to prevent premature *erm* activation in T2NBs. Pnt binds the putative Pnt-binding sites in the 9D11 enhancer *in vitro*, and knocking down *pnt* function reduces Erm expression in immature INPs. Pnt is highly expressed in T2NBs suggesting that Pnt functions opposingly to Dpn, Klu and E(spl)mγ to maintain the 9D11 enhancer in a

poised state in T2NBs for rapid activation in newborn immature INPs (Figure 1.5). As such, down-regulation of Klu, Dpn and E(spl)mγ activity in the newborn immature INP alleviates Hdac1-mediated repression of the 9D11 enhancer, permitting a rapid burst of histone acetylation and activating Erm expression (Figure 1.5) (Janssens et al., 2017). Thus, Notch signaling promotes T2NB maintenance by poising activation of the cell type-specific enhancer of *erm* via Hdac1-mediated histone deacetylation.

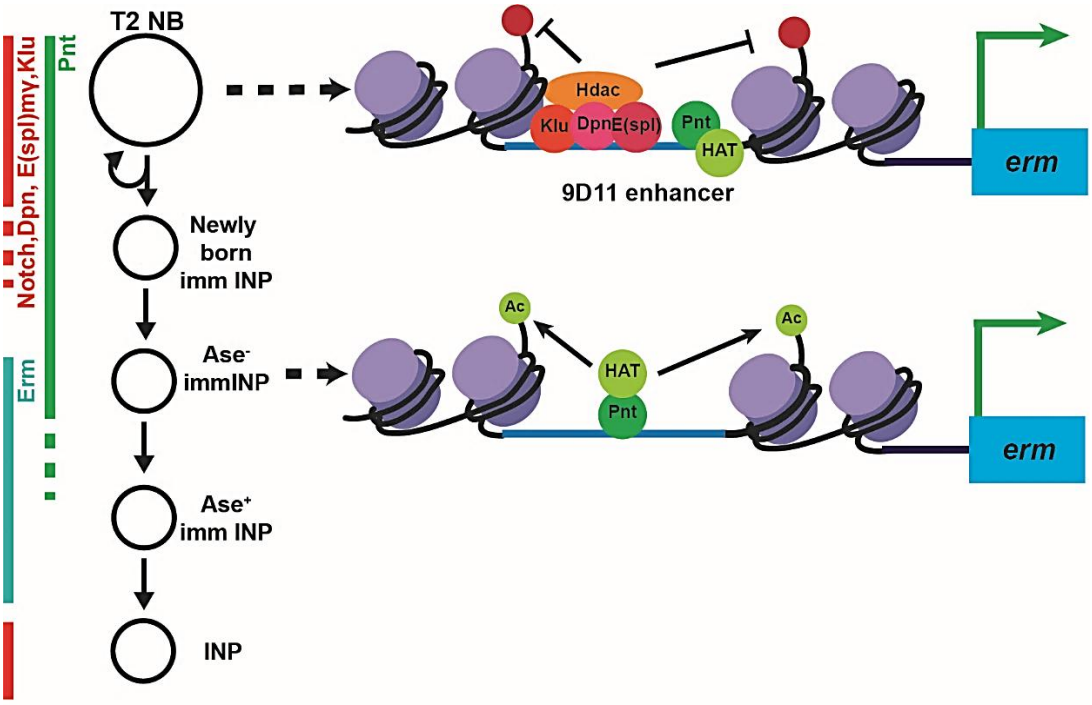


Figure 1.5 9D11 enhancer for *erm* is kept poised for rapid activation

Notch effectors Dpn, E(spl)mγ, and Klu bind 9D11 immature INP (immature INP) specific enhancer and recruit histone deacetylases (HDACs) to repress *erm* activation in T2NB NBs. Upon generation of the immature INP, Dpn, E(spl)mγ, and Klu will be silenced, and the repression of 9D11 enhancer is relieved. Pnt will then allow the recruited histone acetyltransferase (HAT) to acetylate the enhancer and promote *erm* activation within 90 minutes of immature INP generation

Erm- and Ham-induced chromatin changes at T2NB gene loci limit the ability of reactivated Notch signaling from reinstating a T2NB genetic program in INPs (Figure 1.6). Erm restricts the developmental and proliferative potential of INPs because *erm*-

null INPs spontaneously revert into T2NBs in a Notch-dependent manner and mis-expression of Erm triggers premature NB differentiation.(Janssens et al., 2014; Weng et al., 2010) It has been found that *erm* genetically interacts with *histone deacetylase 3* (*hdac3*) and genes that encode core components of the Brahma (Brm) complex to restrict the potential of INPs.(Janssens et al., 2014) Erm co-immunoprecipitates with Brm and Hdac3 when they are overexpressed in *Drosophila* S2 cells (Koe et al., 2014). Brm is the core ATPase subunit of the evolutionarily conserved SWI/SNF nucleosome-remodeling complex that plays a key role in regulating chromatin remodeling (Cenik & Shilatifard, 2021; Jancewicz et al., 2019; Lu & Allis, 2017; Runge et al., 2016). As such, Erm likely functions through histone deacetylases and ATP-dependent chromatin remodelers to inactivate enhancers associated with T2NB gene expression. Reducing *ham* function strongly enhances the supernumerary T2NB phenotype in *erm*-mutant brains. Overexpressed Ham can partially substitute for endogenous Erm and suppress the *erm*-mutant phenotype by repressing target gene transcription. Because Ham protein becomes detectable in immature INPs after Erm and remains expressed in all INPs, sequential activation of *erm* and *ham* likely maintain T2NB genes in a stably inactivated state in INPs (Figure 1.6). Reducing *hdac3* function significantly enhances the supernumerary T2NB phenotype in *ham*-heterozygous brains while reducing the activity of the Brm complex does not.(Quinto-Rives et al., 2020) This genetic interaction suggests that Ham functions through histone deacetylation to maintain T2NB genes in an inactive state in INPs. Thus, continual inactivation of enhancers associated with T2NB genes by Erm and Ham via histone deacetylation allows INPs to exclusively

generate differentiated cells instead of NBs despite reactivation of Notch signaling (Figure 1.6).

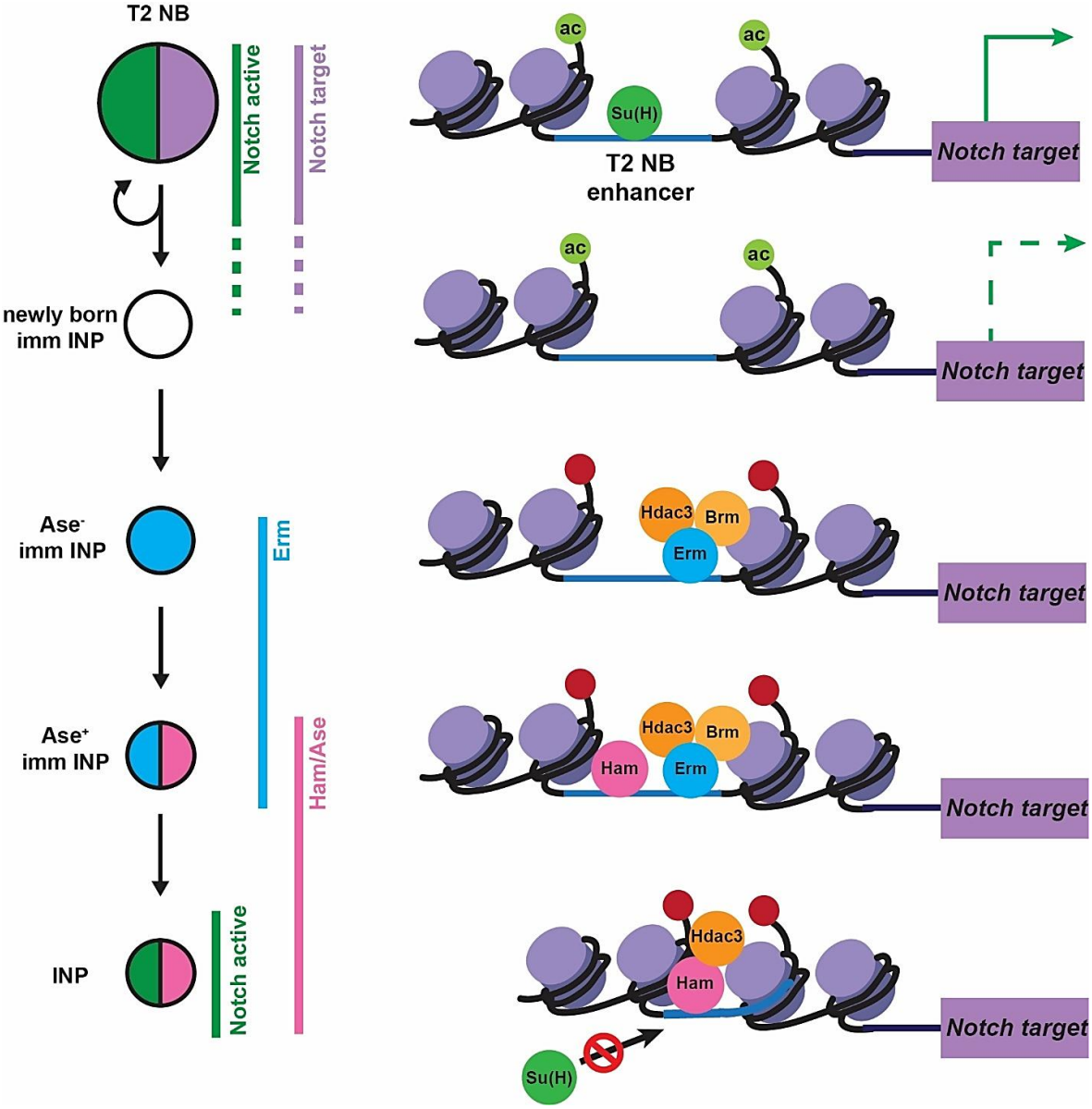


Figure 1.6 Erm and Ham likely act to prevent reactivation of a Notch target subset in INPs.

Notch functions through Su(H) to activate genes in T2NB, likely via acetylation. Erm works with Hdac3 and Brm to rapidly inactivate a subset of targets. Ham works with Hdac3 to maintain inactivity, preventing target reactivation when Notch signaling becomes reactivated in INPs.

Regulation of NB identity

The progeny identity of a T1NB or T2NB is invariable in the wild-type brain, suggesting that the capability to generate an INP or a GMC is determined when NB lineage identities are specified. This intuitive model was challenged by findings from several studies that are summarized below.(Komori, Xiao, Janssens, et al., 2014; Hakes & Brand, 2020; Quinto-Rives et al., 2020; Xie et al., 2014) An unbiased assessment of the regulation of NB lineage identities defined by progeny output necessitates study into cell-type-specific gene regulation by utilizing genomic analyses to define changes in gene activity (**see Chapter 2 for more detail**).

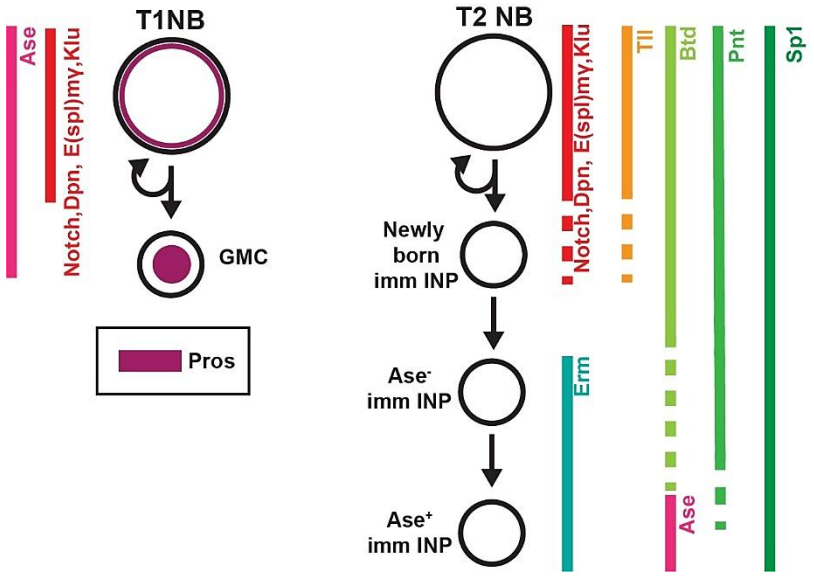


Figure 1.7 T1 and T2NB lineages express separate sets of lineage specific transcription factors

T1NBs normally generate an Ase^{+} while T2 NBs are Ase^{-}. Notch activity and expression of Notch downstream effectors Dpn, E(spl)mγ, and Klu are found in both T1 and T2 NBs. Tll, Btd, Pnt, and Sp1 can be detected in T2NBs but not T1NBs where Tll and Btd promote INP generation and Pnt promotes timely *erm* activation.

Trithorax (Trx)

Analyses of *trithorax* (*trx*), a member of the SET1/MLL complex which promotes gene activation, provided the first evidence suggesting that NB lineage identity defined

by the functional characteristics of their progeny can be altered during fly larval brain neurogenesis. (Komori, Xiao, Janssens, et al., 2014) Post-embryonically removing *trx* function in T2NBs results in their conversion to T1NBs based on the following : *trx*-mutant T2NBs express Ase and display asymmetric localization of Pros during mitosis to directly generate $Pros^{+}$ GMCs, two characteristics that are exclusively associated with T1NBs in wild-type brains (Table 1.1). Consistently, *trx*-mutant T2NBs also lack *pnt* and *buttonhead* (*btd*) expression, genes unique to T2NBs in wild-type brains. Thus, loss of *trx* function molecularly transforms T2NBs into T1NBs. (Komori, Xiao, Janssens, et al., 2014) Interestingly, loss of *brat* or *erm* function alone in T2NBs results in a severe supernumerary T2NB phenotype due to defective INP differentiation leading to a high frequency of INP reversion to T2NBs yet does not affect T1NB progeny differentiation to GMCs. Normally loss of *pros* only in T2NB lineages results in supernumerary INP formation because Pros is kept repressed until INP maturation. (Bayraktar et al., 2010) But in *trx*-mutant T2NBs, loss of *pros* leads to supernumerary T1NB formation. Because *pros* is required for T1NB progeny differentiation to GMCs, these results suggest that the progeny of *trx*-mutant T2NBs assume a GMC identity instead of immature INP. Consistently, most progeny that are in direct contact with *trx*-mutant T2NBs do not turn on the immature INP gene *erm* (Table 1.1). The component *trx* encodes is a conserved histone methyltransferase complex that deposits the monomethylation mark at the histone H3 lysine 4 residue (H3K4me1). (Tie et al., 2014) The Trx complex maintains chromatin in an active state at target gene loci. (Breen & Harte, 1993; Yu et al., 1995) Thus, following establishment of lineage identity during embryogenesis, a Trx-mediated maintenance mechanism is required for continual T2NB function to generate INPs.

Tailless (Tll)

Tll is highly expressed in T2NBs and is a key determinant of T2NB lineage identity (Figure 1.7). (Hakes & Brand, 2020; Quinto-Rives et al., 2020) Post-embryonically removing *tll* function in T2NBs leads to upregulation of T1NB marker Ase and leads to cortical expression of Pros but downregulation of T2NB marker Pnt. The progeny of *tll*-mutant T2NBs display the expression of GMC markers Ase and Pros but do not express Erm or Ham (Table 1.1). These data suggest that loss of *tll* function converts T2NBs into T1NBs. Thus, *tll* is necessary for maintaining T2NB lineage identity.

Over-expressing Tll is sufficient to molecularly and functionally convert T1NBs into T2NBs. It was observed that over-expressing Tll resulted in loss of Ase expression but increased expression of the T2NB lineage specific factor Sp1 (Figure 1.4). Furthermore, the progeny of T1NBs with high levels of Tll were able to generate Erm^{+} progeny corresponding to an immature INP fate. Additionally expressing Tll in INPs was sufficient to induce their reversion into supernumerary T2NBs suggesting that Tll promotes activation of the T2NB genetic program that would normally shut down in INPs. The similarity between the effect of loss of *trx* and *tll* on T2NBs suggests that Tll might function to specifically target Trx to gene loci to maintain T2NB lineage identity since Trx is also active in T1NBs but is not sufficient to induce a T2NB state alone. Elucidating the Tll downstream-effector gene regulatory network that promotes Tll-mediated control of larval brain NB lineage identity and determining whether Tll and Trx directly interact to promote T2NB identity or if other factors is necessary to mechanistically define regulation of NB function.

Buttonhead (Btd)

Trx and Tll are required for to maintain T2NB lineage identity, and their downstream-effector genes should include specific regulators of NB capability to generate INPs. Pnt and Btd are two candidates because their transcripts are highly enriched in T2NBs relative to T1NBs and both Trx and active histone mark it deposits, H3K4me1, are enriched in regulatory regions of *pnt* and *btd* (Figure 1.4).(Carney et al., 2012; Komori, Xiao, Janssens, et al., 2014; Xie et al., 2014) Pnt is required for the activation of *erm* expression in newborn immature INPs (Figure 1.5). (Janssens et al., 2017) Loss of *pnt* function in T2NBs leads to supernumerary T2NB formation which is consistent with loss of *erm* phenotype.(Komori, Xiao, Janssens, et al., 2014) These data indicate that Pnt specifically acts to promote immature INP differentiation to INPs through *erm*.

		wild-type T1NB	wild-type T2NB	Trx $^{-/-}$	Btd$^{-/-}$	Tll$^{-/-}$
NB	**Ase**	+	-	+	-	+
	Dpn	+	+	+	+	+
Progeny	**Pros**	+	-	+	+	+
	Erm	-	+	-	-	-

Table 1.1 Genes expression profile differences in Trx, Btd, and Tll mutant T2 NBs compared to wild-type T1 and T2 NBs.

Loss of *btd* function in T2NBs does not affect the profile of T2NB marker expression since Pnt remains active but Ase stays off. Btd mutants do not generate Erm^{+} progeny but make progeny that adopt a GMC identity as indicated by Ase and Pros expression (Table 1.1). Similar to the *trx*-mutant, removing *brat* function in *btd*-mutant T2NBs results in a mild supernumerary T2NB phenotype, which indicates the Btd mutant progeny are insensitive to Brat loss, consistent with a GMC fate. Over-

expressing Btd in *trx*-mutant T2NBs is sufficient to restore their capability to generate INPs which further suggest *btd* is downstream of Trx. Thus, *btd* is necessary for T2NBs to generate INPs. Furthermore, mis-expressing *btd* expression is sufficient to induce T1NBs to generate immature INPs marked by Erm expression. These ectopic immature INPs require *brat* and *erm* function to properly differentiate into INPs similar to wild-type immature INPs. Thus, Btd uniquely specifies generation of INPs without affecting the T2NB lineage identity. Current insight into if Tll directly regulates Btd expression in T2NBs and insight into what the regulatory relationship between key factors associated with T2NB identity and immature INP specification is still needed. Furthermore, identification of Btd downstream-effectors that are required for T2NBs to generate INPs and insight into if Btd works at the NB level or progeny level is critical to assemble the gene regulatory network that controls NB capability to generate INPs.

Precise regulation of gene expression in T2NBs

Due to the capability to generate INPs, T2NB lineages are significantly more susceptible to perturbations in differentiation that leads to reversion to a NB state. (Bowman et al., 2008; Quinto-Rives et al., 2020; Weng et al., 2010; Xiao et al., 2012) Notch signaling plays a key role in maintaining T2NBs in an undifferentiation state .(Zacharioudaki et al., 2012; Zacharioudaki et al., 2019; Zacharioudaki et al., 2016) Levels of Notch downstream-effector gene expression in T2NBs must be carefully controlled to ensure that their activity can be robustly downregulated in newborn immature INPs to allow for timely onset of differentiation to INPs. Characterization of positive and negative modulators of Notch downstream-effector gene expression in

T2NBs would provide insight into control of enhancer activity critical for cell differentiation in the T2NB lineage.

Zelda (Zld)

Zld is a transcription factor that binds thousands of *cis*-regulatory elements of genes in T2NBs, and likely bookmarks enhancers that become activated in cells at various stages of differentiation in the T2NB lineage during neurogenesis. (Larson et al., 2021; Marques et al., 2021; Michki et al., 2021; Rajan et al., 2023) Some of these genes are highly transcribed in T2NBs, but transcripts of many of these genes only become detectable in NB progeny. Zld binds many non-promoter *cis*-regulatory elements of Notch downstream-effector genes that are transcribed in NBs suggesting that Zld regulates their expression (Figure 1.8). Consistently, removing *zld* function enhances premature differentiation of T2NBs when Notch activity is reduced. Zld overexpression in T2NBs or immature INPs is sufficient to induce supernumerary T2NB formation similar to aberrant activation of Notch signaling. Zld and Suppressor of Hairless (Su(H)), the DNA-binding partner of Notch, bind a NB-specific enhancer associated with the Notch effector *dpn*. Mutating either Zld- or Su(H)-binding sites alone mildly reduces *dpn* enhancer activity while mutating both Zld- and Su(H)-binding sites completely abolishes the enhancer activity (Figure 1.8). These results suggest that Zld functions together with Notch transcriptional activator complex to promote gene expression in NBs by binding cell-type-specific enhancers.

Zld also binds cell-type-specific enhancers associated with genes that are highly expressed in T2NBs including *tll* and *btd.* (Larson et al., 2021).Chromatin accessibility appears to determine the ability of Zld to bind DNA in NBs and their progeny. Zld

occupancy at the cell-type-specific enhancer of *tll* diminishes in NB progeny undergoing differentiation to INPs as chromatin at the enhancer becomes progressively inaccessible. Thus, Zld-bound non-promoter regions of genes are candidate cell-type-specific enhancers in T2NBs.

Fruitless (Fru)

If gene transcript levels, especially those that encode Notch downstream transcription factors that prevent *erm* activation, are too high, the onset of INP differentiation can be impaired leading to supernumerary T2NB formation. (Berger et al., 2012; Komori, Xiao, McCartney, et al., 2014; San-Juán & Baonza, 2011; Xiao et al., 2012; Zacharioudaki et al., 2012; Zhu et al., 2011; Komori et al., 2018; Zacharioudaki et al., 2016) The C isoform for the gene Fruitless (Fru^C) plays an important role in maintaining proper gene transcript levels including Notch downstream-effectors in NBs by dampening their transcription. (Rajan et al., 2023) Loss of fru^C function is not sufficient to perturb the onset of differentiation in immature INPs but robustly enhances their reversion to supernumerary T2NBs when Notch effector gene activity is increased due to reduced *numb* or *brat* function (Figure 1.8). Over-expressing wild-type or a constitutive transcriptional repressor form of Fru^C is sufficient to partially restore differentiation in immature INPs that express elevated levels of Notch downstream-effector genes. The majority (>90%) of Su(H)-bound regions in T2NBs also overlap with Fru^C-bound peaks including promoters and enhancers of *Notch* and Notch effectors like *dpn* as well as *tll*. These results suggest that Fru^C negatively regulates Notch downstream-effector gene activity in T2NBs. Genetic and genomic analyses reveal that Fru^C dampens Notch downstream-effector gene transcription by promoting deposition of

the repressive histone mark H3K27me3 which is associated with the conserved Polycomb Repressive Complex 2 (PRC2). Thus, Fru^C negatively regulate gene transcription in NBs to ensure that their transcript levels are not high enough to potentially overwhelm controls that downregulates their activity in newborn immature INPs and perturb timely onset of differentiation (Figure 1.8). Of note, both Zld and Fru^C are expressed in T1NBs and are likely to serve the same role as observed in T2NBs, specific data testing this is still limited. In T2NB lineages, enhancers bound by Zld and Fru^C in NBs likely play important roles in controlling cell-type-specific gene expression during various stages of differentiation. Defining these enhancers and identifying specific epigenetic patterns associated with these enhancers could provide important insight into how NB function is controlled.

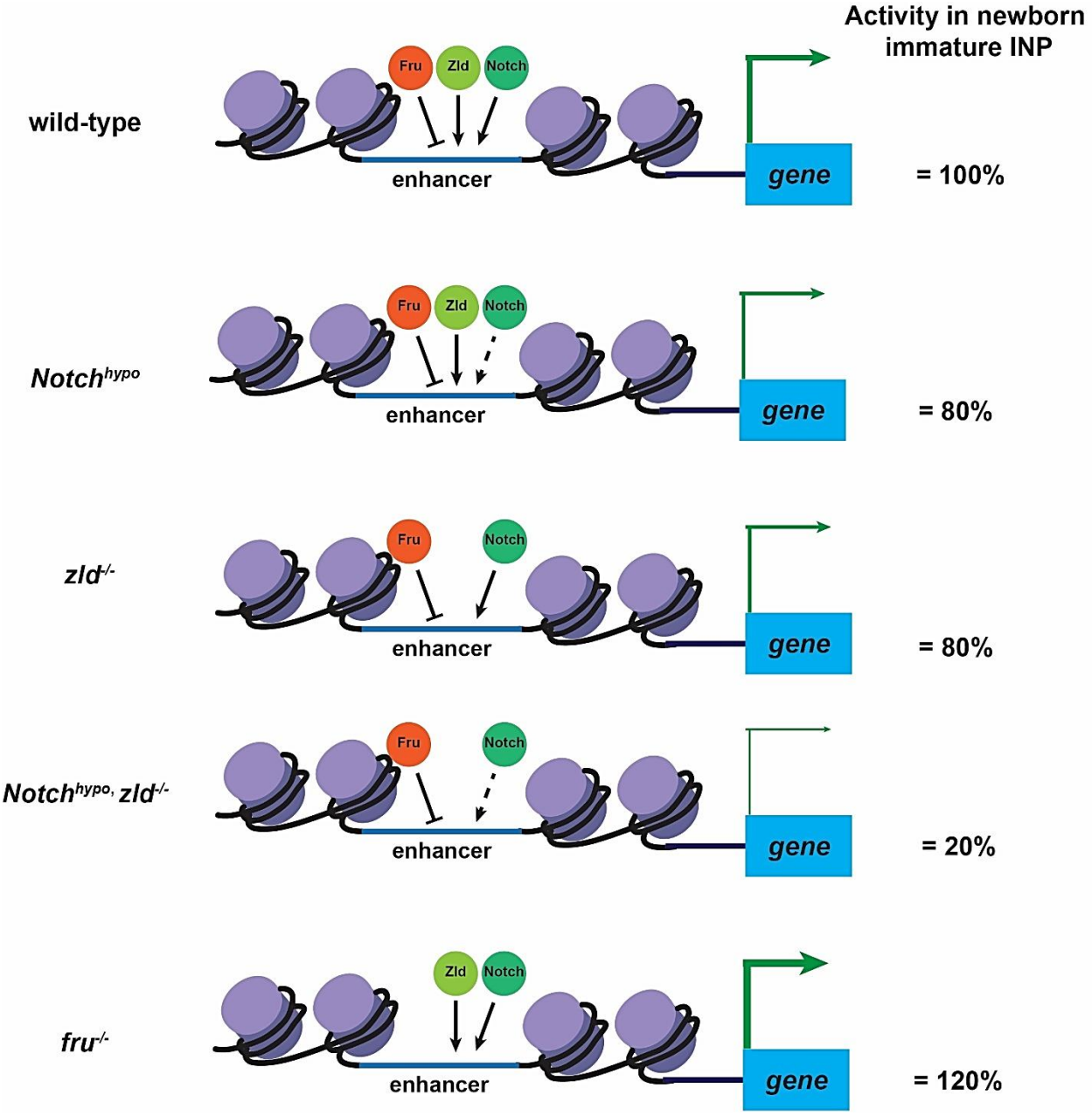


Figure 1.8 Fru and Zld modulate NB related gene activity

In wild-type brains, the activity of NB related genes like *dpn*, is set at 100%. Zld functions to promote gene activation, while Fru dampens activity. In *Notch*^{hypo} (hypomorphic: reduced function) brains, NB related gene activity in newborn progeny is 80%. In *zld*-null brains (-/-), NB gene activity would also be around 80%. In contrast, combining a *Notch*^{hypo} background with *zld*-null reduces NB gene activity to 20% and can result in premature differentiation of NBs. Fru^{c} dampens the activity of NB related genes, where a *fru*-null will show NB related gene activity increases to around 120% in the newborn progeny. Loss of *fru* function alone has no phenotype but can enhance the supernumerary NB phenotype when Notch is overactive in NB progeny.

Investigating stem cell capability to generate high vs low potential TAPs using fly NBs

Significant limitations exist that prevent investigation of radial glial capability to generate specific TAP subtypes which include lack of insight into cell type hierarchy, knowledge of key determinant transcription factors and epigenetic regulators that drive generation of TAPs, as well as cell-type-specific enhancers that specify transcription factor expression. Fly larval brain neural stem cell lineages provide a system where cell type hierarchy is well-defined, and high-potential TAPs and low-potential TAPs can be unambiguously identified. Furthermore, previous studies have identified and characterized key transcription factors and associated epigenetic regulators that promote generation of distinct TAPs subtypes. Genetic systems exist that can be used to enrich for specific neural stem cell types and are well-characterized. This allows for various genomic analyses include ATAC-seq and Cut&Run to define patterns of chromatin accessibility, transcription factor occupancy and histone mark profiles. The patterns of transcription factor binding and histone mark profiles provide in depth approach to define cell-type-specific enhancers that function at various stage of cell differentiation during neurogenesis. The availability of these tools can be combined to assess how neural stem cell capability to generate high- vs. low-potential TAPs is determined and how to reprogram neural stem cells to alter the developmental and proliferative of their progeny. This can be expanded to investigate the plasticity of high-potential TAPs vs. low-potential TAPs and uncover strategies to interconvert these TAPs. Lastly, the fly adult brain can be used to assess if tumor cells originated from a specific TAP subtype that are unable to properly differentiate can be reprogrammed to bypass differentiation blockades and reduce tumor burden. Taken together, larval brain

NB lineages provide a powerful paradigm to define mechanistic control of neural stem cell progeny output during neurogenesis that are unmatched by other experimental models.

References

Álvarez, J. A. D.-B., F.J.(2018). Origin and specification of type II neuroblasts in the Drosophila embryo. *Development*, *145*(7), dev158394.

Attardo, A., Calegari, F., Haubensak, W., Wilsch-Bräuninger, M., & Huttner, W. B.(2008). Live imaging at the onset of cortical neurogenesis reveals differential appearance of the neuronal phenotype in apical versus basal progenitor progeny. *PLoS One*, *3*(6), e2388. https://doi.org/10.1371/journal.pone.0002388

Bahrampour, S., Gunnar, E., Jonsson, C., Ekman, H., & Thor, S.(2017). Neural Lineage Progression Controlled by a Temporal Proliferation Program. *Developmental Cell*, *43*(3), 332-348.e334. https://doi.org/https://doi.org/10.1016/j.devcel.2017.10.004

Bayraktar, O. A., Boone, J. Q., Drummond, M. L., & Doe, C. Q.(2010). Drosophilatype II neuroblast lineages keep Prospero levels low to generate large clones that contribute to the adult brain central complex. *Neural Development*, *5*(1), 26. https://doi.org/10.1186/1749-8104-5-26

Bello, B., Reichert, H., & Hirth, F.(2006). The brain tumor gene negatively regulates neural progenitor cell proliferation in the larval central brain of Drosophila. *Development*, *133*(14), 2639-2648. https://doi.org/10.1242/dev.02429

Bello, B. C., Izergina, N., Caussinus, E., & Reichert, H.(2008). Amplification of neural stem cell proliferation by intermediate progenitor cells in Drosophila brain development. *Neural Develop*, *3*(1), 5.

Berger, C., Harzer, H., Burkard, T. R., Steinmann, J., van der Horst, S., Laurenson, A. S., Novatchkova, M., Reichert, H., & Knoblich, J. A.(2012). FACS purification and transcriptome analysis of drosophila neural stem cells reveals a role for Klumpfuss in self-renewal. *Cell Rep*, *2*(2), 407-418. https://doi.org/10.1016/j.celrep.2012.07.008

Betizeau, M., Cortay, V., Patti, D., Pfister, S., Gautier, E., Bellemin-Ménard, A., Afanassieff, M., Huissoud, C., Douglas, Rodney J., Kennedy, H., & Dehay, C.(2013). Precursor Diversity and Complexity of Lineage Relationships in the Outer Subventricular Zone of the Primate. *Neuron*, *80*(2), 442-457. https://doi.org/https://doi.org/10.1016/j.neuron.2013.09.032

Betschinger, J., Mechtler, K., & Knoblich, J. A.(2006). Asymmetric segregation of the tumor suppressor brat regulates self-renewal in Drosophila neural stem cells. *Cell*, *124*(6), 1241-1253. https://doi.org/10.1016/j.cell.2006.01.038

Boone, J. Q., & Doe, C. Q.(2008). Identification of Drosophila type II neuroblast lineages containing transit amplifying ganglion mother cells. *Dev Neurobiol.*, *68*(9), 1185-1195.

Borrell, V., & Reillo, I.(2012). Emerging roles of neural stem cells in cerebral cortex development and evolution. *Developmental Neurobiology*, *72*(7), 955-971. https://doi.org/https://doi.org/10.1002/dneu.22013

Bowman, S. K., Rolland, V., Betschinger, J., Kinsey, K. A., Emery, G., & Knoblich, J. A.(2008). The Tumor Suppressors Brat and Numb Regulate Transit-Amplifying Neuroblast Lineages in Drosophila. *Dev Cell*, *14*(4), 535-546.

Breen, T. R., & Harte, P. J.(1993). Trithorax regulates multiple homeotic genes in the bithorax and Antennapedia complexes and exerts different tissue-specific, parasegment-specific and promoter-specific effects on each. *Development*, *117*(1), 119-134.

Carney, T. D., Miller, M. R., Robinson, K. J., Bayraktar, O. A., Osterhout, J. A., & Doe, C. Q.(2012). Functional genomics identifies neural stem cell sub-type expression profiles and genes regulating neuroblast homeostasis. *Dev Biol*, *361*(1), 137-146.

Cenik, B. K., & Shilatifard, A.(2021). COMPASS and SWI/SNF complexes in development and disease. *Nat Rev Genet*, *22*(1), 38-58.

Chen, Y. C., & Konstantinides, N.(2022). Integration of Spatial and Temporal Patterning in the Invertebrate and Vertebrate Nervous System. *Front Neurosci*, *16*, 854422.

De Juan Romero, C., & Borrell, V.(2015). Coevolution of radial glial cells and the cerebral cortex. *Glia*, *63*(8), 1303-1319. https://doi.org/10.1002/glia.22827

Eroglu, E., Burkard, T. R., Jiang, Y., Saini, N., Homem, C. C., Reichert, H., & Knoblich, J. A.(2014). SWI/SNF complex regulates Prdm protein Hamlet to ensure lineage directionality in Drosophila neural stem cells. *Cell*, *156*(6), 1259-1273.

Faheem, M., Naseer, M. I., Rasool, M., Chaudhary, A. G., Kumosani, T. A., Ilyas, A. M., Pushparaj, P., Ahmed, F., Algahtani, H. A., Al-Qahtani, M. H., & Saleh Jamal, H.(2015). Molecular genetics of human primary microcephaly: an overview. *BMC Med Genomics*, *8 Suppl 1*(Suppl 1), S4. https://doi.org/10.1186/1755-8794-8-S1-S4

Fernández, V., Llinares-Benadero, C., & Borrell, V.(2016). Cerebral cortex expansion and folding: what have we learned? *EMBO J*, *35*(10), 1021-1044. https://doi.org/10.15252/embj.201593701

Fietz, S. A., Kelava, I., Vogt, J., Wilsch-Brauninger, M., Stenzel, D., Fish, J. L., Corbeil, D., Riehn, A., Distler, W., Nitsch, R., & Huttner, W. B.(2010). OSVZ progenitors of human and ferret neocortex are epithelial-like and expand by integrin signaling. *Nat Neurosci*, *13*(6), 690-699. https://doi.org/10.1038/nn.2553

Finlay, B. L., & Darlington, R. B.(1995). Linked regularities in the development and evolution of mammalian brains. *Science*, *268*(5217), 1578-1584. https://doi.org/10.1126/science.7777856

Florio, M., & Huttner, W. B.(2014). Neural progenitors, neurogenesis and the evolution of the neocortex. *Development*, *141*(11), 2182-2194. https://doi.org/10.1242/dev.090571

Franco, S. J., Gil-Sanz, C., Martinez-Garay, I., Espinosa, A., Harkins-Perry, S. R., Ramos, C., & Müller, U.(2012). Fate-Restricted Neural Progenitors in the Mammalian Cerebral Cortex. *Science*, *337*(6095), 746-749. https://doi.org/doi:10.1126/science.1223616

Frise, E., Knoblich, J. A., Younger-Shepherd, S., Jan, L. Y., & Jan, Y. N.(1996). The Drosophila Numb protein inhibits signaling of the Notch receptor during cell-cell interaction in sensory organ lineage. *Proc Natl Acad Sci U S A*, *93*(21), 11925-11932. https://doi.org/10.1073/pnas.93.21.11925

Genovese, S., Clément, R., Gaultier, C., Besse, F., Narbonne-Reveau, K., Daian, F., Foppolo, S., Luis, N. M., & Maurange, C.(2019). Coopted temporal patterning governs cellular hierarchy, heterogeneity and metabolism in Drosophila neuroblast tumors. *eLife*, *8*, e50375. https://doi.org/10.7554/eLife.50375

Geschwind, D. H., & Rakic, P.(2013). Cortical evolution: judge the brain by its cover. *Neuron*, *80*(3), 633-647. https://doi.org/10.1016/j.neuron.2013.10.045

Guo, M., Jan, L. Y., & Jan, Y. N.(1996). Control of daughter cell fates during asymmetric division: interaction of Numb and Notch. *Neuron*, *17*(1), 27-41. https://doi.org/10.1016/s0896-6273(00)80278-0

Hakes, A. E., & Brand, A. H.(2020). Tailless/TLX reverts intermediate neural progenitors to stem cells driving tumourigenesis via repression of asense/ASCL1. *eLife*, *9*, e53377. .

Hansen, D. V., Lui, J. H., Parker, P. R., & Kriegstein, A. R.(2010). Neurogenic radial glia in the outer subventricular zone of human neocortex. *Nature*, *464*(7288), 554-561.

Haubensak, W., Attardo, A., Denk, W., & Huttner, W. B.(2004). Neurons arise in the basal neuroepithelium of the early mammalian telencephalon: a major site of neurogenesis. *Proc Natl Acad Sci U S A*, *101*(9), 3196-3201.

Hildebrandt, K., Kübel, S., Minet, M., Fürst, N., Klöppel, C., Steinmetz, E., and Walldorf, U.(2021). Enhancer analysis of the Drosophila zinc finger transcription factor Earmuff by gene targeting. . Hereditas *158*, 41.

Hirata, J., Nakagoshi, H., Nabeshima, Y., & Matsuzaki, F.(1995). Asymmetric segregation of the homeodomain protein Prospero during Drosophila development. *Nature*, *377*(6550), 627-630. https://doi.org/10.1038/377627a0

Hu, W. F., Chahrour, M. H., & Walsh, C. A.(2014). The diverse genetic landscape of neurodevelopmental disorders. *Annu Rev Genomics Hum Genet*, *15*, 195-213. https://doi.org/10.1146/annurev-genom-090413-025600

Ikeshima-Kataoka, H., Skeath, J. B., Nabeshima, Y.-i., Doe, C. Q., & Matsuzaki, F.(1997). Miranda directs Prospero to a daughter cell during Drosophila asymmetric divisions. *Nature*, *390*(6660), 625-629. https://doi.org/10.1038/37641

Jancewicz, I., Siedlecki, J. A., Sarnowski, T. J., & Sarnowska, E.(2019). BRM: the core ATPase subunit of SWI/SNF chromatin-remodelling complex-a tumour suppressor or tumour-promoting factor? *Epigenetics Chromatin*, *12*(1), 68. https://doi.org/10.1186/s13072-019-0315-4

Janssens, D. H., Hammn, D. C., Anhezini, L., Xiao, X., Siller, K. H., Siegrist, S. E., Harrison, M. M., & Lee, C.-Y.(2017). A Hdac1/Rpd3-poised circuit balances continual self-renewal and rapid restriction of developmental potential during asymmetric stem cell division. *Dev Cell*, *40*(4), 367-380.

Janssens, D. H., Komori, H., Grbac, D., Chen, K., Koe, C. T., Wang, H., & Lee, C. Y.(2014). Earmuff restricts progenitor cell potential by attenuating the competence to respond to self-renewal factors. *Development*, *141*(5), 1036-1046.

Jayaraman, D., Bae, B. I., & Walsh, C. A.(2018). The Genetics of Primary Microcephaly. *Annu Rev Genomics Hum Genet*, *19*, 177-200. https://doi.org/10.1146/annurev-genom-083117-021441

Knoblich, J. A., Jan, L. Y., & Jan, Y. N.(1995). Asymmetric segregation of Numb and Prospero during cell division. *Nature*, *377*(6550), 624-627. https://doi.org/10.1038/377624a0

Koe, C. T., Li, S., Rossi, F., Wong, J. J., Wang, Y., Zhang, Z., Chen, K., Aw, S. S., Richardson, H. E., Robson, P., Sung, W. K., Yu, F., Gonzalez, C., & Wang, H.(2014). The Brm-HDAC3-Erm repressor complex suppresses dedifferentiation in Drosophila type II neuroblast lineages. *eLife*, *3*, e01906.

Komori, H., Golden, K. L., Kobayashi, T., Kageyama, R., & Lee, C. Y.(2018). Multilayered gene control drives timely exit from the stem cell state in uncommitted progenitors during Drosophila asymmetric neural stem cell division. *Genes Dev*, *32*(23-24), 1550-1561.

Komori, H., Xiao, Q., Janssens, D. H., Dou, Y., & Lee, C. Y.(2014). Trithorax maintains the functional heterogeneity of neural stem cells through the transcription factor Buttonhead. *eLife*, *10.7554/eLife.03502*.

Komori, H., Xiao, Q., McCartney, B. M., & Lee, C. Y.(2014). Brain tumor specifies intermediate progenitor cell identity by attenuating β-catenin/Armadillo activity. *Development*, *141*(1).

Kowalczyk, T., Pontious, A., Englund, C., Daza, R. A., Bedogni, F., Hodge, R., Attardo, A., Bell, C., Huttner, W. B., & Hevner, R. F.(2009). Intermediate neuronal progenitors (basal progenitors) produce pyramidal-projection neurons for all layers of cerebral cortex. *Cereb Cortex*, *19*(10), 2439-2450.

Larson, E. D., Komori, H., Gibson, T. J., Ostgaard, C. M., Hamm, D. C., Schnell, J. M., Lee, C. Y., & Harrison, M. M.(2021). Cell-type-specific chromatin occupancy by the pioneer factor Zelda drives key developmental transitions in Drosophila *Nat Commun*, *12*, 7153.

Lee, C. Y., Andersen, R. O., Cabernard, C., Manning, L., Tran, K. D., Lanskey, M. J., Bashirullah, A., & Doe, C. Q.(2006). Drosophila Aurora-A kinase inhibits neuroblast self-renewal by regulating aPKC/Numb cortical polarity and spindle orientation. *Genes Dev*, *20*(24), 3464-3474. https://doi.org/10.1101/gad.1489406

Lee, C. Y., Robinson, K. J., & Doe, C. Q.(2006). Lgl, Pins and aPKC regulate neuroblast self-renewal versus differentiation. *Nature*, *439*(7076), 594-598.

Lee, C. Y., Wilkinson, B. D., Siegrist, S. E., Wharton, R. P., & Doe, C. Q.(2006). Brat is a Miranda cargo protein that promotes neuronal differentiation and inhibits neuroblast self-renewal. *Dev Cell*, *10*(4), 441-449. https://doi.org/10.1016/j.devcel.2006.01.017

Lewitus, E., Kelava, I., & Huttner, W. B.(2013). Conical expansion of the outer subventricular zone and the role of neocortical folding in evolution and development [Hypothesis and Theory]. *Frontiers in Human Neuroscience*, *Volume 7 - 2013*. https://doi.org/10.3389/fnhum.2013.00424

Lewitus, E., Kelava, I., Kalinka, A. T., Tomancak, P., & Huttner, W. B.(2014). An Adaptive Threshold in Mammalian Neocortical Evolution. *PLOS Biology*, *12*(11), e1002000. https://doi.org/10.1371/journal.pbio.1002000

Llinares-Benadero, C., & Borrell, V.(2019). Deconstructing cortical folding: genetic, cellular and mechanical determinants. *Nat Rev Neurosci*, *20*(3), 161-176.

Llinares Benadero, C., & Borrell, V.(2019). Deconstructing cortical folding: genetic, cellular and mechanical determinants. *Nature Reviews Neuroscience*, *20*. https://doi.org/10.1038/s41583-018-0112-2

Lu, C., & Allis, C. D.(2017). SWI/SNF complex in cancer. *Nat Genet*, *49*(2), 178-179. https://doi.org/10.1038/ng.3779

Marques, G. S., Teles-Reis, J., Konstantnides, N., Brito, P. H., & Homem, C. C. F.(2021). Fate transitions in Drosophila neural lineages: a single cell road map to mature neurons. *bioRxiv*, doi: https://doi.org/10.1101/2021.1106.1122.449317

Martínez-Cerdeño, V., Cunningham, C. L., Camacho, J., Antczak, J. L., Prakash, A. N., Cziep, M. E., Walker, A. I., & Noctor, S. C.(2012). Comparative analysis of the subventricular zone in rat, ferret and macaque: evidence for an outer subventricular zone in rodents. *PLoS One*, *7*(1), e30178. https://doi.org/10.1371/journal.pone.0030178

Martínez-Martínez, M., Ciceri, G., Espinós, A., Fernández, V., Marín, O., & Borrell, V.(2019). Extensive branching of radially-migrating neurons in the mammalian cerebral cortex. *J Comp Neurol*, *527*(10), 1558-1576. https://doi.org/10.1002/cne.24597

Michki, N. S., Li, Y., Sanjasaz, K., Zhao, Y., Shen, F. Y., Walker, L. A., Lee, C.-Y., & Cai, D.(2021). The molecular landscape of neural differentiation in the developing Drosophila brain revealed by targeted scRNA-seq and multi-informatic analysis. *Cell Report*, *35*(4), 109039.

Narbonne-Reveau, K., Lanet, E., Dillard, C., Foppolo, S., Chen, C.-H., Parrinello, H., Rialle, S., Sokol, N. S., & Maurange, C.(2016). Neural stem cell-encoded temporal patterning delineates an early window of malignant susceptibility in Drosophila. *eLife*, *5*, e13463. https://doi.org/10.7554/eLife.13463

Noctor, S. C., Martínez-Cerdeño, V., Ivic, L., & Kriegstein, A. R.(2004). Cortical neurons arise in symmetric and asymmetric division zones and migrate through specific phases. *Nat Neurosci*, *7*(2), 136-144.

Ostgaard, C. M., Rajan, A., Davison, S. R., & Lee, C.-Y.(2025). A double-assurance mechanism restrains generation of high potential transit-amplifying progenitors during neurogenesis. *bioRxiv*, 2025.2009.2016.676671. https://doi.org/10.1101/2025.09.16.676671

Pebworth, M. P., Ross, J., Andrews, M., Bhaduri, A., & Kriegstein, A. R.(2021). Human intermediate progenitor diversity during cortical development. *Proc Natl Acad Sci U S A*, *118*(26), e2019415118.

Pilz, G. A., Shitamukai, A., Reillo, I., Pacary, E., Schwausch, J., Stahl, R., Ninkovic, J., Snippert, H. J., Clevers, H., Godinho, L., Guillemot, F., Borrell, V., Matsuzaki, F., & Götz, M.(2013). Amplification of progenitors in the mammalian telencephalon includes a new radial glial cell type. *Nat Commun*, *4*, 2125. https://doi.org/10.1038/ncomms3125

Quinto-Rives, N., Komori, H., Janssens, D. H., Kondo, S., Dai, Q., Moore, A. W., & Lee, C.-Y.(2020). Sequential activation of transcriptional repressors promotes progenitor commitment by silencing stem cell identity genes. *eLife*(9), e56187.

Rajan, A., Anhezini, L., Rives-Quinto, N., Chhabra, J. Y., Neville, M. C., Larson, E. D., Goodwin, S. F., Harrison, M. M., & Lee, C.-Y.(2023). Low-level repressive histone marks fine-tune gene transcription in neural stem cells. *eLife*, *12*, e86127. https://doi.org/10.7554/eLife.86127

Rakic, P.(2009). Evolution of the neocortex: a perspective from developmental biology. *Nat Rev Neurosci*, *10*(10), 724-735. https://doi.org/10.1038/nrn2719

Reichardt, I., Bonnay, F., Steinmann, V., Loedige, I., Burkard, T. R., Meister, G., & Knoblich, J. A.(2018). The tumor suppressor Brat controls neuronal stem cell lineages by inhibiting Deadpan and Zelda. *EMBO Rep*, *19*(1), 102-117.

Reillo, I., & Borrell, V.(2012). Germinal zones in the developing cerebral cortex of ferret: ontogeny, cell cycle kinetics, and diversity of progenitors. *Cereb Cortex*, *22*(9), 2039-2054. https://doi.org/10.1093/cercor/bhr284

Reillo, I., de Juan Romero, C., Garcia-Cabezas, M. A., & Borrell, V.(2011). A role for intermediate radial glia in the tangential expansion of the mammalian cerebral cortex. *Cereb Cortex*, *21*(7), 1674-1694. https://doi.org/10.1093/cercor/bhq238

Rolls, M. M., Albertson, R., Shih, H. P., Lee, C. Y., & Doe, C. Q.(2003). Drosophila aPKC regulates cell polarity and cell proliferation in neuroblasts and epithelia. *J Cell Biol*, *163*(5), 1089-1098.

Runge, J. S., Raab, J. R., & Magnuson, T.(2016). Chapter One - Epigenetic Regulation by ATP-Dependent Chromatin-Remodeling Enzymes: SNF-ing Out Crosstalk. In P. M. Wassarman (Ed.), *Current Topics in Developmental Biology* (Vol. 117, pp. 1-13). Academic Press. https://doi.org/https://doi.org/10.1016/bs.ctdb.2015.10.009

San-Juán, B. P., & Baonza, A.(2011). The bHLH factor deadpan is a direct target of Notch signaling and regulates neuroblast self-renewal in Drosophila. *Dev Biol*, *352*(1), 70-82.

Sessa, A., Mao, C. A., Hadjantonakis, A. K., Klein, W. H., & Broccoli, V.(2008). Tbr2 directs conversion of radial glia into basal precursors and guides neuronal amplification by indirect neurogenesis in the developing neocortex. *Neuron*, *60*(1), 56-69.

Shen, C. P., Jan, L. Y., & Jan, Y. N.(1997). Miranda is required for the asymmetric localization of Prospero during mitosis in Drosophila. *Cell*, *90*(3), 449-458. https://doi.org/10.1016/s0092-8674(00)80505-x

Smart, I. H., Dehay, C., Giroud, P., Berland, M., & Kennedy, H.(2002). Unique morphological features of the proliferative zones and postmitotic compartments of the neural epithelium giving rise to striate and extrastriate cortex in the monkey. *Cereb Cortex*, *12*(1), 37-53.

Spana, E. P., & Doe, C. Q.(1995). The prospero transcription factor is asymmetrically localized to the cell cortex during neuroblast mitosis in Drosophila. *Development*, *121*(10), 3187-3195. https://doi.org/10.1242/dev.121.10.3187

Tanaka, T., & Gleeson, J. G.(2000). Genetics of brain development and malformation syndromes. *Curr Opin Pediatr*, *12*(6), 523-528. https://doi.org/10.1097/00008480-200012000-00002

Taverna, E., Gotz, M., & Huttner, W. B.(2014). The cell biology of neurogenesis: toward an understanding of the development and evolution of the neocortex. *Annu Rev Cell Dev Biol*, *30*, 465-502. https://doi.org/10.1146/annurev-cellbio-101011-155801

Tie, F., Banerjee, R., Saiakhova, A. R., Howard, B., Monteith, K. E., Scacheri, P. C., Cosgrove, M. S., & Harte, P. J.(2014). Trithorax monomethylates histone H3K4 and interacts directly with CBP to promote H3K27 acetylation and antagonize Polycomb silencing. *Development*, *141*(5), 1129-1139. https://doi.org/10.1242/dev.102392

Walsh, K. T., & Doe, C. Q.(2017). Drosophila embryonic type II neuroblasts: origin, temporal patterning, and contribution to the adult central complex. *Development*, *144*(24), 4552-4562.

Wang, H., Ouyang, Y., Somers, W. G., Chia, W., & Lu, B.(2007). Polo inhibits progenitor self-renewal and regulates Numb asymmetry by phosphorylating Pon. *Nature*, *449*(7158), 96-100.

Wang, H., Somers, G. W., Bashirullah, A., Heberlein, U., Yu, F., & Chia, W.(2006). Aurora-A acts as a tumor suppressor and regulates self-renewal of Drosophila neuroblasts. *Genes Dev*, *20*(24), 3453-3463.

Wang, L., Wang, C., Moriano, J. A., Chen, S., Zuo, G., Cebrián-Silla, A., Zhang, S., Mukhtar, T., Wang, S., Song, M., de Oliveira, L. G., Bi, Q., Augustin, J. J., Ge, X., Paredes, M. F., Huang, E. J., Alvarez-Buylla, A., Duan, X., Li, J., & Kriegstein, A. R.(2025). Molecular and cellular dynamics of the developing human neocortex. *Nature*. https://doi.org/10.1038/s41586-024-08351-7

Wang, X., Tsai, J. W., LaMonica, B., & Kriegstein, A. R.(2011). A new subtype of progenitor cell in the mouse embryonic neocortex. *Nat Neurosci*, *14*(5), 555-561. https://doi.org/10.1038/nn.2807

Weng, M., Golden, K. L., & Lee, C. Y.(2010). dFezf/Earmuff maintains the restricted developmental potential of intermediate neural progenitors in Drosophila. *Dev Cell*, *18*(1), 126-135.

Wirtz-Peitz, F., Nishimura, T., & Knoblich, J. A.(2008). Linking Cell Cycle to Asymmetric Division: Aurora-A Phosphorylates the Par Complex to Regulate Numb Localization. *Cell*, *135*(1), 161-173. https://doi.org/https://doi.org/10.1016/j.cell.2008.07.049

Wu, P.-S., Egger, B., & Brand, A. H.(2008). Asymmetric stem cell division: Lessons from Drosophila. *Seminars in Cell & Developmental Biology*, *19*(3), 283-293. https://doi.org/https://doi.org/10.1016/j.semcdb.2008.01.007

Xiao, Q., Komori, H., & Lee, C. Y.(2012). klumpfuss distinguishes stem cells from progenitor cells during asymmetric neuroblast division. *Development*, *139*(15), 2670-2680.

Xie, Y., Li, X., Zhang, X., Mei, S., Li, H., Urso, A., & Zhu, S.(2014). The Drosophila Sp8 transcription factor Buttonhead prevents premature differentiation of intermediate neural progenitors. *eLife*, *3*(eLife.03596).

Yu, B. D., Hess, J. L., Horning, S. E., Brown, G. A., & Korsmeyer, S. J.(1995). Altered Hox expression and segmental identity in Mll-mutant mice. *Nature*, *378*(6556), 505-508.

Zacharioudaki, Srivathsa, M., & C, D.(2012). bHLH-O proteins are crucial for Drosophila neuroblast self-renewal and mediate Notch-induced overproliferation. *Development*.

Zacharioudaki, E., Falo Sanjuan, J., & Bray, S.(2019). Mi-2/NuRD complex protects stem cell progeny from mitogenic Notch signaling. *eLife*, *8*, e41637.

Zacharioudaki, E., Housden, B. E., Garinis, G., Stojnic, R., Delidakis, C., & Bray, S.(2016a). Genes implicated in stem-cell identity and temporal-program are directly targeted by Notch in neuroblast tumours. *Development*, pii: dev.126326.

Zhu, S., Barshow, S., Wildonger, J., Jan, L. Y., & Jan, Y. N.(2011). Ets transcription factor Pointed promotes the generation of intermediate neural progenitors in Drosophila larval brains. *Proc Natl Acad Sci U S A.*, *108*(51), 20615-20620.

Chapter 2 A Double-Assurance Mechanism Restrains Generation of High Potential Transit-Amplifying Progenitors During Neurogenesis

Summary

Stem cells can generate differentiated progeny directly or indirectly through transit-amplifying progenitors (TAPs), which are vulnerable to tumorigenic transformation. Despite clinical relevance, how stem cells regulate TAP production is unclear. Drosophila brains contain Asense^{+} stem cells (Type1 neuroblasts; T1NBs) that generate low neurogenic potential TAPs and Asense- stem cells (Type2 neuroblasts; T2NBs) that produce high-potential TAPs [Intermediate Neural Progenitors (INPs)]. Unexpectedly, cell-type-specific enhancers of genes essential for INP formation are poised in T1NBs despite never generating INP progeny. Thus, both NB types are competent to generate INPs. Inducing T1NBs to generate INPs is more efficient upon asense knockdown. The progeny of T2NBs expressing elevated Asense adopt a low-potential TAP identity instead of INPs. Elevated Asense expression limits tumor NB expansion driven by stalled INPs halting tumor expansion. We propose that a double-assurance mechanism characterized by dynamic superimposition of lineage-specific activators upon basal-state determinants defines NB capability to generate high-potential TAPs.

Introduction

TAPs are transient stem cell progeny that function to increase the output of differentiated cells during development and homeostasis. TAPs can vary widely in terms of proliferative and developmental potential.(Hevner, 2019) During vertebrate neurogenesis, radial glial progenitors function as neural stem cells and can generate neurons indirectly through TAPs, also known as intermediate progenitors.(Huilgol et al., 2023; Kalebic & Huttner, 2020; Lin et al., 2021; Pipicelli et al., 2025; Thor, 2024) Most intermediate progenitors display low neurogenic potential and canonically divide once to produce two neurons. In developing primate and human brains, a subset of intermediate progenitors exhibit higher neurogenic potential and can divide multiple times to increase neuron generation.(Betizeau et al., 2013; Hansen et al., 2010; Pebworth et al., 2021) It remains unclear whether chromatin accessibility or histone modification patterns at enhancers of genes that drive the formation of specific intermediate progenitors define radial glial capability to generate high- or low-potential TAP subtypes.

The fly larval brain contains two distinct NB lineages that are well-defined providing an excellent *in vivo* paradigm for investigating how heterogenous stem cells regulate generation of distinct types of TAPs.(Doe, 2017; Homem et al., 2015; Janssens & Lee, 2014) Approximately 100 NBs are specified per brain lobe during embryogenesis and undergo repeated asymmetric division to self-renew and to produce an identical TAP subtype every division.(Álvarez, 2018; Walsh & Doe, 2017) Most of these are T1NBs, which generate ganglion mother cells (GMCs) that exhibit low neurogenic potential and divide only once to produce two neurons. Eight are T2NBs, which invariably produce an immature INP that is Asense (Ase; Ascl1) negative but will

upregulate Ase as the differentiation to an INP progresses.(Bello et al., 2008; Boone & Doe, 2008; Bowman et al., 2008) An INP exhibits high neurogenic potential compared to a GMC. An INP undergoes 5-6 rounds of asymmetric division, generating a GMC each division, leading to an overall output of more than a dozen differentiated cells including neurons and glia in its lifetime.(Bayraktar & Doe, 2013; Viktorin et al., 2011) Due to the invariability of the NB progeny and that which NBs produce INPs is determined when the NBs are first generated during the embryonic stage, the ability to generate INPs is thought to be genetically determined by the developmental program that specifies T2NB identity. This “deterministic model” predicts that nucleosomes at enhancers that drive the expression of genes essential for INP formation are closely spaced from each other (chromatin inaccessible) making these *cis*-regulatory elements inaccessible to TF binding in T1NBs resulting in the lack of INP progeny.

Post-embryonically removing *trithorax* (*trx*) gene activity converts T2NBs to T1NBs as indicated by (1) loss of T2NB-specific marker expression, (2) gain of T1NB-specific gene expression and (3) direct generation GMCs (Komori, Xiao, Janssens, et al., 2014). Trx is an evolutionarily conserved histone methyltransferase and maintains chromatin in an active state through H3K4 methylation at target gene loci.(Breen & Harte, 1993; Yu et al., 1995) Trx maintains expression of transcription factors (TFs) essential for T2NB identity. These genes include Tailless (Tll) which is necessary and sufficient for T2NB identity with high levels of Tll expression promoting T2NB maintenance, likely by suppressing the T1NB genetic program.(Hakes & Brand, 2020; Quinto-Rives et al., 2020) Pointed (Pnt) promotes immature INP differentiation into INPs.(Janssens et al., 2014; Komori, Xiao, Janssens, et al., 2014; Xie et al., 2014; Zhu

et al., 2011) Additionally, T2NBs mutant for *buttonhead* (*btd*) generate GMCs instead of INPs while maintaining T2NB-specific marker gene expression.(Komori, Xiao, Janssens, et al., 2014; Xie et al., 2014) *btd* encodes a C_2H_2 zinc finger TF that likely functions as a positive regulator of gene expression (Cohen & Jürgens, 1990; Schöck et al., 1999; Wimmer et al., 1993). Mis-expressing *btd* is sufficient to induce T1NBs to generate INPs. These data suggest that GMC identity is the basal-state for NB progeny fate in both lineages. This “hierarchical model” predicts that chromatin at enhancers that drive gene expression essential for INP formation are loosely wrapped around histone octamers (chromatin accessible) but post-translational modifications of histones maintain inactivity of these *cis*-regulatory elements (chromatin state) in T1NBs. Trx, Tll and Btd can promote activation of these cell-type-specific enhancers in T2NBs leading to generation of INPs instead of GMCs.

The basic-helix-loop-helix TF Ase is expressed in T1NBs throughout development and has been implicated in determining T1NB lineage identity.(Álvarez, 2018; Bahrampour et al., 2017; Bayraktar et al., 2010; Bello et al., 2008; Boone & Doe, 2008; Bowman et al., 2008; Chen et al., 2022; Walsh & Doe, 2017) Surprisingly, deletion of the *ase* locus has no effect on viability or on T1NB lineage progression. This suggests that Ase is not necessary to maintain T1NB identity or for the generation of GMCs. Although increasing Ase expression is sufficient to block premalignant T2NB formation when Tll is overexpressed in T1NBs, the functional significance and underlying mechanism of this result is currently unclear.(Hakes & Brand, 2020) As such, Ase mainly serves as a reliable marker for identifying T1NBs and INPs.

We hypothesized that the chromatin state at enhancers that drive gene expression in immature INPs to promote INP formation serves as a functional readout for the capability of NBs to generate INPs. Thus, identifying genes that are highly transcribed in immature INPs and defining enhancers that drive their cell-type-specific expression are critical for investigation of NB capability to generate INPs. We leveraged published single-cell mRNA sequencing datasets of wild-type NB lineages (Marques et al., 2023; Michki et al., 2021; A. Rajan et al., 2023) to identify genes that are high transcribed in immature INPs. We searched for active neurogenic enhancers, which are defined as non-promoter *cis*-regulatory regions that display accessible chromatin and are bound by Zelda (Zld; a positive regulator of gene transcription (Larson et al., 2021; Reichardt et al., 2018)) and Fruitless^{C} (Fru^{C}; a negative regulator of gene transcription (A. Rajan et al., 2023)) in T2NBs. We identified 3839 active neurogenic enhancers including cell-type-specific enhancers associated with genes that promote immature INP differentiation to INPs. Enhancers of genes essential for INP formation and functions display features that are typically associated with poised enhancers including accessible chromatin, high H3K27me3/H3K4me1 and low H3K27Ac in T1NBs. Thus, the chromatin state and not accessibility at enhancers associated with genes essential for INP formation and functions correlates with NB capability to give rise to an INP or GMC. Inducing T1NBs to generate INPs by mis-expressing Btd becomes more efficient when *ase* function is knocked down, while high levels of Ase promote T2NBs to generate GMCs, via bypassing the INP stage. We identified the TF Prospero (Pros) as the key Ase downstream-effector that reprograms T2NBs to generate GMCs by activating the GMC genetic program in immature INPs. Furthermore, elevating Ase expression in

tumor NBs that form a continual positive feedback loop with immature INPs that are stalled in differentiation suppresses tumor expansion. These results led us to propose a double-assurance mechanism in which dynamic superimposition of lineage-specific activators (Btd) upon basal-state determinants (Ase and Pros) defines NB capability to generate INPs or GMCs.

Transcriptional states regulate NB capability to generate INPs

To determine whether chromatin accessibility or post-translational modification of histones at enhancers of genes essential for INP formation correlates with the capability of NBs to generate INPs (Fig. 2.2A), we first defined gene transcripts that are high enriched in T2NBs, immature INPs or INPs. Of the 255 genes which showed transcript enrichment in T2NBs, immature INPs or INPs based on previously published single-cell mRNA sequencing datasets of wild-type larval brains (Marques et al., 2023; Michki et al., 2021; A. Rajan et al., 2023), 174 showed region of open accessibility (Appendix Table A.1). These genes are assigned to one of four groups based on the cell type where their transcripts first become detectable (Fig. 2.2B; Appendix Table A.1). Transcripts encoded by the Group 1 genes (e.g. *btd* and *pnt*) become detectable prior to or coinciding with the onset of immature INP differentiation marked by Earmuff (Erm) protein expression.(Komori, Xiao, Janssens, et al., 2014; Xie et al., 2014) Gene transcripts in the Group 2 (e.g. *erm*) were first detected in the early stage of immature INP differentiation ($Erm^{+}Ase^{-}$)(Janssens et al., 2017; Janssens et al., 2014; Weng et al., 2010). Gene transcripts in the Group 3 (e.g. *hamlet* (*ham*), *Dichaete* (*D*)) are detected starting in the late stages of immature INP differentiation ($Erm^{+}Ase^{+}$).(Bayraktar & Doe, 2013; Quinto-Rives et al., 2020) Transcripts encoded by the Group 4 genes (e.g. *odd-*

paired (*opa*) and *eyeless* (*ey*)) are detected in various INP life stages.(Abdusselamoglu et al., 2019; Bayraktar & Doe, 2013) Combined, there are 81 genes in group 3 & 4 that are highly enriched during immature INP differentiation and 62 have associated chromatin accessible regions. Assessing the chromatin state at enhancers that drive their cell-type-specific expression should unravel whether chromatin accessibility or histone modifications correlates with NB capability to generate INPs.

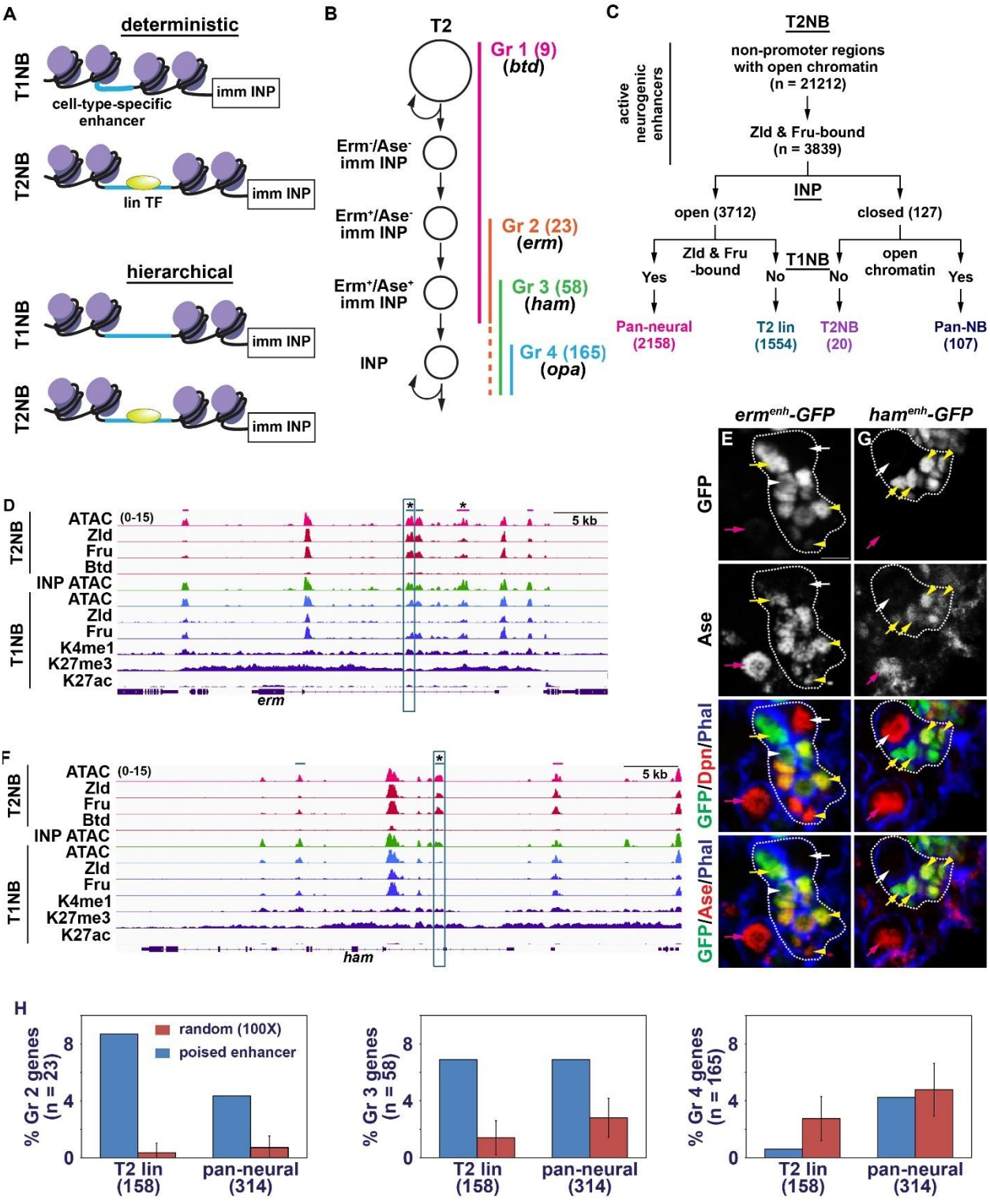


Figure 2.1 Cell-type-specific enhancers associated with genes essential for INP formation are poised in T1NBs

(A) Models for the regulation of NB capability to generate INPs. The deterministic model holds true if cell-type-specific enhancers associated with genes that function to promote immature INP (immature INP) differentiation to are inaccessible in T1NBs. The hierarchal model holds true if immature INP enhancers are accessible but inactive in T1NBs. Lineage-specific transcription factor (lin. TF) promotes activation of these enhancers in T2NBs.(B) 255 genes showed transcript enrichment in T2NBs, immature INPs or INPs based on previously published single-cell mRNA sequencing datasets of wild-type larval brains.(Marques et al., 2023; Michki et al., 2021; A. Rajan et al., 2023) These genes are assigned to one of four groups based on the cell type in which their transcripts first become detectable.(C) Flowchart for the identification of cell-type-specific enhancers in fly larval brain NB lineages. Pan-neural: Pan-neural enhancer. T2 lin: T2 lineage enhancer. T2NB: T2NB enhancer. Pan-NB: pan-NB enhancer (D,F) Genome browser track of the erm and ham locus showing patterns of chromatin accessibility, TF occupancy and histone marks in indicated cell types. The magenta bars correspond to pan-neural enhancers, and teal bars correspond to T2-lin enhancers. Teal box designates enhancer that recapitulates the onset of erm or ham expression in the T2 lineage. * indicates poised enhancers.(E) GFP reporter expression driven by an erm T2 lin enhancer (teal box in D) becomes detectable in Ase- immature INPs but is undetectable in T1 and T2NBs.(G) GFP reporter expression driven by a ham T2 lin enhancer (teal box in F) becomes detectable in Ase+ immature INPs but is undetectable in T1 and T2NBs. White dotted line circles T2NB lineage. White arrow: T2NB. White arrowhead: Ase- immature INP. Yellow arrow: Ase+ immature INP. Yellow arrowhead: INP. Magenta arrow: T1NB. Scale bar: 10μm.

We took an unbiased approach to identify active neurogenic enhancers, which are defined as non-promoter *cis*-regulatory regions that display accessible chromatin and are bound by Zld and Fru^{C} in T2NBs using published datasets.(Larson et al., 2021; A. Rajan et al., 2023) 3839 *cis*-regulatory regions fulfilled these criteria and were referred to as active neurogenic enhancers in T2NBs (Fig. 2.1C). Chromatin accessibility in INPs separates these enhancers into the NB-specific cohort from the NB lineage cohort. Enhancers in the NB-specific cohort are divided into Pan-NB enhancers or T2NB enhancers based on their chromatin accessibility in T1NBs (Fig. 2.1C). Pan-NB enhancers display accessible chromatin in T1NBs and likely promote gene expression in both NB types (Fig. 2.2B; Appendix Table A.1-6). T2NB enhancers display inaccessible chromatin in T1NBs and likely regulate the expression of genes (including *btd* and *tll*) exclusively in T2NBs (Fig. 2.2B; Appendix Table A.1-6).

Enhancers in the NB lineage cohort are grouped into Pan-neural enhancers or T2 lineage (T2 lin) enhancers depending on chromatin accessibility and occupancy by Zld and Fru^C in T1NBs (Fig. 2.1C). Pan-neural enhancers show accessible chromatin and are bound by Zld and Fru^C and likely regulate gene expression in both NB lineages (Fig. 2.2B; Appendix Table A.1-6). This category includes 1 enhancer from the *btd* locus active in T2NBs and 2 enhancers from the *D* and *opa* loci active only in INPs (Fig. 2.2C,D). Lack of Zld binding in T1NBs, which suggests inactivity, is used to define T2 lin enhancers. These include 6 enhancers from the *pnt*, *H6-like-homeobox* (*hmx*), *optix* (*opt*) and other loci that are active exclusively in T2NB lineages and 3 enhancers from the *erm* and *ham* loci active only in immature INPs (Fig. 2.1D,F; Fig. 2.2B; Appendix Table A.1-6). We confirmed that T2 lin enhancers in the *erm* and *ham* loci indeed activate GFP reporter expression in immature INPs consistent with their endogenous protein expression patterns (Fig. 2.1E,G).(Eroglu et al., 2014; Quinto-Rives et al., 2020; Weng et al., 2010) T2 lin enhancers are prevalent in loci containing genes highly expressed in immature INPs suggesting that chromatin accessibility at cell-type-specific enhancers of genes essential for INP formation does not correlate with NB capability to generate INPs (Fig. 2.1A).

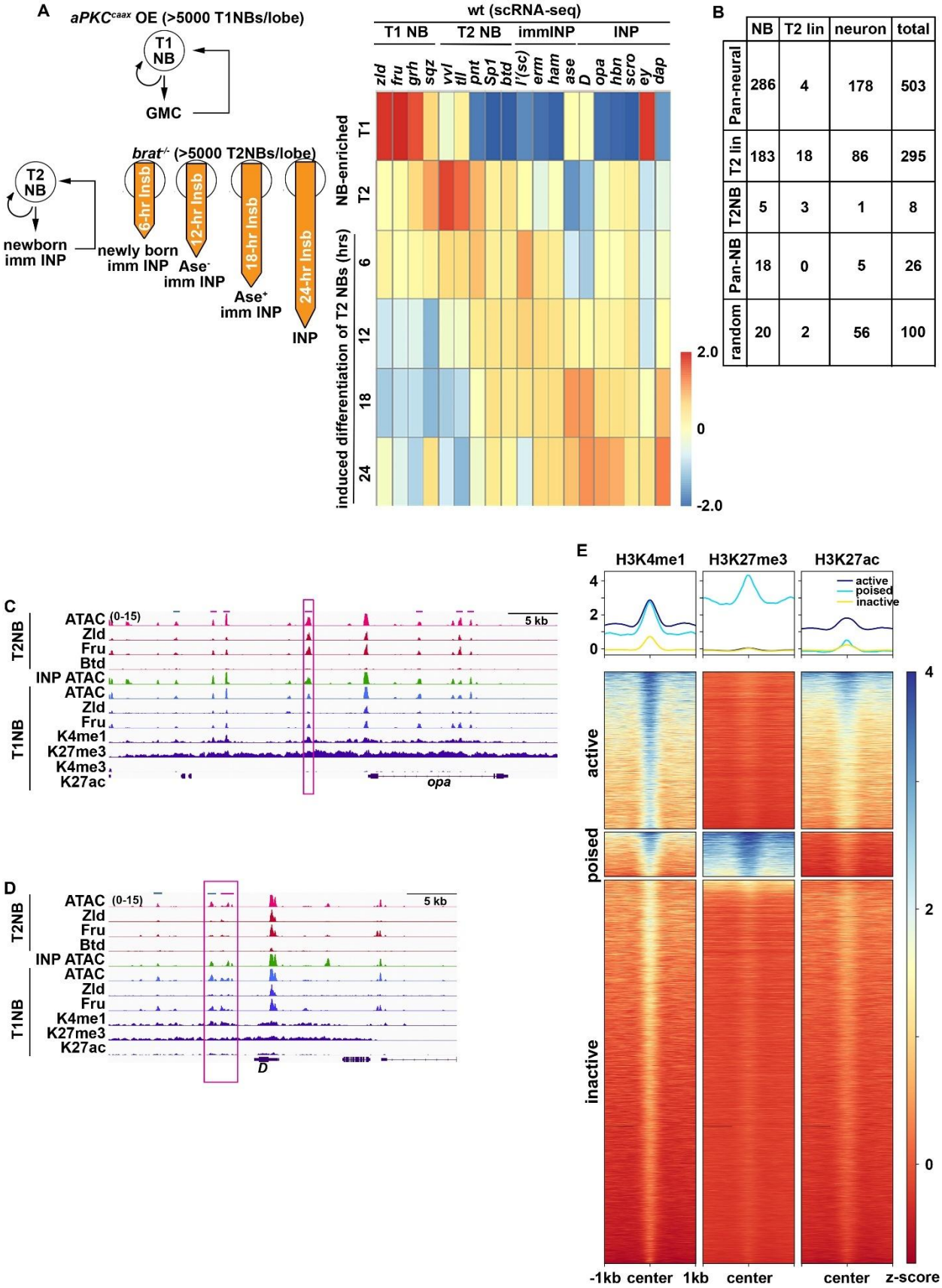

A
aPKCcaax OE (>5000 T1NBs/lobe)
T1 NB
GMC
brat-/- (>5000 T2NBs/lobe)
T2 NB
newborn imm INP
newly born imm INP
Ase- imm INP
Ase+ imm INP
INP
6-hr Insb
12-hr Insb
18-hr Insb
24-hr Insb
wt (scRNA-seq)
T1 NB
T2 NB
immINP
INP
zld fru grh sqz vvl til pnt Sp1 btd l'(sc) erm ham ase D opa hbn scro ey dap
NB-enriched
T1
T2
induced differentiation of T2 NBs (hrs)
6
12
18
24
2.0
0
-2.0
B
NB
T2 lin
neuron
total
Pan-neural
286
4
178
503
T2 lin
183
18
86
295
T2NB
5
3
1
8
Pan-NB
18
0
5
26
random
20
2
56
100
C
T2NB
T1NB
ATAC (0-15)
Zld
Fru
Btd
INP ATAC
ATAC
Zld
Fru
K4me1
K27me3
K4me3
K27ac
5 kb
opa
D
T2NB
T1NB
ATAC (0-15)
Zld
Fru
Btd
INP ATAC
ATAC
Zld
Fru
K4me1
K27me3
K27ac
5 kb
D
E
H3K4me1
H3K27me3
H3K27ac
active
poised
inactive
4
2
0
active
poised
inactive
4
2
0
-1kb center 1kb
center
center
z-score

Figure 2.2 Identification of active neurogenic enhancers in fly larval brain NBs

(A) Schematic for enrichment of NBs and INPs used for isolating Bulk-NB or INP lysate. The distribution of representative gene transcripts in cell types of T1 and T2 lineages derived from single cell RNA-seq of wild-type larval brains shows transcripts abundance consistent with the enriched NB or INP system.(B) Table summarizing the activity pattern of enhancers determined by the flowchart in Fig. 1C. We assessed enhancer activity patterns using lab-generated reporters or against an existing database to validate our approach.(Jenett et al., 2012) Random refers to randomly selected non-promoter enhancers whose activity pattern was available from the Janelia Flylight website.(C-D) Genome browser tracks showing patterns of chromatin accessibility, TF occupancy and histone marks in indicated cell types in opa and D loci where the magenta bars correspond to pan-neural enhancers, and teal bars correspond to T2-lin enhancers. Magenta box designates enhancer with INP-specific activity.(E) Heatmap of k-means clustering of H3K4me1, H3K27ac, and H3K27me3 in regions of accessible enhancers in T2 NBs (n=21212, Fig. 1C). Active, poised, and inactive labels are determined based on pattern of histone marks within cluster.

To correlate post-translational modifications of histones at cell-type-specific enhancers of genes essential for INP formation with the lack of INP progeny generated by T1NBs, T1NB-enriched chromatin was used to examine the patterns of active and repressive histone marks. Three histone modification profiles were established based on the combined pattern of active histone marks (H3K4me1, H3K4me3 and H3K27ac) and repressive histone mark (H3K27me3) $\pm$ 1kb from the center of the 21212 non-promoter regions with open chromatin in T2NBs. An active state (high H3K4me1/H3K27ac and low H3K27me3), a poised state (high H3K4me1/H3K27me3 and low H3K27ac) and an inactive state (low H3K4me1/H3K27ac/H3K27me3) (Fig. 2.2E). 10.1% of T2 lin enhancers and 14.5% of pan-neural enhancers display histone mark combination that is correlated with a poised state (Fig. 2.1H). The percentage of poised T2 lin enhancers and pan-neural enhancers that are associated with Ase^{-} and Ase^{+} immature INP genes (e.g. *Sp-1*, *erm*, *ham*, *Tfap2*, *D* and *Hmx*) was over-represented relative to randomized control in these two groups (Fig. 2.1H). Furthermore, the poised T2 lin and pan-neural enhancer category encompasses cell-

type-specific enhancers that recapitulate the activation of endogenous *erm*, *ham*, *D* and *Hmx* expression (Fig. 2.1D-G). Thus, we conclude that post-translational modification of histones at enhancers of genes essential for INP formation correlates with the capability of NBs to generate INPs (Fig. 2.1A).

Ase limits the capability to generate INPs in T1NBs

Accumulation of repressive histone mark H3K27me3 at cell-type-specific enhancers of genes essential for INP formation could contribute to their inactivity in T1NBs and limit INP generation. Yet, loss of Polycomb Repressive Complex 2 (PRC2) activity, the only enzymatic complex known to catalyze H3K27me3 deposition (Laugesen et al., 2019; Piunti & Shilatifard, 2021), had no apparent effect on GMC generation.(Bello et al., 2007) Thus, it is unlikely that high levels of H3K27me3 alone maintain inactivity of these cell-type-specific enhancers. Poised enhancers can be activated by developmental TFs during lineage commitment in vertebrates.(Lara-Astiaso et al., 2014; Rada-Iglesias et al., 2011) Btd is necessary for T2NBs to generate INPs.(Komori, Xiao, Janssens, et al., 2014) *btd* transcripts are highly enriched in T2NBs and immature INPs, and Btd protein binds T2 lineage enhancers of erm in T2NBs (Fig. 2.1D,F; Appendix Table A.1). As such, lack of expression of T2 lineage-specific TFs including Btd could contribute to the inactivity of cell-type-specific enhancers that drive gene expression essential for INP formation in T1NBs.

High Btd expression can induce T1NBs to generate INPs, but with limited frequency.(Komori, Xiao, Janssens, et al., 2014) Thus, barriers limiting Btd-induced INP generation likely exist in T1NBs. We hypothesized that genes encoding these barrier proteins should be expressed exclusively in T1NBs or in T1NBs and INPs since these

two cell types display similar transcriptomes and directly generate GMCs.(Marques et al., 2023; Michki et al., 2021; A. Rajan et al., 2023) Comparison of the transcriptome of wild-type T1NBs, T2NBs and INPs identified 37 genes that encode TFs and show transcripts enriched in T1NBs (Fig. 2.3A)(Marques et al., 2023; Michki et al., 2021; A. Rajan et al., 2023). We examined protein expression patterns for 35 of these genes and none were found to be uniquely expressed in all T1NBs at the protein level (Appendix Table B.1). We next assessed 86 of 95 genes that encode TFs which show enrichment of transcripts in T1NBs and INPs but found ase and pros were the only genes whose proteins are detected in T1NBs but not in T2NBs (Appendix Table B.1). Pros was excluded from further analyses because Pros functions in GMCs to promote cell cycle exit and differentiation.(Bello et al., 2008; Boone & Doe, 2008; Bowman et al., 2008; Farnsworth et al., 2015) We conclude that Ase is a candidate regulator that limits INP generation in T1NBs.

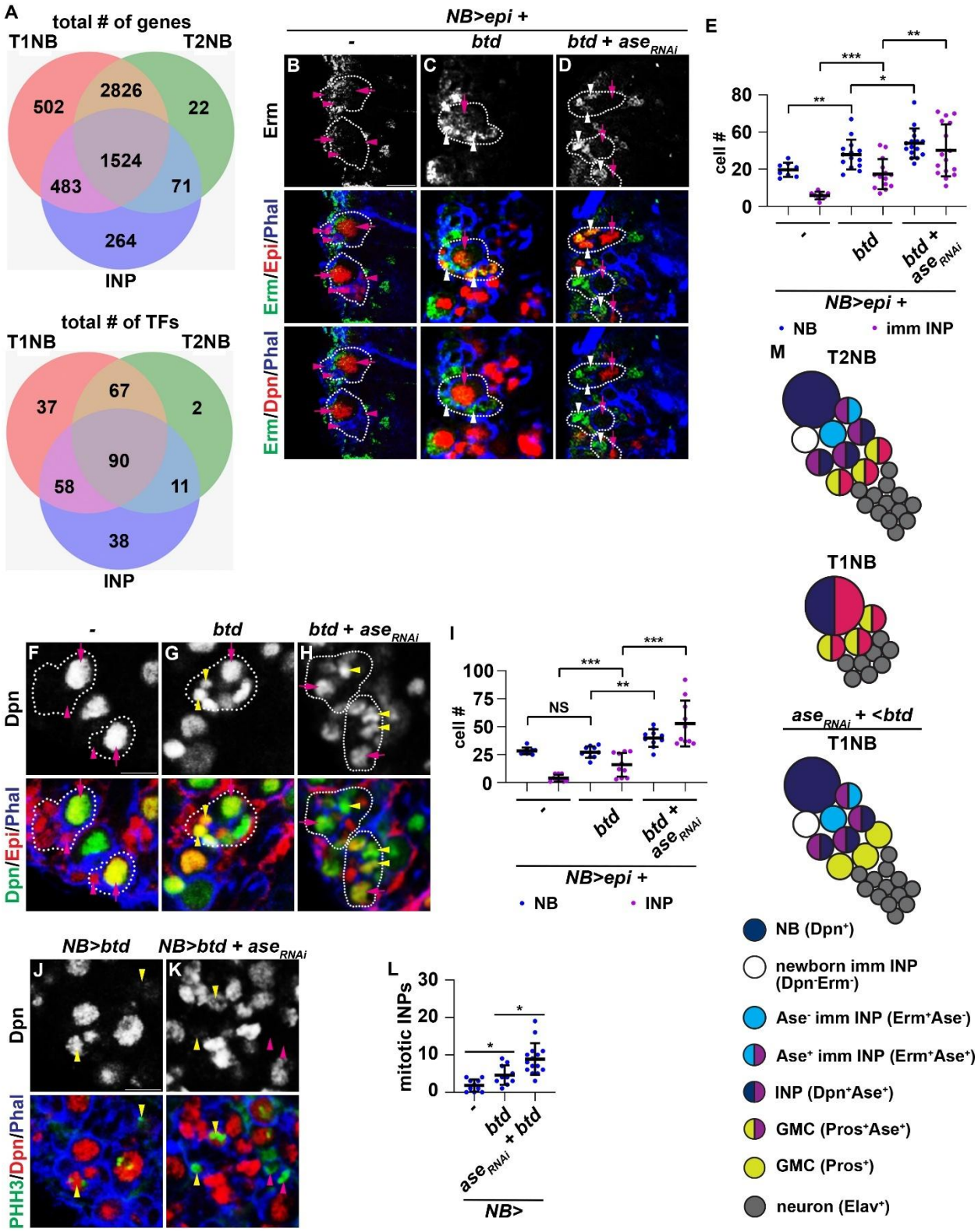


Figure. 2.3 Ase limits the capability of T1NBs to generate INPs induced by Btd

(A) Single-cell transcriptomic comparisons of enriched transcripts (all transcripts – top; TFs only -bottom) across T1NBs, T2NBs and INPs from published single-cell mRNA sequencing datasets of wild-type NB lineages.(Marques et al., 2023; Michki et al., 2021; A. Rajan et al., 2023) (B-D) Images showing that ase knockdown with pan-NB driver (*wor-Gal4*) increases the efficiency of Btd mis-expressing T1NBs, located on the ventral surface of the larval brain, to generate immature INPs (small epitope+Erm+Dpn- cells).(E) Quantification of number of ventral NBs and ventral immature INPs showing knockdown of ase increased number of immature INPs compared to NBs upon Btd mis-expression.(F-H) Images showing that ase knockdown with pan-NB driver increases the efficiency of Btd mis-expressing T1NBs to generate INPs (small epitope+Dpn+ cells).(I) Quantification of number of ventral NBs and ventral INPs showing knockdown of ase increased number of INPs compared to NBs upon Btd mis-expression.(J-K) Images showing that ase knockdown with pan-NB driver increases the efficiency of Btd mis-expressing T1NBs to generate mitotic INPs (small $PHH3^{+}Dpn^{+}$ cells).(L) Quantification of number of mitotic INPs found on the ventral side of the brain showing knockdown of ase increased number of mitotic INPs compared to Btd mis-expression.(M) Diagram summarizing the expression patterns of cell identity markers in T1NBs, T2NBs, and Btd mis-expressing T1NBs combined with ase knockown and their progeny. T1NBs lacking Ase and mis-expressing Btd generate Erm+ immature INPs that mature into proliferative INPs. White dotted line marks NB lineage. Magenta arrow: T1NB. Magenta arrowhead: GMC. White arrowhead: Erm^{+} immature INP. Yellow arrowhead: INP. Scale bar: 10 μm. P-value; NS: Not significant, , *<.05. , **<.005. , ***<.0005. ****<.00005.

If Ase functions as a barrier to INP generation, reducing ase function should allow Btd to more efficiently induce T1NBs to generate INPs. We used a NB-Gal4 driver (*wor-Gal4*) to induce *UAS-btd::myc* expression in all NBs and assessed the identity of their newly generated progeny marked by the perdurance of the Myc epitope expression. We focused on the ventral surface of larval brains which contains exclusively T1NBs under wild-type conditions.(Bello et al., 2008; Boone & Doe, 2008; Bowman et al., 2008) Control brains that expressed a Myc epitope reporter transgene contain NBs that produce GMCs that do not express the immature INP marker Erm (Fig. 2.3B,E). In contrast, high levels of Btd expression in T1NBs led to generation of small Dpn-Erm+ cells (induced immature INPs) which are found in direct contact with the NB (Fig. 2.3C, E). Importantly, after reducing ase function in tandem with high levels of Btd, the number of induced immature INPs produced significantly increased (Fig. 2.3D, E).

To confirm differentiation of these induced immature INPs into INPs we used the following 2 criteria: reactivation of Dpn expression to validate INP identity, and positive phospho-histone H3 (PHH3) to confirm mitotic potential. None of the small Myc+ cells in control brains express Dpn (Fig. 2.3F, I). Btd mis-expressing brains contain 16±11 small Myc+ cells that express Dpn, while knocking down ase function increased the total number of small $Myc^{+}Dpn^{+}$ cells to 53±21 per brain lobe (Fig. 2.3G-I). We detected 5±3 small $Myc^{+}Dpn_{+}$ cells that are mitotically active marked by PHH3 in brains that expressed elevated levels of Btd (Fig. 2J,L). Reducing ase function significantly increased the total number of small $Myc^{+}Dpn^{+}PHH3^{+}$ cells per lobe (Fig. 2.3K,L). These results support a role for Ase in limiting the ability of T1NBs to generate INPs (Fig. 2.3M). Thus, we conclude that Ase functions as a barrier to INP generation in T1NBs.

Elevated Ase expression promotes T2NBs to generate GMCs via bypassing INPs

We tested whether Ase is sufficient to limit the ability of T2NBs to generate INPs by elevating Ase expression. Instead of relying on the lack of Ase expression for identifying T2NBs in this experiment, we overexpressed a *UAS-GFP* transgene driven of a T2NB-specific Gal4 driver (*Tll-Gal4)* to positively mark T2NB lineages.(Hakes & Brand, 2020; Quinto-Rives et al., 2020) 83% of T2NBs in wild-type brains produce Erm+ immature INPs which are found in direct contact with the NB (Fig. 2.4A,C). In contrast, elevating Ase expression drastically reduced the percentage of T2NBs that produce immature INPs with most NBs producing Erm- cells. This result suggests that Ase inhibits T2NBs from generating immature INPs (Fig. 2.4B,C). Consistent with a reduced number of immature INPs, high levels of Ase expression led to significantly fewer INPs

marked by Dpn expression per lobe (20±8 per lobe) than wild-type brains (129±15 per lobe) (Fig. 2.5A,B,D). Similar to Ase, mis-expression the human homolog Ascl1 led to significantly fewer INPs per brain lobe (24±7 per lobe) and T2NBs in these brains are directly surrounded by small Dpn-Ase+ cells that are likely GMCs (Fig. 2.5C,D). We could unambiguously quantify INPs in this experiment because the antibody we used against fly Ase does not cross-react with human Ascl1. We further confirmed the identity of these small Dpn-Ase+ cells using nuclear localization of Pros, an indicator of GMC identity. We found that 98% of T2NBs upon Ase mis-expression were found with GMCs in direct contact with the NB whereas wild-type T2NBs had GMCs distal to NB (Fig. 2.4D-F). Altogether, these results suggest that T2NBs expressing elevated levels of Ase generate GMCs instead of INPs.

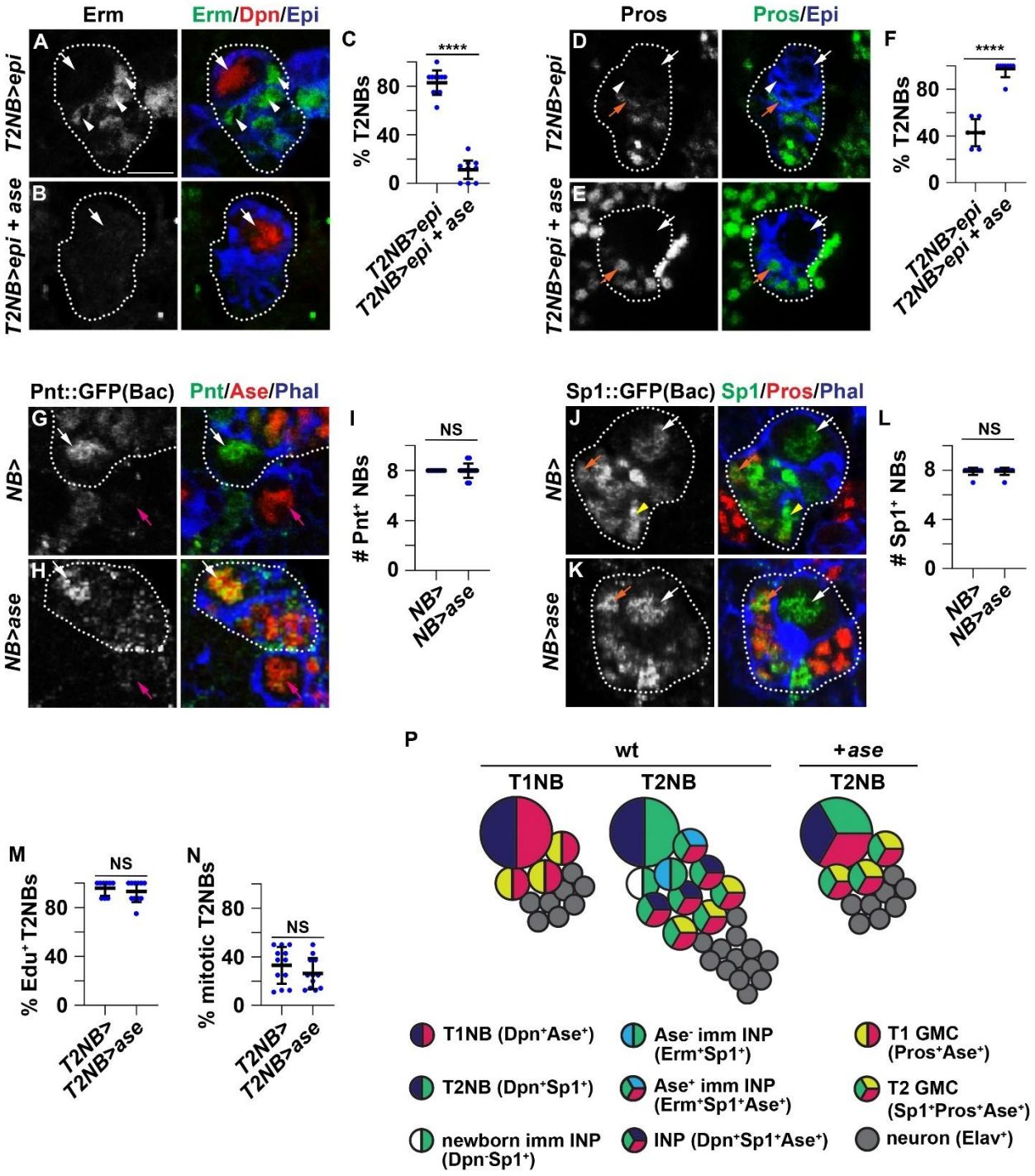


Figure 2.4 Elevated Ase expression promotes T2NBs to generate GMCs via bypassing INPs

(A-B) Images showing that mis-expressing Ase with a T2NB driver (*Tll-Gal4*) results in T2NBs no longer generating immature INPs. A wild-type T2NB marked by GFP expression is always in contact with immature INP progeny that express Erm. An Ase mis-expressing T2NB is in contact with progeny lacking Erm expression.(C) The

percentage of Ase mis-expressing T2NBs surrounded by Erm-positive progeny is significantly lower than control T2NBs.(D-E) Images showing that mis-expressing Ase with a T2NB driver results in T2NBs generating GMCs directly. GMCs identified by Pros expression are usually located at least one-cell away from a control T2NB but are found in contact with the Ase mis-expressing T2NBs.(F) The percentage of Ase mis-expressing T2NBs in direct contact with GMCs is significantly higher than control T2NBs.(G-H) Images showing T2NBs mis-expressing Ase using a pan-NB driver (*Wor-Gal4*) still maintain T2NB-specific marker Pnt expression.(I) The number of NBs demonstrating high Pnt expression is not significantly different between control versus Ase mis-expression.(J-K) Images showing T2NBs mis-expressing Ase using a pan-NB driver still maintain T2NB-specific marker Sp1 expression.(L) The number of NBs demonstrating Sp1 expression is not significantly different between control versus Ase mis-expression.(M-N) The percentage of control versus Ase mis-expressing T2NBs displaying positive EdU incorporation or PHH3 is statistically indistinguishable.(P) Diagram demonstrating how T2NBs mis-expressing Ase bypass INPs to generate GMCs while maintaining their lineage identity. White dotted line marks NB lineage. White arrow: T2NB. White arrowhead: Erm^{+} immature INP. Yellow arrowhead: INP. Magenta arrow: T1NB. Orange arrow: GMC. Scale bar: 10 μm. P-value; NS: Not significant, ****<.00005.

To test if Ase induced T2NBs to generate GMCs by converting their identity to a T1NB state, we used four methods to assess T2NB identity in control brains carrying a NB-specific Gal4 driver alone and in brains that expressed elevated levels of Ase (Fig. 2.5E). The pnt::GFP(Bac) transgene recapitulates endogenous PntP1 expression in larval brains including T2NB-specific expression.(Hakes & Brand, 2020) The number of Pnt::GFP+ NBs appears statistically indistinguishable between control and elevated Ase samples (Fig. 2.4G-I). Due to lack of reliable antibodies or reporter transgenes, we performed single-molecule fluorescent in situ hybridization (sm-FISH) to assess btd transcript patterns. T2NBs were marked by RFP driven by a T2NB-specific Gal4 and *btd* transcript levels were normalized against transcripts of the ribosomal gene mRpl15. The relative levels of btd transcripts in T2NBs are not significantly different between control and elevated Ase samples (Fig. 2.5F-H). The tll::GFP(Bac) transgene mimics endogenous Tll expression in larval brains including higher levels in T2NBs compared to T1NBs.(Hakes & Brand, 2020; Quinto-Rives et al., 2020) The number of NBs

expressing high levels of Tll per lobe appears statistically indistinguishable between control and elevated Ase samples (Fig. 2.5I-K). The Sp1::GFP(Bac) transgene is expressed throughout the entire T2 lineage.(Michki et al., 2021; Quinto-Rives et al., 2020) The number of Sp1::GFP+ NBs per lobe appears statistically indistinguishable between control and elevated Ase samples (Fig. 2.4J-L). GMCs in direct contact with T2NBs that expressed high levels of Ase maintained Sp1::GFP expression, indistinguishable from GMCs generated by T2NBs in control brains (Fig. 2.4J,K). Together, these results support a model that high levels of Ase induce T2NBs to generate GMCs without altering their lineage identity.

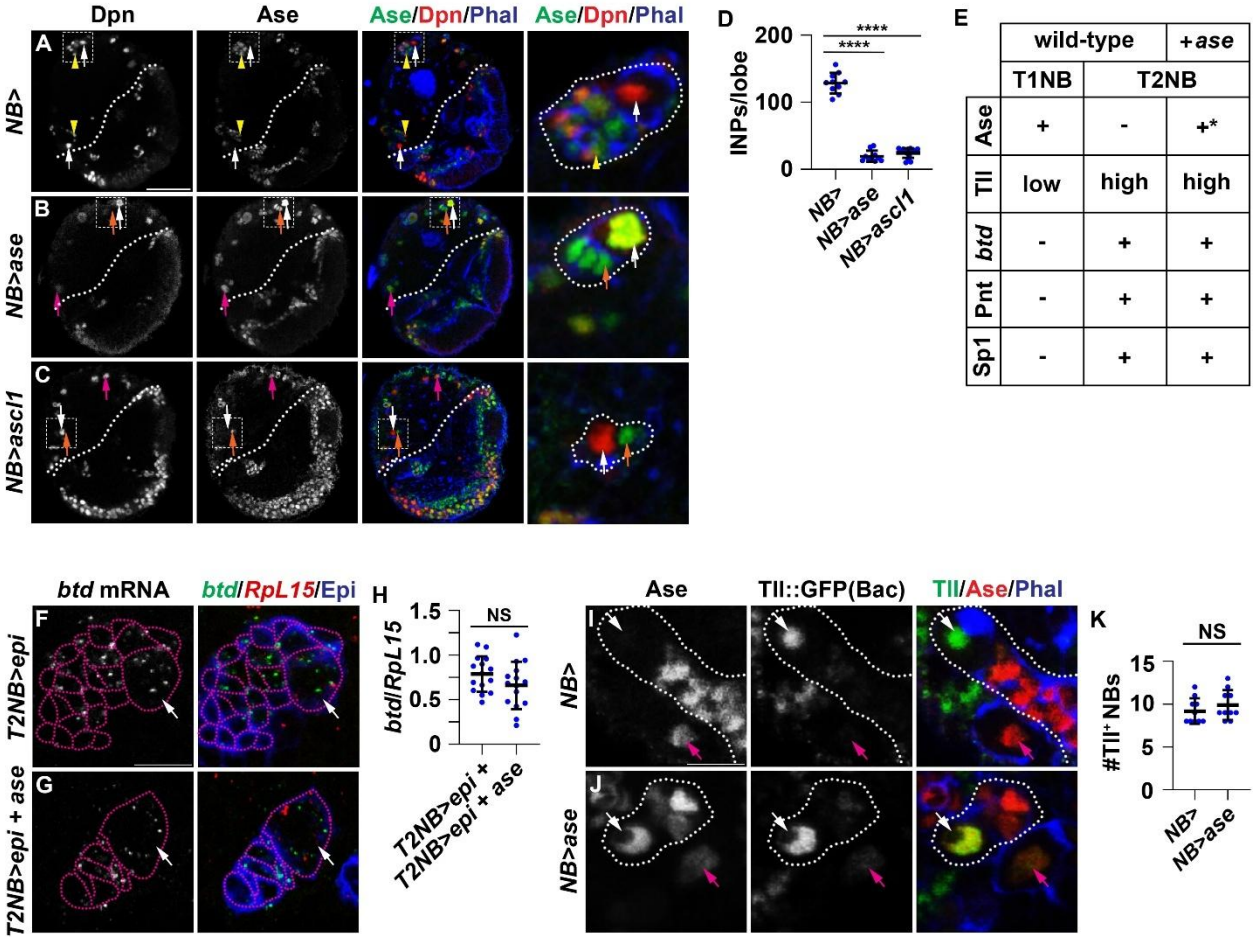


Figure 2.5 Elevated Ase expression promotes T2NBs to generate GMCs and bypass INPs

(A-C) Images showing that mis-expressing Ase and Ascl1 with a pan-NB driver (*Wor-Gal4*) results in loss of INPs (small $Ase^{+}Dpn^{+}$ cells). Scale bar: 50 μm (D) Quantification showing significant decrease in the number of INPs upon mis-expression of Ase or Ascl1 in T2NBs.(E) Table describing the marker profile of wild-type T1 and T2NBs compared to marker profile after Ase mis-expression in T2NBs.(F-G) Images showing that mis-expressing Ase with a T2NB driver (*Tll-Gal4*) does not alter *btd* transcript abundance.(H) Quantification showing no significant change in the ratio of *btd* vs *Rpl15* transcripts in T2NBs with and without Ase mis-expression.(I-J) Images showing T2NBs mis-expressing Ase using a pan-NB driver (*Wor-Gal4*) still maintain T2NB-specific marker Tll expression.(K) The number of NBs demonstrating high Tll expression is not significantly different between control versus Ase mis-expression. White dotted line circles NB lineage. White dotted line demarcates optic lobe boundary. Magenta dotted line marks the T2NB lineage. White arrow: T2NB. Yellow arrowhead: INP. Magenta arrow: T1NB. Orange arrow: GMC. Scale bar: 10 μm. P-value; NS: Not significant, ****<.00005.

To exclude the possibility that changes in cell proliferation led T2NBs to generate GMCs instead of INPs, we examined Edu incorporation and the mitotic marker PHH3 in T2NBs that expressed high levels of Ase compared to wild-type samples. We observed no changes in Edu incorporation upon Ase mis-expression, with all T2NBs taking up Edu after a three-hour feeding similar to control samples (Fig. 2.4M). Furthermore, the percentage of PHH3+ T2NBs in brains that expressed elevated levels of Ase in T2NBs is indistinguishable from control (Fig. 2.4N). Thus, it is unlikely that high levels of Ase induces T2NBs to generate GMCs instead of INPs by altering cell proliferation. We conclude that high levels of Ase promote T2NBs to generate GMCs via bypassing INPs (Fig. 2.4P).

Ase functions through Prospero to promote generation of GMCs by T2NBs

A key first step to identify the downstream-effectors that mediate Ase-induced reprogramming of T2NBs to generate GMCs is to define whether Ase limits INP generation by activating or repressing gene transcription. We took advantage of a

previously published *UAS-ase::VP16* transgene (Bahrampour et al., 2017) that encodes a constitutive transcriptional activator form of Ase and mis-expressed Ase::VP16 in T2NBs. The Ase antibody does not recognize Ase::VP16, nor does Ase::VP16 appear to promote expression of endogenous Ase, allowing us to unambiguously identify T2NBs and INPs ($Dpn^{+}Ase^{+}$). Ase::VP16 mis-expression in T2NBs phenocopies the effect of full-length Ase and Ascl1 mis-expression showing a significant reduction in the number of INPs per lobe without affecting the expression of T2NB-specific markers including Sp1 (Fig. 2.6A-F). Importantly, T2NBs mis-expressing Ase::VP16 are also surrounded by GMCs ($Dpn^{-}Ase^{+}$) instead of INPs (Fig. 2.6B). These results indicate that Ase induces T2NBs to generate GMCs by activating gene expression.

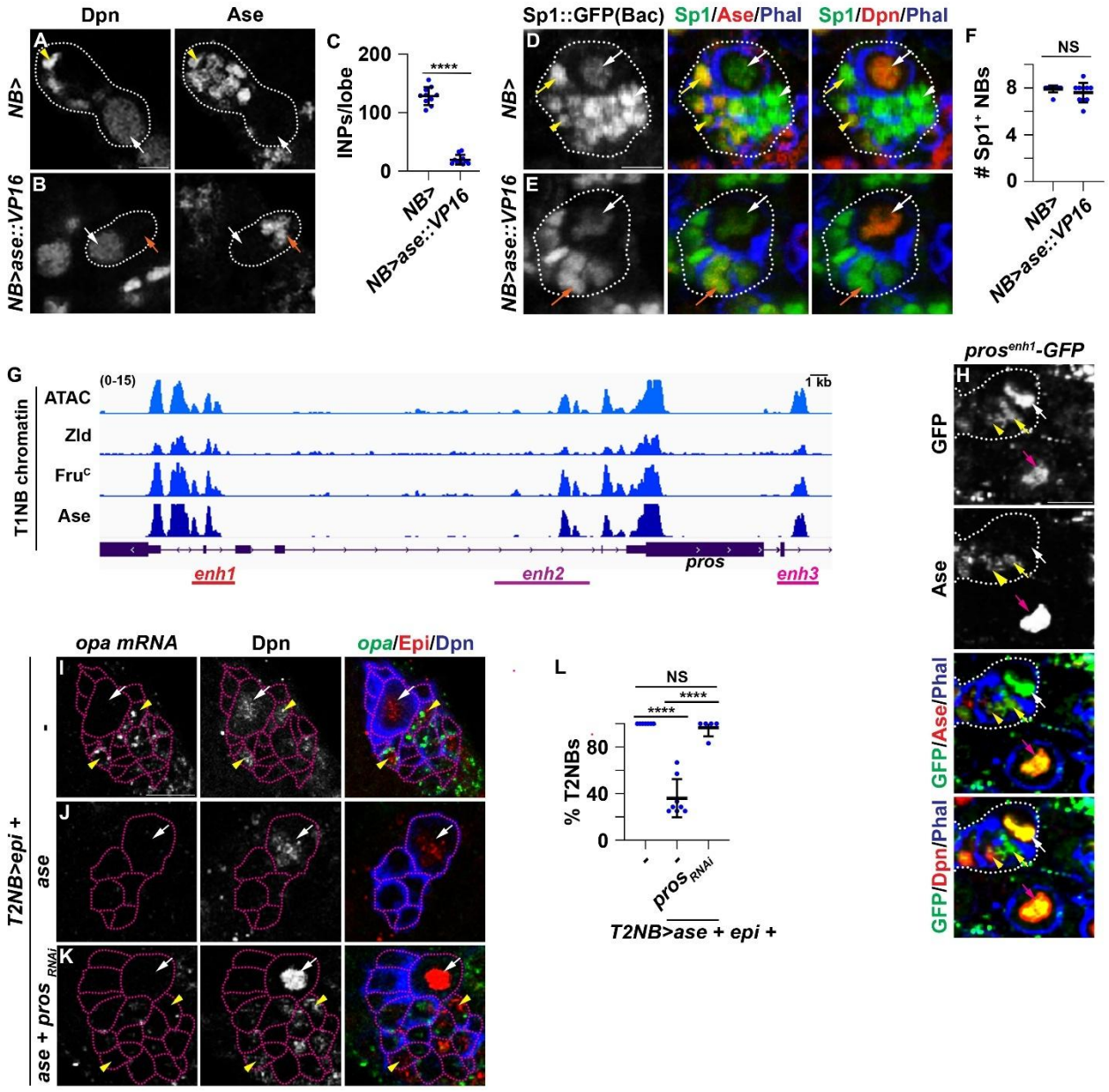


Figure 2.6 Pros mediates Ase-induced bypass of INP generation in the T2NB lineage

(A,B) Images showing T2NBs mis-expressing a transcriptional activator form of Ase (Ase::Vp16) with pan-NB driver (*Wor-Gal4*) are surrounded by GMCs (small $Dpn^{-}Ase^{+}$ cells) while control T2NBs are surrounded by immature INPs (small $Dpn^{-}Ase^{+}$ cells) and INPs (small $Dpn^{+}Ase^{+}$ cells).(C) Quantification showing that larval brains that mis-express Ase::VP16 in NBs contains drastically fewer INPs per lobe than control brains.(D,E) T2NBs mis-expressing Ase::VP16 with pan-NB driver still maintain T2NB lineage-specific maker Sp1 expression.(F) Upon Ase mis-expression the number T2NBs that display nuclear Sp1::GFP expression is statistically indistinguishable from control T2NBs.(G) Genome browser track of the *pros* locus with patterns of chromatin

accessibility and TF occupancy showing three Pan-neural enhancers that are bound by Ase.(H) The expression of a GFP reporter controlled by enhancer 1 from the *pros* locus (*pros*^{enh1}-GFP) is expressed in T1NBs, T2NBs and INPs.(I-K) Knocking down *pros* function in Ase mis-expressing T2NBs restores their ability to generate INPs. INPs are identified by the expression of *opa* mRNAs and Dpn protein.(L) The percentage of Ase mis-expressing T2NBs generating INPs is restored to a level indistinguishable from wild-type T2NBs following *pros* knockdown. Ase mis-expressing T2NBs are surrounded by drastically fewer INPs than wild-type T2NBs but knocking down *pros* function in Ase mis-expressing T2NBs rescues this defect. White dotted line circles NB lineage. Magenta dotted line marks the T2NB lineage. White arrow: T2NB. Yellow arrow: Ase^{+} immature INP. Yellow arrowhead: INP. Magenta arrow: T1NB. Orange arrow: GMC. Scale bar: 10 μm. P-value; NS: Not significant, ****<.00005.

To identify the downstream-effectors of Ase in inducing GMC generation, we used a previously established genetic strategy to enrich for T1NBs (Fig. 2.2A).(Carney et al., 2012; Komori, Xiao, Janssens, et al., 2014) We confirmed that the transcriptome of enriched T1NBs is highly similar to wild-type T1NBs determined by sc-RNA sequencing (Fig. 2.2A).(Marques et al., 2023) T1NB-enriched chromatin was used to identify 2993 active neurogenic enhancers defined as non-promoter cis-regulatory regions that display accessible chromatin and are bound by Zld and FruC (Fig. 2.7A). 2589 of these enhancers are bound by Ase in T1NBs. Because Ase is highly expressed in T1NBs and INPs, gene transcripts that are nearest to Ase-bound neurogenic enhancers and are enriched in T1NBs alone or in T1NBs and INPs are considered as candidate Ase downstream-effectors (Appendix Table B.1). 18 of these 113 genes encode TFs, with *ase* and *pros* being the only two genes whose protein products are specifically expressed in T1NBs and INPs (Appendix Table B.2). We focused on *pros* and confirmed that high levels of Ase were sufficient to induce *pros* transcript enrichment in T2NBs (Fig. 2.7B-D). Thus, *pros* is an excellent candidate downstream-effector of Ase.

We assessed enhancer activity under the control of each of three putative Ase-bound enhancers in the *pros* locus (Fig. 2.6G). GFP expression driven by enhancer 1 or 2 was detected in T2NBs in addition to T1NBs and INPs or detected only in a small subset of T1NBs suggesting that these two regulatory elements are not activated by Ase (Fig. 2.6G,H). In contrast, the expression of pros-GFP reporter driven by enhancer 3 was detected in T1NBs and INPs but not T2NBs, a pattern consistent with endogenous Ase expression patterns (Fig 2.6G, Fig. 2.7E,). Elevated levels of Ase were also sufficient to activate *pros-GFP* expression in T2NBs (Fig. 2.7F,G). Enhancer 3 contains 4 putative Ase-binding sequences.(Southall & Brand, 2009) The expression pattern and intensity of the *prosΔAse*-GFP reporter, which carries deletion of all 4 Ase-binding sites, appeared indistinguishable from pros-GFP in control brains (Fig. 2.7H,I). Most importantly, elevated levels of Ase cannot activate *prosΔAse-GFP* expression in T2NBs (Fig. 2.7J,K). Thus, we conclude Ase functions through enhancer 3 to regulate Pros expression.

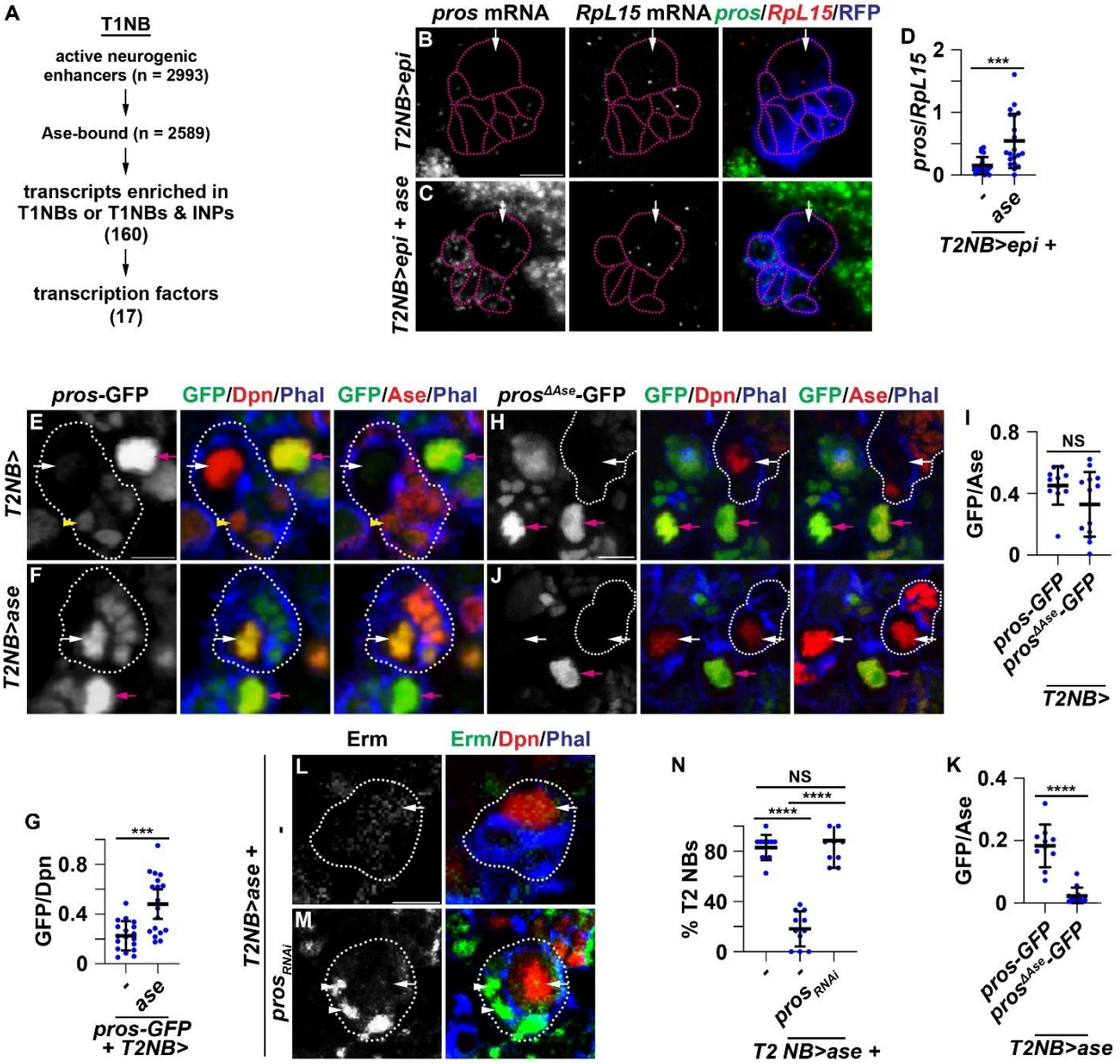


Figure 2.7 Ase functions through Pros to promote generation of GMCs by T2NBs

(A) A flow chart for identifying candidate Ase downstream-effector genes that encode transcription factors.(B,C) Images showing Ase mis-expression is sufficient to induce *pros* transcription in T2NBs. *pros* transcripts are undetectable in control T2NBs but robustly detected in Ase mis-expressing T2NBs. *RpL15* transcripts serve as an internal control.(D) Levels of *pros* transcripts relative to *RpL15* transcripts in Ase mis-expressing T2NBs are significantly higher than control T2NBs.(E,F) The expression of a GFP reporter controlled by enhancer 3 from the *pros* locus bound by Ase can be activated in T2NBs by Ase mis-expression. *pros*^{enh3}-GFP (abbreviated as *pros*-GFP) is expressed in T1NBs and INPs but not in T2NBs in wild-type brains mimicking endogenous Ase expression. *pros*-GFP expression is detected in T2NBs mis-expressing Ase.(G) Levels of *pros*-GFP expression relative to Dpn expression are significantly higher in T2NBs

mis-expressing Ase than control T2NBs.(H) Removing all Ase-binding sites in the enhancer 3 from the *pros* locus has no effect on its cell-type-specific expression pattern. The *pros*$^{enh3\Delta Ase}$-GFP (abbreviated as *pros*$^{\Delta Ase}$-GFP) reporter transgene lacks all Ase-binding sites and is expressed in T1NBs and INPs but not in T2NBs.(I) Levels of *pros*$^{\Delta Ase}$-GFP expression relative to background Ase staining are statistically indistinguishable from *pros*-GFP expression.(J) The *pros*$^{\Delta Ase}$-GFP reporter transgene is not activated in T2NBs upon Ase mis-expression.(K) Levels of *pros*$^{\Delta Ase}$-GFP relative to Ase staining are significantly lower than *pros*-GFP expression.(L-M) Images showing that knocking down *pros* function in Ase mis-expressing T2NBs restores their ability to generate immature INPs. An Ase mis-expressing T2NB is surrounded by progeny lacking Erm expression but become surrounded by immature INPs marked by Erm expression when *pros* function is knocked down.(N) The percentage of Ase mis-expressing T2NBs surrounded by Erm$^+$ immature INPs is restored to a level indistinguishable from wild-type T2NBs following *pros* knockdown. White dotted line marks NB lineage. White arrow: T2NB. White arrowhead: Erm$^+$ immature INP. Yellow arrowhead: INP. Magenta arrow: T1NB. Scale bar: 10 μm. P-value; NS: Not significant, ****<.00005, ***<.0005.

If Pros mediates Ase-induced reprogramming of T2NBs to generate GMCs, knocking down pros function upon Ase misexpression should restore INP generation. Indeed, reducing Pros function in T2NBs that mis-express Ase restored the generation of immature INPs marked by Erm expression (Fig. 2.7L-N). These immature INPs were able to differentiate into INPs marked by *odd paired* (opa) transcripts and Dpn protein (Fig 2.6I-L). Thus, we conclude that Ase functions through *pros* to reprogram T2NBs to generate GMCs.

Prospero reprograms immature INPs to bypass an INP state and adopt a GMC fate

Although *pros* is required for Ase-induced reprogramming of T2NBs to generate GMCs (Fig. 2.6I-K, Fig. 2.7L,M,), nuclear Pros protein first becomes detectable in immature INPs in direct contact with these NBs rather than in the NB (Fig. 2.4E, Fig 2.6C). This result suggests that high levels of Ase expression in T2NBs leads to activation of the GMC genetic program in immature INPs. This hypothesis predicts that GMCs are more closely related to immature INPs than NBs or INPs. We used published

single-cell mRNA sequencing datasets of wild-type larval brains to find the transcriptomic similarity between NBs, immature INPs, INPs, GMCs and neurons, using the Euclidean distance between average gene expression of each cell-type (Fig. 2.8A).(Marques et al., 2023; Michki et al., 2021; A. Rajan et al., 2023) GMCs in both NB lineages are the most closely related cell type to each other, while Ase^{-} and Ase^{+} immature INPs are most closely related to one another (Fig. 2.8A). Consistent with our hypothesis, the next most closely related cell type to GMCs is Ase^{-} immature INPs followed by Ase^{+} immature INPs (Fig. 2.8A). We tested whether elevated Pros levels can activate the GMC genetic program in immature INPs by expressing a *UAS-pros* transgene under the control of an immature INP Gal4 driver (*erm*-GAL4) (Fig. 2.8B). Brains expressing elevated levels of Pros contained significantly fewer INPs per lobe than control brains (Fig. 2.8C-E). While T2NBs in control brains were surrounded primarily by INPs ($Dpn^{+}Ase^{+}$), cells in direct contact with T2NBs in brains that expressed elevated levels of Pros appeared to be GMCs ($Dpn^{-}Ase^{+}$) (Fig. 2.8C,D). These data suggest that Pros expression can activate the GMC genetic program in immature INPs.

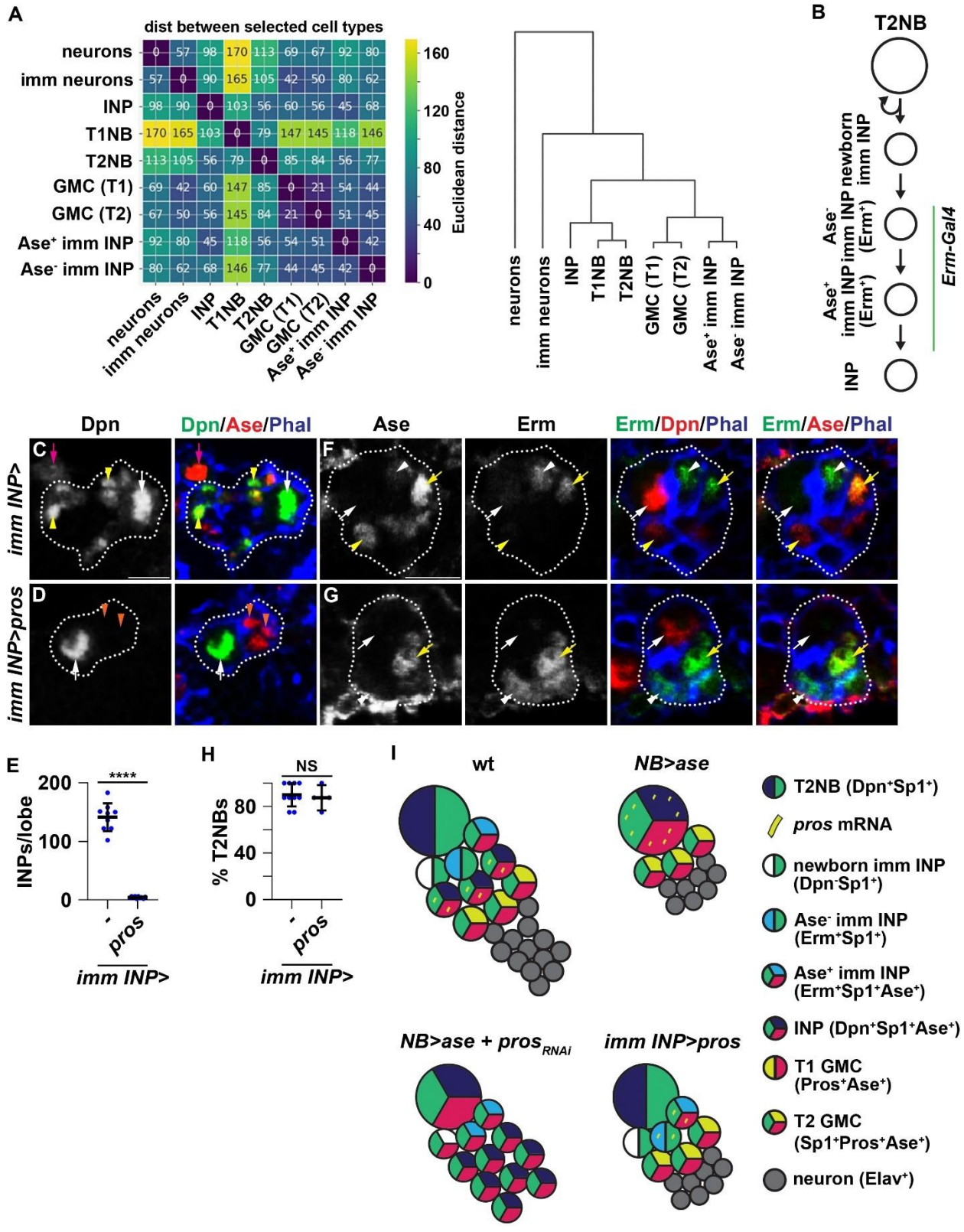

A
dist between selected cell types
neurons
imm neurons
INP
T1NB
T2NB
GMC (T1)
GMC (T2)
Ase+ imm INP
Ase- imm INP
Euclidean distance
B
T2NB
Ase- imm INP newborn imm INP (Erm+)
Ase+ imm INP (Erm+)
INP
Erm-Gal4
Dpn
Dpn/Ase/Phal
Ase
Erm
Erm/Dpn/Phal
Erm/Ase/Phal
imm INP>
imm INP>pros
C
D
F
G
E
INPs/lobe
****
pros
imm INP>
H
% T2NBs
NS
I
wt
NB>ase
NB>ase + pros RNAi
imm INP>pros
T2NB (Dpn+Sp1+)
pros mRNA
newborn imm INP (Dpn-Sp1+)
Ase- imm INP (Erm+Sp1+)
Ase+ imm INP (Erm+Sp1+Ase+)
INP (Dpn+Sp1+Ase+)
T1 GMC (Pros+Ase+)
T2 GMC (Sp1+Pros+Ase+)
neuron (Elav+)

Figure 2.8 Pros reprograms immature INPs to bypass an INP state and adopt a GMC fate

(A) The Euclidean distance between average gene expression of NBs, immature INPs, INPs, GMCs and neurons using published single-cell mRNA sequencing datasets of wild-type larval brains.(Marques et al., 2023; Michki et al., 2021; A. Rajan et al., 2023) GMCs from the T1 and T2 lineages are highly similar to immature INPs. Dendrogram based on Pearson correlation summarizes the degree of similarity between sell types.(B) Diagram depicting at what stage of immature INP *Erm-Gal4* is active in the T2 lineage.(C-D) Images showing Pros mis-expression in immature INPs by *Erm-Gal4* promotes premature adoption of a GMC fate. A wild-type T2NB lineage contains INPs (small $Dpn^{+}Ase^{+}$ cells) whereas a T2NB lineage that mis-expresses *pros* in immature INPs only contains small $Dpn^{-}Ase^{+}$ progeny (E) Quantification showing the number of INPs per brain lobe where Pros is mis-expressed in immature INPs is drastically lower than wild-type brain lobe.(F-G) Images showing Pros mis-expression in immature INPs does not prevent specification of Erm^{+} immature INPs or Ase^{+} immature INPs.(H) Quantification showing the fraction of T2NBs producing Erm^{+} immature INPs upon Pros mis-expression in immature INPs not significantly different from wild-type T2NBs.(I) A schematic summarizing the data that suggest Pros mediates Ase-induced bypassing of INP production to generate GMCs by T2NBs. White dotted line marks NB lineage. White arrow: T2NB. White arrowhead: Erm^{+}/Ase^{-} immature INP. Yellow arrow: Ase^{+} immature INP. Yellow arrowhead: INP. Magenta arrow: T1NB. Orange arrow: T2 lineage GMC. Scale bar: 10 μm. P-value; NS: Not significant, ****<.00005

We tested whether Pros activates the GMC genetic program in immature INPs in part by overriding immature INP gene expression. Newborn immature INPs transition to Ase^{-} immature by upregulating Erm expression 90 minutes following asymmetric division of the T2NB.(Janssens et al., 2017; Janssens et al., 2014) As such, Erm protein expression is the earliest marker that indicates the onset of differentiation in a newborn immature INP. Pros mis-expression in immature INPs had no effect on endogenously expressed Erm protein and upregulation of Ase expression (Fig. 2.8F-H). Thus, we conclude that Pros-induced reprogramming of immature INPs into GMCs occurs through superimposition of the GMC genetic program upon endogenously expressed immature INP genes (Fig. 2.8I).

Reprogramming tumor NB progeny fate bypasses differentiation blockades and halts tumor growth

The ability to control the generation of specific TAP subtypes could provide a strategy to bypass differentiation blockades in TAPs that leads to tumorigenesis. The RNA-binding protein Brain Tumor (Brat) promotes the onset of differentiation in newborn immature INPs, and loss of *brat* function blocks immature INP differentiation to INPs, resulting in a transformation into premalignant T2NBs.(Bello et al., 2008; Betschinger et al., 2006; Boone & Doe, 2008; Bowman et al., 2008; Komori et al., 2025; Komori, Xiao, McCartney, et al., 2014; Lee, Wilkinson, et al., 2006; Xiao et al., 2012) A subset of these premalignant T2NBs bypass cell cycle exit and immortalize into tumor NBs in adult *brat*-mutant brains.(Genovese et al., 2019; Narbonne-Reveau et al., 2016) Adult *brat*-mutant tumor NBs lack Ase expression suggesting that they maintain T2NB identity and likely generate immature INPs that are stalled in differentiation and revert to tumor NBs (Fig. 2.9A; Fig. 2.10A).

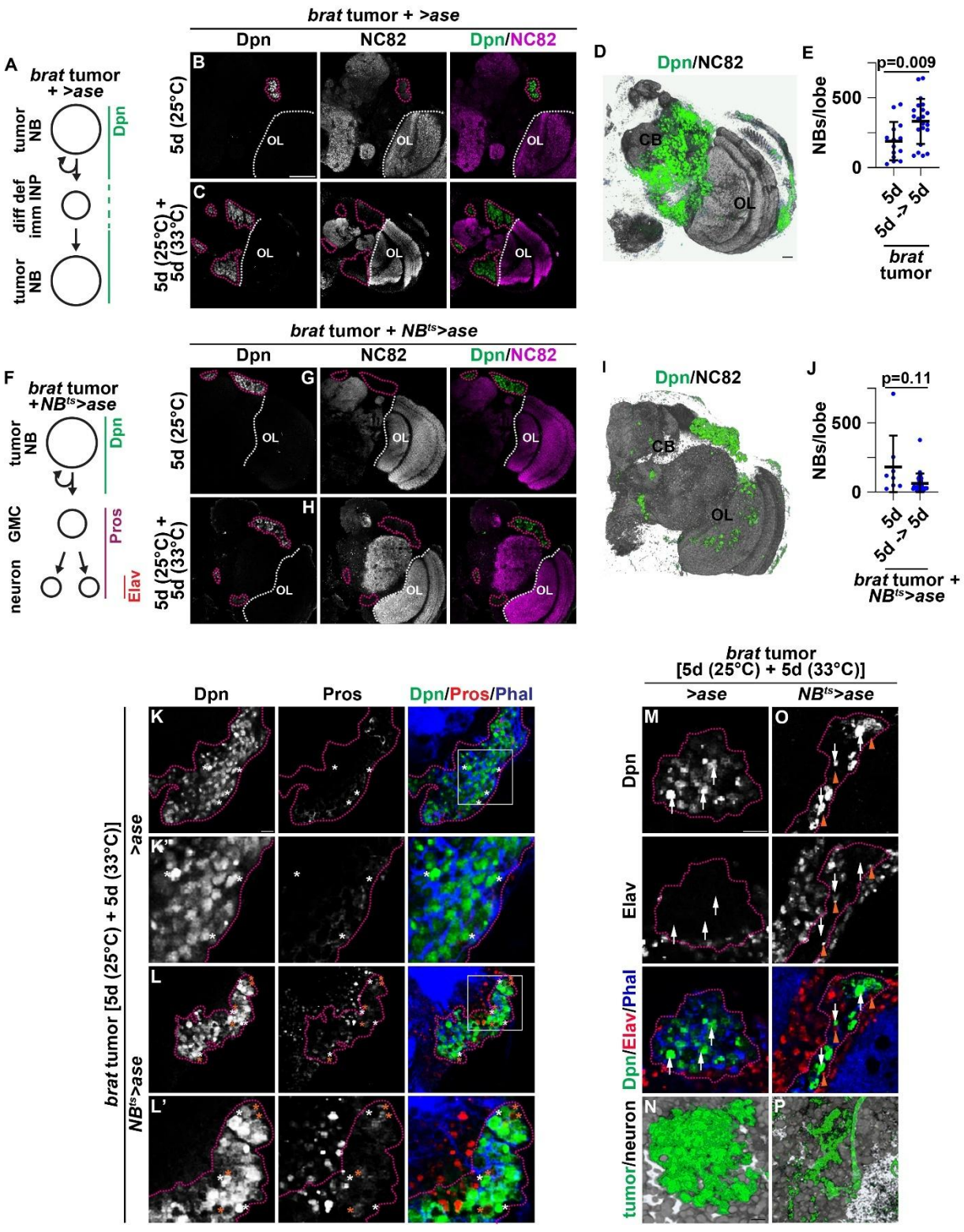


Figure 2.9 Reprogramming tumor NBs to generate GMCs halts tumor growth driven by defective INPs

(A) Diagram showing that upon loss of *brat* function, immature INPs fail to differentiate into INPs and revert back to tumor NBs.(B-C) Images showing tumor NBs continually grow in adult fly brains in a *brat*-, *patr-1* hypomorphic background. Tumor cells are marked by Dpn expression, and neurons are marked by NC82 expression. Scale bar: 50 μm.(D) 3-D reconstruction of an adult brain showing tumor mass (pseudo colored in green) 10 days after eclosion. Scale bar: 10 μm.(E) Quantification showing that the number of tumor NBs (Dpn^+ cells) increases over time.(F) Diagram showing that mis-expression of Ase upon loss of Brat function will produce progeny that bypass immature INP state and restore generation of differentiated progeny marked with Pros (GMCs) or Elav (neurons).(G-H) Images showing tumor NBs stop growing or may become ablated in adult fly brains upon Ase mis-expression in a *brat*-, *patr-1* hypomorphic background.(I) 3-D reconstruction of an adult brain showing tumor mass (pseudo colored in green) 10 days after eclosion is much smaller in the Ase mis-expressing samples.(J) Quantification showing that the number of tumor NBs (Dpn^+ cells) upon Ase mis-expression is not significantly different and is likely decreasing over time.(K-L) Images showing tumor NBs are induced to produce GMC progeny ($Pros^+$) upon Ase mis-expression in adult fly brains in a *brat*-, *patr-1* hypomorphic background. Scale bar: 20 μm.(M,O) Images showing tumor NBs are induced to produce neurons progeny ($Elav^+$) upon Ase mis-expression in adult fly brains in a *brat*-, *patr-1* hypomorphic background. White dotted line marks OL boundary. Magenta dotted line marks tumor boundary. Scale bar: 20 μm.(N,P) 3-D reconstruction of an adult brain showing tumor mass (pseudo colored in green) is invaded by neurons (pseudo colored gray) upon Ase misexpression. Scale bar: 20 μm.

If tumor cells-of-origin in adult *brat*-mutant brains are indeed immature INPs stalled in differentiation, Ase-induced reprogramming of immature INPs into GMCs should limit tumor expansion. Brat promotes degradation of gene transcripts that encode proteins inhibiting the onset of differentiation in immature INPs.(Komori et al., 2018; Reichardt et al., 2018) Protein associated with topo II related-1 (Patr-1) is a component of the RNA decapping protein complex, which contributes to mRNA decay.(Pradhan et al., 2012) Brat and Patr-1 function together to promote immature INP differentiation to INPs.(Komori et al., 2025) Larval brains carrying *brat* and *patr-1* hypomorphic alleles ($brat^{hypo}$,$patr\text{-}1^{hypo}$) display a moderate premalignant T2NB phenotype originating from immature INPs stalled in differentiation (Fig. 2.10B-D,F,G). High levels of Ase expression significantly suppressed the premalignant T2NB

phenotype in *brat^{hypo},patr-1^{hypo}* larval brains (Fig. 2.10D-F). Wild-type adult brains do not contain NBs, whereas *brat^{hypo},patr-1^{hypo}* adult brains displayed detectable tumor NBs marked by Dpn expression with high penetrance at eclosion (Fig. 2.10G). We used *brat^{hypo},patr-1^{hypo}* animals that carry a *UAS-ase* transgene alone as control animals that receive no treatment. *brat^{hypo},patr-1^{hypo}* animals that carried a heat-inducible *NB-Gal4* driver and a *UAS-ase* transgene were experimental animals where Ase expression can be induced in tumor NBs shifting from 25°C to 33°C. Tumor masses were identified using Dpn to mark NBs and NC82 to mark the neuropil. Tumor masses were clearly visible in controls 5 days post-eclosion at 25°C and increased their volume and total number of tumor NBs following additional 5 days of incubation at 33°C (Fig. 2.9B-E, Supplementary Movie 1). Although tumor masses were also visible in experimental animals 5 days post-eclosion at 25°C, tumor NB number and tumor burden failed to increase upon induction of Ase expression for 5 days (Fig. 2.9F-J, Supplementary Movie 2). These results demonstrate that Ase-induced reprogramming of immature INPs to adopt a GMC fate can bypass differentiation blockades in immature INPs and halt tumor growth.

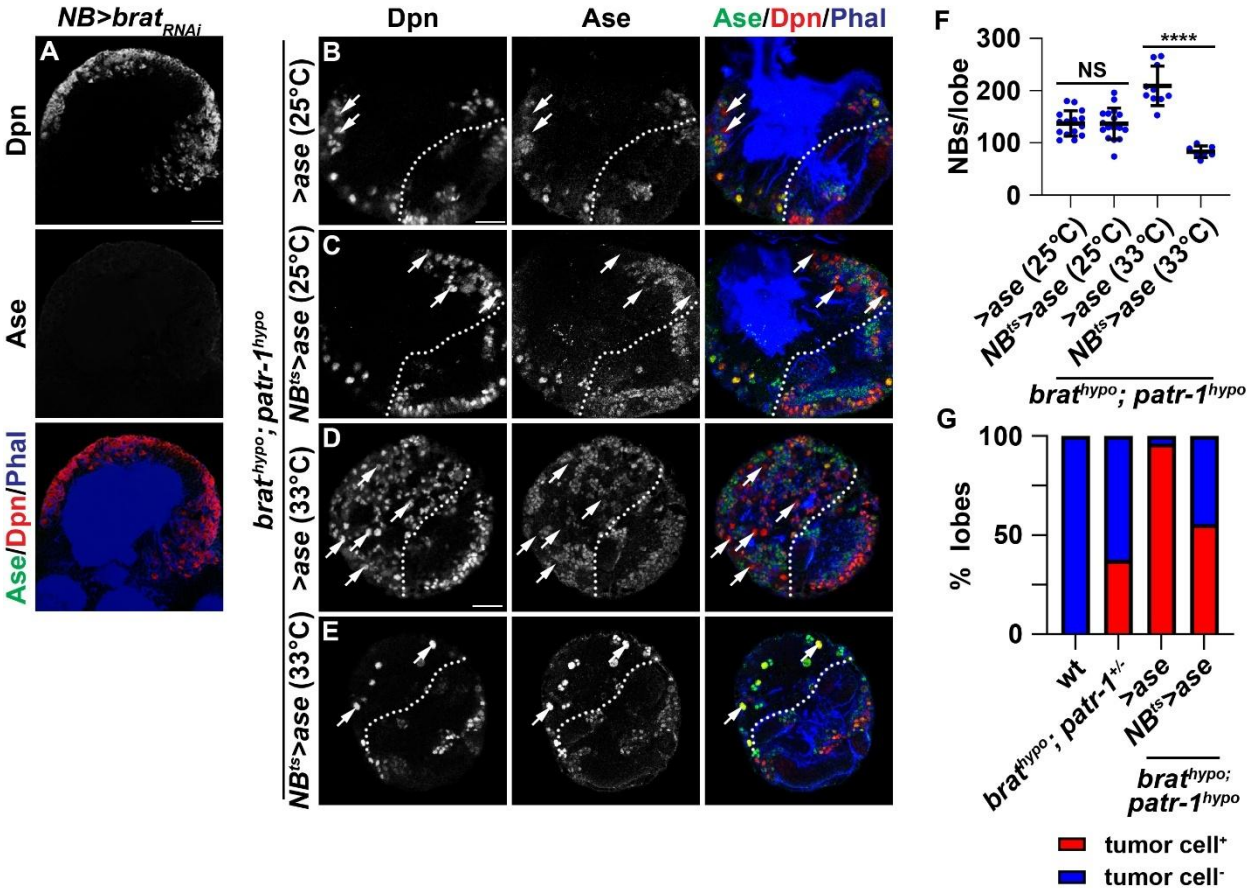


Figure 2.10 Elevating Ase expression suppresses premalignant NBs formation in *brat*,*patr-1*-hypomorphic brains

(A) Images showing brat knockdown since larval stage produces T2NBs (Ase^{-}Dpn^{+}) that persisted into the adult brain.(B-E) Images showing that *brat^{hypo}*,*patr-1^{hypo}* compound larval brains with and without NB-gal4 (*Dpn-Gal4*) when kept at 25^{o}C do not have a significantly different number of NBs, while induction at 33^{o}C will drive Ase mis-expression in the presence of NB-Gal4. Ase mis-expression is sufficient to result in decreased number of T2NBs.(F) Quantification showing that keeping *brat^{hypo}*,*patr-1^{hypo}* compound brain samples at 25^{o}C was able to keep Ase suppressed and with no significant change in the number of NBs. Shifting to 33^{o}C was able to induce Ase mis-expression resulted in a significant decrease in the number of NBs.(G) Quantification showing the fraction of brain lobes where tumors (Dpn^{+}) could be detected from between wild-type, *brat^{hypo}*,*patr-1$^{+/-}$*, *brat^{hypo}*,*patr-1^{hypo}*, and *brat^{hypo}*,*patr-1^{hypo}* with NB-Gal4 driving Ase samples.

We further examined whether Ase expression indeed halts *brat^{hypo}*,*patr-1^{hypo}* tumor expansion by reprogramming tumor NBs to generate GMCs marked by nuclear

Pros. We also assessed if these GMCs were able to differentiate into neurons by utilizing the neuron marker Elav. The *brat*^{hypo}*,patr-1*^{hypo} control brains consists of mostly tumor NBs marked by Dpn expression and very few GMCs and neurons (Fig. 2.9K,M,N). We did not detect any GMCs and neurons immediately adjacent to tumor NBs (Fig. 2.9K',M). In contrast, in *brat*^{hypo}*,patr-1*^{hypo} brains that had Ase expression induced, it could be observed that GMCs and neurons were interspersed among tumor NBs (Fig. 2.9L,O,P). Importantly, we could easily detect GMCs and neurons located adjacent to tumor NBs (Fig. 2.9L',M). This result is consistent with GMCs surrounding T2NBs that expressed high levels of Ase in larval brains (Fig. 2.4E). Thus, we conclude that the Ase-instilled barrier to generate INPs can halt tumor expansion by reprogramming tumor NBs to generate GMCs via bypassing stalled INPs that are the cells-of-origin in *brat*-mutant brains.

Discussion

Despite significant advance in our understanding of the genomic landscape and transcriptome of various cell types in the developing vertebrate cortex (Pebworth et al., 2021; Wang et al., 2025), how radial glia decide to generate specific TAP subtypes remain unknown. We investigated how NBs decide to generate INPs instead of GMCs during fly larval brain neurogenesis. The capability to generate INPs was defined by chromatin accessibility at cell-type-specific enhancers of genes that drive INP formation in the T2 lineage (Fig. 2.1C). Surprisingly, these enhancers are maintained in a poised state in T1NBs despite never generating INPs in their lifetime (Fig. 2.11A). Thus, both NB types are competent to generate INPs. The mutually exclusive expression and

functions of Btd and Ase/Pros maximizes the efficiency of INP generation in T2NBs and GMC production in T1NBs in wild-type brains (Fig. 2.11B). Because cell-type-specific enhancers of genes essential for INP formation are maintained in a poised state in T1NBs, endogenously expressed Ase safeguards GMC generation by constraining INP production induced by aberrant expression of T2NB TFs such as Btd (Fig. 2.11B). Elevating Ase expression in T2NBs functions through Pros to reprogram immature INPs into GMCs bypassing the INP state. Our study suggests that a double-assurance mechanism in which dynamic superimposition of lineage-specific activators (Btd) upon basal-state determinants (Ase/Pros) defines NB capability to generate INPs or GMCs.

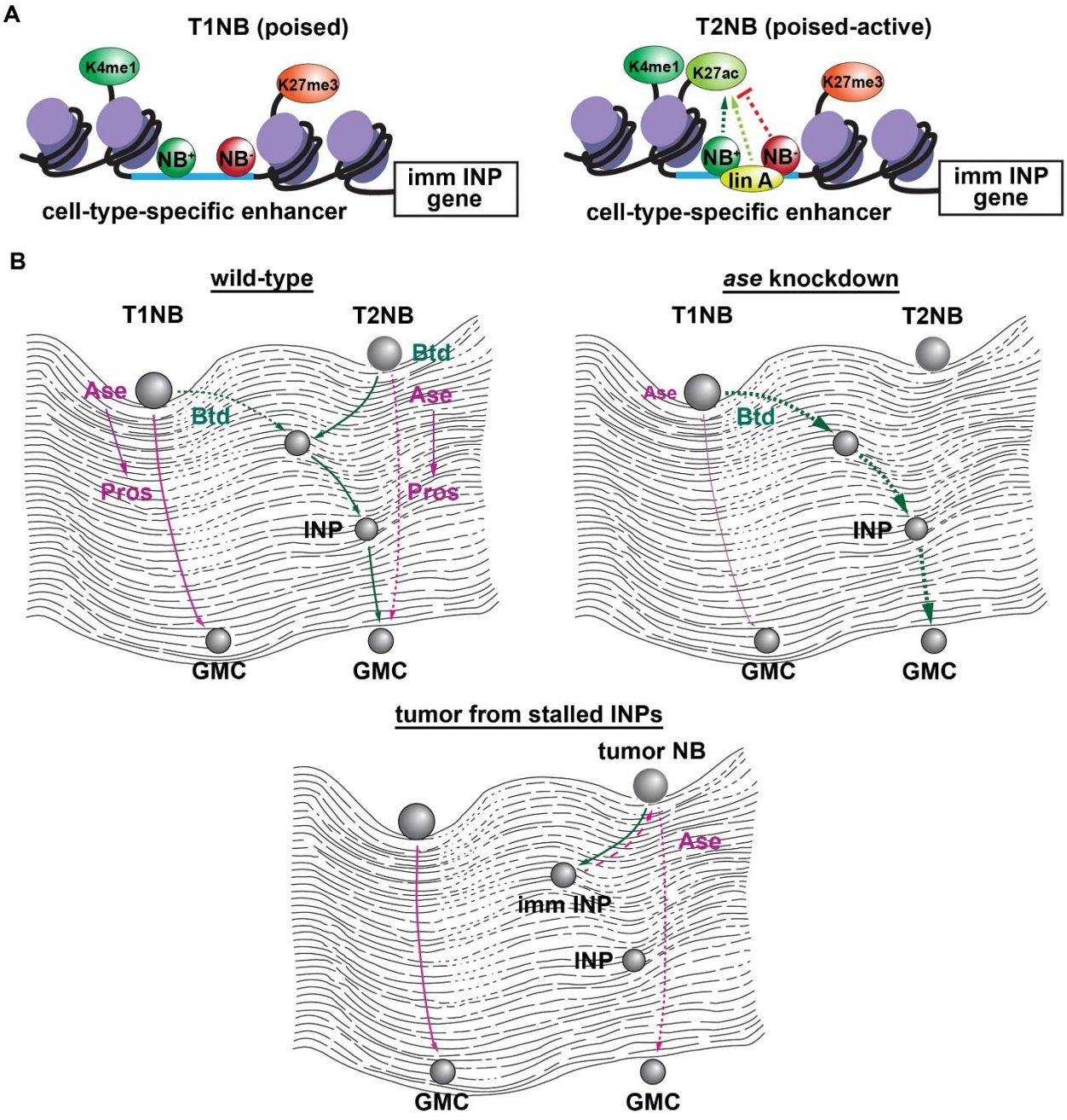


Figure 2.11 The capability to generate INPs is inherent to both NB types but activated exclusively in T2NBs

(A) Enhancers associated with genes that promote INP generation are maintained in a poised state in T1NBs but are in a poised-activate state in T2NB through binding of lineage specific TFs. NB^{+}: NB-specific transcriptional activator, NB^{-}: NB-specific transcriptional repressor, Lin A: Lineage-specific transcriptional activator.(B) Chromatin landscape diagram showing that both T1 and T2NBs are capable to generate INPs or GMCs directly based on cues from TFs. Stoichiometric superimposition of basal-state

transcription factors (Ase and Pros) and lineage-specific transcription factor (Btd) defines NB decision to generate INPs or GMCs. Reprogramming tumor NBs to bypass defective immature INPs and generate GMCs instead halt tumor growth in *brat*,*patr-1* hypomorphic brains.

Regulation of cell intrinsic competency to generate transit-amplifying progenitors

The inability to directly assess the capability of radial glia to generate TAP subtypes *in situ* has hindered our understanding of the generation of diverse cell types during neurogenesis. The obstacle mainly stems from lack of insight into cell-type-specific enhancers that are functionally relevant to TAP formation. We leveraged the well-established cell type hierarchy in NB lineages to define a large cohort of active neurogenic enhancers in T2NBs including cell-type-specific enhancers of genes essential for INP formation during fly larval brain neurogenesis (Fig. 2.1C). Two models for the regulation of NB capability to generate INPs can be deduced from previous studies (Álvarez, 2018; Bahrampour et al., 2017; Bayraktar et al., 2010; Bello et al., 2008; Boone & Doe, 2008; Bowman et al., 2008; Chen et al., 2022; Walsh & Doe, 2017). The deterministic model suggests that cell-type-specific enhancers of genes that promote INP formation are inaccessible in T1NBs leading to their inability to generate INPs. This model predicts that inducing T1NBs to generate INPs would necessitate re-establishment of chromatin accessibility at these enhancers (Fig. 2.1A). By contrast, the hierarchical model suggests that enhancers driving gene expression essential for INP generation are accessible in both NB types but are inactive in T1NBs (Fig. 2.1A). Our study revealed that these cell-type-specific enhancers display characteristics that are indicative of poised enhancers including accessible chromatin, high H3K27me3/H3K4me1 and low H3K27ac in T1NBs (Fig. 2.1D,F; 2.2D,E). These data

support the hierarchical model that the capability to generate INPs is inherent to both NBs but activated by lineage-specific transcription factors such as Btd in T2NBs.

What prevents poised enhancers of genes essential for INP formation from activation in T1NBs? Lack of T1NB-intrinsic activators that function analogously to Btd is likely a major factor. This study uncovered a previously unknown function of Ase that instills a barrier mechanism limiting the ability of T1NBs to generate INPs. We identified Pros as a key downstream-effector of Ase-instilled barrier mechanism (Fig. 2.5;Fig. 2.7). Ase likely limits INP generation by promoting Pros expression, which does not appear necessary for NB function (Bayraktar et al., 2010), suggesting that the barrier mechanism does not directly inhibit activation of poised cell-type-specific enhancers in T1NBs (Fig. 2.7). Instead, the barrier mechanism likely functions in GMCs to limit reprogramming into immature INPs due their similarity in the transcriptome and genomic landscape (see discussion below). Thus, we propose that Btd and Ase function opposingly in a double-assurance mechanism to ensure the capability to generate INPs is maximally activated in T2NBs while safeguarding this ability in T1NBs.

A perplexing question arose from our study: why are cell-type-specific enhancers of genes essential for INP formation maintained in a poised state in T1NBs despite lacking INP progeny? Genomic studies in embryonic, hematopoietic and skin stem cell lineages have reported the identification of a large cohort of poised enhancers (Lara-Astiaso et al., 2014; Ma et al., 2020; Rada-Iglesias et al., 2011). Subsets of these poised enhancers transition to an active state marked by increased H3K27ac and concomitant decrease in H3K27me3. Thus, a function of the poised chromatin state is likely to bookmark developmental enhancers for rapid activation in a response to

signaling and developmental cues. Many poised developmental enhancers do not appear to become activated and eventually lose chromatin accessibility in differentiated cell types. These enhancers might serve as a reservoir of *cis*-regulatory elements that are in a low-barrier state allowing stem cells to adapt to environmental changes by readily changing gene expression. Our study suggests that similar poising mechanisms appear to regulate cell-type-specific enhancers of genes in neural differentiation programs in neural stem cells likely to ensure timely and rapid neuronal differentiation.

Transit-amplifying progenitor plasticity

It is currently unknown what constrains radial glial progeny to assume the identity of a specific TAP subtype and whether their identities can be interconverted. In *Drosophila*, an INP can undergo 5-6 rounds of asymmetric division to generate a GMC each time, but a GMC always divides symmetrically to generate 2 neurons suggesting that these two types of NB progeny exhibit drastically different neurogenic potential. Post-embryonically removing *btd* function in T2NBs has no effects on their lineage-specific marker gene expression and does not detectably upregulate Ase and Pros protein expression. Yet, their presumptive immature INPs assume a GMC fate marked by Pros protein expression (Komori, Xiao, Janssens, et al., 2014). Similarly, elevating Ase expression in T2NBs does not affect lineage-specific marker expression but leads to their progeny to assume a GMC fate (Fig. 2.4E). These findings suggest that (1) GMC fate is the default cell identity for NB progeny in both lineages and (2) the expanded neurogenic potential in immature INPs arise from superimposition of the immature INP-specific genetic program upon the GMC identity. Consistently, analyses of published single-cell mRNA sequencing datasets of wild-type larval brains indicate that

GMCs in both NB lineages are most closely related to Ase^{-} immature INPs followed by Ase^{+} immature INPs (Fig. 2.8A). Furthermore, the vast majority of active neurogenic enhancers in T2NBs remain accessible in immature INPs and likely in GMCs (Fig. 2.1C)(Larson et al., 2021). Elevated Pros expression is sufficient to reprogram Ase^{-} immature INPs into GMCs without altering their lineage identity as indicated by their progeny extending bifurcating axon projections that are characteristic of T2 lineage-specific neurons (Fig. 2.7D,G)(Bayraktar et al., 2010). Thus, the identities of GMCs and immature INPs can be interconverted by regulators of NB capability to generate INPs. In agreement with this model, elevated Ase expression in tumor NBs in adult *brat*-mutant brains results in bypassing the generation of differentiation-deficient INPs, which serve of cells-of-origin for tumor cells, and generate GMCs instead halting tumor expansion (Fig. 2.9, Fig 2.11B).

Poised enhancers identified in vertebrate stem cell types likely represent regulatory potential of a large repertoire of gene expression programs that can be activated in their TAP progeny (Lara-Astiaso et al., 2014; Ma et al., 2020; Rada-Iglesias et al., 2011). Although subset of these enhancers become activated in TAPs to promote lineage-specific differentiation programs, most remain in a poised state and display diminished accessibility much later in development. Similar to *Drosophila*, vertebrate TAPs likely are significantly more plastic than what their classifying subtypes suggest, potentially increasing their susceptibility to tumorigenic transformation and leading to childhood malignancies (Balgobind et al., 2011; Jessa et al., 2019). Insight into reprogramming the activity of developmentally poised enhancers in tumor cells might

allow for the generation of distinct TAP subtypes bypassing differentiation blockades that drive tumor expansion.

References

Abdusselamoglu, M. D., Eroglu, E., Burkard, T. R., & Knoblich, J. A.(2019). The transcription factor odd-paired regulates temporal identity in transit-amplifying neural progenitors via an incoherent feed-forward loop. *eLife*, *8*, e46566.

Albertson, R., & Doe, C. Q.(2003). Dlg, Scrib and Lgl regulate neuroblast cell size and mitotic spindle asymmetry. *Nat Cell Biol*, *5*(2), 166-170.

Álvarez, J. A. D.-B., F.J.(2018). Origin and specification of T2NB neuroblasts in the Drosophila embryo. *Development*, *145*(7), dev158394.

Amemiya, H. M., Kundaje, A., & Boyle, A. P.(2019). The ENCODE Blacklist: Identification of Problematic Regions of the Genome. *Sci Rep*, *9*(1), 9354.

Bahrampour, S., Gunnar, E., Jonsson, C., Ekman, H., & Thor, S.(2017). Neural Lineage Progression Controlled by a Temporal Proliferation Program. *Dev Cell*, *43*(3), 332-348.

Balgobind, B. V., Zwaan, C. M., Pieters, R., & Van den Heuvel-Eibrink, M. M.(2011). The heterogeneity of pediatric MLL-rearranged acute myeloid leukemia. *Leukemia*, *25*(8), 1239-1248.

Bayraktar, O. A., Boone, J. Q., Drummond, M. L., & Doe, C. Q.(2010). Drosophila T2NB neuroblast lineages keep Prospero levels low to generate large clones that contribute to the adult brain central complex. *Neural Dev*, *5*, 26.

Bayraktar, O. A., & Doe, C. Q.(2013). Combinatorial temporal patterning in progenitors expands neural diversity. *Nature*, *498*(7455), 449-455.

Bello, B., Holbro, N., & Reichert, H.(2007). Polycomb group genes are required for neural stem cell survival in postembryonic neurogenesis of Drosophila. *Development*, *134*(6), 1091-1099.

Bello, B. C., Izergina, N., Caussinus, E., & Reichert, H.(2008). Amplification of neural stem cell proliferation by intermediate progenitor cells in Drosophila brain development. *Neural Develop*, *3*(1), 5.

Betizeau, M., Cortay, V., Patti, D., Pfister, S., Gautier, E., Bellemin-Ménard, A., Afanassieff, M., Huissoud, C., Douglas, R. J., Kennedy, H., & Dehay, C.(2013). Precursor diversity and complexity of lineage relationships in the outer subventricular zone of the primate. *Neuron*, *80*(2), 442-457.

Betschinger, J., Mechtler, K., & Knoblich, J. A.(2006). Asymmetric segregation of the tumor suppressor brat regulates self-renewal in Drosophila neural stem cells. *Cell*, *124*(6), 1241-1253.

Bischof, J., Maeda, R. K., Hediger, M., Karch, F., & Basler, K.(2007). An optimized transgenesis system for Drosophila using germ-line-specific φC31 integrases. *Proceedings of the National Academy of Sciences*, *104*(9), 3312-3317. https://doi.org/doi:10.1073/pnas.0611511104

Boone, J. Q., & Doe, C. Q.(2008). Identification of Drosophila T2NB neuroblast lineages containing transit amplifying ganglion mother cells. *Dev Neurobiol.*, *68*(9), 1185-1195.

Bowman, S. K., Rolland, V., Betschinger, J., Kinsey, K. A., Emery, G., & Knoblich, J. A.(2008). The Tumor Suppressors Brat and Numb Regulate Transit-Amplifying Neuroblast Lineages in Drosophila. *Dev Cell*, *14*(4), 535-546.

Breen, T. R., & Harte, P. J.(1993). Trithorax regulates multiple homeotic genes in the bithorax and Antennapedia complexes and exerts different tissue-specific, parasegment-specific and promoter-specific effects on each. *Development*, *117*(1), 119-134.

Carney, T. D., Miller, M. R., Robinson, K. J., Bayraktar, O. A., Osterhout, J. A., & Doe, C. Q.(2012). Functional genomics identifies neural stem cell sub-type expression profiles and genes regulating neuroblast homeostasis. *Dev Biol*, *361*(1), 137-146.

Chen, R., Deng, X., & Zhu, S.(2022). The Ets protein Pointed P1 represses Asense expression in T2NB neuroblasts by activating Tailless. *PLoS Genet*, *18*(1), e1009928.

Cohen, S. M., & Jürgens, G.(1990). Mediation of Drosophila head development by gap-like segmentation genes. *Nature*, *346*(6283), 482-485.

Daul, A. L., Komori, H., & Lee, C. Y.(2010). EdU (5-ethynyl-2'-deoxyuridine) labeling of Drosophila mitotic neuroblasts. *Cold Spring Harb Protoc*, *2010*(7), pdb.prot5461. https://doi.org/10.1101/pdb.prot5461

Doe, C. Q.(2017). Temporal Patterning in the Drosophila CNS. *Annu Rev Cell Dev Biol*, *33*, 219-240.

Eroglu, E., Burkard, T. R., Jiang, Y., Saini, N., Homem, C. C., Reichert, H., & Knoblich, J. A.(2014). SWI/SNF complex regulates Prdm protein Hamlet to ensure lineage directionality in Drosophila neural stem cells. *Cell*, *156*(6), 1259-1273.

Farnsworth, D. R., Bayraktar, O. A., & Doe, C. Q.(2015). Aging Neural Progenitors Lose Competence to Respond to Mitogenic Notch Signaling. *Curr Biol*, *25*(23), 3058-3068.

Faust, G. G., & Hall, I. M.(2014). SAMBLASTER: fast duplicate marking and structural variant read extraction. *Bioinformatics*, *30*(17), 2503-2505.

Gaspar, J. M.(2018). NGmerge: merging paired-end reads via novel empirically-derived models of sequencing errors. *BMC Bioinformatics*, *19*(1), 536.

Genovese, S., Clément, R., Gaultier, C., Besse, F., Narbonne-Reveau, K., Daian, F., Foppolo, S., Luis, N. M., & Maurange, C.(2019). Coopted temporal patterning governs cellular hierarchy, heterogeneity and metabolism in Drosophila neuroblast tumors. *Elife*, *8*, e50375.

Gibson, T. J., Larson, E. D., & Harrison, M. M.(2024). Protein-intrinsic properties and context-dependent effects regulate pioneer factor binding and function. *Nature Structural & Molecular Biology*, *31*(3), 548-558. https://doi.org/10.1038/s41594-024-01231-8

Hakes, A. E., & Brand, A. H.(2020). Tailless/TLX reverts intermediate neural progenitors to stem cells driving tumourigenesis via repression of asense/ASCL1. *eLife*, *9*, e53377. .

Hansen, D. V., Lui, J. H., Parker, P. R., & Kriegstein, A. R.(2010). Neurogenic radial glia in the outer subventricular zone of human neocortex. *Nature*, *464*(7288), 554-561.

Harrison, M. M., Botchan, M. R., & Cline, T. W.(2010). Grainyhead and Zelda compete for binding to the promoters of the earliest-expressed Drosophila genes. *Dev Biol*, *345*(2), 248-255.
Heinz, S., Benner, C., Spann, N., Bertolino, E., Lin, Y. C., Laslo, P., Cheng, J. X., Murre, C., Singh, H., & Glass, C. K.(2010). Simple combinations of lineage-determining transcription factors prime cis-regulatory elements required for macrophage and B cell identities. *Mol Cell*, *38*(4), 576-589.
Hevner, R. F.(2019). Intermediate progenitors and Tbr2 in cortical development. *J Anat*, *235*(3), 616-625.
Hildebrandt, K., Kübel, S., Minet, M., Fürst, N., Klöppel, C., Steinmetz, E., & Walldorf, U.(2021). Enhancer analysis of the Drosophila zinc finger transcription factor Earmuff by gene targeting. . *Hereditas*, *158*(1), 41.
Homem, C. C., Repic, M., & Knoblich, J. A.(2015). Proliferation control in neural stem and progenitor cells. *Nat Rev Neurosci*, *16*(11), 647-659.
Huilgol, D., Russ, J. B., Srivas, S., & Huang, Z. J.(2023). The progenitor basis of cortical projection neuron diversity. *Curr Opin Neurobiol*, *81*, 102726.
Janssens, D. H., Hammn, D. C., Anhezini, L., Xiao, X., Siller, K. H., Siegrist, S. E., Harrison, M. M., & Lee, C.-Y.(2017). A Hdac1/Rpd3-poised circuit balances continual self-renewal and rapid restriction of developmental potential during asymmetric stem cell division. *Dev Cell*, *40*(4), 367-380.
Janssens, D. H., Komori, H., Grbac, D., Chen, K., Koe, C. T., Wang, H., & Lee, C. Y.(2014). Earmuff restricts progenitor cell potential by attenuating the competence to respond to self-renewal factors. *Development*, *141*(5), 1036-1046.
Janssens, D. H., & Lee, C. Y.(2014). It takes two to tango, a dance between the cells of origin and cancer stem cells in the Drosophila larval brain. *Semin Cell Dev Biol.*
Jenett, A., Rubin, G. M., Ngo, T. T., Shepherd, D., Murphy, C., Dionne, H., Pfeiffer, B. D., Cavallaro, A., Hall, D., Jeter, J., Iyer, N., Fetter, D., Hausenfluck, J. H., Peng, H., Trautman, E. T., Svirskas, R. R., Myers, E. W., Iwinski, Z. R., Aso, Y., . . . Zugates, C. T.(2012). A GAL4-driver line resource for Drosophila neurobiology. *Cell Rep*, *2*(4), 991-1001.
Jessa, S., Blanchet-Cohen, A., Krug, B., Vladoiu, M., Coutelier, M., Faury, D., Poreau, B., De Jay, N., Hébert, S., Monlong, J., Farmer, W. T., Donovan, L. K., Hu, Y., McConechy, M. K., Cavalli, F. M. G., Mikael, L. G., Ellezam, B., Richer, M., Allaire, A., . . . Kleinman, C. L.(2019). Stalled developmental programs at the root of pediatric brain tumors. *Nat Genet*, *51*(12), 1702-1713.
Kalebic, N., & Huttner, W. B.(2020). Basal Progenitor Morphology and Neocortex Evolution. *Trends Neurosci*, *43*(11), 843-853.
Kent, W. J., Zweig, A. S., Barber, G., Hinrichs, A. S., & Karolchik, D.(2010). BigWig and BigBed: enabling browsing of large distributed datasets. *Bioinformatics*, *26*(17), 2204-2207.
Kim, D., Paggi, J. M., Park, C., Bennett, C., & Salzberg, S. L.(2019). Graph-based genome alignment and genotyping with HISAT2 and HISAT-genotype. *Nat Biotechnol*, *37*(8), 907-915.
Koe, C. T., Li, S., Rossi, F., Wong, J. J., Wang, Y., Zhang, Z., Chen, K., Aw, S. S., Richardson, H. E., Robson, P., Sung, W. K., Yu, F., Gonzalez, C., & Wang,

H.(2014). The Brm-HDAC3-Erm repressor complex suppresses dedifferentiation in Drosophila T2NB neuroblast lineages. *eLife*, *3*, e01906.
Komori, H., Golden, K. L., Kobayashi, T., Kageyama, R., & Lee, C. Y.(2018). Multilayered gene control drives timely exit from the stem cell state in uncommitted progenitors during Drosophila asymmetric neural stem cell division. *Genes Dev*, *32*(23-24), 1550-1561.
Komori, H., Rastogi, G., Bugay, J. P., Luo, H., Lin, S., Angers, S., Smibert, C. A., Lipshitz, H. D., & Lee, C. Y.(2025). mRNA decay pre-complex assembly drives timely cell-state transitions during differentiation. *Cell Rep*, *44*(1).
Komori, H., Xiao, Q., Janssens, D. H., Dou, Y., & Lee, C. Y.(2014). Trithorax maintains the functional heterogeneity of neural stem cells through the transcription factor Buttonhead. *eLife*, *10.7554/eLife.03502*.
Komori, H., Xiao, Q., McCartney, B. M., & Lee, C. Y.(2014). Brain tumor specifies intermediate progenitor cell identity by attenuating β-catenin/Armadillo activity. *Development*, *141*(1).
Langmead, B., & Salzberg, S. L.(2012). Fast gapped-read alignment with Bowtie 2. *Nat Methods*, *9*(4), 357-359.
Lara-Astiaso, D., Weiner, A., Lorenzo-Vivas, E., Zaretsky, I., Jaitin, D. A., David, E., Keren-Shaul, H., Mildner, A., Winter, D., Jung, S., Friedman, N., & Amit, I.(2014). Immunogenetics. Chromatin state dynamics during blood formation. *Science*, *345*(6199), 943-949.
Larson, E. D., Komori, H., Gibson, T. J., Ostgaard, C. M., Hamm, D. C., Schnell, J. M., Lee, C. Y., & Harrison, M. M.(2021). Cell-type-specific chromatin occupancy by the pioneer factor Zelda drives key developmental transitions in Drosophila *Nat Commun*, *12*, 7153.
Laugesen, A., Højfeldt, J. W., & Helin, K.(2019). Molecular Mechanisms Directing PRC2 Recruitment and H3K27 Methylation. *Mol Cell*, *74*(1), 8-18.
Lee, C. Y., Robinson, K. J., & Doe, C. Q.(2006). Lgl, Pins and aPKC regulate neuroblast self-renewal versus differentiation. *Nature*, *439*(7076), 594-598.
Lee, C. Y., Wilkinson, B. D., Siegrist, S. E., Wharton, R. P., & Doe, C. Q.(2006). Brat is a Miranda cargo protein that promotes neuronal differentiation and inhibits neuroblast self-renewal. *Dev. Cell*, *10*(4), 441-449.
Liao, Y., Smyth, G. K., & Shi, W.(2014). featureCounts: an efficient general purpose program for assigning sequence reads to genomic features. *Bioinformatics*, *30*(7), 923-923.
Lin, Y., Yang, J., Shen, Z., Ma, J., Simons, B. D., & Shi, S. H.(2021). Behavior and lineage progression of neural progenitors in the mammalian cortex. *Curr Opin Neurobiol*(66), 144-157.
Love, M. I., Huber, W., & Anders, S.(2014). Moderated estimation of fold change and dispersion for RNA-seq data with DESeq2. *Genome Biol*, *15*(12), 550.
Ma, S., Zhang, B., LaFave, L. M., Earl, A. S., Chiang, Z., Hu, Y., Ding, J., Brack, A., Kartha, V. K., Tay, T., Law, T., Lareau, C., Hsu, Y. C., Regev, A., & Buenrostro, J. D.(2020). Chromatin Potential Identified by Shared Single-Cell Profiling of RNA and Chromatin. *Cell*, *183*(4), 1103-1116.

Manning, L., & Doe, C. Q.(1999). Prospero distinguishes sibling cell fate without asymmetric localization in the Drosophila adult external sense organ lineage. . *Development*, *126*(10), 2063-2071.
Marques, G. S., Teles-Reis, J., Konstantinides, N., Brito, P. H., & Homem, C. C. F.(2023). Asynchronous transcription and translation of neurotransmitter-related genes characterize the initial stages of neuronal maturation in Drosophila. *PLoS Biol*, *21*(5), e3002115.
Michki, N. S., Li, Y., Sanjasaz, K., Zhao, Y., Shen, F. Y., Walker, L. A., Lee, C.-Y., & Cai, D.(2021). The molecular landscape of neural differentiation in the developing Drosophila brain revealed by targeted scRNA-seq and multi-informatic analysis. *Cell Report*, *35*(4), 109039.
Narbonne-Reveau, K., Lanet, E., Dillard, C., Foppolo, S., Chen, C. H., Parrinello, H., Rialle, S., Sokol, N. S., & Maurange, C.(2016). Neural stem cell-encoded temporal patterning delineates an early window of malignant susceptibility in Drosophila. *Elife*, *5*, e13463.
Orchard, P., Kyono, Y., Hensley, J., Kitzman, J. O., & Parker, S. C. J.(2020). Quantification, Dynamic Visualization, and Validation of Bias in ATAC-Seq Data with ataqv. . *Cell Syst*, *10*(3), 298-306.
Pebworth, M. P., Ross, J., Andrews, M., Bhaduri, A., & Kriegstein, A. R.(2021). Human intermediate progenitor diversity during cortical development. *Proc Natl Acad Sci U S A*, *118*(26), e2019415118.
Pipicelli, F., Villalba, A., & Hippenmeyer, S.(2025). How radial glia progenitor lineages generate cell-type diversity in the developing cerebral cortex. *Curr Opin Neurobiol*, *93*, 103046.
Piunti, A., & Shilatifard, A.(2021). The roles of Polycomb repressive complexes in mammalian development and cancer. *Nat Rev Mol Cell Biol*, *22*(5), 326-345.
Pradhan, S. J., Nesler, K. R., Rosen, S. F., Kato, Y., Nakamura, A., Ramaswami, M., & Barbee, S. A.(2012). The conserved P body component HPat/Pat1 negatively regulates synaptic terminal growth at the larval Drosophila neuromuscular junction. *J Cell Sci*, *125*((Pt 24)), 6105-6116.
Quinlan, A. R., & Hall, I. M.(2010). BEDTools: a flexible suite of utilities for comparing genomic features. *Bioinformatics*, *26*(6), 841-842.
Quinto-Rives, N., Komori, H., Janssens, D. H., Kondo, S., Dai, Q., Moore, A. W., & Lee, C.-Y.(2020). Sequential activation of transcriptional repressors promotes progenitor commitment by silencing stem cell identity genes. *eLife*(9), e56187.
Rada-Iglesias, A., Bajpai, R., Swigut, T., Brugmann, S. A., Flynn, R. A., & Wysocka, J.(2011). A unique chromatin signature uncovers early developmental enhancers in humans. *Nature*, *470*(7333), 279-283.
Rajan, A., Anhezini, L., Rives-Quinto, N., Chhabra, J. Y., Neville, M. C., Larson, E. D., Goodwin, S. F., Harrison, M. M., & Lee, C.-Y.(2023). Low-level repressive histone marks fine-tune gene transcription in neural stem cells. *eLife*, *12*, e86127. https://doi.org/10.7554/eLife.86127
Rajan, A., Anhezini, L., Rives-Quinto, N., Chhabra, J. Y., Neville, M. C., Larson, E. D., Goodwin, S. F., Harrison, M. M., & Lee, C.-Y.(2023). Low-level repressive histone marks fine-tune stemness gene transcription in neural stem cells. *Elife*, *12*, e86127.

Ramírez, F., Dündar, F., Diehl, S., Grüning, B. A., & Manke, T.(2014). deepTools: a flexible platform for exploring deep-sequencing data. *Nucleic Acids Res*, *42(Web Server issue)*, W187-191.

Reichardt, I., Bonnay, F., Steinmann, V., Loedige, I., Burkard, T. R., Meister, G., & Knoblich, J. A.(2018). The tumor suppressor Brat controls neuronal stem cell lineages by inhibiting Deadpan and Zelda. *EMBO Rep*, *19*(1), 102-117.

Robinson, M. D., McCarthy, D. J., & Smyth, G. K.(2010). edgeR: a Bioconductor package for differential expression analysis of digital gene expression data. *Bioinformatics*, *26*(1), 139-140.

Schöck, F., Sauer, F., Jäckle, H., & Purnell, B. A.(1999). Drosophila head segmentation factor buttonhead interacts with the same TATA box-binding protein-associated factors and *in vivo* DNA targets as human Sp1 but executes a different biological program. *Proc Natl Acad Sci U S A.*, *96*(9), 061-065.

Sotillos, S., Díaz-Meco, M. T., Caminero, E., Moscat, J., & Campuzano, S.(2004). DaPKC-dependent phosphorylation of Crumbs is required for epithelial cell polarity in Drosophila. *J Cell Biol*, *166*(4), 549-557.

Southall, T. D., & Brand, A. H.(2009). Neural stem cell transcriptional networks highlight genes essential for nervous system development. *The EMBO Journal*, *28*(24), 3799-3807-3807. https://doi.org/https://doi.org/10.1038/emboj.2009.309

Thor, S.(2024). Indirect neurogenesis in space and time. *Nat Rev Neurosci*, *25*(8), 519-534.

Thorvaldsdóttir, H., Robinson, J. T., & Mesirov, J. P.(2013). Integrative Genomics Viewer (IGV): high-performance genomics data visualization and exploration. *Brief Bioinform*, *14*(2), 178-192.

Viktorin, G., Riebli, N., Popkova, A., Giangrande, A., & Reichert, H.(2011). Multipotent neural stem cells generate glial cells of the central complex through transit amplifying intermediate progenitors in Drosophila brain development. *Dev Biol*, *356*(2), 553-565.

Virtanen, P., Gommers, R., Oliphant, T. E., & Contributors., S.(2020). SciPy 1.0: fundamental algorithms for scientific computing in Python. *Nat Methods*, *17*(3), 261-272.

Walsh, K. T., & Doe, C. Q.(2017). Drosophila embryonic T2NB neuroblasts: origin, temporal patterning, and contribution to the adult central complex. *Development*, *144*(24), 4552-4562.

Wang, L., Wang, C., Moriano, J. A., Chen, S., Zuo, G., Cebrián-Silla, A., Zhang, S., Mukhtar, T., Wang, S., Song, M., de Oliveira, L. G., Bi, Q., Augustin, J. J., Ge, X., Paredes, M. F., Huang, E. J., Alvarez-Buylla, A., Duan, X., Li, J., & Kriegstein, A. R.(2025). Molecular and cellular dynamics of the developing human neocortex. *Nature*, *doi: 10.1038/s41586-024-08351-7*.

Weng, M., Golden, K. L., & Lee, C. Y.(2010). dFezf/Earmuff maintains the restricted developmental potential of intermediate neural progenitors in Drosophila. *Dev Cell*, *18*(1), 126-135.

Wimmer, E. A., Jäckle, H., Pfeifle, C., & Cohen, S. M.(1993). A Drosophila homologue of human Sp1 is a head-specific segmentation gene. *Nature*, *366*(6456), 690-694.

Wingett, S. W., & Andrews, S.(2018). FastQ Screen: A tool for multi-genome mapping and quality control. *F1000Res*, *7*, 1338.

Wolf, F. A., Angerer, P., & Theis, F. J.(2018). SCANPY: large-scale single-cell gene expression data analysis. *Genome Biol*, *19(*(1), 15.
Xiao, Q., Komori, H., & Lee, C. Y.(2012). klumpfuss distinguishes stem cells from progenitor cells during asymmetric neuroblast division. *Development*, *139*(15), 2670-2680.
Xie, Y., Li, X., Zhang, X., Mei, S., Li, H., Urso, A., & Zhu, S.(2014). The Drosophila Sp8 transcription factor Buttonhead prevents premature differentiation of intermediate neural progenitors. *eLife*, *3*(eLife.03596).
Yang, C. P., Samuels, T. J., Huang, Y., Yang, L., Ish-Horowicz, D., Davis, I., & Lee, T.(2017). Imp and Syp RNA-binding proteins govern decommissioning of Drosophila neural stem cells. *Development*, *144*(19), 3454-3464.
Yashar, W. M., Kong, G., VanCampen, J., Curtiss, B. M., Coleman, D. J., Carbone, L., Yardimci, G. G., Maxson, J. E., & Braun, T. P.(2022). GoPeaks: histone modification peak calling for CUT&Tag. . *Genome Biol*, *23*(1), 144.
Yu, B. D., Hess, J. L., Horning, S. E., Brown, G. A., & Korsmeyer, S. J.(1995). Altered Hox expression and segmental identity in Mll-mutant mice. *Nature*, *378*(6556), 505-508.
Yu, F., Sankaran, V. G., & Yuan, G. C.(2021). CUT&RUNTools 2.0: a pipeline for single-cell and bulk-level CUT&RUN and CUT&Tag data analysis. *Bioinformatics*, *38*(1), 252-254.
Zerbino, D. R., Johnson, N., Juettemann, T., Wilder, S. P., & Flicek, P.(2014). WiggleTools: parallel processing of large collections of genome-wide datasets for visualization and statistical analysis. *Bioinformatics*, *30*(7), 1008-1009.
Zhang, Y., Liu, T., Meyer, C. A., Eeckhoute, J., Johnson, D. S., Bernstein, B. E., Nusbaum, C., Myers, R. M., Brown, M., Li, W., & Liu, X. S.(2008). Model-based analysis of ChIP-Seq (MACS). *Genome Biol*, *9*(9), R137.
Zhu, S., Barshow, S., Wildonger, J., Jan, L. Y., & Jan, Y. N.(2011). Ets transcription factor Pointed promotes the generation of intermediate neural progenitors in Drosophila larval brains. *Proc Natl Acad Sci U S A.*, *108*(51), 20615-20620.
Zhu, S., Lin, S., Kao, C. F., Awasaki, T., Chiang, A. S., & Lee, T.(2006). Gradients of the Drosophila Chinmo BTB-zinc finger protein govern neuronal temporal identity. *Cell*, *127*(2), 409-422.

Material and Methods

Table 2.1 Key Resources for Chapter 2

REAGENT or RESOURCE	SOURCE	IDENTIFIER
Antibodies		
Chicken anti-GFP IF (1:2000)	Aves Labs, INC.	Cat#GFP-1020
Rabbit anti-RFP IF (1:200)	Rockland	Cat.#600-401-379, Lot#31089
Rabbit anti-Ase IF (1:400), Cut&Run (0.5 ul)	(Weng et al., 2010)	
Rabbit anti-Btd Cut&Run (0.5 µl)	This study	

Rat anti-Dpn IF (1:1000)	(Lee, Robinson, et al., 2006)	clone 11D1BC7.14
Guinea Pig anti-Ase IF (1:100)	(Koe et al., 2014)	
Rabbit anti-Phospho-Histone-H3(Ser10) IF (1:1000)	EMD Millipore, Billerica, MA	Cat. #06-570
Mouse anti-cMyc IF (1:100)	Roche, Basel, Switzerland	Cat.# 11 667 149 001
Rabbit anti-Pros IF (1:500)	DSHB, Iowa city, IA	MR1A
Rabbit anti-Scrib IF (1:500)	(Albertson & Doe, 2003)	
Rabbit anti-Erm IF (1:200)	(Hildebrandt et al., 2021)	
Rabbit anti-Elav IF (1:100)	DSHB	9F8A9
Rabbit H3K4me1 Cut&Run (0.5 ul)	Abcam	Ab8895
Rabbit H3K27ac Cut&Run (0.5 ul)	Active motif	39136
Rabbit H3K27me3 Cut&Run (0.5 ul)	Sigma Aldrich	07-449
Rabbit anti-Zld Cut&Run (0.5 ul)	(Harrison et al., 2010)	
Rabbit anti-Fru^{com} Cut&Run (0.5 ul)	D. Yamamoto	
Alexa Fluor® 488 AffiniPure Donkey Anti-Chicken IgY (IgG) (H+L) (IF: 1:500)	Jackson Immuno Research Laboratories, INC.	Cat#703-545-155
Alexa Fluor® 647 AffiniPure Goat Anti-Rat IgG (H+L) (IF: 1:500)	Jackson Immuno Research Laboratories, INC.	Cat#112-605-167
Goat anti-Mouse IgG (H+L) Highly Cross-Adsorbed Secondary Antibody, Alexa Fluor 488	ThermoFisher Scientific	Cat#A-11029
Goat anti-Rabbit IgG (H+L) Highly Cross-Adsorbed Secondary Antibody, Alexa Fluor 488 (IF 1:500)	ThermoFisher Scientific	Cat#A-11034
Goat anti-Rabbit IgG (H+L) Highly Cross-Adsorbed Secondary Antibody, Alexa Fluor 546 (IF: 1:500)	ThermoFisher Scientific	Cat#A-11035
Goat anti-Guinea Pig IgG (H+L) Highly Cross-Adsorbed Secondary Antibody, Alexa Fluor 488 (IF: 1:500)	Invitrogen	Cat#A-11073
Chemicals, peptides, and recombinant proteins		
Alexa Fluor Plus 405 Phalloidin IF(1:500)	Invitrogen	Cat#: A30104
Alexa Fluor 488 phalloidin IF(1:500)	Invitrogen	Cat#: A12379
Rhodamine Phalloidin IF(1:500)	ThermoFisher Scientific	Cat#R415
ProLong™ Gold Antifade Mount	ThermoFisher SCIENTIFIC	Cat#P36934
Sodium butyrate	Sigma Aldrich	Cat#: B5887
Critical commercial assays		
HCR RNA-FISH amplifiers	Molecular Instruments, Inc	

Click-iT™ EdU Cell Proliferation Kit for Imaging, Alexa Fluor™ 555 dye	ThermoFisher Scientific	C10338
RNeasy Micro Kit	Qiagen	Cat#74004
CUTANA ChIC/CUT&RUN Kit	Epicypher	SKU: 14–1048
Illumina Tagment and DNA enzyme and Buffer	Illumina	20034210
IDT for Illumina DNA/RNA UD Indeces	Illumina	20026121
NEBNext Ultra II DNA Library Prep Kit for Illumina	New England Biolabs	Cat#: E7645L
NEBNext Multiplex Oligos for Illumina (96 Unique Dual Index Primer Pairs)	New England Biolabs	Cat#: E6440L
ProLong Gold Antifade Mountant	Invitrogen	Cat#: P36930
Agencourt AMPure XP - 5 mL	Beckman Coulter	Cat#: A63880
HCR RNA-FISH amplifiers	Molecular Instruments, Inc	
Deposited data		
ATAC-seq of T1NBneuroblast enriched brains	Cheng-yu Lee's Laboratory	NIH GEO Accession: GSE305703 (this study)
CUT&RUN of T1NBneuroblast enriched brains TFs and histone marks and T2NB neuroblast enriched brains for btd	Cheng-yu Lee's Laboratory	NIH GEO Accession: GSE305704 (this study)
Bulk RNA of T1NBneuroblast, T2NB neuroblast, or INP enriched brains	Cheng-yu Lee's Laboratory	NIH GEO Accession: GSE305705 (this study)
Single cell RNA-seq of T2NB neuroblast lineage and CUT&RUN of Fru^{c} in T2NB neuroblast enriched brains	Cheng-yu Lee's Laboratory	NIH GEO Accession: GSE218257(A. Rajan et al., 2023)
Single cell RNA-seq of INP lineage	Dawen Cai's Laboratory	NIH GEO Accession: GSE153723 (Michki et al., 2021)
Single cell RNA-seq of neuroblast lineages	Catarina Homem's Laboratory	NIH GEO Accession: GSE179763 (Marques et al., 2023)
Bulk ATAC-seq of T2NB neuroblast lineage and CUT&RUN of zld in T2NB neuroblast enriched brains	Melissa Harrison's Laboratory	NIH GEO Accession: GSE150931 (Larson et al., 2021)
Experimental models: Organisms/strains		
D. melanogaster: brat11/CyO, Actin-GFP	(Lee, Wilkinson, et al., 2006)	N/A
D. melanogaster: y1, w67c23; P{y+t7.7, w+mC=wHy}bratDG19310	(Xiao et al., 2012)	N/A

D. melanogaster: P{EPgy2-Δd3}Patr-1d3	(Pradhan et al., 2012)	N/A
D. melanogaster: P{EPgy2-Δd17}Patr-1d17		
D. melanogaster: y1, M{vas-int.Dm}ZH-2A w*; M{UAS-insbFL-myc}ZH-86Fb	(Komori et al., 2018)	N/A
D. melanogaster: *Wor-Gal4*(II)	(Lee, Robinson, et al., 2006)	N/A
D. melanogaster: *Wor-Gal4*(III)	(Weng et al., 2010)	N/A
D. melanogaster: P{dpn-GAL4.EE}	(Yang et al., 2017)	N/A
D. melanogaster: Ase-Gal4(II)	(Zhu et al., 2006)	N/A
D. melanogaster: UAS-apkcCaax	(Sotillos et al., 2004)	N/A
D. melanogaster: UAS-Pros.L	(Manning & Doe, 1999)	N/A
D. melanogaster: VanGlow reporter fly: PBac{tll enh-GFP::Luc(nls)}VK31	(Larson et al., 2021)	N/A
D. melanogaster: VanGlow reporter fly: PBac{btd enh-GFP::Luc(nls)}VK22	This study	N/A
D. melanogaster: VanGlow reporter fly: PBac{erm enh-GFP::Luc(nls)}VK22	This study	N/A
D. melanogaster: VanGlow reporter fly: PBac{ham enh-GFP::Luc(nls)}VK22	This study	N/A
D. melanogaster: VanGlow reporter fly: PBac{pntp1 enh-GFP::Luc(nls)}VK22	This study	N/A
D. melanogaster: VanGlow reporter fly: PBac{pntp3 enh-GFP::Luc(nls)}VK22	This study	N/A
D. melanogaster: VanGlow reporter fly: PBac{pros1 enh-GFP::Luc(nls)}VK22	This study	N/A
D. melanogaster: VanGlow reporter fly: PBac{pros3 enh-GFP::Luc(nls)}VK22	This study	N/A
D. melanogaster: y1, M{vas-int.Dm}ZH-2A w*; M{UAS-Tll1-244-3xmyc}ZH-86Fb	This study	N/A
D. melanogaster: y1, M{vas-int.Dm}ZH-2A w*; M{UAS-Btd-3xmyc}ZH-86Fb	This study	N/A
D. melanogaster: VanGlow reporter fly: PBac{pros3ΔAse enh-GFP::Luc(nls)}VK22	This study	N/A
D. melanogaster: y1 w*; PBac{y[+mDint2] w[+mC]=tll-EGFP.S}VK00037	Bloomington Drosophila Stock Center	BDSC: 30874
D. melanogaster: w1118; Df(2L)Exel8040/CyO	Bloomington Drosophila Stock Center	BDSC: 7847
D. melanogaster: w1118; PBac{Sp1- EGFP.S}VK00033	Bloomington Drosophila Stock Center	BDSC: 38669
D. melanogaster: w1118; PBac{pnt-GFP.FPTB}VK00037	Bloomington Drosophila Stock Center	BDSC: 42680
D. melanogaster: y1, w1118; PBac{UAS-ase.MYC}VK00002	Bloomington Drosophila Stock Center	BDSC: 83298
D. melanogaster: y1, w1118; PBac{UAS-ase.VP16.MYC}VK00002	Bloomington Drosophila Stock Center	BDSC: 83296
D. melanogaster: y1 w*; P{w+mC=UAS-Hsap\ASCL1}3	Bloomington Drosophila Stock Center	BDSC: 39711

D. melanogaster: w1118; P{y+t7.7 w+mC=GMR31F04-GAL4}attP2 (*Tll-Gal4*)	Bloomington Drosophila Stock Center	BDSC: 46187
D. melanogaster: w*; P{y+t7.7 w+mC=10XUAS-IVS-mCD8::RFP}attP40	Bloomington Drosophila Stock Center	BDSC: 32219
D. melanogaster: y1 w*; P{w+mC=UAS-mCD8::GFP.L}LL5, P{UAS-mCD8::GFP.L}2	Bloomington Drosophila Stock Center	BDSC: 5137
D. melanogaster: w*; P{w+mC=UAS-Dcr-2.D}2, P{w[+mC]=UAS-mCherry.CAAX.S}2; TM2/TM6B, Tb1	Bloomington Drosophila Stock Center	BDSC: 59022
D. melanogaster: Oregon-R-C	Bloomington Drosophila Stock Center	BDSC: 5
D. melanogaster: pr1 pwn1 P{ry+t7.2=hsFLP}38/CyO; Ki1 kar1 ry506	Bloomington Drosophila Stock Center	BDSC: 5258
D. melanogaster: y1 v1; P{y+t7.7 v+t1.8=UAS-LUC.VALIUM10}attP2	Bloomington Drosophila Stock Center	BDSC: 35788
D. melanogaster: eGFPRNAi y1 sc* v1 sev21; P{y+t7.7 v+t1.8=VALIUM22-EGFP.RNAi.4}attP4	Bloomington Drosophila Stock Center	BDSC: 41550
D. melanogaster: P{UAS-lacZ.B}Bg4-1-2	Bloomington Drosophila Stock Center	BDSC: 1776
D. melanogaster: w1118; P{w+mC=UAS-EGFP}34/TM3, Sb1	Bloomington Drosophila Stock Center	BDSC: 5430
D. melanogaster: AseRNAi w1118; P{GD12444}v28280	Vienna Drosophila Resource Center	VDRC:v28280
D. melanogaster: ProsRNAi y1 v1; P{y+t7.7 v+t1.8=TRiP.JF02308}attP2/TM3, Sb1	Bloomington Drosophila Stock Center	BDSC: 26745
D. melanogaster: ProsRNAi y1 v1; P{TRiP.HMJ02107}attP40	Bloomington Drosophila Stock Center	BDSC: 42538
D. melanogaster: w1118; P{w[+mC]=UAS-Dcr-2.D}2	Bloomington Drosophila Stock Center	BDSC: 24650
D. melanogaster: w*; P{w[+mC]=tubP-GAL80[ts}10; TM2/TM6B, Tb1	Bloomington Drosophila Stock Center	BDSC: 7108
D. melanogaster: w*; P{w[+mC]=tubP-GAL80ts}20; TM2/TM6B, Tb1	Bloomington Drosophila Stock Center	BDSC: 7019
D. melanogaster: w*; sna[Sco]/CyO; P{w[+mC]=tubP-GAL80ts]ncd[GAL80ts-7]	Bloomington Drosophila Stock Center	BDSC: 7018
D. melanogaster: w1118; PBac{achi-GFP.FPTB}VK00033	Bloomington Drosophila Stock Center	BDSC: 55828
D. melanogaster: w1118; PBac{Atf-2-GFP.FLAG}VK00033	Bloomington Drosophila Stock Center	BDSC: 38627

D. melanogaster: y1 w* Mi{PT-GFSTF.2}biMI01347-GFSTF.2 lncRNA:CR32773MI01347-GFSTF.2/FM7c	Bloomington Drosophila Stock Center	BDSC: 59290
D. melanogaster: y1 w*; PBac{CG11247-GFP.FPTB}VK00037	Bloomington Drosophila Stock Center	BDSC: 92317
D. melanogaster: w1118; PBac{CG11398-GFP.FPTB}VK00033	Bloomington Drosophila Stock Center	BDSC: 56784
D. melanogaster: y1 w*; PBac{CG11456-GFP.FPTB}VK00037	Bloomington Drosophila Stock Center	BDSC: 92318
D. melanogaster: y1 w*; PBac{CG11560-GFP.FPTB}VK00037	Bloomington Drosophila Stock Center	BDSC: 92319
D. melanogaster: y1 w*; PBac{CG11906-GFP.FPTB}VK00031/TM6B, Tb1	Bloomington Drosophila Stock Center	BDSC: 96787
D. melanogaster: w1118; PBac{CG12236-GFP.FPTB}VK00033	Bloomington Drosophila Stock Center	BDSC: 68182
D. melanogaster: w1118; PBac{CG12236-GFP.FPTB}VK00033	Bloomington Drosophila Stock Center	BDSC: 64803
D. melanogaster: y1 w*; PBac{CG12391-GFP.FPTB}VK00033	Bloomington Drosophila Stock Center	BDSC: 79610
D. melanogaster: w1118; PBac{CG12659-GFP.FPTB}VK00033	Bloomington Drosophila Stock Center	BDSC: 66747
D. melanogaster: w1118; PBac{CG12744-GFP.FPTB}VK00033	Bloomington Drosophila Stock Center	BDSC: 55832
D. melanogaster: w1118; PBac{CG15011-GFP.FPTB}VK00033	Bloomington Drosophila Stock Center	BDSC: 64805
D. melanogaster: w1118; PBac{CG15073-GFP.FPTB}VK00033	Bloomington Drosophila Stock Center	BDSC: 59978
D. melanogaster: w1118; PBac{CG1602-GFP.FPTB}VK00033	Bloomington Drosophila Stock Center	BDSC: 59970
D. melanogaster: w1118; PBac{CG1663-GFP.FPTB}VK00033	Bloomington Drosophila Stock Center	BDSC: 67710
D. melanogaster: y1 w*; P{CG17186-GFP.FPTB}attP40	Bloomington Drosophila Stock Center	BDSC: 67391
D. melanogaster: y1 w*; PBac{CG17568-GFP.FPTB}VK00033	Bloomington Drosophila Stock Center	BDSC: 68185
D. melanogaster: y1 w*; P{CG17612-GFP.FPTB}attP40	Bloomington Drosophila Stock Center	BDSC: 92312
D. melanogaster: y1 w*; P{CG18764-GFP.FPTB}attP40	Bloomington Drosophila Stock Center	BDSC: 66442
D. melanogaster: y1 w*; P{CG2712-GFP.FPTB}attP40	Bloomington Drosophila Stock Center	BDSC: 81263

D. melanogaster: y1 w*; PBac{CG30020-GFP.FPTB}VK00031	Bloomington Drosophila Stock Center	BDSC: 81255
D. melanogaster: w1118; PBac{CG3065-GFP.FPTB}VK00033	Bloomington Drosophila Stock Center	BDSC: 59971
D. melanogaster: y1 w*; P{CG31365-GFP.FPTB}attP40	Bloomington Drosophila Stock Center	BDSC: 67724
D. melanogaster: y1 w*; PBac{CG31388-GFP.FPTB}VK00037	Bloomington Drosophila Stock Center	BDSC: 59994
D. melanogaster: y1 w*; P{CG31441-GFP.FPTB}attP40	Bloomington Drosophila Stock Center	BDSC: 81254
D. melanogaster: y1 w*; P{CG32772-GFP.FPTB}attP40	Bloomington Drosophila Stock Center	BDSC: 92385
D. melanogaster: w1118; P{CG3281-GFP.FPTB}attP40	Bloomington Drosophila Stock Center	BDSC: 864830
D. melanogaster: y1 w*; P{CG34376-GFP.FPTB}attP40/CyO	Bloomington Drosophila Stock Center	BDSC: 67394
D. melanogaster: w1118; P{CG4424-GFP.FPTB}attP40	Bloomington Drosophila Stock Center	BDSC: 66404
D. melanogaster: w1118; PBac{CG4707-GFP.FPTB}VK00033	Bloomington Drosophila Stock Center	BDSC: 67722
D. melanogaster: y1 w*; P{CG4730-GFP.FPTB}attP40	Bloomington Drosophila Stock Center	BDSC: 83680
D. melanogaster: y1 w*; PBac{CG4820-GFP.FPTB}VK00037	Bloomington Drosophila Stock Center	BDSC: 59988
D. melanogaster: y1 w*; PBac{CG5245-GFP.FPTB}VK00037	Bloomington Drosophila Stock Center	BDSC: 59989
D. melanogaster: w1118; P{CG6254-GFP.FPTB}attP40	Bloomington Drosophila Stock Center	BDSC: 66591
D. melanogaster: w1118; P{CG6765-GFP.FPTB}attP40	Bloomington Drosophila Stock Center	BDSC: 64833
D. melanogaster: w1118; P{CG6813-GFP.FPTB}attP40	Bloomington Drosophila Stock Center	BDSC: 56840
D. melanogaster: w1118; PBac{CG8388-GFP.FPTB}VK00033/TM6C, Sb1	Bloomington Drosophila Stock Center	BDSC: 64832
D. melanogaster: w1118; PBac{CG8478-GFP.FPTB}VK00037	Bloomington Drosophila Stock Center	BDSC: 56782
D. melanogaster: y1 w*; PBac{CG8924-GFP.FPTB}VK00033	Bloomington Drosophila Stock Center	BDSC: 81259
D. melanogaster: w1118; PBac{CG9609-GFP.FPTB}VK00033	Bloomington Drosophila Stock Center	BDSC: 67708

D. melanogaster: w1118; PBac{CrebB-GFP.FPTB}VK00033	Bloomington Drosophila Stock Center	BDSC: 66399
D. melanogaster: w1118; P{D19B-GFP.FPTB}attP40	Bloomington Drosophila Stock Center	BDSC: 65296
D. melanogaster: y1 w*; P{dati-GFP.FPTB}attP40	Bloomington Drosophila Stock Center	BDSC: 93571
D. melanogaster: y1 w*; PBac{Dref-GFP.FPTB}VK00037	Bloomington Drosophila Stock Center	BDSC: 92325
D. melanogaster: y1 w*; PBac{dwg-GFP.FPTB}VK00037	Bloomington Drosophila Stock Center	BDSC: 92310
D. melanogaster: y1 w*; P{E(bx)-GFP.FPTB}attP40	Bloomington Drosophila Stock Center	BDSC: 68180
D. melanogaster: y1 w*; PBac{emc-GFP.FPTB}VK00037	Bloomington Drosophila Stock Center	BDSC: 55825
D. melanogaster: w1118; PBac{ERR-GFP.FSTF}VK00037	Bloomington Drosophila Stock Center	BDSC: 38638
D. melanogaster: y1 w*; P{fs(1)h-GFP.FPTB}attP40	Bloomington Drosophila Stock Center	BDSC: 83402
D. melanogaster: y1 w*; P{fuss-GFP.FPTB}attP40	Bloomington Drosophila Stock Center	BDSC: 83410
D. melanogaster: w1118; PBac{GATAd-GFP.FPTB}VK00033/TM3, Sb1	Bloomington Drosophila Stock Center	BDSC: 43952
D. melanogaster: w1118; PBac{insv-GFP.FPTB}VK00033	Bloomington Drosophila Stock Center	BDSC: 56189
D. melanogaster: y1 w*; Mi{PT-GFSTF.0}jumuMI00438-GFSTF.0/TM6C, Sb1 Tb1	Bloomington Drosophila Stock Center	BDSC: 59764
D. melanogaster: w1118; PBac{Lpt-GFP.FPTB}VK00033	Bloomington Drosophila Stock Center	BDSC: 64738
D. melanogaster: y1 w*; P{M1BP-GFP.FPTB}attP40	Bloomington Drosophila Stock Center	BDSC: 66739
D. melanogaster: w1118; PBac{Mad-GFP.FLAG}VK00033	Bloomington Drosophila Stock Center	BDSC: 38663
D. melanogaster: y1 w*; PBac{MBD-R2-GFP.FPTB}VK00037	Bloomington Drosophila Stock Center	BDSC: 83669
D. melanogaster: y1 w*; P{mirr-GFP.FPTB}attP40	Bloomington Drosophila Stock Center	BDSC: 38663
D. melanogaster: y1 w*; PBac{MTA1-like-GFP.FPTB}VK00037	Bloomington Drosophila Stock Center	BDSC: 94327
D. melanogaster: w1118; PBac{Nf-YB-GFP.FPTB}VK00033	Bloomington Drosophila Stock Center	BDSC: 56158

D. melanogaster: y1 w*; P{Nf-YC-GFP.FPTB}attP40	Bloomington Drosophila Stock Center	BDSC: 81266
D. melanogaster: w1118; P{nom-GFP.FPTB}attP40	Bloomington Drosophila Stock Center	BDSC: 65297
D. melanogaster: w1118; PBac{oc-GFP.FPTB}VK00033	Bloomington Drosophila Stock Center	BDSC: 66393
D. melanogaster: y1 w*; P{phol-GFP.FPTB}attP40	Bloomington Drosophila Stock Center	BDSC: 66456
D. melanogaster: y1 w*; P{Phs-GFP.FPTB}attP40/CyO	Bloomington Drosophila Stock Center	BDSC: 83407
D. melanogaster: w1118; PBac{prg-GFP.FPTB}VK00033	Bloomington Drosophila Stock Center	BDSC: 64798
D. melanogaster: y1 w*; P{pzg-GFP.FPTB}attP40	Bloomington Drosophila Stock Center	BDSC: 68198
D. melanogaster: y1 w*; PBac{ranshi-GFP.FPTB}VK00037	Bloomington Drosophila Stock Center	BDSC: 83671
D. melanogaster: y1 w*; PBac{sd-GFP.FPTB}VK00033	Bloomington Drosophila Stock Center	BDSC: 79614
D. melanogaster: w1118; PBac{sima-GFP.B.FPTB}VK00037	Bloomington Drosophila Stock Center	BDSC: 43957
D. melanogaster: y1 w*; P{tef-GFP.FPTB}attP40	Bloomington Drosophila Stock Center	BDSC: 83389
D. melanogaster: y1 w*; P{toy-GFP.FPTB}attP40	Bloomington Drosophila Stock Center	BDSC: 83390
D. melanogaster: y1 w*; PBac{zf30C-GFP.FPTB}VK00033	Bloomington Drosophila Stock Center	BDSC: 67397
Software and algorithms		
LAS AF	Leica Microsystems	N/A
ImageJ	Abramoff et al.18,19	N/A
Imaris	Oxford Instruments	N/A
Other		
B5-labeled HCR RNA-FISH iprobe (btd-RA)	Molecular Instruments, Inc	btd-RA
B3-labeled HCR RNA-FISH iprobe (pros-RJ)	Molecular Instruments, Inc	pros-RJ
B5-labeled HCR RNA-FISH iprobe (EGFP)	Molecular Instruments, Inc	EGFP
B2-labeled HCR RNA-FISH iprobe (mRpL15)	Molecular Instruments, Inc	mRpL15-RA

B1-labeled HCR RNA-FISH iprobe (opa)	Molecular Instruments, Inc	opa-RA
B2-labeled HCR RNA-FISH iprobe (dpn)	Molecular Instruments, Inc	dpn-RA

Fly genetics and transgenes

For experiments driving a *UAS*-transgene and the matched controls, crosses were carried out in 6-oz plastic bottles, and eggs were collected on apple caps in 8-hour intervals. Larvae were kept at 25°C and 24 hours after collection were genotypes and transferred to cornmeal caps. Larvae were shifted to 33°C for 72 hours to induce *UAS*-transgene expression for overexpression or knock down unless otherwise specified. *Tubulin-Gal80^{ts}* was used to prevent transgene expression in the embryo for all experiments without heat shock induction. *Worniu-Gal4* was used to drive Pan-NB expression, *31F04-Gal4* (*Tll-Gal4*) was used to drive T2NB specific expression, and *9D11-Gal4* on the second chromosome (*Erm-Gal4*) was used to drive immature INP expression. Experiments shown in Fig. 2.3A and Fig. 2.7L-N utilized the same number of *UAS*-transgenes between control and experimental to account for driver dilution.

GFP reporter transgenes used were cloned with Gateway LR Clonase (ThermoFisher Scientific, Waltham, MA) to insert PCR-amplified genomic regions into the VanGlow vector with the DSCP (Addgene#83338). Coordinates and validated sequences for the enhancers used are included in Appendix Table C.1. For *pros$^{\Delta Ase}$-GFP*, gBlocks (Integrated DNA Technologies, Coralville, IA) were ordered with Ase binding sites (CAGCTG) deleted. The reporters were integrated into the VK22 site on chromosome 2 using φC31-mediated integration (Genetivision Inc). Transgenic flies were identified in

the F1 generation based on their red eye color. Expression was validated by dissecting and imaging wandering third instar larvae.

For generation of *UAS-btd::3XMyc*, open reading frame for *btd-RA* with a 3XMyc epitope added, was cloned into the *pUASt-attB* vector through use of standard PCR, restriction digest and ligation procedures. The Transgene were inserted into the *pUAST-attB M(3xP3-RFP.attP)ZH-86Fb* docking site using ΦC31 integrase-mediated transgenesis.(Bischof et al., 2007) DNA injections were carried out by Genetivision Inc.

Immunofluorescent staining and antibodies

Larval brains were dissected in phosphate buffered saline (1X PBS) before fixation for 23 minutes at 25°C in a solution containing 100 mM PIPES (pH 6.9), 1 mM EGTA, 0.3% Triton X-100 and 1 mM MgSO4 and 4% formaldehyde. Samples were then washed in a solution 1X PBS and 0.3% Triton X-100 (1X PBST). Samples were incubated in a solution of 1X PBST and primary antibody (found in Key Resources Table) for 3 hours at. Samples were washed with 1X PBST before incubated overnight at 4°C in a solution of 1X PBST and secondary antibodies or phalloidin (found in Key Resources Table). The following day samples were washed in 1X PBST before equilibrating in ProLong Gold antifade mount (ThermoFisher Scientific). Adult brain samples were prepared using the same protocol with the adjustment of performing both primary and secondary antibody incubation steps overnight at 4°C.

Hybridization Chain Reaction (HCR) and immunofluorescent staining

Experiments where mRNA transcripts in larval brains were quantified, was done by performing in situ HCR v3.087. All cDNA sequences utilized NCBI to generate HCR

probes. HCR probes can be found in the Key Resources Table. Samples were dissected in 1X PBS and fixed for 23 minutes in a solution of 100 mM PIPES (pH 6.9), 1 mM EGTA, 0.3% Triton X-100 and 1 mM MgSO4 with 4% formaldehyde concentration. After fixing, samples were washed in a solution 1X PBS and 0.3% Triton X-100 (1X PBST). Samples were then incubated in a hybridization buffer (10% formamide, 5×SSC, 0.3% Triton X-100 and 10% dextran sulfate) at 37°C for 1 hr. Following the incubation, 5 nM of primary mRNA HCR probes (Molecular Instruments, Los Angeles, CA) were added to each sample and incubated overnight at 37°C. The following day, samples were washed with SSC buffer (10% formamide, 5×SSC, 0.3% Triton X-100) and were incubated for 30 minutes at 25°C with incubated with amplification buffer (5×SSC, 0.3% Triton X-100 and 10% dextran sulfate). Secondary hairpins (Molecular Instruments, Los Angeles, CA) were denatured at 95°C for 2 minutes and incubated on ice for 5 minutes before 3 μM of each hairpin were added to each sample. Samples were incubated overnight at 25°C. The following day samples were washed in 1X PBST before fixing for 12 minutes to initiate immunofluorescent staining protocol as listed above.

Edu Labeling

Larvae for Edu labeling were collected in 6-oz plastic bottles, and eggs were collected on apple caps in 8-hour intervals. Newly hatched larvae were genotyped and allowed to grow on corn meal caps at 25°C before shifting to 33°C for 48 hours to induce *UAS-ase* expression. This was to ensure the larvae would not be too old to take up Edu containing food. Kankel-White medium caps were prepared with bromophenol blue and with Edu concentration 0.2 mM as previously described.(Daul et al., 2010) Feeding was carried out for three hours. Larvae that took up the Edu containing food as

indicated by blue food in the guts were dissected and processed for antibody staining as described above. After staining, samples were treated with Click-iT™ EdU Cell Proliferation Kit for Imaging, Alexa Fluor™ 555 dye (ThermoFisher Scientific) as per manufacturer instructions. Following this, samples were washed in 1X PBST before equilibrating in ProLong Gold antifade mount (ThermoFisher Scientific).

Imaging and Quantification of immunofluorescent samples

Images of samples were acquired on a Leica SP5 scanning confocal microscope (Leica Microsystems Inc) using a 63X glycerol immersion objective. Images were taken at 1.5X zoom for whole lobe, or 3X zoom for single neuroblasts or clonal lineages. Whole brain lobe images were taken with z-stacks of 1.51 µm thickness, while 3X zoom images and all smFISH images used 0.5 µm thickness.

Quantification was done where the observer was blind to the genotypes. All statistical analyses were performed using a two-tailed Student's t-test with p-values <0.05 (*), <0.005(**), <0.0005 (***), and <0.00005 (****). GraphPad Prism was used to generate dot-plots. Only the central brain was looked at and identified based on morphology. T1NBand T2NB NBs were identified based on size (>7 µm) and expected marker profile or labeling with mcd8:GFP or mcd8:RFP. INPs were identified by small size (<5 µm) and were $Dpn^{+}Ase^{+}$. Experiments targeting T1NBs in Fig 2.3 used the ventral side of the brain where only T1NBs are present.

The number of INPs was manually counted using only one brain lobe per brain. Fractions of T2NBs were calculated by counting all T2NBs in one brain lobe per brain and counting the number of T2NBs that met criteria outlined in each experiment. Fraction of T1NBs generating immature INPs was calculated by counting all T1NBs on

the ventral side of the brain and counting the number of T1NBs that had $Myc^{+}Erm^{+}Dpn^{-}$ small cells directly adjacent. Quantification of foci was done by manually counting the number of foci found in the T2NB in every other z-stack and normalizing to mRpl15 foci. Only one NB per brain was quantified to ensure biological variability. For pixel intensity comparisons, the pixel intensities of Dpn or Ase were measured in nucleus of cells of interest by using Image J software and selecting an ROI and the pixel intensities of GFP reporter in the identical area were measured.

Collection of brains for ATAC-seq, CUT&RUN, and bulk RNA-seq

T2NB enriched brains were acquired as previously described (Larson et al., 2021; Quinto-Rives et al., 2020) where *brat*$^{11/Df}$ brains were collected in 8 hour windows incubated for 120 hours at 25°C. Immature INP and INP enriched brains were acquired as described where pan-NB driver WorGal4 was used to drive *UAS-insb* in *brat*$^{11/Df}$ brains to induce synchronous differentiation by using *Tub-Gal80*^{ts} to control when Insb expression is activated. (Larson et al., 2021; Quinto-Rives et al., 2020) Samples were collected in 8-hour windows and kept at 25°C for 96 hours before shifting to 33°C to induce Insb expression. All INP labeled samples utilized a 24-hour induction. T1NB enriched brains utilized a T1NB specific driver *Ase-Gal4* to mis-express *UAS-aPKC*^{caax} to prevent T1NBs from differentiating as previously described.(Lee, Robinson, et al., 2006) These samples were collected in 8-hour windows and were shifted to 33°C for 72 hours after larval hatching. All samples were dissected in 1X PBS before further processing.

ATAC-seq on NB or INP enriched brains

ATAC-seq was performed as described in (Gibson et al., 2024). Three replicates were collected with at least 5 brains per sample. Samples were collected in 1X PBS and spun down for 3 minutes at 600 g. Supernatant was removed and the brains were resuspended in 50 µl lysis buffer (10 mM Tris pH 7.5, 10 mM NaCl, 3 mM MgCl2, 0.1% NP-40). Samples were transferred to a dounce homogenizer and were dounced at least 40 times on ice. Dounce was washed with 50 µl lysis buffer. 100 µl of sample was transferred to a PCR tube and spun for ten minutes at 500 g at 4°C. Supernatant was removed and pellet was resuspended in a mix containing 5 µl Transposase Buffer, 2.5 µl sterile water, and 2.5 µl Tn5 transposase all sourced from Tagment Illumina. Samples were incubated at 37°C for 30 minutes. DNA was then purified using Qiagen MiniElute Reaction Cleanup Kit (Qiagen) and eluted in 10 µl EB Buffer. DNA was combined with 10 µl Illumina Index, 5 µl water, and 25 µl NEB Next Hi-Fi 2x PCR master mix. DNA was then PCR amplified 12 cycles using the following conditions: 72°C for 5 minutes, 98°C for 30 seconds and then followed by 12 cycles of 98°C for 10 seconds, 63°C for 30 seconds and 72°C for 1 minute. Libraries were purified using 1.1 x AMPure Beads without size selection.(Beckman Coulter). Sequencing utilized IlluminaNovaSeq-6000 chip (University of Michigan Advanced Genomics Core) with 150-bp paired-end reads.

CUT&RUN on NB enriched brains

Samples were prepared as previously described.(Gibson et al., 2024; Arjun Rajan et al., 2023) Brains were dissected in under 45 minutes with at least 50 brains per replicate for TFs and 25 brains per replicate for histone marks. Two replicates were collected for each sample. . Larval brains were dissected in 1X PBS, transferred to 0.5mL Eppendorf tubes, and spun down for 3 minutes at 600 g and supernatant was

removed. Samples were then prepared using CUTANA ChIC/CUT&RUN (Epicypher) per the manufacturer's protocol with some modifications. Brains were resuspended in 100 µl wash buffer before being transferred to a dounce homogenizer and were dounced at least 40 times on ice. Sample was transferred to a 1.5 ml tube and spun for 3 minutes at 600 g. Pellet was processed using CUT&RUN kit. For each sample, 0.5 µg of antibody was used (or 0.5 µl if antibody concentration was unknown). Additionally, 0.5 ng of *Escherichia coli* spike-in DNA was added into every sample as a spike-in control. Samples targeting acetylation utilized 10 mM of sodium butyrate (Sigma Aldrich) in all buffers. Samples using mouse antibodies were processed with an additional antibody incubation step, in which samples were washed twice with cell permeabilization buffer after primary antibody incubation, and then were incubated for 1 hour with 0.5 µg of rabbit anti-mouse IgG (Abcam, ab46540).

DNA was diluted to 50 µl in 0.1x TE which was followed by library prep using the NEBNext Ultra II DNA Library Prep Kit for Illumina (E7645) along with NEBNext Multiplex Oligos for Illumina (E6440). The manufacturer's protocol was followed with modifications. Adaptor was diluted by a ratio 1:25. The bead clean-up steps were performed using 1.1 x AMPure Beads without size selection. The PCR cycle was adjusted to match the settings listed in CUTANA ChIC/CUT&RUN kit. DNA was eluted in 20 µL 0.1 x TE. Agilent TapeStation was used to assess DNA quality and concentration. If samples had greater than 1% adaptor, additional bead cleanup was done. Samples were sequenced on IlluminaNovaSeq-6000 chip (University of Michigan Advanced Genomics Core) with 151-bp end reads.

RNA-seq on NB or INP enriched brains

Samples were prepared as previously described.(Quinto-Rives et al., 2020) Samples were dissected in 20-minute intervals and at least 50 brains were collected. All samples were prepared in triplicate. Samples were prepared in RNase-free conditions. RNA was isolated using TRIzol (ThermoFisher Scientific) and mRNA was then purified using the RNeasy Micro Kit (Qiagen) according to the manufacturer's instructions. Libraries were prepped using SMART-Seq Stranded Kit (Takara, 634444) according to manufacturer's instructions. RNA was sequenced on IlluminaNovaSeq-6000 chip with 150bp end paired reads (University of Michigan Advanced Genomics Core).

Re-analysis of scRNA-seq data

Processed scRNA-seq data from L3 brains consisting of all NB lineages(Marques et al., 2023), T2 lineage(A. Rajan et al., 2023), and INPs(Michki et al., 2021) were downloaded from NIH GEO. Datasets were merged, and QC filtering was performed using scanpy(Wolf et al., 2018) (min genes per cell = 200, min cells per gene = 3, mitochondrial percent < 5). Due to batch effect across datasets, we re-annotated the merged dataset using known marker genes (T2NB: *fru*$^{+}$, *pnt*$^{+}$, *dpn*$^{+}$, *erm*$^{-}$, *ase*$^{-}$; Ase^{-} immature INP: *fru*$^{-}$, *pnt*$^{+}$, *erm*$^{+}$, *ase*$^{-}$, *dpn*$^{-}$, *opa*$^{-}$, *dap*$^{-}$; Ase^{+} immature INP: *fru*$^{-}$, *pnt*$^{+}$, *erm*$^{+}$, *dpn*$^{-}$, *opa*$^{-}$, *dap*$^{-}$; INP: *dpn*$^{+}$, *ase*$^{+}$, *fru*$^{-}$, *opa*$^{+}$, *dap*$^{-}$; T1NB: *fru*$^{+}$, *ase*$^{+}$, *dpn*$^{+}$, *pnt*$^{-}$, *erm*$^{-}$; T1 GMC: *dpn*$^{-}$, *ase*$^{+}$, *Sp1*$^{-}$, *opa*$^{+}$; T2 GMC: *dpn*$^{-}$, *ase*$^{+}$, *Sp1*$^{+}$, *opa*$^{+}$; immature neurons: *Hey*$^{+}$, *fru*$^{-}$, *ase*$^{-}$; neurons: *nSyb*$^{+}$, *ase*$^{-}$). Known marker genes were visualized by cell-type using scanpy dotplot.

Gene were declare on or off based on whether they were expressed above average (z-score > 0) within a given cell-type. Overlapping and differential genes were visualized

using matplotlib venn3 [doi: 10.1109/MCSE.2007.55]. Transcription factors were annotated based on FlyBase's (release FB2024_04) transcription factor category.

Cell type similarity was assessed in two ways. Dendogram based on pearson correlation between cell-types was generated using scanpy dendrogram function. Eucledian distance of the average gene expression between cell-types was caulculated using scipy pdist module (Virtanen et al., 2020), and visualized using seaborn heatmap [doi: https://doi.org/10.21105/joss.03021.].

Data processing and analysis of ATAC-seq

ATAC-seq datasets for T2 and INP enriched brains(Larson et al., 2021) as well as T1 enriched brains were processed. Quality control was performed on FASTQ files using FastQC and FastQ-Screen (https://www.bioinformatics.babraham.ac.uk/projects/fastqc/).(Wingett & Andrews, 2018) Illumina adapters were trimmed from FASTQ files using NGmerge.(Gaspar, 2018) Trimmed reads were aligned to the dm6 genome using bowtie2 using flags: --very-sensitive -I 10 -X 2000.(Langmead & Salzberg, 2012) Duplicate reads were removed using samblaster(Faust & Hall, 2014), and data quality was checked using ATAQV(Orchard et al., 2020). Preliminary bigwig files were generated using deeptools bamCoverage.(Ramírez et al., 2014) MACS2 was used to call peaks using default parameters.(Zhang et al., 2008)

TMM (Trimmed Mean of M-Values) normalization was performed to accout for difference in library composition and sequencing depth. First, all peaks from MACS2 were merged, and blacklisted regions determined by ENCODE were removed.(Amemiya et al., 2019) Then, reads in peaks were counted using featureCounts on each individual

replicate.(Liao et al., 2014) EdgeR calcNormFactors (method = TMM) was colled on each count matrix, and the normalization factor was calculated as 1,000,000/(normFactor * number of reads in peaks).(Robinson et al., 2010) Bigwig files were generated for individual replicates using deeptools bamCoverage on aligned bam files with the scaleFactor equal to the final normalization factor that was calculated, and only mono/sub nucleosomal fragments were kept using maxFragmentSize 120. Bigwigs were then merged using wiggletools write_bg(Zerbino et al., 2014), converted back to bigwig files using bedGraphToBigWig(Kent et al., 2010) and z score bigwig files for histone marks were generated and visualized in IGV(Thorvaldsdóttir et al., 2013).

Data processing and analysis of CUT&RUN

CUT&RUN datasets for T2 enriched brains as well as T1 enriched brains were processed.(Larson et al., 2021; A. Rajan et al., 2023) Quality control was performed on FASTQ files using FastQC and FastQ-Screen. Illumina adapters were trimmed from FASTQ files using NGmerge. Trimmed reads were aligned to the dm6 genome using bowtie2 using flags: --very-sensitive -I 10 -X 2000. Duplicate reads were removed using samblaster. Preliminary bigwig files were generated using deeptools bamCoverage. Transcription factor peaks were called following the CUT&RUNTools2 pipeline(Yu et al., 2021), blacklist regions were removed, and the remaining peaks were merged using bedtools.

TMM (Trimmed Mean of M-Values) normalization was performed to accout for difference in library composition and sequencing depth for bigwig files. First, all peaks from each histone mark were called using gopeaks(Yashar et al., 2022), broad peak calling was used for H3K27me3 and H3K27ac, and narrow peak calling was used for

H3K4me1 and H3K4me3, Peaks for each type of histone mark were merged, and blacklisted regions determined by ENCODE were removed. For transcription factors, peaks generated from CUT&RUNTools2 were used. Reads in peaks were counted using featureCounts on each individual replicate. EdgeR calcNormFactors (method = TMM) was colled on each count matrix, and the normalization factor was calculated as 1,000,000/(normFactor * number of reads in peaks). Bigwig files were generated for individual replicates using deeptools bamCoverage on aligned bam files with the --scaleFactor equal to the final normalization factor that was calculated. Bigwigs were then merged using deeptools bigwigCompare, and z score bigwig files were generated and visualized in IGV.

Data processing and analysis of RNA-seq data

Bulk RNA-seq datasets for T1, T2, immature INP, and INP enriched brains were processed. Quality control was performed on FASTQ files using FastQC and FastQ-Screen. Illumina adapters were trimmed from FASTQ files using cutadapt [doi: https://doi.org/10.14806/ej.17.1.200]. Trimmed reads were aligned to the dm6 transcriptome using hisat2 using flags: --no-mixed –no-discordant.(Kim et al., 2019) A gene by count matrix was generated using featureCounts to count alignments from the hisat2 output to the annotated dm6 transcriptome (refGene). The resulting matrix was processed using DESEQ2 (Love et al., 2014), and a z-score scaled heatmap of known marker genes was generated from the variance stabilized transformed matrix.

Flowcharts, heatmap, and gene list analyses

To determine regions that fulfilled designed criteria, we used bedtools to filter regions based on overlapping peak criteria.(Quinlan & Hall, 2010) ATAC-seq peaks

called by MACS2 were interesected across all replicates (keeping only peaks that are called in every replicate), merged, and ENCODE blacklist regions were removed. Promoters were determined as 1000bp upstream of TSS, and regions overlapping with promoters were also removed. For all analyses, we started from the set of accessible regions that are open in T2NB neuroblasts, as T2NB accessibility is a superset of all accessible regions by visual inspection. Transcription factor peaks were called following the CUT&RUNTools2 pipeline(Yu et al., 2021), merged using bedtools, and ENCODE blacklist regions were removed. Peaks were associated with their nearest gene using homer annotatePeaks(Heinz et al., 2010), and genes lists from the scRNA-seq data were used to associate regions with cell-types that were enriched for the associated gene. Some peaks were manually reassigned to their nearest gene, in the case where Homer misannotates due to the presence of ncRNAs. These cases are highlighted. Data was integrated using pandas [10.25080/Majora-92bf1922-00a] in python, and resulting tables are included within the supplemental data.

We performed k-means clustering on the H3K4me1, H3K27ac, and H3K27me3 CUT&RUN data from T1NB enriched brains using deeptools computeMatrix and plotHeatmap. We performed k-means clustering with n=3 clusters on the set of regions defined by as being accessible in T2NB neuroblasts, not including promoters, and used the z-scored bigwig files for each histone mark. Clusters were extracted from the matrix using plotHeatmap, named based on the histone mark pattern (Active: H3K4me1^{+}, H3K27ac^{+}; Poised: H3K4me1^{+}, H3K27me3^{+}; Inactive: H3K4me1^{-}, H3K27ac^{-}), and interesected using pandas in python as well as visualized

Appendices

Appendix A: Activity for Characterized Enhancers

Table 2.2 Enhancers and genes corresponding to Fig 2.1B

Activity pattern identified manually using Flylight: Gal4 corresponds to Janelia Flylight Line ((Jenett et al., 2012; Li et al., 2014). Red denotes manually reannotated gene name.

Gene Name	Location	Gal4 or reporter	Pattern	Gal4 or reporter	Pattern
Group 1					
btd	chrX: 9689615-9689712	85C07	T2NB		
pnt	chr3R: 23333973-23334697	46C10	No CB expression	45 E10	No CB expression
btd	chrX: 9697466-9697902				
btd	chrX: 9703294-9703423	85C01	No expression		
btd	chrX: 9704175-9704601	85C01	No expression		
eya	chr2L: 6537777-6538106	20C10	T1 NB		
eya	chr2L: 6545012-6545589	20 E04	Neuron Subset		
eya	chr2L: 6533582-6533973	20 E01	T1NB + T2NB		
grn	chr3R: 8187271-8188332	27B03	T1NB + T2NB		
pnt	chr3R: 23300895-23301631	44C09	T2NB		
pnt	chr3R: 23298682-23299026	pntp1 VG	T2NB		
pnt	chr3R: 23297821-23298357				
pnt	chr3R: 23297212-23297609				
pnt	chr3R: 23315163-23315596	pntp3 VG	T2NB		
zfh2	chr4: 517141-517761	73G07	Neuron Subset		
btd	chrX: 9692609-9692921	btd enh VG	T2NB		
Dll	chr2R: 24813545-24814021				
pnt	chr3R: 23293008-23293491				

zfh2	chr4: 502281-503018				
zfh2	chr4: 507193-508782	73G10	Neuron Subset		
btd	chrX:9709732-9709969	85C10	Neuron Subset	85C05	Neuron Subset
btd	chrX:9706789-9707198				
btd	chrX:9703678-9703999	85C01	No CB expression		
btd	chrX:9706018-9706175				
btd	chrX:9707809-9707982	85C08	Neuron Subset		
btd	chrX:9710377-9710610	85C10	Neuron Subset	85C05	Neuron Subset
Dcr-2	chr2R:17580290-17580378				
Dcr-2	chr2R:17580790-17581092				
Dll	chr2R:24819818-24819950	35B01	No CB expression	35A05	No CB expression
Dll	chr2R:24812005-24812330	35D07	Neuron Subset		
Dll	chr2R:24823594-24824074	35C12	Neuron Subset		
Dll	chr2R:24825075-24825171	35C12	Neuron Subset	35C06	Neuron Subset
Dll	chr2R:24821220-24821356	35B01	Neuron Subset		
eya	chr2L:6540421-6540792	21C02	T1 NB		
eya	chr2L:6529390-6529547				
eya	chr2L:6544149-6544294	20 E04	Neuron Subset		
eya	chr2L:6548178-6548333	20C01	Neuron Subset		
eya	chr2L:6540982-6541284	21C02	T1 NB		
eya	chr2L:6527050-6527242				
eya	chr2L:6528008-6528859				
eya	chr2L:6539546-6540121				
grn	chr3R:8162382-8162469				
grn	chr3R:8156347-8156564	26G11	Neuron Subset	26B03	Neuron Subset
grn	chr3R:8157414-8157590	26B03	Neuron Subset	26H11	
grn	chr3R:8164501-8164873				

grn	chr3R:8165187-8165390				
grn	chr3R:8176202-8176348	26 E03	Neuron Subset	26 E06	Neuron Subset
grn	chr3R:8165596-8166242				
grn	chr3R:8167140-8167255				
grn	chr3R:8166891-8166999				
grn	chr3R:8170796-8171281	26G09	T1NB	26B06	T1NB
pnt	chr3R:23306170-23306383	45F08	Neuron Subset	45C12	No CB expression
pnt	chr3R:23303163-23303318	45F08	Neuron Subset	45C12	No CB expression
pnt	chr3R:23309968-23310137	46B11	Neuron Subset		
pnt	chr3R:23323451-23323871	46C12	Neuron Subset		
pnt	chr3R:23343602-23344100				
pnt	chr3R:23341893-23342034	44C01	Neuron Subset		
pnt	chr3R:23319904-23320232	45D11	T2 NB		
pnt	chr3R:23312039-23312213				
pnt	chr3R:23312591-23312935	43D09	Neuron Subset		
zfh2	chr4:522939-523390	73G01	Glia		
zfh2	chr4:527859-528424	73G02	No CB expression		
zfh2	chr4:527552-527758	73G02	No CB expression		
zfh2	chr4:506833-507070	73G10	Neuron Subset		
zfh2	chr4:506297-506421	73G12	Pan neuronal		
zfh2	chr4:519445-520018	73F12	T1 NB		
zfh2	chr4:505174-505734	73G12	Pan neuronal		
Group 2					
lncRNA:cherub	chr3R: 11269201..11269287				
lncRNA:cherub	chr3R: 11268526..11268868				
lncRNA:cherub	chr3R: 11265207..11265862				
lncRNA:cherub	chr3R: 11272748..11272991				
Nrt	chr3L: 16765023..16765312				
lncRNA:cherub	chr3R: 11275985..11276339				

Nrt	chr3L: 16768558..16768959	38B06	T2NB	38C04	T1NB + T2NB
sty	chr3L: 3438743..3439242				
lncRNA:cherub	chr3R: 11279405..11279648				
Sp1	chrX: 9743993..9744660				
jar	chr3R: 24269268..24269707	45F03	T1 NB		
Mmp2	chr2R: 9662046..9662711				
l(1)sc	chrX: 411214..411913				
asRNA:CR43933	chr3L: 21498907..21499094				
jar	chr3R: 24265053..24265336				
erm	chr2L: 1963517..1964072	9D11	Immature INP		
erm	chr2L: 1962787..1963374	9D10	Immature INP		
Trl	chr3L: 14758844..14759415	77G01	T1NB + T2NB		
snRNA:7SK	chr3R: 7474561..7475375				
sty	chr3L: 3418299..3418898				
sty	chr3L: 3420255..3420612				
Nrt	chr3L: 16765560..16765763				
lncRNA:cherub	chr3R: 11269755..11270611				
Trl	chr3L: 14754909..14755758	77F12	T1NB + T2NB		
lncRNA:cherub	chr3R: 11280259..11280417				
lncRNA:cherub	chr3R: 11261068..11261731				
sty	chr3L: 3417226..3417356				
wge	chr3R: 22719077..22719638				
lncRNA:cherub	chr3R: 11254535..11255156				
lncRNA:cherub	chr3R: 11255907..11257101				
lncRNA:cherub	chr3R: 11253854..11254107				
lncRNA:cherub	chr3R: 11278667..11279109				
sty	chr3L: 3438263..3438592				

sty	chr3L: 3426989..3427419				
edl	chr2R: 18671991..18672589				
erm	chr2L: 1967059..1967771				
jar	chr3R: 24264379..24264840				
lncRNA:cherub	chr3R: 11271410..11271513				
lncRNA:cherub	chr3R: 11270720..11271036				
lncRNA:cherub	chr3R: 11263620..11263861				
sty	chr3L: 3440078..3440710				
lncRNA:cherub	chr3R: 11271785..11272040				
Trl	chr3L: 14746651..14746864				
wge	chr3R: 22716334..22716549				
sty	chr3L: 3425350..3425494				
sty	chr3L: 3419901..3420104				
snRNA:7SK	chr3R: 7475699..7476032				
sty	chr3L: 3428165..3428577				
sty	chr3L: 3423412..3423634				
wge	chr3R: 22720599..22720782				
Nrt	chr3L: 16769123..16769275	38B06	T2 NB		
wge	chr3R: 22717931..22718340				
wge	chr3R: 22717586..22717794				
Nrt	chr3L: 16769917..16770329	38C04	T1NB + T2NB		
lncRNA:cherub	chr3R: 11279960..11280158				
lncRNA:cherub	chr3R: 11277378..11277835				
wge	chr3R: 22719830..22720019				
Nrt	chr3L: 16770663..16770799	38C04	T1NB + T2NB		
Mmp2	chr2R: 9659943..9660179				
Sp1	chrX: 9749537..9749646				

Mmp2	chr2R: 9648049..9648429				
Traf4	chr2L: 4375158..4375439				
twit	chr2L: 20853982..20854659				
Sp1	chrX: 9741968..9742109				
Mmp2	chr2R: 9687119..9687285				
Sp1	chrX: 9738071..9738350				
Mmp2	chr2R: 9661612..9661855				
Mmp2	chr2R: 9651886..9652093				
Sp1	chrX: 9738773..9738954				
Mmp2	chr2R: 9660421..9660752				
Mmp2	chr2R: 9661142..9661239				
jar	chr3R: 24269871..24270134	92F12	T1NB + T2NB		
Sp1	chrX: 9746388..9746746				
l(1)sc	chrX: 412676..413041				
erm	chr2L: 1959960..1960123	9D10	Immature INP		
erm	chr2L: 1953137..1953685				
VepD	chr2R: 22407623..22407906				
Mmp2	chr2R: 9675907..9676168				
l(1)sc	chrX: 407625..407756	13B12	Neuron Subset		
erm	chr2L: 1965330..1965445	9D11	Immature INP		
l(1)sc	chrX: 406185..406433	13B12	Neuron Subset		
jar	chr3R: 24270243..24270481	92F12	T1NB + T2NB		
edl	chr2R: 18671478..18671643				
Mmp2	chr2R: 9649770..9650057				
Traf4	chr2L: 4357777..4357882				
Traf4	chr2L: 4358949..4359100				
Mmp2	chr2R: 9680612..9680821				

Sp1	chrX: 9736900..9737165				
edl	chr2R: 18675371..18675715				
jar	chr3R: 24263136..24263326	45A05	Neuron Subset		
asRNA:CR43933	chr3L: 21499403..21499497				
twit	chr2L: 20851776..20852061				
Sp1	chrX: 9735798..9735935				
erm	chr2L: 1964859..1965073	9D11	Immature INP		
Sp1	chrX: 9730161..9730631				
gogo	chr3L: 20293056..20293381	92F12	T1NB + T2NB		
Traf4	chr2L: 4372275..4372561				
l(1)sc	chrX: 405722..405946	13B12	Neuron Subset		
Mmp2	chr2R: 9655283..9655685				
Group 3					
Hmx	chr3R:17572143-17572395				
Mnt	chrX:3684956-3685151	13F01	T1NB + T2NB		
shep	chr3L:5184256-5184372				
Alh	chr3R:7122825-7123485				
cas	chr3R:5719338-5719730	71G07	T1NB + T2NB		
cas	chr3R:5729216-5729718	71C09	INP + GMC		
CenG1A	chr2L:13876131-13876619				
CG17716	chr2R:13617039-13617344				
CG17716	chr2R:13621200-13621697				
CG31998	chr4:207056-207812				
D	chr3L:14163784-14164218	73B07	T1NB + T2NB		
D	chr3L:14170112-14170680	73B10	T1NB		
Dmtn	chr3R:6395925-6396333				
Eip63E	chr3L:3536749-3537349				

Eph	chr4:611015-611234				
Gug	chr3L:8470680-8470985				
Gug	chr3L:8455087-8455480				
Gug	chr3L:8460296-8460693				
ham	chr2L:18786487-18787125	80G10	ImmINP		
hdc	chr3R:30334310-30334915				
hdc	chr3R:30275991-30276597				
hdc	chr3R:30332537-30332777				
hdc	chr3R:30284817-30285431				
Hmx	chr3R:17572911-17573625	80C12	T2NB		
Hmx	chr3R:17573981-17574524	80C12	T2NB		
kek5	chrX:19359416-19359859				
Kr-h1	chr2L:6086783-6087729				
lncRNA:roX2	chrX:11578978-11579117				
MEP-1	chr3L:2636081-2636457				
Mnt	chrX:3690876-3691383	13D03	T1NB + T2NB		
Mnt	chrX:3686571-3687417	12B10	T1NB + T2NB		
OtopLa	chrX:5649860-5650149				
OtopLa	chrX:5639320-5640047				
pico	chrX:19842129-19842975				
Ptpmeg	chr3L:349138-349544				
RhoGEF2	chr2R:17028257-17028555				
shep	chr3L:5174050-5174446				
shep	chr3L:5178911-5179644				
TfAP-2	chr3L:21611700-21612174	23 E06	T1NB + T2NB		
Agpat1	chrX:12765599-12765867				
Alh	chr3R:7104133-7104622	83A06	T1NB + T2NB		

Alh	chr3R:7103298-7103827	83A03	T1NB + T2NB		
alpha-Man-Ia	chrX:10302430-10302660				
beta-Spec	chrX:17658206-17659264				
CenG1A	chr2L:13890112-13891196				
CenG1A	chr2L:13837041-13837906				
CenG1A	chr2L:13877834-13878335				
CenG1A	chr2L:13887056-13887397				
CG11360	chr4:682443-683243				
CG17716	chr2R:13617486-13617951				
CG5004	chrX:17124140-17125096				
D	chr3L:14171612-14172568	73C02	INPs		
D	chr3L:14156874-14157570	73B12	INPs		
Dg	chr2R:16096556-16096823				
Eip63E	chr3L:3542456-3542820				
Gug	chr3L:8458735-8459270				
hdc	chr3R:30276772-30277264				
Hmx	chr3R:17566637-17567504				
Hmx	chr3R:17557483-17557931	80C09	Neuron Subset		
kek5	chrX:19393486-19393811				
kek5	chrX:19360939-19361630				
kek5	chrX:19364104-19364376				
Kr-h1	chr2L:6087844-6088875				
Kr-h1	chr2L:6081185-6081724				
Mnt	chrX:3678196-3678438	12C10	T1NB + T2NB		
Mnt	chrX:3672091-3672383				
Mnt	chrX:3694703-3695030	13A06	T1NB + T2NB		
Mnt	chrX:3676712-3677221	13G02	T1NB		

Mnt	chrX:3677401-3677964	13G02	T1NB		
Mnt	chrX:3685532-3685819	13F01	T1NB + T2NB		
Mnt	chrX:3691647-3691887	13D03	T1NB + T2NB		
OtopLa	chrX:5646514-5647039				
OtopLa	chrX:5649227-5649747				
OtopLa	chrX:5636653-5637184				
OtopLa	chrX:5638414-5639197				
pico	chrX:19847228-19847592				
Rbfox1	chr3L:10517494-10517877				
Rbfox1	chr3L:10525506-10526064				
Rbfox1	chr3L:10526314-10526922				
Rbfox1	chr3L:10516253-10517030				
Rbfox1	chr3L:10508085-10508266				
sgg	chrX:2652343-2652745				
shep	chr3L:5182711-5183257				
shep	chr3L:5249159-5249420				
Swip-1	chr2L:18982709-18983380				
TfAP-2	chr3L:21610330-21610972	23F12	T1NB + T2NB		
TfAP-2	chr3L:21584704-21585199	24G06	Pan neuronal		
TfAP-2	chr3L:21604425-21604661	25A02	T1NB + T2NB		
Alh	chr3R:7105525-7105932	83A05	T1NB + T2NB		
Alh	chr3R:7102888-7103135	83A03	T1NB + T2NB		
alpha-Man-Ia	chrX:10290702-10290904				
alpha-Man-Ia	chrX:10307899-10308642				
alpha-Man-Ia	chrX:10324541-10324839				
alpha-Man-Ia	chrX:10320223-10320362				
alpha-Man-Ia	chrX:10318498-10319005				

alpha-Man-Ia	chrX:10319199-10319563				
Ank	chr4:128897-129008				
Ank	chr4:130656-130810				
cas	chr3R:5716330-5716494				
CASK	chr3R:21821466-21821598	66B01	Neuron Subset		
CASK	chr3R:21816163-21816506	64B02	Neuron Subset		
CASK	chr3R:21809332-21809576	64F03	Neuron Subset		
CenG1A	chr2L:13877003-13877351	64D06	No CB expression		
CenG1A	chr2L:13892041-13892457				
CenG1A	chr2L:13893286-13893586				
CenG1A	chr2L:13875631-13875892				
CenG1A	chr2L:13894484-13895055				
CG11360	chr4:670383-670526				
CG11360	chr4:682115-682323				
CG11399	chr3L:20784513-20784757				
CG13784	chr2L:7219339-7219544				
CG13784	chr2L:7218942-7219097				
CG17716	chr2R:13629741-13630186				
CG17716	chr2R:13639197-13639586				
CG17716	chr2R:13626890-13627464				
CG17716	chr2R:13634857-13635016				
CG17716	chr2R:13628320-13628564				
CG17716	chr2R:13638107-13638220				
CG17716	chr2R:13638856-13639098				
CG5004	chrX:17110625-17111094				
CG5004	chrX:17108736-17109144				
CG5004	chrX:17112424-17112822				
CG5004	chrX:17113599-17113790				

CG5004	chrX:17137048-17137452				
D	chr3L:14165934-14166283	73C01	Neuron Subset		
D	chr3L:14165431-14165594	73C01	Neuron Subset		
D	chr3L:14161847-14162061	73C03	Neuron Subset		
D	chr3L:14181474-14181847	12G08	No CB expression	13B02	Neuron Subset
D	chr3L:14172853-14173019	73C02	INPs		
D	chr3L:14160860-14161038				
Dab	chr3L:16714018-16714155				
Dbp80	chr3L:27279729-27279851				
Dbp80	chr3L:27280566-27280764				
Dbp80	chr3L:27291715-27291876				
Dbp80	chr3L:27289725-27289941				
Dbp80	chr3L:27288368-27288613				
Dg	chr2R:16091225-16091687				
Dg	chr2R:16097228-16097687				
Dg	chr2R:16095604-16095727				
DIP2	chr3L:256843-257166				
DIP2	chr3L:257286-257436				
Dmtn	chr3R:6396649-6396886				
Dmtn	chr3R:6402912-6403069				
Eip63E	chr3L:3518095-3518391				
Eip63E	chr3L:3537675-3537883				
Eip63E	chr3L:3516623-3516774				
EndoA	chr3R:18906144-18906283				
EndoA	chr3R:18907401-18907638				
Eph	chr4:612443-612551				
Gug	chr3L:8451746-8452065				

Gug	chr3L:8455780-8456242	83B10	T1NB + T2NB	83C02	Neuron Subset
Gug	chr3L:8459607-8459977	83B11	T1NB + T2NB		
Gug	chr3L:8457950-8458082	83B10	T1NB + T2NB		
Gug	chr3L:8460850-8460940	83B11	T1NB + T2NB		
Gug	chr3L:8457485-8457737	83B10	T1NB + T2NB		
Gug	chr3L:8461537-8461771	83B11	T1NB + T2NB		
ham	chr2L:18793975-18794233	80G04	No CB expression		
ham	chr2L:18772411-18772853	80G12	Neuron Subset		
ham	chr2L:18785914-18786227	80G10	ImmINP		
ham	chr2L:18785113-18785345	80G10	ImmINP	80F10	Neuron Subset
ham	chr2L:18793169-18793270	80G08	Neuron Subset	80G04	
hdc	chr3R:30351675-30352017				
hdc	chr3R:30347350-30347640				
hdc	chr3R:30281171-30281321				
hdc	chr3R:30344230-30344596				
hdc	chr3R:30284301-30284611				
hdc	chr3R:30291331-30291525				
hdc	chr3R:30281897-30282204				
hdc	chr3R:30335216-30335410				
hdc	chr3R:30338111-30338376				
hdc	chr3R:30346679-30346913				
Hmx	chr3R:17556251-17556515	80C09	Neuron Subset		
Hmx	chr3R:17562128-17562412				
Hmx	chr3R:17552998-17553221				
Hmx	chr3R:17567713-17567874				
Hmx	chr3R:17575171-17575722				
Hmx	chr3R:17576220-17576631				

Hmx	chr3R:17569296-17569458				
kek5	chrX:19397782-19398012				
kek5	chrX:19385510-19385718				
kek5	chrX:19396762-19397092				
kek5	chrX:19354342-19354639				
kek5	chrX:19399609-19399887				
kek5	chrX:19403380-19403703				
kek5	chrX:19401587-19401920				
kek5	chrX:19400788-19401134				
kek5	chrX:19354881-19355040				
kek5	chrX:19384533-19384743				
kek5	chrX:19359004-19359311				
kek5	chrX:19371836-19372422				
kek5	chrX:19377232-19377363				
kek5	chrX:19364476-19364715				
kek5	chrX:19375499-19375794				
Kr-h1	chr2L:6082952-6083397				
Kr-h1	chr2L:6085645-6086076	81C08	T1NB + T2NB		
Kr-h1	chr2L:6089043-6089404	81C06	T1NB + T2NB		
MFS17	chr2R:2566336-2566444				
MFS17	chr2R:2587007-2587210				
MFS17	chr2R:2693909-2694032				
MFS17	chr2R:2564153-2564526				
MFS17	chr2R:2600714-2600872				
MFS17	chr2R:2596895-2596996				
MFS17	chr2R:2567064-2567227				
MFS17	chr2R:2630402-2630507				

MFS17	chr2R:2694140-2694246				
MFS17	chr2R:2564939-2565051				
MFS17	chr2R:2562492-2562930				
Mnt	chrX:3681797-3681928	13G05	Neuron Subset		
Mnt	chrX:3673928-3674071	12D10	Neuron Subset		
Mnt	chrX:3672867-3673017	12D10	Neuron Subset		
Mnt	chrX:3681169-3681339	13G05	Neuron Subset		
Mnt	chrX:3692456-3692623	13D03	T1NB + T2NB		
Mnt	chrX:3690518-3690709	13D03	T1NB + T2NB		
Mnt	chrX:3682053-3682231	13G05	Neuron Subset		
Mnt	chrX:3682435-3682726	13G05	Neuron Subset		
Mnt	chrX:3694180-3694290	13A06	T1NB + T2NB		
onecut	chr4:608199-608458				
onecut	chr4:608010-608102				
onecut	chr4:606941-607162				
OtopLa	chrX:5640639-5640770				
OtopLa	chrX:5647740-5648096				
OtopLa	chrX:5630821-5631385				
pico	chrX:19846967-19847054				
pico	chrX:19843160-19843398				
Ptpmeg	chr3L:329239-329397				
Rbfox1	chr3L:10507377-10507489				
Rbfox1	chr3L:10518072-10518500				
Rbfox1	chr3L:10485469-10485881				
sgg	chrX:2665334-2666063				
sgg	chrX:2659558-2659848				
sgg	chrX:2634939-2635053				
sgg	chrX:2657496-2657746				

sgg	chrX:2663839-2664023				
sgg	chrX:2655137-2655384				
sgg	chrX:2636049-2636595				
sgg	chrX:2636926-2637103				
sgg	chrX:2645705-2645804				
shep	chr3L:5266847-5267193				
shep	chr3L:5187276-5187435				
shep	chr3L:5193107-5193462				
shep	chr3L:5169219-5169498				
shep	chr3L:5247604-5247779				
shep	chr3L:5278768-5279013				
shep	chr3L:5188016-5188128				
shep	chr3L:5186908-5187107				
shep	chr3L:5191970-5192164				
shep	chr3L:5206329-5206453				
shep	chr3L:5211630-5211989				
shep	chr3L:5192777-5192896				
shep	chr3L:5169804-5170311				
shep	chr3L:5194851-5194945				
shep	chr3L:5288115-5288220				
shep	chr3L:5213804-5213892				
shep	chr3L:5296236-5296493				
shep	chr3L:5243956-5244096				
shep	chr3L:5271406-5272052				
shep	chr3L:5246924-5247127				
Swip-1	chr2L:18983683-18983891				
Swip-1	chr2L:18982105-18982304				

TfAP-2	chr3L:21611221-21611467				
TfAP-2	chr3L:21589989-21590352	24F12	T1NB		
TfAP-2	chr3L:21587764-21588289	24B02	Neuron Subset		
TfAP-2	chr3L:21585692-21586337	24G06	Pan neuronal		
TfAP-2	chr3L:21589623-21589797	24F12	T1NB	24B02	Neuron Subset
trio	chr3L:1023784-1024076	24F12	T1NB	16B10	T1NB + T2NB
trio	chr3L:1006180-1006367	17B01	Neuron Subset		
trio	chr3L:1022089-1022267	17A11	Neuron Subset		
ttv	chr2R:14565966-14566329				
ttv	chr2R:14533152-14533470				
ttv	chr2R:14535881-14536218				
ttv	chr2R:14530593-14530702				
Group 4					
Myo81F	chr3R:235696-235807				
Myo81F	chr3R:304167-304270				
dnc	chrX:3285404-3285589	14 E05	Neuron Subset		
dnc	chrX:3189766-3189948	13G04	T1NB		
lncRNA:CR44417	chr2R:17868949-17869068				
Myo81F	chr3R:316767-316899				
Myo81F	chr3R:202059-202548				
Myo81F	chr3R:289643-289755				
Ten-a	chrX:12196993-12197106				
asRNA:CR44029	chr4:879369-879600				
asRNA:CR44029	chr4:879717-879897				
CG11873	chr3R:29073951-29074575				
CG13454	chr3L:15514440-15514704				
CG3408	chr3L:9508447-9508776				

CG3764	chr3L:17010957-17011609				
dnc	chrX:3178591-3178775	14B11	T1NB		
elav	chrX:525643-525949	71C07	T1NB + T2NB		
esg	chr2L:15339081-15339334				
ey	chr4:696784-696999				
glec	chr3R:21854349-21854482				
jim	chr3L:22803794-22804032				
Mkp3	chr3L:19081300-19081687				
Mkp3	chr3L:19079180-19079509				
Myo81F	chr3R:324961-325236				
Myo81F	chr3R:212368-212716				
Myo81F	chr3R:156361-157162				
Myo81F	chr3R:162516-162821				
Myo81F	chr3R:219049-219209				
Myo81F	chr3R:950867-951091				
Myo81F	chr3R:129326-129461				
Myo81F	chr3R:304676-304812				
Myo81F	chr3R:831885-832083				
Myo81F	chr3R:143053-143245				
Myo81F	chr3R:35552-35708				
Myo81F	chr3R:328360-328649				
Myo81F	chr3R:148549-148716				
Myo81F	chr3R:329543-329682				
Nrx-IV	chr3L:12146857-12147430				
Optix	chr2R:8044601-8045079	95A04	T2NB		
Optix	chr2R:8038955-8039388	95A06	Neuron Subset		
Optix	chr2R:8046235-8046846	30D11	Neuron Subset		
Optix	chr2R:8038288-8038771	30D11	Neuron Subset		

RapGAP1	chr2L:7573451-7573913				
RapGAP1	chr2L:7576910-7577393				
rdgB	chrX:13761596-13762391				
Sema1a	chr2L:8542783-8542909				
side	chr3R:27438492-27438639				
sli	chr2R:15922809-15923096				
Thd1	chr4:554906-555205	59H10	T1NB + T2NB		
tkv	chr2L:5247502-5248036				
tkv	chr2L:5240477-5240869				
UbcE2H	chrX:8091237-8091715				
UbcE2H	chrX:8092595-8093681				
unc-5	chr2R:15360277-15360567	93F01	Neuron Subset		
ap	chr2R:5710970-5711649	42B11	T1NB		
ap	chr2R:5735573-5737173	41C10	T1NB + T2NB		
caps	chr3L:13227184-13228097				
CG11873	chr3R:29068629-29069945				
CG11873	chr3R:29086997-29087643				
CG42258	chrX:12470096-12470623				
CG6191	chr2R:13587194-13588023				
crol	chr2L:11807590-11808309	77G08	Glia		
crol	chr2L:11805915-11807452	77G08	Glia		
dnc	chrX:3332459-3332896	13 E05	Glia		
dnc	chrX:3205851-3206430	13G04	T1NB		
dnc	chrX:3190767-3191078				
E(spl)m7-HLH	chr3R:26036231-26036562				
elav	chrX:523881-524791	71C07	T1NB + T2NB		
esg	chr2L:15332666-15332864				

Evi5	chrX:11453144-11453516				
ey	chr4:713103-713524				
Flo2	chrX:14842000-14842526				
fra	chr2R:12531843-12532470				
glec	chr3R:21853626-21854097				
glec	chr3R:21854833-21855127				
His3.3B	chrX:9152310-9152500				
jim	chr3L:22822481-22823161	80 E01	Neuron Subset		
jing	chr2R:6607107-6607805				
jing	chr2R:6612883-6613271				
Lac	chr2R:12455648-12456787				
Lar	chr2L:19590338-19591056				
lncRNA:CR43651	chr2R:9552559-9553079				
lncRNA:CR43724	chr2R:8029224-8030264	29F07	Pan Neuronal		
lncRNA:CR43857	chr2L:7420866-7421400				
lncRNA:CR43857	chr2L:7423506-7423933				
lncRNA:CR43857	chr2L:7420528-7420766				
lncRNA:CR43857	chr2L:7422414-7422749				
lncRNA:CR43857	chr2L:7419986-7420337				
lncRNA:CR43857	chr2L:7418421-7418690				
lncRNA:CR44417	chr2R:17869202-17869694				
lncRNA:CR45054	chr3R:10080562-10081120				
lncRNA:CR45054	chr3R:10079282-10079543				
lncRNA:CR45054	chr3R:10082727-10083354				
lncRNA:CR45054	chr3R:10084039-10084593				
lncRNA:CR45919	chr2L:17558372-17558882				
lncRNA:CR45919	chr2L:17560216-17560951				

lncRNA:CR45919	chr2L:17559206-17559810				
LRP1	chr2R:8183580-8183906				
myo	chr4:695275-695700				
Myo81F	chr3R:306910-307104				
Myo81F	chr3R:140093-140561				
Myo81F	chr3R:164924-165331				
Myo81F	chr3R:41621-41889				
Myo81F	chr3R:314648-315139				
Myo81F	chr3R:137754-138067				
Myo81F	chr3R:172566-173124				
Myo81F	chr3R:315604-316383				
Myo81F	chr3R:36506-37114				
Myo81F	chr3R:327201-327407				
Myo81F	chr3R:141496-141870				
Myo81F	chr3R:125225-125486				
Myo81F	chr3R:142205-142653				
Myo81F	chr3R:38027-38141				
Myo81F	chr3R:293476-293677				
Myo81F	chr3R:123085-124168				
Myo81F	chr3R:173299-175447				
Myo81F	chr3R:40118-40562				
Myo81F	chr3R:296082-296514				
opa	chr3R:4863832-4864255	77B03	T1NB + T2NB		
opa	chr3R:4865213-4865475	77B03	T1NB + T2NB		
opa	chr3R:4858681-4859305				
opa	chr3R:4845050-4845890	77B05	INP		
osa	chr3R:17710704-17711891	59H05	T1NB + T2NB		
ph-p	chrX:2135473-2135806				

ph-p	chrX:2137408-2137800				
ph-p	chrX:2134504-2135236				
Pp2C1	chrX:4684323-4684926				
Pp2C1	chrX:4686352-4686530				
Ptp99A	chr3R:29376250-29376855				
Ptp99A	chr3R:29414527-29415324				
Ptp99A	chr3R:29375737-29376035				
Rac2	chr3L:7433646-7434712				
RapGAP1	chr2L:7550853-7551440				
RapGAP1	chr2L:7534982-7535263				
rgr	chr2R:8601487-8601876				
Sema1a	chr2L:8556167-8557350	34 E08	T1NB + T2NB		
Sema1a	chr2L:8543899-8544315	33 E11	T1NB + T2NB		
Sema1a	chr2L:8550542-8551064	32H10	T1NB + T2NB		
shg	chr2R:21044947-21045678				
sm	chr2R:19631832-19632158				
sm	chr2R:19624510-19625536				
tap	chr3L:17361841-17362305				
tara	chr3R:16247922-16248597				
Ten-a	chrX:12212531-12213339				
tna	chr3L:10855299-10855866	60C09	T1NB + T2NB		
tna	chr3L:10865729-10866162	60B02	T1NB + T2NB		
tna	chr3L:10861443-10862284	60C04	T1NB + T2NB		
tna	chr3L:10856069-10857022	60C04	T1NB + T2NB		
unc-119	chrX:7294456-7294922				
unc-119	chrX:7293026-7294254				
unc-5	chr2R:15339533-15339876	93 E11	No expression		

unc-5	chr2R:15351558-15352652	93 E08	Neuron Subset		
unc-5	chr2R:15349410-15349763				
Wnt4	chr2L:7272138-7272957	25A11	Neuron Subset		
ap	chr2R:5709696-5710306	41C10	T1NB + T2NB		
ap	chr2R:5715439-5715783	40A07	Neuron Subset		
ap	chr2R:5731678-5732608	41D11	Neuron Subset	41D03	Neuron Subset
ap	chr2R:5718875-5719041	39C09	Neuron Subset		
ap	chr2R:5717310-5717602	42B11	T1NB		
ap	chr2R:5735289-5735426	42B11	T1NB		
ap	chr2R:5725852-5725991				
arg	chrX:513715-513951				
asRNA:CR44029	chr4:883083-883300				
asRNA:CR44029	chr4:878860-879061				
Cad74A	chr3L:17375555-17375817				
Cap-G	chr2R:13142238-13142663				
Cap-G	chr2R:13141043-13141258				
Cap-G	chr2R:13133430-13133885				
Cap-G	chr2R:13139953-13140154				
caps	chr3L:13236850-13237184				
caps	chr3L:13226516-13226985				
CG10011	chr3R:28627241-28627678				
CG10011	chr3R:28626913-28627130				
CG10011	chr3R:28621230-28621420				
CG10011	chr3R:28629373-28629610				
CG10011	chr3R:28635629-28635878				
CG10011	chr3R:28629747-28629935				
CG10011	chr3R:28634066-28634228				
CG10082	chr2R:21645595-21645846				

CG10508	chr3L:21212136-21212283				
CG10508	chr3L:21211573-21212016				
CG11873	chr3R:29068098-29068269				
CG11873	chr3R:29070261-29070699				
CG11873	chr3R:29083998-29084215				
CG11873	chr3R:29075527-29075687				
CG11873	chr3R:29081951-29082288				
CG11873	chr3R:29085140-29085327				
CG11873	chr3R:29080850-29081228				
CG11873	chr3R:29078883-29079245				
CG13454	chr3L:15514990-15515155				
CG14200	chrX:19510318-19510465				
CG14200	chrX:19511527-19511755				
CG15744	chrX:13287440-13287756				
CG2225	chr2L:21678240-21678878				
CG31122	chr3R:18422373-18422773				
CG31729	chr2L:13294270-13294372				
CG32640	chrX:13171957-13172188	24A08	T2NB		
CG32640	chrX:13177604-13177753				
CG32640	chrX:13174856-13175437				
CG32640	chrX:13179412-13179561				
CG32809	chrX:1691527-1691707	55A06	No CB expression		
CG3634	chr3L:20807206-20807295				
CG3764	chr3L:17007269-17007398				
CG3764	chr3L:17010082-17010558				
CG3764	chr3L:17004468-17004782				
CG3764	chr3L:17003807-17003969				

CG3764	chr3L:17004066-17004247				
CG42258	chrX:12472903-12473013				
CG42258	chrX:12466938-12467356				
CG42258	chrX:12464014-12464550				
CG42258	chrX:12472162-12472308				
CG6191	chr2R:13591151-13591301				
CG6191	chr2R:13592361-13592500				
CG6420	chr3R:26723741-26724071				
CG7369	chr3L:22743298-22743438				
CG9171	chr2L:5777915-5778284				
CG9171	chr2L:5800980-5801142				
ClC-c	chr3L:16091256-16091605				
crol	chr2L:11804838-11805160	77G10	T1NB + T2NB		
DAAM	chrX:1295279-1295610				
DAAM	chrX:1315747-1316075				
DAAM	chrX:1321088-1321578				
dnc	chrX:3288319-3289005	15C04	Neuron Subset	15D05	Neuron Subset
dnc	chrX:3185556-3185915				
dnc	chrX:3180334-3180463				
dnc	chrX:3273926-3274131	12C07	Neuron Subset	12D12	Neuron Subset
dnc	chrX:3202704-3202886	12H08	Neuron Subset		
dnc	chrX:3298077-3298230	15D06	Neuron Subset		
dnc	chrX:3298969-3299147	15D06	Neuron Subset		
dnc	chrX:3291679-3291804	15D10	Neuron Subset		
dnc	chrX:3306666-3307067	15D10	Neuron Subset		
dnc	chrX:3198634-3198796	13 E11	Neuron Subset	13A03	Neuron Subset
dnc	chrX:3190517-3190653	13G04	T1NB		

dnc	chrX:3191213-3191531	13G04	T1NB		
dnc	chrX:3311240-3311533	15B12	Neuron Subset		
Dsp1	chrX:16334350-16334515	56D11	T1NB + T2NB		
Dsp1	chrX:16334056-16334225				
Dsp1	chrX:16339386-16339749				
Dsp1	chrX:16335391-16335536	56D11	T1NB + T2NB		
E(Pc)	chr2R:11450600-11451344				
E(spl)m7-HLH	chr3R:26034677-26035336				
elav	chrX:522323-522677	27 E08	T1NB		
esg	chr2L:15343343-15343514				
esg	chr2L:15334295-15334486				
esg	chr2L:15327286-15327387				
esg	chr2L:15339474-15340062				
Evi5	chrX:11452892-11453027				
ewg	chrX:278052-278305	51D10	T1NB + T2NB		
ey	chr4:702018-702196	16F06	Neuron Subset		
ey	chr4:713918-714447				
ey	chr4:699282-699530	16F10	INP		
ey	chr4:715578-715847	16 E03	Neuron Subset		
ey	chr4:701145-701451	16F06	Neuron Subset		
ey	chr4:708966-709163	16H11	Neuron Subset		
ey	chr4:702923-703109				
Fas3	chr2L:18317597-18317861				
Fas3	chr2L:18331630-18331738				
Fas3	chr2L:18322744-18322869				
Fas3	chr2L:18327143-18327344				
Fas3	chr2L:18336480-18336678				
Fas3	chr2L:18324060-18324169				
Fas3	chr2L:18332529-18332675				

Fas3	chr2L:18328574-18328835				
Flo2	chrX:14840900-14841314				
fra	chr2R:12532948-12533105	28D08	T1NB + T2NB	28F11	T1NB
fra	chr2R:12536257-12536346	28H03	T1NB		
Fur1	chr3R:25472069-25472386	25H06	Neuron Subset		
Fur1	chr3R:25445220-25445463	26H09	Pan neuronal		
Fur1	chr3R:25454734-25454861	26C12	Neuron Subset		
Fur1	chr3R:25445815-25446190	26H09	Pan neuronal		
Fur1	chr3R:25449577-25449698	25G10	Neuron Subset	27A05	T1NB
Fur1	chr3R:25456810-25457391	26B12	Neuron Subset		
Fur1	chr3R:25446334-25447093	27A05	T1NB		
glec	chr3R:21857909-21858160				
glec	chr3R:21855555-21855872				
hbn	chr2R:20959223-20959547	34G10	INP		
hbn	chr2R:20957942-20958027	35A03	T1NB + T2NB		
hbn	chr2R:20956168-20956373	35A03	T1NB + T2NB		
hbn	chr2R:20955450-20955709				
hbn	chr2R:20963324-20963650				
jim	chr3L:22829143-22829329	80D10	Neuron Subset	80 E02	Neuron Subset
jim	chr3L:22830581-22831194	80D10	Neuron Subset		
jim	chr3L:22823907-22824260	80D09	Neuron Subset	80 E01	Neuron Subset
jim	chr3L:22812511-22812721				
jim	chr3L:22801974-22802377	87 E03	Neuron Subset		
jim	chr3L:22797830-22798164				
jim	chr3L:22805547-22805701				
jim	chr3L:22820293-22820411	80 E03	Neuron Subset		
jim	chr3L:22810791-22811092				

jing	chr2R:6605769-6605885				
jing	chr2R:6606010-6606111				
jing	chr2R:6504491-6504773				
Lac	chr2R:12457402-12457696				
Lac	chr2R:12454124-12454317				
Lac	chr2R:12460111-12460235				
Lar	chr2L:19591273-19591399				
Lar	chr2L:19619710-19619959				
Lar	chr2L:19617155-19617682				
Lar	chr2L:19612391-19612583				
Lar	chr2L:19621134-19621287				
lncRNA:CR42862	chr3L:225236-225433				
lncRNA:CR43651	chr2R:9552099-9552365				
lncRNA:CR43724	chr2R:8024306-8024731				
lncRNA:CR43857	chr2L:7419712-7419875				
lncRNA:CR45054	chr3R:10081648-10081914				
lncRNA:CR45054	chr3R:10082371-10082594				
lncRNA:CR45919	chr2L:17561991-17562364				
LRP1	chr2R:8181281-8181533				
LRP1	chr2R:8176662-8176959				
LRP1	chr2R:8188591-8189178				
LRP1	chr2R:8183111-8183257				
LRP1	chr2R:8180308-8180774				
LRP1	chr2R:8179742-8179966				
mib1	chr3L:16012481-16012769				
Mkp3	chr3L:19086973-19087202				
Mkp3	chr3L:19079852-19080207				

Mkp3	chr3L:19087390-19087868				
Mkp3	chr3L:19077407-19077653				
msl-2	chr2L:3465326-3465757				
myo	chr4:692111-692280				
Myo81F	chr3R:224257-224701				
Myo81F	chr3R:213860-214206				
Myo81F	chr3R:314435-314542				
Myo81F	chr3R:866011-866168				
Myo81F	chr3R:459199-459421				
Myo81F	chr3R:567919-568056				
Myo81F	chr3R:457491-457657				
Myo81F	chr3R:933381-933478				
Myo81F	chr3R:428532-428800				
Myo81F	chr3R:162233-162407				
Myo81F	chr3R:887041-887409				
Myo81F	chr3R:313585-313760				
Myo81F	chr3R:42090-42498				
Myo81F	chr3R:87394-88845				
Myo81F	chr3R:420803-420908				
Myo81F	chr3R:42707-42897				
Myo81F	chr3R:410923-411014				
Myo81F	chr3R:418708-418807				
Myo81F	chr3R:562520-562822				
Myo81F	chr3R:320096-320198				
Myo81F	chr3R:452038-452383				
Myo81F	chr3R:98069-98195				
Myo81F	chr3R:952142-952253				
Myo81F	chr3R:634206-634397				

Myo81F	chr3R:138872-139012				
Myo81F	chr3R:137238-137484				
Myo81F	chr3R:225368-225820				
Myo81F	chr3R:318923-319036				
Myo81F	chr3R:322153-322246				
Myo81F	chr3R:325700-325850				
Myo81F	chr3R:293780-294101				
Myo81F	chr3R:711306-711408				
Myo81F	chr3R:326439-326528				
Myo81F	chr3R:409175-409496				
Myo81F	chr3R:38268-38375				
Myo81F	chr3R:143451-143600				
Myo81F	chr3R:726029-726290				
Myo81F	chr3R:704794-704932				
Myo81F	chr3R:300004-300176				
Myo81F	chr3R:403853-404197				
Myo81F	chr3R:404548-405067				
Myo81F	chr3R:407815-408053				
Myo81F	chr3R:189274-189677				
Myo81F	chr3R:114515-114600				
Myo81F	chr3R:675569-675809				
Myo81F	chr3R:405642-405887				
Myo81F	chr3R:187662-187990				
Myo81F	chr3R:101442-103028				
Myo81F	chr3R:685825-686133				
Myo81F	chr3R:229339-229558				
Myo81F	chr3R:717691-717868				

Myo81F	chr3R:186314-186501				
Myo81F	chr3R:739220-739451				
Myo81F	chr3R:723766-724245				
Myo81F	chr3R:294731-294936				
Myo81F	chr3R:635312-635612				
Myo81F	chr3R:107732-109371				
norpA	chrX:4325111-4325206	14H10	No CB expression		
norpA	chrX:4324524-4324925	14H10	No CB expression		
norpA	chrX:4323926-4324148	14H10	No CB expression		
Oaz	chr2R:14447876-14448263				
Oaz	chr2R:14449947-14450296				
Oaz	chr2R:14456129-14456397				
Oaz	chr2R:14440020-14440230	51C08	T1NB		
Oaz	chr2R:14463946-14464114				
Oaz	chr2R:14448897-14449284				
Oaz	chr2R:14440623-14441078				
Oaz	chr2R:14437537-14437905	51C08	T1NB		
Oaz	chr2R:14463518-14463692				
opa	chr3R:4863009-4863307	77A10	T1NB		
opa	chr3R:4855966-4856240	77B07	Neuron Subset		
opa	chr3R:4850349-4850713	77B04	Neuron Subset		
opa	chr3R:4842803-4843346	77B01	Neuron Subset		
opa	chr3R:4853489-4853613				
Optix	chr2R:8045337-8045756	95A06	Neuron Subset		
Optix	chr2R:8047881-8048346	95A04	T2NB		
Optix	chr2R:8032991-8033388				
osa	chr3R:17714536-17714748				

osa	chr3R:17713010-17713246	95H05	Neuron Subset		
ph-p	chrX:2131173-2131454				
ph-p	chrX:2139705-2139949				
Pi3K92E	chr3R:20635031-20635166				
Pp2C1	chrX:4685763-4686212				
Ptp99A	chr3R:29406886-29407119				
Ptp99A	chr3R:29382061-29382477				
Ptp99A	chr3R:29466762-29467138				
Ptp99A	chr3R:29467269-29467506				
Ptp99A	chr3R:29460507-29460702				
Ptp99A	chr3R:29406175-29406525				
Ptp99A	chr3R:29470726-29470841				
Ptp99A	chr3R:29412628-29413381				
Ptp99A	chr3R:29413575-29413702				
Ptp99A	chr3R:29452937-29453194				
Ptp99A	chr3R:29375499-29375639				
Ptp99A	chr3R:29421666-29421851				
Ptp99A	chr3R:29428418-29428534				
Ptp99A	chr3R:29420898-29421128				
Ptp99A	chr3R:29374399-29374859				
RapGAP1	chr2L:7530871-7531028				
RapGAP1	chr2L:7554582-7554990				
RapGAP1	chr2L:7546089-7546255				
RapGAP1	chr2L:7526693-7527154				
RapGAP1	chr2L:7536315-7536758				
RapGAP1	chr2L:7538187-7538613				
RapGAP1	chr2L:7554313-7554477				

RapGAP1	chr2L:7535639-7535778				
RapGAP1	chr2L:7546949-7547212				
RapGAP1	chr2L:7533020-7533321				
RapGAP1	chr2L:7532197-7532285				
RapGAP1	chr2L:7526397-7526541				
RapGAP1	chr2L:7529240-7529379				
rdgB	chrX:13770779-13770888	37D08	Neuron Subset		
robo1	chr2R:22700121-22700331				
robo2	chr2L:1406871-1407054	28G05	Glia	28D10	INPs and GMC
robo2	chr2L:1409384-1409528	28G05	Glia		
robo2	chr2L:1419826-1420036				
robo2	chr2L:1404954-1405725	28D10	INPs and GMCs?		
robo2	chr2L:1412506-1412775	28D12	Neuron Subset		
robo2	chr2L:1405898-1406228	28D10	INPs and GMCs		
robo2	chr2L:1418222-1418756	28C04	Neuron Subset		
robo2	chr2L:1413035-1413358	28F12	INPs	28D12	Neuron Subset
Sema1a	chr2L:8554595-8554776	34 E08	T1NB		
Sema1a	chr2L:8566339-8566531	33G05	Neuron Subset		
Sema1a	chr2L:8566912-8567001	33G05	Neuron Subset	34B01	Neuron Subset
Sema1a	chr2L:8555615-8555814	34 E08	T1NB		
Sema1a	chr2L:8545526-8545793	33G04	Neuron Subset		
Sema1a	chr2L:8541532-8541846				
Sema1a	chr2L:8563372-8563604	34D11	Neuron Subset		
Sema1a	chr2L:8551245-8551377				
Sema1a	chr2L:8544620-8544887				
shg	chr2R:21047832-21048542				
side	chr3R:27431135-27431340				

side	chr3R:27427014-27427155				
side	chr3R:27426418-27426520				
sli	chr2R:15923445-15924012				
sli	chr2R:15883613-15883875	31B10	Neuron Subset		
sli	chr2R:15886631-15886993	32F01	Neuron Subset		
sli	chr2R:15883994-15884130	31B10	Neuron Subset		
sli	chr2R:15922530-15922669				
sli	chr2R:15880754-15881866				
sli	chr2R:15892972-15893102				
sli	chr2R:15923209-15923312	31C11	Neuron Subset	32A06	Glia
sli	chr2R:15921192-15921622				
sm	chr2R:19569700-19569825				
sm	chr2R:19534626-19535111				
sm	chr2R:19564830-19565096				
sm	chr2R:19543639-19543803				
sm	chr2R:19627773-19628035				
sm	chr2R:19540660-19541181				
sm	chr2R:19620263-19620373				
sm	chr2R:19619720-19619943				
sm	chr2R:19531161-19531372				
sm	chr2R:19535817-19535997				
smash	chr3R:4705340-4705432				
SPARC	chr3R:26869664-26869943				
Spn	chr3L:2548328-2549063				
Spn	chr3L:2552992-2553079				
Spn	chr3L:2550339-2550715				
Spn	chr3L:2532249-2532470				

Spn	chr3L:2537834-2538069				
Spn	chr3L:2538593-2538881				
Spt20	chr3L:13499518-13500382				
stai	chr2L:6112628-6112747				
stai	chr2L:6109135-6109306				
stai	chr2L:6104312-6104788				
stai	chr2L:6121599-6121921				
stai	chr2L:6110878-6111130				
stai	chr2L:6105661-6105936				
stai	chr2L:6110101-6110349				
tap	chr3L:17358527-17358795				
tap	chr3L:17362897-17363079				
tap	chr3L:17357424-17357656				
Ten-a	chrX:12226491-12226651				
Ten-a	chrX:12141158-12141465				
Ten-a	chrX:12202480-12202598				
Ten-a	chrX:12147436-12147692				
Ten-a	chrX:12202931-12203059				
Ten-a	chrX:12196458-12196679				
Ten-a	chrX:12044975-12045185				
Thd1	chr4:545685-546240				
Thd1	chr4:537296-537397				
tkv	chr2L:5241144-5241234				
tkv	chr2L:5231770-5232473				
tkv	chr2L:5270348-5270508				
tkv	chr2L:5246920-5247328				
tkv	chr2L:5236606-5237021				

tkv	chr2L:5270006-5270193				
tkv	chr2L:5245476-5245681				
tna	chr3L:10869116-10869469				
tna	chr3L:10867798-10868203				
tna	chr3L:10864938-10865473	60C09	T1NB + T2NB		
tna	chr3L:10854466-10854685	60C04	T1NB + T2NB		
Tnks	chr3R:25659312-25659425				
UbcE2H	chrX:8090614-8091086				
unc-5	chr2R:15357574-15357671				
unc-5	chr2R:15336211-15336455	74H07	Neuron Subset		
unc-5	chr2R:15337054-15337215	74H07	Neuron Subset		
unc-5	chr2R:15359575-15360127	93 E12	Neuron Subset		
unc-5	chr2R:15337312-15337470				
unk	chr3R:23158190-23158457				
Usp1	chr3R:29229969-29230061				
Usp15-31	chr2R:24749675-24749796				
Usp15-31	chr2R:24741832-24741984				
Vav	chrX:19264019-19264202				
Wnt4	chr2L:7281570-7281730				
Wnt4	chr2L:7273447-7273672	25A11	Neuron Subset		
Wnt4	chr2L:7287254-7287398	17D09	Neuron Subset		
Wnt4	chr2L:7274072-7274457	25A11	Neuron Subset		
Wnt4	chr2L:7281130-7281282				
Wnt4	chr2L:7290402-7290676	17B02	Neuron Subset	17A12	T1NB
Wnt4	chr2L:7282450-7282783				
X11L	chrX:17608313-17608604				
X11L	chrX:17611024-17611188				

X11L	chrX:17603331-17603678				
X11Lbeta	chrX:10628723-10628893				
X11Lbeta	chrX:10636420-10636836				
X11Lbeta	chrX:10628292-10628556				
X11Lbeta	chrX:10635348-10635656				
X11Lbeta	chrX:10637638-10638195				

Table 2.3 Pan Neural enhancers annotated with activity patterns identified from Fig 2.1C

Activity pattern identified manually using Flylight: Gal4 corresponds to Janelia Flylight Line ((Jenett et al., 2012; Li et al., 2014). Red denotes manually reannotated gene name.

Gene Name	Location	Gal4/Reporter	Pattern	Gal4/Reporter	Pattern
Pan Neural					
toy	chr4:984791-985096	9G09	T1NB		
fuss	chr4:979706-980385	9G07	T1NB		
retn	chr2R:23647003-23647363	9F12	Neuron Subset		
Eglp2	chr2R:23621263-23622024	9F01	T1NB		
lncRNA:CR44829	chr2R:24853897-24854584	94H10	T1NB		
lncRNA:CR45239	chr3L:6652910-6653417	94F02	T1NB		
en	chr2R:11551893-11552455	94D05	T1NB + T2NB		
tou	chr2R:11565587-11565996	94D03	Neuron Subset		
lncRNA:CR46095	chr3R:24606948-24607824	94C02	Neuron Subset		
CG46339	chr3R:26917602-26918356	94A07	T1NB		
Pms2	chr2R:15363431-15364177	93F02	T1NB + T2NB		
unc-5	chr2R:15351558-15352652	93 E11	No expression		
unc-5	chr2R:15349410-15349763	93 E08	Neuron Subset		
Dscam2	chr3L:7193713-7194286	89 E11	Neuron Subset		

Dscam2	chr3L:7185370-7185752	89 E06	T1NB + T2NB		
sdt	chrX:8196542-8196965	88H11	T1NB + T2NB		
Art9	chr3R:13929969-13930597	88G08	T1NB + T2NB		
inv	chr2R:11477633-11478175	88B03	Neuron Subset		
inv	chr2R:11469224-11469903	88A11	Neuron Subset & Glia		
E5	chr3R:13877163-13877607	88A06	Neuron Subset		
shn	chr2R:11197206-11197603	87G10	Neuron Subset		
shn	chr2R:11202280-11203789	87G09	T1NB + T2NB		
CG14441	chrX:6700199-6700702	87F05	T1NB + T2NB		
CG42580	chrX:20582804-20583610	87B11	Neuron Subset		
Qsox2	chr3R:21928300-21928798	87A08	No expression		
Kr-h1	chr2L:6081185-6081724	87 E09	T1NB + T2NB		
lncRNA:CR45287	chr2L:5489009-5489637	86H09	No expression		
lncRNA:CR43453	chr3R:21460011-21460306	86C07	Neuron Subset		
CG42684	chrX:17751751-17751976	86B06	Neuron Subset		
klu	chr3L:11010301-11010883	86 E09	No Expression		
MTA1-like	chr3R:5644904-5645276	85H10	Neuron Subset		
shn	chr2R:11199634-11199923	85G03	Neuron Subset		
salm	chr2L:11456664-11457260	85D09	T1NB + T2NB		
nej	chrX:9684763-9685236	85C09	no expression		
btd	chrX:9692609-9692921	85C06	no expression	btd enh VG	T2 NB
lncRNA:CR42651	chr3R:6815234-6815951	84H10	Neuron Subset		
lncRNA:CR45915	chr3R:6810617-6811038	84H03	T1NB + T2NB		
Scr	chr3R:6854336-6854763	84H02	Neuron Subset		
Eip93F	chr3R:21990006-21990628	84C02	T1NB + T2NB		
Gsc	chr2L:585148-585644	84B09	T1NB		

lncRNA:CR44713	chr3L:11246014-11246682	84B05	Pan neuronal		
lncRNA:CR44715	chr3L:11247883-11248115	84B01	T1NB + T2NB		
lncRNA:CR44714	chr3L:11247464-11247774	84B01	T1NB + T2NB		
bon	chr3R:20594715-20594974	84A03	T1NB + T2NB		
run	chrX:20709462-20710325	83H04	T1NB + T2NB		
Cib2	chr2R:20884395-20884898	83D06	Neuron Subset		
CG11294	chrX:8694856-8695535	83C12	Glia		
lncRNA:CR43862	chrX:20687113-20687800	83C05	T1NB + T2NB		
Gug	chr3L:8458735-8459270	83B10	T1NB + T2NB		
Alh	chr3R:7104133-7104622	83A06	T1NB + T2NB		
Alh	chr3R:7103298-7103827	83A03	T1NB + T2NB		
lncRNA:CR43685	chr3R:7090349-7090569	83A03	T1NB + T2NB		
CAH15	chr2R:20906655-20906807	83 E01	T1NB + T2NB		
sba	chr3R:23914123-23915167	82H03	T1NB + T2NB		
CG33111	chr3R:23819594-23820040	82G08	Neuron Subset		
CG33268	chr3L:11591734-11592229	82A10	Neuron Subset		
CG14137	chr3L:11599072-11599366	82A09	Neuron Subset		
jumu	chr3R:10357195-10357572	81F04	T1NB + T2NB		
Kr-h1	chr2L:6087844-6088875	81C06	T1NB + T2NB		
hang	chrX:16426603-16427310	81C01	T1NB + T2NB		
CG18586	chr3L:5877003-5878015	81B11	Neuron Subset		
CG13287	chr3L:5881287-5881649	81B09	Neuron Subset		
CG13287	chr3L:5878908-5879339	81B08	T1NB + T2NB		
CG42758	chr3L:14576375-14576877	81A06	T1NB		
HGTX	chr3L:14600686-14600900	81A02	Neuron Subset		
B-H2	chrX:17345443-17346297	81 E07	T1NB + T2NB		
CG9380	chr2R:25206001-25206805	80H09	T1NB + T2NB		

Kr	chr2R:25214803-25215472	80H07	Neuron Subset		
lncRNA:CR43817	chr2L:18805855-18806513	80H03	T1NB		
CG7587	chr3R:17583564-17584133	80D07	T1NB		
CG7587	chr3R:17582807-17583267	80D07	T1NB		
Hmx	chr3R:17557483-17557931	80C09	Neuron Subset		
Prx3	chr3R:17550773-17551195	80C05	T1NB + T2NB		
jim	chr3L:22822481-22823161	80 E01	Neuron Subset		
lncRNA:CR32730	chrX:7159142-7159447	79F11	Neuron Subset		
lncRNA:CR32730	chrX:7161383-7162329	79F10	T1NB + T2NB		
CG1958	chrX:7252477-7252749	79D01	T1NB + T2NB		
lncRNA:CR45203	chr3R:9488454-9488941	79B12	Neuron Subset		
CG16779	chr3R:9490770-9491565	79B11	Neuron Subset		
CG9650	chrX:7244133-7244718	79 E10	T1NB + T2NB		
CG9650	chrX:7194682-7195180	79 E08	No expression		
CG9650	chrX:7242007-7242613	79 E06	No expression		
Vsx1	chrX:5588536-5588730	78H07	T1NB + T2NB	78H09	T1NB + T2NB
Vsx1	chrX:5579256-5579946	78H06	Neuron Subset	78G12	Neuron Subset
Vsx2	chrX:5573454-5573798	78H03	T1NB + T2NB		
snRNA:U1:21D	chr3R:23826841-23828049	78D12	Neuron Subset		
lncRNA:CR42746	chr2L:12543006-12543612	78D05	Pan Neuronal		
lncRNA:CR44597	chr2L:12574958-12575358	78A02	Neuron subset		
snRNA:U1:95Cb	chr3R:23831746-23832222	78 E01	T1NB + T2NB		
dan	chr3R:25183432-25183896	77H06	Neuron Subset		
dan	chr3R:25174482-25175286	77H05	T1NB + T2NB		
dan	chr3R:25173649-25174313	77H05	T1NB + T2NB		
crol	chr2L:11807590-11808309	77G08	Glia		
crol	chr2L:11805915-11807452	77G08	Glia		

Trl	chr3L:14754909-14755758	77G01	T1NB + T2NB		
Trl	chr3L:14758844-14759415	77F12	T1NB + T2NB		
Act57B	chr2R:20933532-20933995	77F11	Neuron Subset		
Rx	chr2R:20913630-20914603	77F10	T1NB + T2NB		
CG14659	chr3R:4833729-4834024	77B11	T1NB + T2NB		
CG14659	chr3R:4835314-4835848	77B10	T1NB + T2NB		
opa	chr3R:4845050-4845890	77B05	INP		
opa	chr3R:4865213-4865475	77B03	T1NB + T2NB		
opa	chr3R:4863832-4864255	77B03	T1NB + T2NB	77A10	T1NB
Sox21a	chr3L:14111530-14111736	77A06	T1NB + T2NB		
Sox21a	chr3L:14109791-14110194	77A06	T1NB + T2NB		
CG9674	chr3L:16806284-16806817	75F12	T1NB + T2NB		
ab	chr2L:11219984-11220369	75F08	Neuron Subset		
ab	chr2L:11221139-11221640	75D08	No expression		
mamo	chrX:13890306-13890907	75C06	T1NB + T2NB		
CG11068	chrX:13954147-13954688	75B03	Neuron Subset		
l(3)neo38	chr3R:11776033-11776292	75A02	T1NB + T2NB		
ab	chr2L:11244331-11244679	75 E10	Neuron Subset		
ab	chr2L:11247029-11248396	75 E04	Neuron Subset		
lncRNA:CR43856	chr2L:15013409-15013959	74G04	Neuron subset		
lncRNA:CR43856	chr2L:15011854-15012249	74G04	Neuron subset		
sr	chr3R:18111675-18112114	74 E07	T1NB + T2NB		
zfh2	chr4:507193-508782	73G10	Neuron Subset		
D	chr3L:14171612-14172568	73C02	INPs		
D	chr3L:14156874-14157570	73B12	INPs		
lncRNA:CR46001	chr3L:6103192-6103960	72H10	Neuron Subset		
smog	chr2L:4856425-4857113	72A09	T1NB + T2NB		

smog	chr2L:4867375-4868222	72A03	T1NB + T2NB		
sif	chr3L:5665362-5665861	71G10	No expression		
sif	chr3L:5680030-5680413	71G06	Neuron Subset		
Vsx2	chrX:5545775-5546188	71G04	T1NB		
Myc	chrX:3381457-3382465	71F01	T1NB + T2NB		
lncRNA:CR44924	chr3R:5727544-5728227	71D05	T1NB + T2NB		
lncRNA:CR44924	chr3R:5720021-5720951	71D05	T1NB + T2NB		
elav	chrX:523881-524791	71C07	T1NB + T2NB		
Rdl	chr3L:9190250-9190571	70G05	Neuron Subset		
vnd	chrX:595660-596205	69H09	T1NB + T2NB		
ptc	chr2R:8647392-8648099	69F09	Neuron Subset		
br	chrX:1621728-1622398	69B12	No expresson		
br	chrX:1598284-1598798	69B03	T1NB + T2NB		
br	chrX:1593187-1594146	69A12	T1NB + T2NB		
br	chrX:1581187-1581497	69A07	Neuron Subset		
snmRNA:400	chrX:1565612-1566402	69A03	T1NB + T2NB		
eg	chr3L:21807981-21808370	69 E01	Neuron Subset		
Pp1-13C	chrX:15364019-15364491	67C12	T1NB + T2NB		
Pp1-13C	chrX:15356159-15357010	67C03	Neuron Subset		
Abl	chr3L:16634140-16634673	67B05	T1NB + T2NB		
chinmo	chr2L:1649855-1650166	67B04	T1NB + T2NB		
lncRNA:CR44655	chrX:13993387-13993514	65D08	No expression		
ben	chrX:13994776-13995393	65D07	No expression		
arm	chrX:1898275-1899124	65A12	Neuron Subset		
mir-999	chr3R:21793743-21794305	64H08	Neuron Subset		
mamo	chrX:13978723-13979143	64F11	T1NB + T2NB		
Atpalpha	chr3R:20956635-20957228	64D01	Neuron Subset		

Atpalpha	chr3R:20951392-20951982	64C07	T1NB + T2NB		
Gr93a	chr3R:21829288-21829897	64B10	Neuron Subset		
bsh	chr2L:19769734-19769999	64B07			
CG32198	chr3L:18539784-18540211	64A10	Neruon Subset		
CG43248	chr3L:15532401-15532736	64 E07	Neuron Subset		
Abl	chr3L:16645536-16645963	60H11	T1NB + T2NB		
rgr	chr2R:8601487-8601876	60G11	T1NB		
lncRNA:CR45246	chr3L:10832255-10832859	60D02	Pan neuronal		
lncRNA:CR45169	chr3L:10844753-10845184	60C12	T1NB + T2NB		
lncRNA:CR45169	chr3L:10842728-10843289	60C12	T1NB + T2NB		
tna	chr3L:10865729-10866162	60C09	T1NB + T2NB		
HmgD	chr2R:21700356-21700922	60C08	Neuron Subset		
CG13894	chr3L:696224-696831	60C07	T1NB + T2NB		
tna	chr3L:10856069-10857022	60C04	T1NB + T2NB		
tna	chr3L:10855299-10855866	60C04	T1NB + T2NB		
lncRNA:CR45247	chr3L:10817622-10818334	60B08	Neuron Subset		
tna	chr3L:10861443-10862284	60B02	T1NB + T2NB		
lncRNA:CR45823	chr3L:8851384-8852231	60A10	T1NB		
CG32026	chr3L:8833151-8833883	60A10	T1NB		
lncRNA:CR45938	chr3L:18759022-18759625	60A08	Neruon Subset		
lncRNA:CR45938	chr3L:18757183-18757525	60A08	Neruon Subset		
CG13894	chr3L:699570-700085	59H12	T1NB + T2NB		
osa	chr3R:17710704-17711891	59H05	T1NB + T2NB		
CG42831	chr3L:10810832-10811549	59G11	Pan neuronal		
lncRNA:CR44347	chr3L:10809052-10809687	59G11	Pan neuronal		
foxo	chr3R:14061124-14061975	59G09	T1NB + T2NB		
CG13907	chr3L:882884-883130	59G08	No expression		

lncRNA:CR45169	chr3L:10847058-10847688	59G03	T1NB + T2NB		
lncRNA:CR45246	chr3L:10825122-10825583	59G02	Pan neuronal		
HmgZ	chr2R:21706671-21707299	59F10	T1NB + T2NB		
HmgZ	chr2R:21705910-21706313	59F10	T1NB + T2NB		
lin-28	chr3L:5653609-5653992	59F02	Neuron Subset		
CG30222	chr2R:21579697-21580406	59D09	Neuron Subset		
Nlg2	chr2L:6873936-6874491	59B07	Neuron Subset		
lncRNA:CR46265	chr3R:18719246-18720462	59 E04	T1NB + T2NB		
Faa	chr3L:4076902-4077298	58F02	Neuron Subset		
VAChT	chr3R:18707355-18707969	58 E10	Neuron Subset		
lncRNA:CR46036	chr3R:17700658-17701564	56H11	Glia		
ftz-f1	chr3L:18791051-18791689	56G09	Neruon Subset		
ftz-f1	chr3L:18771498-18772120	56D09	Neruon Subset		
CG14291	chr3R:18913712-18914129	56D07	T1NB + T2NB		
HmgD	chr2R:21714416-21714952	56D02	INPs and Neurons		
asRNA:CR43426	chr3L:22851262-22852220	56 E10	T1NB + T2NB		
lncRNA:CR45169	chr3L:10845426-10846133	56 E07	T1NB + T2NB		
Sik3	chr2R:18689846-18690157	55G06	Neuron Subset		
igl	chr2R:15154602-15154928	55C04	Neuron Subset		
CG10132	chr2L:19519466-19520041	55B05	Neuron Subset		
dpr20	chr3L:857697-858063	54C01	T1NB		
dlp	chr3L:14634520-14635029	54B09	Neuron Subset		
lncRNA:CR45888	chr3L:14661537-14662488	53H05	T1NB + T2NB		
CG34286	chr3R:19719396-19719946	53B04	Neuron Subset		
GluClalpha	chr3R:19731017-19731564	53A12	Neuron Subset		
lncRNA:CR45888	chr3L:14660485-14661160	53 E05	T1NB + T2NB		
CG6495	chr2L:10759876-10760651	52B05	T1NB + T2NB		

CG17124	chr2L:10757098-10757259	52B05	T1NB + T2NB		
sqz	chr3R:19165574-19165938	52A06	T1NB		
sff	chr3L:15920794-15921316	51F12	Pan Neuronal		
phyl	chr2R:14430698-14431388	51 E01	T1NB + T2NB		
CG5644	chr3L:8978749-8979075	50F09	Glia		
lncRNA:CR46057	chr3R:21651396-21652110	50D03	Neuron Subset		
beat-IIIc	chr2L:17268092-17268659	50B03	T1NB + T2NB		
beat-IIIc	chr2L:17267377-17267651	50B03	T1NB + T2NB		
apt	chr2R:23573098-23573930	49G06	T1NB + T2NB		
apt	chr2R:23571628-23572039	49G06	T1NB + T2NB		
E2f1	chr3R:21635783-21636360	49F10	T1NB + T2NB		
E2f1	chr3R:21634705-21634897	49F10	T1NB + T2NB		
apt	chr2R:23585822-23586812	49A03	T1NB		
lncRNA:CR46056	chr3R:21640292-21640777	48F11	T1NB + T2NB		
lncRNA:CR46057	chr3R:21649034-21649386	48C06	Neuron Subset		
apt	chr2R:23579019-23579734	48A04	T1NB + T2NB	49A05	T1NB + T2NB
CG12344	chr2R:10832718-10833539	47D02	T1NB + T2NB		
Eip75B	chr3L:18065482-18066030	46C07	Pan neuronal		
Eip75B	chr3L:18063262-18063724	46C07	Pan neuronal		
lilli	chr2L:2894053-2894757	46C03	T1NB + T2NB		
lncRNA:CR43904	chr2R:6158672-6159298	46B10	T1NB + T2NB		
lilli	chr2L:2898258-2898556	46B09	Neuron Subset		
hth	chr3R:10599303-10600360	46B05	T1NB + T2NB		
EcR	chr2R:6151100-6151492	46 E06	T1NB + T2NB		
hth	chr3R:10571118-10571894	46 E04	T1NB + T2NB		
lilli	chr2L:2925068-2925716	46 E03	Neuron Subset		
mir-4944	chr3R:10557295-10558622	45H11	T1NB + T2NB		

lilli	chr2L:2909588-2909891	45G08	Neuron Subset		
lncRNA:CR45392	chr3L:18078948-18079561	45G03	T1NB + T2NB		
EcR	chr2R:6120371-6121381	45D06	Glia		
lncRNA:CR45921	chr3L:17990029-17990271	45D02	Neuron Subset		
Ns1	chr3R:17065241-17065743	45C11	Neuron Subset		
hth	chr3R:10616729-10617397	45B07	T1NB + T2NB		
lncRNA:CR45392	chr3L:18078349-18078609	45B06	T1NB		
lncRNA:CR45392	chr3L:18077670-18078062	45B06	T1NB		
Mef2	chr2R:9954898-9955744	45B04	Pan neuronal		
psq	chr2R:10554076-10554528	44H12	T1NB + T2NB		
lncRNA:acal	chr2R:10551337-10552132	44H12	Pan Neuronal		
hth	chr3R:10640405-10641267	44H07	Neuron Subset		
Eip75B	chr3L:18061777-18062272	44H06	Neuron Subset		
lncRNA:CR43253	chr3L:18083946-18084553	44H05	Neruon Subset		
Rfx	chr3R:10368052-10368695	44G12	Neuron Subset		
Eip75B	chr3L:18016366-18016915	44G04	T1NB + T2NB		
Ars2	chr2R:6103777-6104570	44F12	T1NB		
Ars2	chr2R:6102419-6103173	44F12	T1NB		
mir-4944	chr3R:10535811-10536041	44D09	Neuron Subset		
Eip75B	chr3L:17962185-17962491	44D06	Neuron Subset		
Eip75B	chr3L:18018544-18019482	44D01	Neuron Subset		
Dad	chr3R:17056149-17057006	44C10	Glia		
lncRNA:acal	chr2R:10548225-10548876	44C03	T1NB + T2NB		
lncRNA:acal	chr2R:10546845-10547591	44C03	T1NB + T2NB		
EcR	chr2R:6147848-6148771	44B03	T1NB + T2NB		
tko	chrX:2440215-2440684	44A04	T1NB + T2NB		
lilli	chr2L:2888623-2889447	43H06	T1NB		

grh	chr2R:17828805-17829974	43G07	T1NB + T2NB		
lilli	chr2L:2886648-2887283	43F12	T1NB		
CHES-1-like	chrX:7702631-7702923	42H04	Glia		
Lmx1a	chr3L:12325710-12326315	42H02	T1NB + T2NB		
dve	chr2R:22271173-22271774	42H01	Neuron Subset		
CG10543	chr2R:20998103-20998345	42G11	Neuron Subset		
CG10543	chr2R:20996949-20997488	42G11	Neuron Subset		
KP78a	chr3R:11351593-11352352	42G10	T1NB + T2NB	pros 1 VG	T1NB + T2NB
chinmo	chr2L:1670199-1670953	42G09	Neuron Subset		
tj	chr2L:19462849-19463330	42G01	Neuron Subset		
scrt	chr3L:3978289-3979347	42F10	T1NB + T2NB		
Pdp1	chr3L:7836824-7837354	42F08	Neuron Subset		
SoxN	chr2L:8817435-8818456	42D10	T1NB + T2NB		
CG11883	chr2R:10604161-10604364	42D07	Neuron Subset		
CHES-1-like	chrX:7692412-7692819	42C12	Neuron Subset		
HEATR2	chr3R:14346737-14347380	42C08	Neuron Subset		
dsx	chr3R:7963472-7963961	42C06	Glia		
CG30430	chr2R:25120727-25121251	42C05	T1NB		
ap	chr2R:5735573-5737173	42B11	T1NB		
CHES-1-like	chrX:7697161-7697580	42B03	T1NB + T2NB		
chinmo	chr2L:1654173-1654539	42A12	T1NB + T2NB		
kay	chr3R:29771647-29772310	42A04	T1NB + T2NB		
grh	chr2R:17809465-17809800	42 E09	T1NB + T2NB		
chinmo	chr2L:1662560-1663872	41H08	Neuron Subset		
dmrt99B	chr3R:29690754-29691399	41H02	Neuron susbet		
Pdp1	chr3L:7856171-7856586	41H01	T1NB + T2NB		
CG30430	chr2R:25127570-25127777	41F10	T1NB		

SoxN	chr2L:8809642-8810828	41F09	T1NB + T2NB		
psq	chr2R:10558363-10559118	41F08	T1NB + T2NB		
cpb	chr2L:1688104-1688969	41F07	T1NB + T2NB		
l(2)k14505	chr2L:21250728-21251189	41F02	Neuron Subset		
HEATR2	chr3R:14351765-14352056	41D07	Neuron Subset		
Rbp9	chr2L:2957860-2958317	41D06	Neuron Subset		
ap	chr2R:5710970-5711649	41C10	T1NB + T2NB		
grh	chr2R:17815348-17816439	41C09	T1NB + T2NB		
chinmo	chr2L:1658068-1658535	41C07	Neuron subset		
slou	chr3R:21551560-21551924	41B12	Neuron Subset		
l(2)09851	chr2R:5745159-5745926	41B09	Neuron Subset		
scrt	chr3L:3979956-3980415	41B06	Neuron Subset		
CG12769	chr2R:8060457-8060927	41B01	Neuron Subset		
CG12769	chr2R:8051142-8051520	41B01	Neuron Subset		
Pdp1	chr3L:7863342-7863756	41A09	Glia		
bap	chr3R:21387147-21387887	41A06	T1NB + T2NB		
CG30430	chr2R:25115212-25116105	40H11	Neuron Subset		
lncRNA:CR43437	chr4:418336-419024	40H06	T1NB		
mir-9385	chr4:407944-408337	40H01	T1NB + T2NB		
cnc	chr3R:23214879-23215231	40G07	No expression		
dac	chr2L:16477541-16477911	40F08	T1NB		
lncRNA:CR44024	chr4:426182-427460	40F02	Neuron Subset		
dati	chr4:396046-396869	40D08	T1NB + T2NB		
CG30430	chr2R:25129932-25130307	40C04	Neuron Subset		
fzo	chr3R:23207282-23207604	40C01	T1NB		
Sox102F	chr4:807734-808473	40A12	No expresson		
slou	chr3R:21561328-21562104	39H09	Neuron Subset		

lncRNA:CR45125	chr4:380300-381150	39G02	T1NB + T2NB		
NK7.1	chr3R:14373433-14373836	39F11	Neuron Subset		
cnc	chr3R:23220290-23220580	39D04	Glia		
Rbp9	chr2L:2955670-2956381	39D03	Neuron Subset		
chinmo	chr2L:1651829-1652263	39C11	T1NB + T2NB		
pros	chr3R:11378443-11379163	39B06	T1 and INPs	pros 2 VG	T1 and INPs
CG12071	chr3R:30880025-30880488	39A12	Neuron Subset		
CG42852	chr3L:16747330-16747647	38G12	Pan neuronal		
CG4116	chrX:3060307-3060883	38G10	T1NB + T2NB		
kirre	chrX:3027765-3028582	38G10	Neuron Subset		
kirre	chrX:3025882-3026131	38F12	T1NB		
CG9701	chr3L:16744137-16744854	38F05	T1NB + T2NB		
shot	chr2R:13940539-13941402	38C12	T1NB + T2NB		
rst	chrX:2966841-2967711	38C10	T1NB + T2NB		
kirre	chrX:2987212-2987781	38A02	Neuron Subset		
CG12374	chr2R:12766047-12766455	37H04	Neuron Subset		
lncRNA:CR43653	chr3R:21598643-21599000	37B05	T1NB		
Neu2	chr3L:21483860-21484352	36C10	Neuron Subset		
Eip74EF	chr3L:17606832-17607231	36C03	Neuron Subset		
zfh1	chr3R:30760495-30761326	36B11	Neuron Subset		
croc	chr3L:21479664-21480215	36B04	Neuron Subset		
A16	chr2L:13035731-13036235	36A02	T1NB		
Eip74EF	chr3L:17613915-17614412	36A01	Neuron Subset		
Eip74EF	chr3L:17611626-17612512	36A01	Neuron Subset		
lncRNA:CR44551	chr3L:12304023-12304533	35G09	T1NB + T2NB		
snoRNA:Me28S-A576	chr3L:17569978-17570518	35G07	T1NB + T2NB		
lncRNA:CR45667	chrX:7656645-7657143	35D02	T1NB + T2NB		

ct	chrX:7642269-7643071	35B03	T1NB + T2NB		
aop	chr2L:2174707-2175164	35 E11	T1NB + T2NB		
snoRNA:Me28S-A576	chr3L:17563347-17564175	34H03	T1NB		
CG32532	chrX:19545767-19547115	34G03	Neuron Subset		
mirr	chr3L:12700242-12701007	34D12	Neuron Subset		
lncRNA:CR43855	chr2L:8585291-8586332	34D05	T1NB + T2NB		
ci	chr4:59992-60440	34D04	T1NB + T2NB		
Src64B	chr3L:4624489-4624797	34C10	T1NB + T2NB		
CG32246	chr3L:4618831-4620231	34C08	T1NB + T2NB		
ct	chrX:7603053-7603559	34B09	T1NB + T2NB		
ct	chrX:7604512-7604959	34A08	Pan neuronal		
CG43731	chr2L:19098026-19098617	34A04	Subset Neuron		
lncRNA:CR43855	chr2L:8612096-8612825	34A03	Neuron Subset		
Lim1	chrX:8770201-8771249	34 E12	T1NB + T2NB		
Sema1a	chr2L:8556167-8557350	34 E08	T1 NB		
Lim3	chr2L:19090013-19091133	33H04	T1NB + T2NB		
Lim1	chrX:8785780-8786047	33H03	Neuron Subset		
CG12689	chrX:7595545-7596542	33H01	T1NB + T2NB		
ct	chrX:7615472-7615795	33F07	T1NB + T2NB	33H05	T1NB + T2NB
Src64B	chr3L:4599655-4600345	33C08	T1NB + T2NB		
lncRNA:CR45052	chr3R:31701862-31702556	33A11	T1NB + T2NB		
Sema1a	chr2L:8550542-8551064	33 E11	T1NB + T2NB		
lncRNA:CR45379	chr3L:3855474-3856070	33 E05	T1NB + T2NB		
mirr	chr3L:12681283-12681863	33 E04	T1NB + T2NB		
Sema1a	chr2L:8543899-8544315	32H10	T1NB + T2NB		
CadN	chr2L:17742912-17743448	32D11	T1NB + T2NB		
CG14506	chr3R:29287310-29287830	32D05	T1NB + T2NB		

SNF4Agamma	chr3R:21190772-21191300	32D03	T1NB		
lncRNA:CR45568	chr3R:29282851-29283449	32C11	T1NB + T2NB		
CadN	chr2L:17747426-17747825	32C01	T1NB + T2NB		
CadN	chr2L:17746885-17747173	32C01	T1NB + T2NB		
stan	chr2R:10680859-10681324	32B11	T1NB + T2NB		
CG45544	chr3R:29257897-29258482	32B06	T1NB + T2NB		
stan	chr2R:10682604-10683597	32B02	T1NB + T2NB		
SNF4Agamma	chr3R:21187347-21187968	32A12	No expression		
CadN	chr2L:17754057-17754529	32 E10	Subset Neuron		
CG43231	chr2L:17684303-17684903	32 E04	No expression		
svp	chr3R:12278924-12279410	31G08	Neuron subset		
CadN	chr2L:17735251-17736099	31G01	T1NB + T2NB		
lncRNA:CR45568	chr3R:29279912-29280248	31F07	T1NB + T2NB		
CG43231	chr2L:17702664-17702914	31D02	T1NB + T2NB		
CG43231	chr2L:17702096-17702522	31D02	T1NB + T2NB		
spi	chr2L:19575963-19576683	31C05	T1NB + T2NB		
Rho1	chr2R:16104307-16104870	31B06	No expression		
CG18508	chrX:3161937-3163244	30G07	T1NB + T2NB		
lncRNA:CR45267	chr2R:8021608-8022356	30F05	T1NB + T2NB		
lncRNA:CR44084	chrX:6983579-6984013	30D02	T1NB + T2NB		
N	chrX:3141950-3142603	30C06	T1NB + T2NB		
lncRNA:CR44339	chr2R:12985311-12986030	30B10	T1NB + T2NB		
lncRNA:CR44339	chr2R:12984507-12985137	30B10	T1NB + T2NB		
PIP82	chrX:8523732-8524152	29G07	T1NB + T2NB		
CG33798	chr2R:12990805-12991344	29F09	Neuron Subset		
lncRNA:CR43724	chr2R:8029224-8030264	29F07	Pan Neuronal		
CG30056	chr2R:12554553-12555321	29F05	T1NB + T2NB		

CG18371	chr2R:14024666-14025037	29A01	Neuron Subset		
Psc	chr2R:12979454-12979746	29 E08	T1NB + T2NB		
CG42637	chr3L:19791371-19792055	29 E01	Neuron Subset		
drl	chr2L:19196060-19197286	28H04	T1NB + T2NB		
CG18371	chr2R:14019563-14019966	28G12	T1NB + T2NB		
mam	chr2R:13995561-13996070	28F08	T1NB + T2NB		
mam	chr2R:13994039-13995015	28F08	T1NB + T2NB		
fra	chr2R:12531843-12532470	28D08	T1NB + T2NB		
lncRNA:CR44898	chr2L:1390167-1390564	28D05	T1NB + T2NB		
lncRNA:CR43653	chr3R:21594886-21595087	28A11	T1NB + T2NB		
mam	chr2R:14008264-14008793	28A06	Neuron Subset		
mir-4978	chr2R:14006783-14007293	28A06	Neuron Subset		
lncRNA:CR43302	chr3R:8190736-8191195	26H06	No expression		
Edg84A	chr3R:6683263-6683531	26H01	No expression		
disco	chrX:16231309-16232057	26G01	T1NB + T2NB		
chn	chr2R:15109062-15109785	26C03	Neuron Subset		
lncRNA:CR45304	chr2L:7319803-7320640	25C06	No expression		
Dl	chr3R:19321758-19322308	25B11	T1NB + T2NB		
Him	chrX:18214377-18214817	25B02	Neuron Subset		
Wnt4	chr2L:7272138-7272957	25A11	Neuron Subset		
Dl	chr3R:19319069-19319606	25A03	T1NB + T2NB		
TfAP-2	chr3L:21604425-21604661	25A02	T1NB + T2NB		
TfAP-2	chr3L:21584704-21585199	24G06	Pan neuronal		
Dl	chr3R:19324980-19325383	24B08			
Dl	chr3R:19324516-19324860	24B08	T1NB + T2NB		
Wnt10	chr2L:7358792-7359436	24 E06	Neuron Subset		
TfAP-2	chr3L:21610330-21610972	23F12	T1NB + T2NB		

fru	chr3R:18473994-18474562	23B02	No expression		
nAChRalpha1	chr3R:24457650-24458660	23A11	Neuron Subset		
Egfr	chr2R:21545438-21545825	22F09	T1NB		
fru	chr3R:18546775-18547207	22F06	Neuron Subset		
bif	chrX:11686168-11686626	22D10	No expression		
Egfr	chr2R:21552577-21552882	22D09	T1NB + T2NB		
Wnt2	chr2R:9493426-9493668	22C06	Neuron Subset		
NimC4	chr2L:14049768-14050346	21D05	Neuron subset		
nAChRalpha6	chr2L:9882451-9882962	20H09	Neuron Subset		
CG42758	chr3L:14565021-14565680	20G03	Neuron Subset		
ase	chrX:459414-459822	20B05	T1NB + INP		
cg	chr2R:14175471-14175852	20A05	T1NB + T2NB		
cg	chr2R:14174189-14175083	20A05	T1NB + T2NB		
nAChRalpha7	chrX:19349086-19349565	20 E10	No expression		
Dr	chr3R:29552758-29553405	19D08	Neuron Subset		
lncRNA:CR43613	chr3R:29541636-29541982	19B03	T1NB + T2NB		
lncRNA:CR43613	chr3R:29540809-29541465	19B03	T1NB + T2NB		
nAChRbeta1	chr3L:4431113-4431770	18D07	Neuron Subset		
ase	chrX:456456-457409	18 E10	T1NB + T2NB		
Acsl	chr2R:8668689-8669172	17F05	Glia		
Acsl	chr2R:8667604-8668034	17F05	Glia		
lncRNA:CR44216	chr2L:14244209-14244691	17D03	Neuron subset		
lncRNA:CR45759	chr3L:6785948-6786959	17C04	T1NB		
lncRNA:CR46322	chr2R:10210932-10211652	17 E05	T1NB		
lncRNA:CR44730	chr2L:14454057-14454811	16F09	T1NB + T2NB		
Hr3	chr2R:10224576-10225656	16F05	Neuron Subset		
lncRNA:CR44731	chr2L:14477671-14478383	16F02	T1NB + T2NB		

Hdc	chr2R:10239059-10239372	16D12	Neuron Subset		
sima	chr3R:30100696-30101007	15F07	Pan neuronal		
CG13891	chr3L:432647-433171	15D07	Neuron Subset		
lncRNA:CR45631	chr3R:16423343-16423919	15D03	No expresson		
lncRNA:CR46112	chr3R:30114402-30114967	15A05	Neuron susbet		
lncRNA:CR44203	chr2R:7429058-7429849	15 E10	T1NB + T2NB	14D09	T1NB + T2NB
so	chr2R:7418387-7418816	15 E06	Neuron Subset		
sima	chr3R:30098207-30098715	15 E04	T1NB + T2NB		
sima	chr3R:30090293-30090754	15 E03	Neuron susbet		
CG13891	chr3L:424503-425117	14G10	Neuron Subset		
snoRNA:Or-CD16	chr2L:3504754-3505472	14F08	Neuron Subset		
lncRNA:CR45630	chr3R:16413828-16414046	14C06	Neuron Subset		
nrv2	chr2L:6795180-6795450	14C04	T1 NB		
dnc	chrX:3332459-3332896	14B11	T1NB		
sim	chr3R:13075711-13076282	14A05	T1NB + T2NB		
dnc	chrX:3190767-3191078	13G04	T1NB		
Mnt	chrX:3677401-3677964	13G02	T1NB		
Mnt	chrX:3676712-3677221	13G02	T1NB		
Mnt	chrX:3685532-3685819	13F01	T1NB + T2NB		
Mnt	chrX:3691647-3691887	13D03	T1NB + T2NB		
dpn	chr2R:8233234-8233829	13C02	T1NB + T2NB	dpn VG	T1NB + T2NB
hig	chr2R:9245270-9245846	13B05	T1NB		
net	chr2L:87670-87828	13B04	T1NB		
PNPase	chr3R:31421842-31422636	13A07	Neuron Subset		
lncRNA:CR45102	chrX:3695516-3695761	13A06	T1NB + T2NB		
Mnt	chrX:3694703-3695030	13A06	T1NB + T2NB		
dnc	chrX:3205851-3206430	13 E05	Glia	12F10	Glia

Fer2	chr3R:16152171-16152908	12H11	Neuron Subset		
kn	chr2R:14803121-14803381	12H01	T1NB + T2NB		
lncRNA:CR44411	chr2L:17588240-17588683	12D08	T1NB + T2NB		
Mnt	chrX:3678196-3678438	12C10	T1NB + T2NB		
nub	chr2L:12623138-12623622	12 E08	Neuron Subset		
lncRNA:CR44886	chrX:3346938-3347945	11H01	T1NB + T2NB		
lncRNA:CR44742	chr2L:5287826-5288289	11G11	T1NB + T2NB		
lncRNA:CR44742	chr2L:5287448-5287675	11G11	T1NB + T2NB		
CG3556	chrX:4480052-4480514	11E 05	T1NB + T2NB		
lncRNA:CR45730	chr2L:5296936-5297281	11D11	T1NB + T2NB		
pdm2	chr2L:12655771-12656063	11C12	Neuron Subset		
lncRNA:CR42696	chr2L:21324401-21325151	11C01	Neuron Subset		
Myc	chrX:3379317-3379931	11B06	T1NB + T2NB		
vri	chr2L:5292873-5293685	11B02	Neuron Subset		
vri	chr2L:5292126-5292696	11B02	Neuron Subset		
dimm	chr2L:21330878-21331232	11A10	Neuron Subset		
crp	chr2L:16274929-16275616	11 E12	Neuron subset		
pdm2	chr2L:12681525-12682472	11 E07	Neuron Subset		
bi	chrX:4439740-4440661	11 E06	T1NB + T2NB		
pdm3	chr2R:8382825-8383920	10H09	Neuron Subset		
lncRNA:CR44999	chrX:3369437-3369898	10G10	T1NB + T2NB		
bi	chrX:4452942-4453423	10E 08	T1NB + T2NB	11D01	T1NB + T2NB
hng3	chr3L:776529-777191	10B08	T1NB + T2NB		
vri	chr2L:5306415-5307105	10B06	T1NB + T2NB		

Table 2.4 T2 lin enhancers annotated with activity patterns identified from Fig 2.1C

Activity pattern identified manually using Flylight: Gal4 corresponds to Janelia Flylight Line ((Jenett et al., 2012; Li et al., 2014). Red denotes manually reannotated gene name.

Gene Name	Location	Gal4/Reporter	Pattern	Gal4/Reporter	Pattern
T2 Lin.					
wor	chr2L:15426580-15427235	*Wor-Gal4*	T1NB + T2NB		
Six4	chr3L:20793750-20794213	Six4 VG	T1NB + T2NB		
pnt	chr3R:23297821-23298357	pntp1 VG	T2NB		
fuss	chr4:981086-981445	9G08	T1NB		
lncRNA:CR45153	chr2R:23637961-23638309	9F08	T1NB + T2NB		
erm	chr2L:1963517-1964072	9D11	ImmINP	Erm VG	ImmINP
erm	chr2L:1962787-1963374	9D11	ImmINP	9D10	ImmINP
Optix	chr2R:8044601-8045079	95A06	Neuron Subset		
Optix	chr2R:8046235-8046846	95A04	T2NB		
CG14762	chr2R:8014370-8014578	95A03	T1NB + T2NB		
lncRNA:CR44829	chr2R:24855323-24855644	94H10	T1NB		
Alk	chr2R:16637146-16637499	94G11	Neuron Subset		
dpr5	chr3R:11510375-11510993	94G09	INPs		
en	chr2R:11542022-11542386	94D06	Neuron Subset		
Dbx	chr3L:1916632-1917035	94B04	Neuron Subset		
unc-5	chr2R:15360277-15360567	93F01	Neuron Subset		
CG10182	chr3R:23576368-23577056	93B04	T1NB + T2NB		
TER94	chr2R:9988263-9988666	9 E07	Neuron Subset		
Dscam3	chr3R:17500893-17501689	89H10	T1NB + T2NB		
Dscam3	chr3R:17499108-17499550	89G09	Neuron Subset		
Dscam2	chr3L:7184657-7185111	89 E06	T1NB + T2NB		
snRNA:U4:25F	chr2L:5564868-5565878	88D08	T1NB + T2NB		
inv	chr2R:11493715-11494119	88C04	Neuron Subset		

Qsox2	chr3R:21921268-21921830	87B01	No expression		
Kr	chr2R:25232916-25233613	87 E05	T1NB + T2NB		
klu	chr3L:11016012-11016583	86F06	T1NB + T2NB		
klu	chr3L:11011614-11012256	86 E09	No Expression		
shn	chr2R:11175382-11176113	85G02	Neuron Subset		
sala	chr2L:11473945-11474943	85E 11	Neuron Subset		
btd	chrX:9704175-9704601	85C01	No expression		
btd	chrX:9703294-9703423	85C01	No expression		
dany	chr2R:22003789-22004061	84H12	Neuron Subset		
salr	chr2L:11362745-11363256	84G10	T1NB + T2NB		
lncRNA:CR44586	chr2L:11352813-11353119	84G03	T1NB + T2NB		
Eip93F	chr3R:21936692-21937118	84D11	T1NB		
Eip93F	chr3R:21945873-21946033	84D06	T1NB + T2NB		
Eip93F	chr3R:21951449-21951896	84C11	T1NB + T2NB		
Blimp-1	chr3L:5637742-5638106	83H01	Neuron Subset		
Blimp-1	chr3L:5636762-5637535	83H01	Neuron Subset		
lncRNA:CR46249	chr3L:548559-549077	83G08	No expression		
lncRNA:CR43862	chrX:20688175-20688556	83C05	T1NB + T2NB		
Gug	chr3L:8455087-8455480	83C02	Neuron Subset		
Gug	chr3L:8460296-8460693	83B11	T1NB + T2NB		
CAH15	chr2R:20907057-20907724	83 E01	T1NB + T2NB		
sba	chr3R:23915319-23915724	82H03	T1NB + T2NB		
lncRNA:CR44184	chr2L:19019607-19019847	82G02	Neuron Subset		
lncRNA:CR43491	chrX:17379699-17380035	81D12	T1NB + T2NB		
Kr-h1	chr2L:6086783-6087729	81C06	T1NB + T2NB		
CG18586	chr3L:5875831-5876029	81B11	Neuron Subset		
CG42758	chr3L:14575661-14576018	81A06	T1NB		

lncRNA:CR43817	chr2L:18806818-18807356	80H02	T1NB + T2NB		
ham	chr2L:18786487-18787125	80G10	ImmINP	Ham VG	ImmINP
lncRNA:CR43804	chr2L:18775271-18775858	80G02	Neuron Subset		
AANAT1	chr2R:24141464-24142099	80F06	Neuron Subset		
CG7587	chr3R:17593530-17593821	80D05	Neuron Subset		
Hmx	chr3R:17573981-17574524	80C12	T2NB		
Hmx	chr3R:17572911-17573625	80C12	T2NB		
CG9650	chrX:7235701-7236156	79F06	T1NB + T2NB		
CG1958	chrX:7250013-7250455	79E 01	T1NB + T2NB		
CG9650	chrX:7233291-7234159	79D05	T1NB		
bun	chr2L:12545732-12545910	78B08	T1NB + T2NB		
lncRNA:CR44596	chr2L:12579186-12579463	78B05	No expression		
dan	chr3R:25177665-25177948	77H03	T1NB + T2NB		
CG34435	chrX:5607852-5608569	76C09	Neuron Subset		
for	chr2L:3657943-3658403	75G09	T1NB + T2NB		
ab	chr2L:11219084-11219738	75F08	Neuron Subset		
zfh2	chr4:517141-517761	73G07	Neuron Subset		
CG9205	chr3L:1046288-1046937	73D10	Neuron Subset		
D	chr3L:14170112-14170680	73B10	INPs	73C02	INPs
D	chr3L:14163784-14164218	73B07	T1NB + T2NB		
lncRNA:CR45887	chr3L:14153063-14153534	73A10	T1NB		
lncRNA:CR45887	chr3L:14137100-14137829	73A01	T1NB + T2NB		
Ets65A	chr3L:6114671-6115181	72H06	Neuron Subset		
smog	chr2L:4857411-4857986	72A09	T1NB + T2NB		
cas	chr3R:5719338-5719730	71G07	T1NB + T2NB		
Vsx2	chrX:5553132-5553506	71F05	T1NB + T2NB		
Vsx2	chrX:5552499-5552936	71F05	T1NB + T2NB		

snoRNA:Psi28S-3342	chrX:5533252-5533808	71F02	T1NB + T2NB		
snoRNA:Psi28S-3342	chrX:5531973-5532469	71F02	T1NB + T2NB		
snoRNA:Psi28S-3342	chrX:5541444-5541918	71D06	Neuron Subset		
CG1239	chr3R:5729216-5729718	71C09	INP + GMC		
elav	chrX:525643-525949	71C07	T1NB + T2NB		
lncRNA:CR44281	chr2R:8655338-8656138	69F11	T1NB + T2NB		
Mur2B	chrX:1616758-1617482	69B10	T1NB + T2NB		
br	chrX:1598973-1599441	69B03	T1NB + T2NB		
br	chrX:1566508-1567088	69A03	T1NB + T2NB		
Oct-TyrR	chr3L:22033967-22034392	68A07	Neuron Subset		
Pp1-13C	chrX:15364817-15365556	67C12	T1NB + T2NB		
dco	chr3R:31059602-31059796	66B06	Neuron Susbset		
Hers	chrX:19898081-19898395	66A09	Neuron Subset	64G04	Neuron Subset
Hers	chrX:19897567-19897928	66A09	Neuron Subset		
14-3-3zeta	chr2R:10101365-10101956	64D02	Neuron Subset		
REPTOR	chr3R:24580936-24581171	60A09	T1NB + T2NB		
REPTOR	chr3R:24580153-24580388	60A09	T1NB + T2NB		
Xrp1	chr3R:18923302-18923537	60A04	Neuron Subset		
Thd1	chr4:554906-555205	59H10	T1NB + T2NB		
lncRNA:CR45169	chr3L:10848059-10848668	59G03	T1NB + T2NB		
lin-28	chr3L:5652810-5653035	59F02	Neuron Subset		
foxo	chr3R:14057201-14057655	59 E11	T1NB + T2NB		
CG43049	chr3L:18927560-18928158	58H12	Neuron Subset		
Liprin-gamma	chr2R:22370373-22370629	58D07	T1NB + T2NB		
CG46319	chr2R:10124676-10125230	57G01	Glia		
dally	chr3L:8825201-8825463	56G11	Neuron Subset		
Sep_4	chrX:16693832-16694330	56F07	Pan neuronal		

asRNA:CR43971	chr3L:15108079-15108478	56F05	T1NB + T2NB		
asRNA:CR43971	chr3L:15107275-15107856	56F05	T1NB + T2NB		
Xrp1	chr3R:18918663-18918831	56B06	No expression		
twz	chr2R:21576732-21576982	55H04	T1NB + T2NB		
twz	chr2R:21575258-21575584	55H04	T1NB + T2NB		
VAChT	chr3R:18711200-18711585	55D01	T1NB + T2NB		
Gad1	chr3L:4083495-4083974	55B08	Neuron Subset		
dlp	chr3L:14633976-14634380	54B09	Neuron Subset		
CG1354	chrX:9775368-9775901	53F02	Neuron Subset		
lncRNA:CR45277	chr2R:14433493-14433781	52C04	Pan neuronal		
nvy	chr2R:24280690-24281100	52A08	Neuron Subset		
VGlut	chr2L:2396555-2397549	51G05	T1NB + T2NB		
apt	chr2R:23574397-23574768	50D05	No expression		
apt	chr2R:23572478-23572611	49G06	T1NB + T2NB		
dpr10	chr3L:10181893-10182420	49D03	T1NB + T2NB		
apt	chr2R:23586995-23587542	49A03	T1NB		
CG11298	chr2R:22346911-22347316	48D06	Neuron Subset		
apt	chr2R:23578726-23578890	48A04	T1NB + T2NB		
sd	chrX:15818831-15819054	47B09	Neuron Subset		
lilli	chr2L:2896121-2896486	46C03	T1NB		
lncRNA:CR43904	chr2R:6159708-6159991	46B10	T1NB + T2NB		
hth	chr3R:10594592-10595286	46B08	T1NB		
lncRNA:CR43963	chrX:12718660-12719087	46A08	Neuron Subset		
Dad	chr3R:17053040-17053272	46A01	T1NB + T2NB		
Dad	chr3R:17052400-17052866	46A01	T1NB + T2NB		
Dad	chr3R:17051350-17051778	46A01	T1NB + T2NB		
mir-4944	chr3R:10559108-10559559	45H11	T1NB + T2NB		

CG4364	chr2L:9715129-9715708	45G12	T1NB + T2NB		
CG3841	chr2L:9588282-9588656	45G12	T1NB + T2NB		
lilli	chr2L:2908839-2909094	45G08	Neuron Subset		
lncRNA:CR43963	chrX:12727748-12728230	45G01	Neuron Subset		
snoRNA:Me28S-A30	chr3L:18005358-18005932	45F05	Neuron Subset		
jar	chr3R:24269268-24269707	45F03	T1NB		
EcR	chr2R:6122008-6122489	45D06	Glia		
Eip75B	chr3L:17964850-17965550	45D02	Neuron Subset		
hth	chr3R:10579413-10579666	45D01	Neuron Subset		
lncRNA:CR45922	chr3L:18037777-18038269	45C07	T1NB		
msi	chr3R:25595317-25596109	45C04	T1NB		
lncRNA:CR45392	chr3L:18075825-18076248	45B06	T1NB		
pnt	chr3R:23315163-23315596	45B05	T2NB	pntp3 VG	T2NB
lncRNA:CR43963	chrX:12725094-12725526	45B01	T1NB + T2NB		
lncRNA:CR43963	chrX:12724281-12724767	45B01	T1NB + T2NB		
hth	chr3R:10605891-10606553	45 E04	T1NB		
gt	chrX:2434961-2435400	44H04	Neuron Subset		
apt	chr2R:23565516-23565924	44G01	Neuron Subset		
Eip75B	chr3L:18029012-18029191	44D01	Neuron Subset		
lncRNA:CR44811	chr2R:24369448-24370156	44C12	T1NB		
pnt	chr3R:23300895-23301631	44C09	T2NB	45B10	Glia
Dad	chr3R:17059139-17059438	43G11	Neuron Subset		
CHES-1-like	chrX:7703440-7704015	42H04	Glia		
KP78b	chr3R:11353472-11353749	42G11	T1NB + T2NB		
SoxN	chr2L:8819259-8820028	42D10	T1NB + T2NB		
kay	chr3R:29764081-29764798	42 E11	Neuron Susbet		
cnc	chr3R:23211718-23211973	42 E02	Neuron Subset		

CG42710	chr2L:8787873-8788703	41H10	T1NB + T2NB		
CG30430	chr2R:25128094-25128359	41F10	T1NB		
SoxN	chr2L:8808962-8809432	41F09	T1NB + T2NB		
dve	chr2R:22252533-22253075	41F05	Neuron Subset		
l(2)k14505	chr2L:21251824-21252166	41F02	Neuron Subset		
pros	chr3R:11368465-11368788	41B05	T1NB		
grh	chr2R:17806426-17807747	41A10	Neuron Subset		
psq	chr2R:10581616-10582073	41 E12	Neuron Subset		
mir-9374	chr2L:21243863-21244469	41 E08	T1NB + T2NB		
l(2)09851	chr2R:5741488-5742708	41 E03	T1NB + T2NB		
lncRNA:CR44943	chr3R:14378512-14378896	41 E02	T1NB		
mir-9385	chr4:402221-402525	40H08	T1NB		
CG10026	chr2L:19459339-19459981	40H07	T1NB + T2NB		
lncRNA:CR43437	chr4:419681-419976	40H06	T1NB		
CHES-1-like	chrX:7691746-7692061	40H02	Neuron Subset		
Sfp60F	chr2R:25170571-25171002	40G03	No expression		
lncRNA:CR45695	chr2L:1644441-1644673	40F08	T1NB + T2NB		
mir-9385	chr4:411027-411241	40F01	T1NB + T2NB		
mir-9385	chr4:411661-412289	40C06	Pan neuronal		
CG42710	chr2L:8800127-8800522	40 E11	Neuron Subset		
dve	chr2R:22275817-22276192	40 E08	Neuron Subset		
dve	chr2R:22267686-22268448	39H01	T1NB + T2NB		
CG42710	chr2L:8794007-8794775	39F10	T1NB + T2NB		
lov	chr2R:25140758-25141394	39 E03	T1NB + T2NB		
kirre	chrX:3024562-3024993	38F12	Neuron Subset		
CG9701	chr3L:16743576-16743974	38F05	T1NB + T2NB		
shot	chr2R:13934351-13935089	38C03	T1NB		

shot	chr2R:13924709-13925147	38C02	T1NB + T2NB		
Nrt	chr3L:16768558-16768959	38B06	T2NB	38C04	T1NB + T2NB
CG4116	chrX:3055301-3055918	38 E12	T1NB + T2NB		
lncRNA:CR43653	chr3R:21599612-21600030	37B05	T1NB		
lncRNA:CR43653	chr3R:21597392-21597831	37B05	T1NB		
Dl	chr3R:19315537-19316002	37A05	T1NB		
CG44355	chr3L:12319471-12320102	36B06	T1NB + T2NB		
CG44355	chr3L:12318576-12319074	36B06	T1NB + T2NB		
Oatp58Dc	chr2R:22230498-22230871	36A10	Neuron Subset		
lncRNA:CR43238	chr3R:30749858-30750650	35C10	Neuron Susbset		
aop	chr2L:2166769-2167558	35C02	T1NB + T2NB		
ct	chrX:7621081-7621315	35B07	T1NB + T2NB		
aop	chr2L:2175274-2175703	35 E11	T1NB + T2NB		
aop	chr2L:2162280-2162764	34H06	T1NB + T2NB		
lncRNA:CR43855	chr2L:8584601-8585183	34D05	T1NB + T2NB		
ci	chr4:60548-60844	34D04	T1NB + T2NB		
ci	chr4:58836-59371	34D04	T1NB + T2NB		
ct	chrX:7602221-7602811	34B09	T1NB + T2NB		
ct	chrX:7605714-7606035	34A08	Pan neuronal		
lncRNA:CR43431	chr3L:12651304-12652008	33H11	T1NB + T2NB		
Lim1	chrX:8795785-8796248	33F01	Neuron Subset		
CadN	chr2L:17743580-17744159	32D11	T1NB + T2NB		
lncRNA:CR45568	chr3R:29273351-29273981	32C12	T1NB + T2NB		
lncRNA:CR46014	chr3R:12276015-12276387	32C04	T1NB + T2NB		
CadN	chr2L:17748750-17749084	32C01	T1NB + T2NB		
CG45544	chr3R:29257084-29257621	32B06	T1NB + T2NB		
SNF4Agamma	chr3R:21186704-21187094	32A12	No expression		

lncRNA:CR45568	chr3R:29271008-29271370	32 E06	No expression		
lncRNA:CR45568	chr3R:29269515-29269670	32 E06	No expression		
lncRNA:CR45568	chr3R:29268770-29269259	32 E06	No expression		
Ubx	chr3R:16719711-16720350	31F12	T1NB		
CG45544	chr3R:29264655-29265195	31F05	Neuron Subset		
CG43231	chr2L:17715428-17716134	31B04	No expression		
spi	chr2L:19573016-19573402	31 E08	T1NB + T2NB		
Optix	chr2R:8038955-8039388	30D11	Neuron Subset		
Optix	chr2R:8038288-8038771	30D11	Neuron Subset		
PIP82	chrX:8524939-8525342	30D07	T1NB + T2NB		
msn	chr3L:2579591-2579990	30C02	Neuron Subset		
CG30056	chr2R:12555823-12556261	29F05	T1NB + T2NB		
IntS4	chrX:8548874-8549795	29D06	T1NB		
CG33752	chr2R:12549510-12550303	28G07	T1NB + T2NB		
d4	chr2R:5260582-5260791	28B10	T1NB		
Tab2	chr2R:19292914-19293571	28B07	No expression		
Dscam1	chr2R:7372563-7372803	28 E05	T1NB		
gish	chr3R:16280029-16280625	27H10	Glia		
hh	chr3R:23143438-23143811	27G12	T1NB + T2NB		
lncRNA:CR44898	chr2L:1386077-1386628	27F07	T1NB + T2NB		
grn	chr3R:8187271-8188332	27B03	T1NB + T2NB		
slim	chr2R:18442659-18443003	27 E11	Neuron Subset		
gish	chr3R:16281217-16281686	27 E03	T1NB + T2NB		
Btk29A	chr2L:8277960-8278192	26F10	T1NB		
chn	chr2R:15132297-15132770	26F08	Neuron Subset		
chn	chr2R:15130578-15131231	26F08	Neuron Subset		
chn	chr2R:15129491-15129887	26F08	Neuron Subset		

Arl8	chr3R:8149970-8150885	26F04	T1NB		
snRNA:U5:14B	chrX:16236360-16236735	26D09	Neuron Subset		
milt	chr2L:7038201-7039017	25G12	T1NB		
Eph	chr4:611015-611234	25F09	Neuron Subset		
Dl	chr3R:19318235-19318948	25A03	T1NB + T2NB		
aos	chr3L:16476947-16477677	24G11	T1NB		
CG44174	chr3R:19310562-19311067	24D04	Neuron Subset		
CG30283	chr2R:21541062-21541405	23C11	No expression		
fru	chr3R:18445035-18445330	23A02	T1NB + T2NB		
TfAP-2	chr3L:21611700-21612174	23 E06	T1NB + T2NB		
lncRNA:CR45950	chr3R:24446474-24447151	22G06	Neuron Subset		
Egfr	chr2R:21547172-21547691	22F09	T1NB		
fru	chr3R:18448726-18449062	22B06	Glia		
fru	chr3R:18448068-18448514	22B06	Glia		
bif	chrX:11686765-11687210	22 D10	No expression		
bif	chrX:11685562-11685930	22 D10	No expression		
crb	chr3R:24295447-24296020	21D08	Neuron Subset		
lncRNA:CR43766	chr2L:9849626-9850366	20G02	T1NB + T2NB		
eya	chr2L:6537777-6538106	20C10	T1NB		
eya	chr2L:6545012-6545589	20 E04	Neuron Subset		
eya	chr2L:6533582-6533973	20 E01	T1NB + T2NB		
nAChRalpha4	chr3L:23279118-23279339	17H04	Neuron Subset		
lncRNA:CR45759	chr3L:6784779-6785173	17C04	T1NB		
lncRNA:CR44731	chr2L:14483402-14483815	17A06	T1NB + T2NB		
lncRNA:CR44731	chr2L:14479802-14480007	16F02	T1NB + T2NB		
lncRNA:CR45630	chr3R:16406668-16407010	15B07	T1NB		
lncRNA:CR44753	chrX:393668-394082	15 E09	T1NB		

sima	chr3R:30097007-30097385	15 E04	T1NB + T2NB		
sima	chr3R:30095289-30096461	15 E04	T1NB + T2NB		
nrv2	chr2L:6792018-6792353	14B09	Glia		
Mnt	chrX:3690876-3691383	13D03	T1NB + T2NB		
kn	chr2R:14788307-14788972	13C11	Neuron Subset		
BEAF-32	chr2R:14776679-14776983	13B08	Neuron Subset		
net	chr2L:88532-88906	13B04	T1NB		
mir-1010	chr3R:22271156-22271629	13A10	INPs		
Pex7	chr3L:8658898-8659833	12H06	Neuron Subset		
kn	chr2R:14803608-14803819	12H01	T1NB + T2NB		
Mnt	chrX:3686571-3687417	12B10	T1NB + T2NB		
bi	chrX:4403117-4404497	12B05	T1NB + T2NB		
pdm2	chr2L:12661429-12661950	11G10	Neuron Subset		
lncRNA:CR45730	chr2L:5294862-5295299	11D11	T1NB + T2NB		
bi	chrX:4462057-4462436	11C04	T1NB + T2NB		
Nepl7	chr2L:12672396-12672618	11A01	Neuron Subset		
pdm2	chr2L:12682827-12683087	11 E07	Neuron Subset		
CG3556	chrX:4507251-4507478	10D01	T1NB + T2NB	11F04	T1NB + T2NB
emc	chr3L:745095-745621	10C04	T1NB + T2NB	10B05	T1NB + T2NB
crp	chr2L:16280009-16280306	10B02	T1NB + T2NB		
lncRNA:CR43644	chr3R:26020661-26021232	10 E02	T1NB + T2NB		

Table 2.5 T2 NB enhancers annotated with activity patterns identified from Fig 2.1C

Activity pattern identified manually using Flylight: Gal4 corresponds to Janelia Flylight Line ((Jenett et al., 2012; Li et al., 2014). Red denotes manually reannotated gene name.

Gene Name	Location	Gal4/Reporter	Pattern	Gal4/Reporter	Pattern
T2NB					
btd	chrX:9689615-9689712	85C07	T2NB	85C03	Neuron Subset
N	chrX:3139258-3139451	30D10	T1NB + T2NB		
tll	chr3R:30848277-30849071	31F04	T2NB	Tll enh VG	T2NB
pnt	chr3R:23333973-23334697	46C10	No CB expression	45 E10	No CB expression
gem	chr2R:10134775-10134975	27F04	T1 NB		

Table 2.6 Pan NB enhancers annotated with activity patterns identified from Fig 2.1C

Activity pattern identified manually using Flylight: Gal4 corresponds to Janelia Flylight Line ((Jenett et al., 2012; Li et al., 2014). Red denotes manually reannotated gene name.

Gene Name	Location	Gal4/Reporter	Pattern	Gal4/Reporter	Pattern
Pan NB					
Dscam3	chr3R:17502699-17502898	89H10	T1NB + T2NB		
CG14441	chrX:6701646-6702006	87F05	T1NB + T2NB		
Qsox2	chr3R:21927803-21928172	87A08	No expression		
lncRNA:CR42746	chr2L:12544043-12544208	78B08	T1NB + T2NB	78D05	T1NB + T2NB
Ets65A	chr3L:6115828-6115913	72H06	Neuron Subset		
Slc45-1	chr3L:9196724-9196967	70G04	T1NB + T2NB		
REPTOR	chr3R:24579772-24579884	60A09	T1NB + T2NB		
lncRNA:CR44514	chr3L:702994-703425	56G05	T1NB + T2NB	59H12	Pan Neuronal
lin-28	chr3L:5655734-5656221	56C11	T1NB + T2NB		
snoRNA:Me28S-A30	chr3L:18007609-18007954	46 E12	No expression		
mir-4944	chr3R:10538429-10538643	46 E01	T1NB + T2NB	44C06	No expression

lncRNA:CR45922	chr3L:18038403-18038554	45C07	T1NB		
CHES-1-like	chrX:7698778-7698928	42B03	T1NB + T2NB		
lncRNA:CR43437	chr4:421435-421674	40C10	T1NB + T2NB		
rst	chrX:2962057-2962726	38C10	T1NB + T2NB		
ct	chrX:7613662-7614045	34C09	T1NB + T2NB	33F07	T1NB + T2NB
lncRNA:CR44039	chr3R:12268204-12268536	31H02	T1NB + T2NB		
Pkcdelta	chrX:12437812-12437942	22 E03	Neuron Subset		
dnc	chrX:3285404-3285589	14 E05	Neuron Subset	15D05	Neuron Subset
dnc	chrX:3189766-3189948	13G04	T1NB		
Mnt	chrX:3684956-3685151	13F01	T1NB + T2NB		

Table 2.7 Random non-promoter enhancers patterns from Janelia Flyight.

Activity pattern identified manually using Flylight: Gal4 corresponds to Janelia Flylight Line ((Jenett et al., 2012; Li et al., 2014). Red denotes manually reannotated gene name.

Name	Pattern
52H01	Neuron subset
82C02	none
14G12	none
59D11	T1NB + T2NB
14C01	none
24A08	T1NB + T2NB
25C03	Neuron subset
59F06	Glia
75D05	None in CB
15A01	Neuron subset
22B05	Neuron subset
34G05	Pan Neuronal
35C11	T2NB
38F04	Neuron subset
47G12	none
49D02	T1NB + T2NB

59H02	Neuron subset
78G09	Neuron subset
11F07	Neuron subset
67B09	Neuron subset
19D12	T1NB + T2NB
28G05	Neuron subset
35F04	Glia
39F02	Neuron subset
43F04	Neuron subset
48F08	Neuron subset
76C04	Neuron subset
77C12	Neuron subset
79H09	Glia
81H11	T1NB + T2NB
20A02	Neuron subset
35F04	Glia
40B09	T1NB + T2NB
78A04	Neuron subset
78D01	Glia
36C07	Neuron subset
55G05	Neuron subset
78B02	Neuron subset
80F09	T1NB + T2NB
85A11	No expression
14A08	Glia
16B09	No expression
24G08	Neuron subset
30B01	Neuron subset
32A02	Neuron subset
35C06	Neuron subset
41H12	Neuron subset
50A04	Neuron subset
50C01	T1NB
56G08	Neuron subset
14F05	Neuron subset
24C07	Neuron subset
30B08	T1NB
31A03	T1NB

80B05	Neuron subset
16H09	Neuron subset
37G06	T1NB + T2NB
38G04	T1NB
44B12	T1NB + T2NB
83D12	Neuron subset
13D10	Neuron subset
42F04	No expression
53F07	Neuron subset
75H05	No expression
80F02	T1NB
33H09	Neuron subset
41H09	Neuron subset
48H11	Neuron Subset
71F03	Neuron Subset
83G12	Glia
33H06	T1NB + T2NB
40C02	Neuron Subset
43G03	No expression
49H09	No expression
56D08	No expression
56H01	Neuron Subset
67C11	Neuron Subset
71C10	Neuron Subset
73D01	Glia
95C07	No expression
19D07	T1NB + T2NB
31G02	No expression
46C12	Neuron Subset
46D05	Neuron Subset
51H09	Neuron Subset
89B01	Neurons Subset
92H07	Neuron Subset
94H08	Pan neuronal
53F01	T1NB + T2NB
83F06	Neuron Subset + Glia
24H03	Neuron Subset
25C05	T2NB

27C05	Neuron Subset
36A06	Neuron Subset
43F05	T1NB
50A01	Neuron subset
52C05	Neuron Subset
82C10	Neuron Subset
93D11	Neuron Subset
94A08	Glia

Appendix B: Expression Patterns for Genes with mRNA Associated with T1 NBs or INPs

Table 2.8 Expression pattern in CB validated using GFP reporters, antibodies, or published data for TFs identified in Fig. 2.3A as T1NB or T1NB and INP enriched

Gene	Expression Pattern
achi	Weak Pan NB
Antp	No central brain expression
ase	T1 NBs and INPs
Atf-2	Weak Pan NB
bi	No central brain expression
CG10321	
CG11247	Weak Pan NB
CG11398	No central brain expression
CG11456	Weak Pan NB
CG11560	Weak Pan NB
CG11906	No central brain expression
CG12054	(No reporter)
CG12219	Moderate pan NB
CG12236	No central brain expression
CG12391	Subset of NBs
CG12659	Pan NB
CG12744	Weak Pan NB
CG15011	No central brain expression
CG15073	No central brain expression
CG15435	(No reporter)
CG1602	No central brain expression
CG1663	No central brain expression
CG17186	Weak Pan NB
CG17568	Weak pan NB
CG17612	Weak Pan NB
CG18764	Weak Pan NB
CG2712	Weak Pan NB
CG30020	Weak Pan NB
CG3065	Pan NB

CG31365	No central brain expression
CG31388	No central brain expression
CG31441	Ubiquitous, slightly higher in NBs
CG32767	
CG32772	Ubiquitous
CG3281	Weak Pan NB
CG34376	No central brain expression
CG4424	Subset of Neurons
CG4707	Pan NB
CG4730	Weak Pan NB
CG4820	Weak Pan NB
CG5245	No central brain expression
CG6254	Ubiquitous, slightly higher in NBs
CG6654	No central brain expression
CG6765	Weak Pan NB
CG6813	No central brain expression
CG8388	Ubiquitous
CG8478	Pan NB, cortical
CG8924	Pan NB
CG9609	Pan NB
Clamp	Ubiquitous slightly higher in NBs
Cp190	(No reporter)
CrebB	Weak Pan NB
D19B	Pan NB
danr	Pan NB
dati	No central brain expression
dbr	(No reporter)
Dref	Ubiquitous, slightly higher in NBs
dwg	Pan NB
E(bx)	Ubiquitous, slightly higher in NBs
E(spl)m8-HLH	Pan NB
emc	Pan NB
ERR	Ubiquitous
fs(1)h	All cortical membranes and neuropil
fuss	Subset of neurons
GATAd	Ubiquitous, slightly higher in NBs
insv	Pan NB
jumu	Pan NB
lola	immature Neurons
Lpt	Ubiquitous, slightly higher in NBs
M1BP	Pan NB
Mad	Pan NB, higher in INPs
MBD-R2	Ubiquitous, slightly higher in NBs

mirr	Subset of neurons
MTA1-like	Subset of neurons
MTF-1	Weak Pan NB
Nf-YB	Weak Pan NB
nom	No central brain expression
oc	Subset of T1NBNBs and GMCs
p53	Not expressed
Pbp95	(No reporter)
phol	Pan NB
Phs	Pan NB
prg	Cortical T1 NBS and INPs, nuclear GMCs and Neurons
pros	Ubiquitous, slightly higher in NBs
pzg	Weak Pan NB
ranshi	Weak Pan NB
run	Subset of NBs
sd	Pan NB, higher in INPs
sima	Weak Pan NB
Su(H)	Pan NB
tef	Ubiqutous higher in NB
toy	No central brain expression
Usf	(No reporter)
wdn	
zf30C	Ubiquitous, slightly higher in NBs

Table 2.9 Expression pattern in CB validated using GFP reporters, antibodies, or published data for candidate Ase target TFs identified in Figure 2.7

Gene	Expression Pattern
Ase	T1 NBs and INPs
CG32772	Ubiquitous but weak throughout central brain
CrebB	Weak pan NB
Dati	No expression
Lola	immature Neurons
Emc	Pan NB, higher in INPs
fs(1)h	All cortical membranes and neuropil
HmgD	Pan NB
HmgZ	Pan NB
Mad	Pan NB
Pros	Cortical T1 NBs and INPs, nuclear GMCs and Neurons
Sd	Pan NB, higher in INPs
sima	Very weak pan NB

jumu	Pan NB
Eip75B	(No reporter)
Su(H)	Very weak pan NB or not expressed
klu	Pan NB
E2f1	Pan NB

Appendix C: Enhancer Reporter Construction

Table 2.10 Coordinates and sequences for newly made enhancer reporters

Enhancer name	Coordinate	Sequence
erm	2L:1963434-1964066	actcactgatgaaaaaggtctcaaaaacataaatgcaatcaaattaaactgtaaattatcaaggtgatttttttcaagtgtatgatcatctctagccttgattatcctgccgagaaaccggttgctcctgcggggcgttgttcgttttttccgctactggcctgacatttgatttcgctttcggcggcgatggcagcggaaatgctttttctttctacggttgttgacacgcgatcctgcgattcacgaggatcctgcgtcggtgtgccgatcatcctgttcgagtcctgtttttcgtcctggcgcgtgtgccgcgcttccggttaattatattccgcaatgccaaagtccccgcaacgaaagcgaaatcgtcgctttcggttcgagaatcaaatgcatatgctctcggctttttgtgctccctacgctgggctcgaattcctttattccgcctgtcagtcgtcgtctccgaggtcctggcattgtccttcgagtgcctcgccgctcgaacaactgctcattaattgccggttatgtgcgcttttctttcccaaacgctgacgaatttggcattctaaattggctcgtgccagcttgcttgtaatgcgagtaggcgacaggatgttgatcc
ham	2L:18786466-18787132	agtttaccctccactgtgcgaatttgtatatcaatctgcgctgatcctgtaagcctggcaacttcaactgtgtgtgtgtgtgtctcattgacaggacaggactcactgctattgccatagcgattcccgttcggatgccgatgccgatgcctattccgattctgattctgattgctattgctattgcaaggaccgctgttccattgttctgccttcgaggcggagcggaagtcgctcttctctgccgaaaaggaccccaaggaaaaagtgaagcagggcaagttctcaagtcaaaatgcgcgagacagacgagcggggtcaggactataattatggcaaggtcaaaccgttacgagtgccgttgaagatcgcgtctgtgcagaaggaggaggggagagggaggcgtgaactaagaagatcgtaacttaataccagccaaagctgcaaactctggaatctggatcaagattcgaacccatccctgcagcacgcgccctcgaatcgagtttacccaagtgcaatttgcagtgtgcaacggaaatggtagaagaggagcagatacctctgcttcctgtcttggcacactttccactaaaatcacatctgccaggatctcgattgcagcagggtggttcaggtacaaccggtgatcagacacactgggg

pros1	3R:11352885-11353685	gcacaacggacgcaagataaggcattctggtacccaagggatacgatcggacttatctgacaatggat gcgaaactctggaactcacagtgaccaccgcgtgcttgcttaattacgctctttacttacgcatcggtccatt ggcgatccccccctggcggcaatcaaaaacgaattagcgttaatccactccacaagtgtaccatatcgttt cgtatccgtatcgttgagcgagaccgaactttcagatacaaggcgcgccgtagtactgaaacgcattga gcggaatatctgaagacaggtcttgaactggaactgaaacgtctgagacgggctgagcaaagagaga gcgaagagcgtctttgtgctcttcttacgctcaaaaaaatggccaactgattgcgatcgtgtgctcgtgcag cggatttgaaaagaaacgcattattaagatttacgcctgcttcaacttttctctttcgtcgtctttaaacataaa atttaaaaagagaaaattaaaattttaagcagtttgattttctctctttctttttcactcaatttttgaattatgttgctc ttccttctctcaatatcgtttccttgagcgtttcttgaggtgtgacgtcacggatgcgaaggggaggcacttcg ggtgtttcgtgcttcgtctttgttcgtctttgcggcgaatttggcctttgtcgtggtcttcgtcttcgtttgagtttcttc attggtatgggttatcttgcggtggtggtgctggcgactgcgatggtgtatgtgtgccatcaagacttcccc
pros3	3R:11378481-11379125	cgcaagaagttgccaaaaagagcagaaagacaacgactacggaaaaacgacagctgccagatagt ccgtggtgtgggtaaattcggatatacggttattccgtggaaggagtgggctgttctcaatggaacagagc caaagtgaagtgaggtaggcccgcatgcagtcgccgtgatttgcgcgccaaatccgggccgcatctgtc cgccccgaagtgaataccataccgaaggaaaacagagaaccgagctgaaaacagagcgtggcac aaggtctcacctggatttataacttgcaaccctctttcatcgtcggcttagcagctgcccgtctccgatttgtct aagacatgcgcaacgtcttaaggaattgtccgcaagacaccctaagaaattcccctacctgcgcacaa gcgaacagcacaaaagacaacaaatcaagacccggcggcgcggggtttgttcggaatttcttatgggg gttgctacccttgcgcgatgtgccctaaccctactttgcatgggaatcggggagttggcatcttgtctttgcctt cgacgacttcggcgacttcttgggcgagaggttaaaatgggtgggaatattttctgatttcctaactggtact cgattgtttgtttccg
Pros3ΔAse	3R:11378481-11379125	cgcaagaagttgccaaaaagagcagaaagacaacgactacggaaaaacgaccagatagtccgtgg tgtgggtaaattcggatatacggttattccgtggaaggagtgggctgttctcaatggaacagagccaaagt gaagtgaggtaggcccgcatgcagtcgccgtgatttgcgcgccaaatccgggccgtccgccccgaagt gaataccataccgaaggaaaacagagaaccgaaaacagagcgtggcacaaggtctcacctggattt ataacttgcaaccctctttcatcgtcggcttagcccgtctccgatttgtctaagacatgcgcaacgtcttaag gaattgtccgcaagacaccctaagaaattcccctacctgcgcacaagcgaacagcacaaaagacaa caaatcaagacccggcggcgcggggtttgttcggaatttcttatgggggttgctacccttgcgcgatgtgcc ctaaccctactttgcatgggaatcggggagttggcatcttgtctttgccttcgacgacttcggcgacttcttgg gcgagaggttaaaatgggtgggaatattttctgatttcctaactggtactcgattgtttgtttccg

btd	X:9692412-9693152	agtattgagtcatatcagttggttaaacattaaatctcatattatcccaagaaatcccctacataatgatattcatcttaacaatgggtagcttaagagtcgagatgcacttccgtgagcttgttccgttttgggagtcatcattatctttcacagcagcagcaagtcgtaaaatttgtggctcagacccacgttgcgtatgcgtaataaaaaagacgccgcgtaataaaaagggagcgaaaacaacaacagcaacagcaattgtgattaatatgcggcacacaagcatacacaaacgcacgcacacacgaaacgggcgcaggccatgcgagagagagagagcgaaggagagagctgctgtctcttttgtggtggtgtttggtcaacgccccttaaatacagttatttcattgggccgcgaccacaaatttattagtttttattgttattgtattgatatttgaattatgcacgctccctcttcgtcttctaacgttacttttatcattgggatcctctggagaaaaatgccattaaacagaaattttaatttaattaaagtgatgagccatacttctttctctctgtctgcttactttcatcgaaacaaattgatggtctgagtgggcaaggggata
pntp1	3R:23297691-23298300	agcggaaaatcaagaaacctcaaagttaaagctacaaaagcaattaatccttaagcttatactaatatttctagccttaaattgcattaatccaaaacgtttctttctgtgtaccaaataataagatggtgtgtgccaaaaacaaaaaaaaaaagaaggagcaaaatggtataagcatactttcagttgaatttcaattaaaactcgttctgttcgcacaaaaggattacacatttaatgcaataaggattgtcagggaggaggagttgcaggaagcgcctacgggaagaacaaaggcggatgggcaaggtactcccgaatctagggattccttcggatgggcctgccaacaacagctgtcgactgacactcgagatcatcagcccattcaattgatatcaaattggagtaggatccttgccagaatctcgctcgatcctgtgcacgtgtacaaattgcactctctgagctctgagctctgagctctgtatcctataatatggtctgagccctatgctctgtcttttgtaccatatagcactgcaagcacttccggccccatcccgctaatgtaaatcggatgtcaatgcattgcgcgtgaggcatatc
pntp3	3R:23315128-23315676	ggcaaatctactcatgtttctccgccccctcccctgcaatgactcgagaaatgcccaggcacacaggcaatttatgaatgaatttcttgtgttgcctcacacgcgcattcttctcaaaagaaactccagacaacgaacacaacgaaaacaacaacaactaaaaagaagaagacaccgatattgtagtaagggaacgcttcgtatttcgaagatacaatacctccaggcgatagaagcaacaacaacaatcgatcgagacgtcgacgtcgacagaggccgcttccgctgcttccgttcgatgtattgatatagggtgcaaaagagatggctagatgcagaacggccagcgtggaaaagagaagatagtggccagggcaaaggagaggaggaggataagataaagctattattatgatgactacgcgaccaggtaaatttatgaatgggatacgaaacgaaacgagacgcgaaacattgactccgcggcttaacgtctatgaatgaattgaaattacgtgcgacggcgacggagacgtaagggagatca

Chapter 3 Regulation of T2NB Functional Identity and Lineage Progression

Summary

The ability of neural stem cells to generate an increased number of neurons through transit amplifying cells is thought to play an important role in promoting complex brain development. T2NB neuroblasts generate intermediate progenitor cells (INPs) that can divide multiple times to amplify overall neuronal output. Transcription factors Tailless (Tll) and Buttonhead (Btd) are known to be necessary for promoting INP generation but how these genes function mechanistically has been limited. Here we show that Trithorax (Trx) is needed to promote activation of *tll*, which appears to function as a transcriptional repressor in T2NBs. We identified *hmx* and *vsx2* as genes that are likely repressed by Tll and appear to promote proper differentiation of INPs into GMCs. We also provide proposed schemes to identify Tll and Btd targets that influence T2NB function. We also showed a new means of assaying enhancer activity which could be used to provide better insight into how genes like *tll* are shut down during T2NB lineage progression.

Introduction

Previous work has identified roles for Trx and Tll in maintaining T2NB identity (Hakes & Brand, 2020; Komori et al., 2014; Quinto-Rives et al., 2020). Previous work has identified that *trithorax* (*trx*) and *retinoblastoma binding protein 5* (*rbbp5*) are components of the SET1/MLL complex to promote gene activation through deposition of H3K4me3, an active histone mark associated with enhancers (Krogan et al., 2002;

Miller et al., 2001). Loss of either component results in apparent loss of T2NB identity, but does not appear to cause global gene misregulation due to other

redundancies in in SET1/MLL complex function outside of Trx or Rbbp5 (Komori et al., 2014).

Trx is likely working with specific TFs to preferentially activate genes needed for T2NB activity. Previous work has shown that Trx activates *btd,* which is required for proper specification of immature INPs from T2NBs (Komori et al., 2014). Btd is likely to work as an activator, but loss of Btd does not result in loss of Pnt as is observed upon Trx loss (Hakes & Brand, 2020; Komori et al., 2014). Both this observation and evidence that indicates *btd* is a target of Trx suggests that there factors not including Btd that work in complex with Trx. Previous work has also shown that some factors associated with T2NB identity are down regulated upon Trx and Tll loss, but new methods and greater knowledge of genes expressed in T2NBs has been made available since that provide a more in depth means to investigate if loss of either factor results in a true conversion to a T1NB identity and what the gene regulatory network that underlies T2NB identity is.

Tll plays an important role in promoting neurogenesis, but aberrant activation of Tll in the T2NB lineage causes reversion of INPs to a NB state resulting in a tumorigenic phenotype (Hakes & Brand, 2020; Quinto-Rives et al., 2020). Understanding what genes Tll might be regulating that facilitate stem cell maintenance could have important implications for suppressing tumorigenesis. Tll is likely a target of Notch and needs to be maintained in NBs but not reactivated in INPs (Hakes & Brand, 2020; Quinto-Rives et al., 2020; Zacharioudaki et al., 2016). A T2NB specific enhancer of *tll* has been identified that becomes inaccessible shortly after immature INP generation which evidence suggests is mediated by Earmuff (Erm), but the ability to visualize rapid

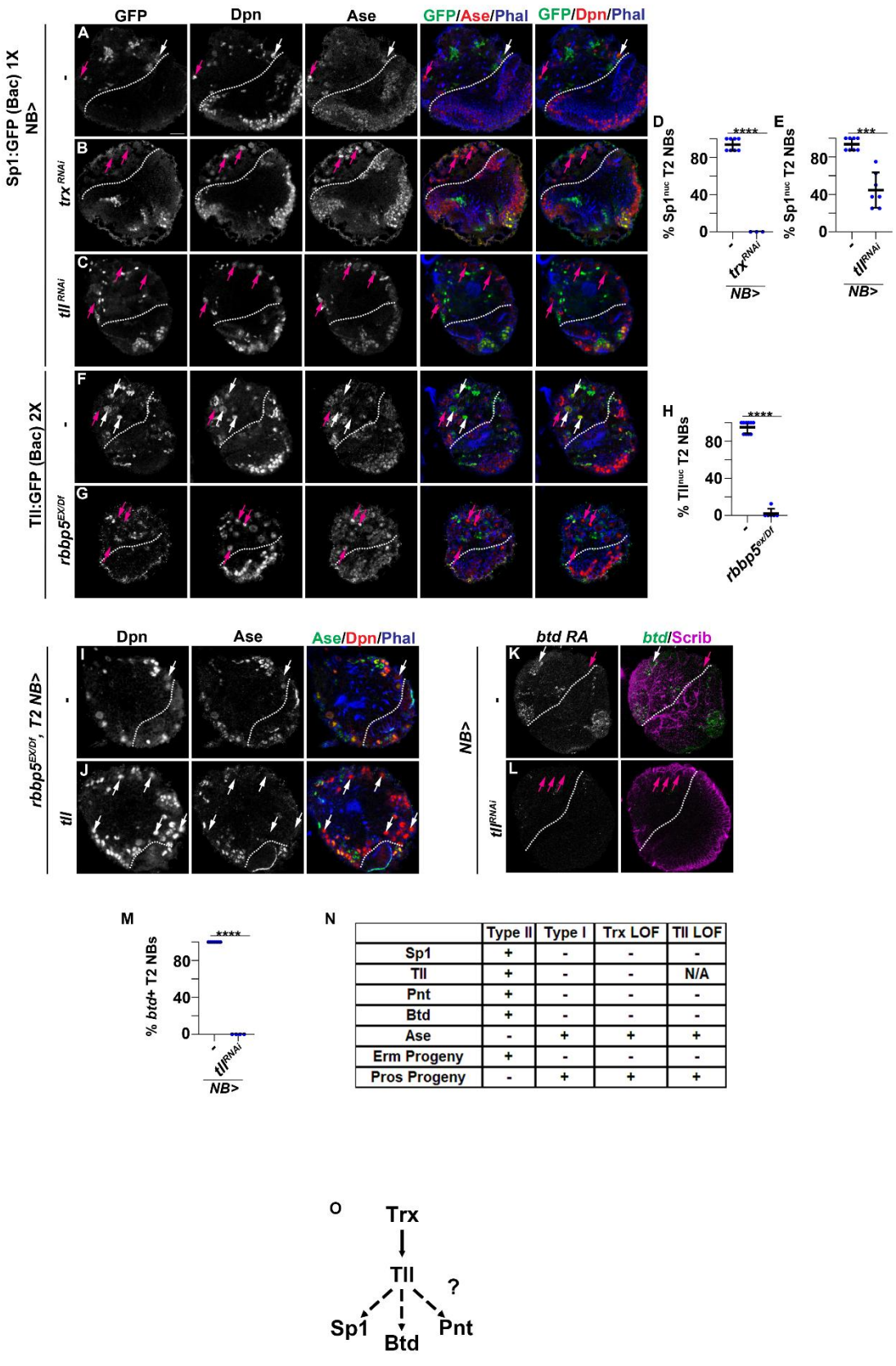
changes in enhancer activity and has been limited thus far (Larson et al., 2021; Quinto-Rives et al., 2020).

Additionally, insight into the role of Btd and how it promotes immature INP specification has been limited. Btd, as the apparent downstream most regulator that promotes INP generation is of interest in terms of understanding mechanistically how INP generation is specified. One limitation into study on Btd has been due to a lack of information on where exactly Btd is expressed due to no available reporters or functional antibodies. New technological developments in mRNA in situ could be utilized to provide insight into where *btd* is transcribed in the T2NB lineage, potentially shedding light on the role Btd might play. Further understanding of what Btd targets and how gene expression changes in T2NB lineages upon loss of Btd expression may be needed to better understand molecularly what happens to specify the generation of INPs.

Tll and Trx are necessary to maintain T2NB functional identity

We recently identified that the Sp family TF Sp1 is known to be expressed in T2NBs and throughout the T2NB lineage, but is not detected in T1NBs in the central brain (Quinto-Rives et al., 2020). Sp1 is known to play a role in specification of T2NBs during embryonic development, but postembryonic removal of Sp1 has no apparent phenotype (Álvarez, 2018; Chen et al., 2021; Quinto-Rives et al., 2020). Sp1 was concluded to be a positive marker for T2NB identity. We then tested whether Tll or Trx are needed to maintain Sp1 expression in T2NBs. We knocked down *tll* and *trx* using previously validated RNAi lines and compared how many T2NBs could be positively identified based on the presence of nuclear Sp1:GFP signal. We found that by knocking

down either *tll* or *trx*, the fraction of T2NBs that retained Sp1:GFP signal was significantly reduced (Fig. 3.1A-E). We conclude that both Trx and Tll are necessary to maintain Sp1 expression in T2NBs.



N

	Type II	Type I	Trx LOF	Tll LOF
Sp1	+	-	-	-
Tll	+	-	-	N/A
Pnt	+	-	-	-
Btd	+	-	-	-
Ase	-	+	+	+
Erm Progeny	+	-	-	-
Pros Progeny	-	+	+	+

Figure 3.1 Tll likely functions downstream of Trx to maintain T2NB cell identity

(A-C) Images of Sp1:GFP expression in T2NB lineages upon *trx* and *tll* knockdown with pan-NB driver (*Wor-Gal4*).(D-E) Quantification of fraction of T2NBs with nuclear Sp1:GFP expression upon *tll* or *trx* knockdown with NB driver (*Wor-Gal4*). Tll and Trx are needed to maintain Sp1 expression in T2NB lineages.(F-G) Images of Tll:GFP (two copies of transgene) expression in T2NB lineages in control and *rbbp5* mutant ($rbbp5^{DF}$/$rbbp5^{ex}$ brains.(H) Quantification of fraction of T2NBs with nuclear Tll:GFP expression in control vs *rbbp5* mutant ($rbbp5^{DF}$/$rbbp5^{ex}$) brains. Trx complex activity is needed to maintain high Tll expression in T2NBs.(I-J) Images showing supernumerary T2NBs ($Dpn^{+}Ase^{-}$) are able to be generated upon Tll misexpression for 24 hours in T2NB lineages with T2NB driver (*Wor-Gal4*, Ase-Gal80) in a *rbbp5* mutant ($rbbp5^{DF}$/$rbbp5^{ex}$) background. Tll is likely downstream of Trx and Rbbp5 activity (K-L) Images of *btd* transcripts in T2NB lineages upon *tll* knockdown with pan-NB driver (*Wor-Gal4*).(M) Quantification of fraction of T2NBs with detectable *btd* transcript enrichment upon *tll* knockdown with pan-NB driver (*Wor-Gal4*). Tll is necessary to maintain *btd* transcription in T2NB lineages.(N) Summary of gene profile of wild-type T1NBand T2NBs and the immature progeny generated compared with gene profile of T2NBs with Tll and Trx loss of function. Tll and Trx are necessary to maintain T2NB identity.(O) Potential model for regulation of T2NB identity. Trx activates *tll* and Tll may activate (indirectly or directly) T2NB genes *sp1*, *btd*, and *pnt* . White arrow: T2NB neuroblast; magenta arrow: T1NBneuroblast; Prog:Progeny; White dashed line separates central brain from optic lobe; Scale bar: 20 μm. Graphs show mean number ± standard deviation. p-value: ***<0.0005, and ****<0.00005.

Next, we wanted to identify the relationship between Tll and Trx and test if Trx was necessary for Tll expression, or if *tll* could be activated independently of Trx and might potentially be working with Trx in a complex. We looked at Tll expression with a GFP reporter using a background with two copies of the Tll:GFP transgene for clear detection and to better distinguish T2NBs from T1NBs in which Tll is also expressed, but at lower levels. Due to Tll:GFP and trx^{RNAi} transgenes both being inserted on the second chromosome; we instead utilized a *rbbp5* mutant background. We examined Tll:GFP in $rbbp5^{-/-}$ background vs control and found that there were significantly less Tll:GFP positive T2NBs in the *rbbp5* mutant brains (Fig. 3.1F-H). We next tested if Tll could still function in a *rbbp5* mutant NBs. We misexpressed Tll using a T2NB specific

driver (*Wor-Gal4*, *Ase-Gal80)* and induced expression for 24 hours. The upregulation of Ase in *rbbp5* mutants does not always manifest in every T2NB, so this driver is expected to be active in at least a subset of T2NBs. We observed that Tll misexpression resulted in the generation of supernumerary T2NBs, based on the presence of larger $Dpn^{+}Ase^{-}$ cells (Fig. 3.1I-J). This phenotype is consistent with previous studies that showed misexpression of full length Tll in T2NB lineages results in supernumerary T2NBs being generated (Hakes & Brand, 2020; Quinto-Rives et al., 2020). From these data we conclude that *tll* is likely activated by Trx which exists in complex with Rbbp5. Further validation through using mosaic analysis with a repressible cell marker (MARCM) to label a single NB lineage clone and induce a *trx* knockout in combination with Tll misexpression will be able to clearly demonstrate if Tll can restore T2NB function independent of Trx.

Previously, Trx was found to activate Btd to promote generation of INPs from T2NBs (Komori et al., 2014). We sought to see if Tll may also play a role in regulating expression of Btd. We knocked down *tll* in all neuroblasts using a pan NB driver (*Wor-Gal4*). Due to lack of reporter transgenes or antibodies that work for immunofluorescence, we utilized small molecule in situ hybridization (sm-FISH) to look at if *btd* was transcribed in T2NBs. We observed the number of NB enriched in *btd* transcripts was significantly lower than in control NBs (Fig. 3.1K-M). This indicates that high Tll expression is necessary for *btd* to remain transcribed in T2NBs. Previous studies established that both Tll and Trx expression are necessary to maintain expression of the T2NB lineage specific factor Pointed (Pnt). Pnt is known to promote activation of *erm*, a gene necessary for immature INP commitment, so it is unsurprising

that T2NB mutant for *tll* or *trx* do not generate Erm^{+} immature INPs. Instead, Pros^{+} GMCs are observed to be directly generated, consistent with a conversion to a T1NB identity (Hakes & Brand, 2020; Komori et al., 2014; Quinto-Rives et al., 2020). A summary of the gene profile of wild-type T1NBand T2NBs in addition to *trx* and *tll* mutant T2NBs is shown in Fig. 3.1N. These results further confirm that Tll and Trx activity are necessary to maintain T2NB identity, and that loss of either gene results in a full conversion to a T1NB identity. This brings up the question of how Tll is functioning to promote T2NB identity. Is Tll promoting activation of genes like *pnt*, *btd*, and *sp1* (Fig. 3.1O)? The data suggests *tll* is downstream target of Trx, but previous work also seems to indicate Trx deposits H3K4me3 to specifically activate *btd* and *pnt* suggesting activation of these genes is parallel to activation of *tll*. To better elucidate the details of the gene regulatory network, it is necessary to know how Tll is acting mechanistically to promote T2NB identity.

Tll is likely acting to repress gene function in T2NBs

We sought to establish if Tll is directly activating or repressing target genes in T2NBs. To do this we created a Tll transgene where we took the nucleotide sequence corresponding to the first 244 amino acids and added to the C-terminus of this construct either a constitutive transcriptional activator domain (Vp16) or constitutive transcriptional repressor domain (ERD) (Fig. 3.2A). This portion of Tll from the first 244 amino acids includes the entire DNA binding domain (DBD) in addition to a small portion of the ligand binding domain (LBD). This was designed as such because a previous version of the construct using only the DBD with Vp16 or ERD attached was insufficient to produce a phenotype upon overexpression in T2NB lineages. We also added three copies of a

Myc epitope tag to be able to confirm transgene presence (Fig. 3.1A). In addition to the Vp16 and ERD containing constructs we designed a construct with only the Myc tag added to verify that overexpression without activator or repressor domains will not result in a phenotype.

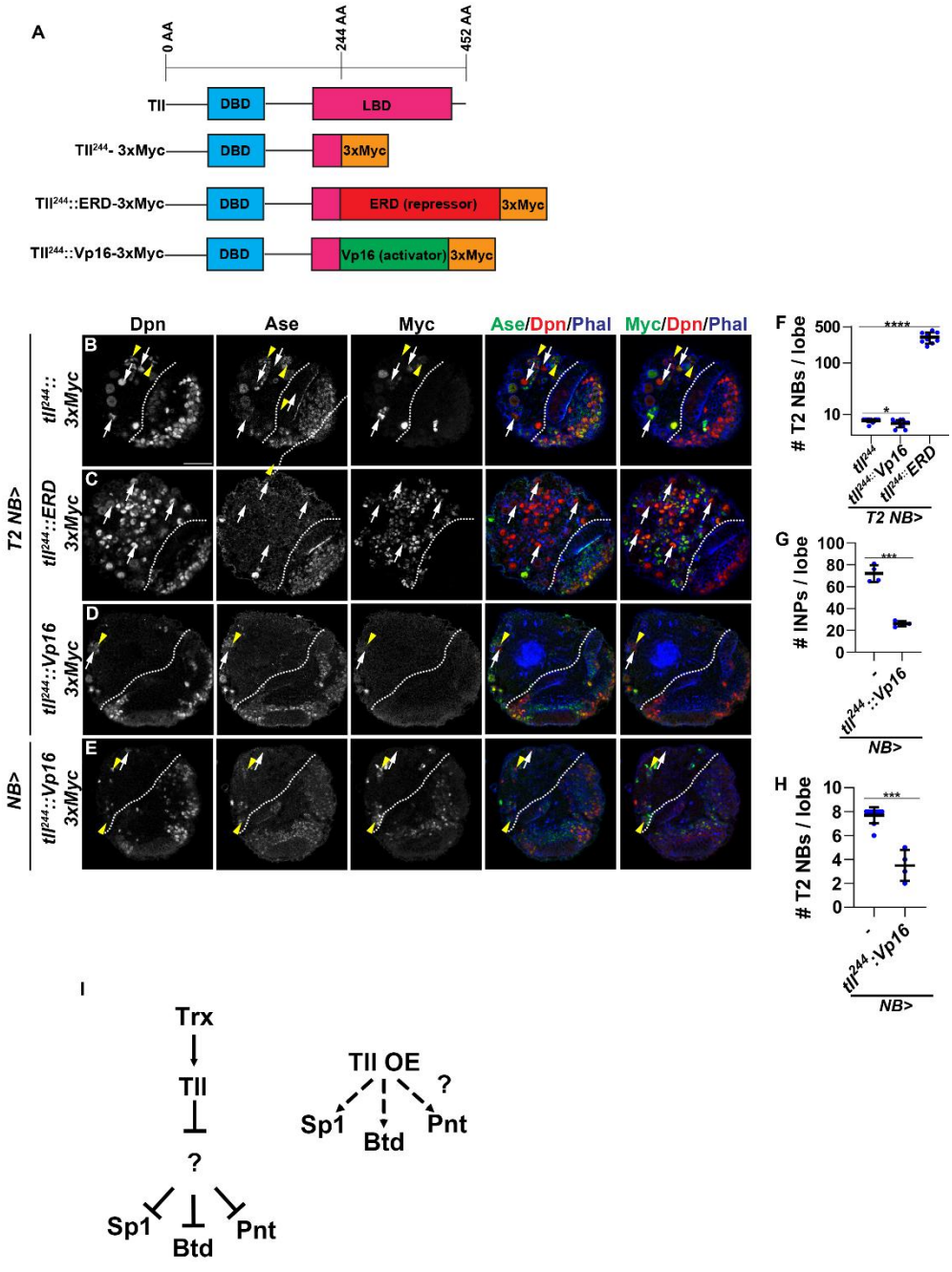


Figure 3.2 Tll likely functions as a repressor to promote T2NB functional identity

(A) Schematic for design of UAS-Tll chimeric constructs. Tll gene structure shows DNA-binding domain (DBD) and ligand binding domain (LBD) and the corresponding amino acid (AA) length. Chimeric constructs utilize activator domain (Vp16) or repressor domain (ERD) attached to the C-terminus with a 3xMyc epitope tag added.(B-D) Images showing phenotypes observed upon Tll chimera misexpression in T2NB lineages with T2NB driver (*Wor-Gal4*, Ase-Gal80).(F) Quantification of number of T2NBs ($Dpn^{+}Ase^{-}$) upon Tll chimera misexpression with T2NB driver (*Wor-Gal4*, Ase-Gal80). Tll^{244}::ERD misexpression causes supernumerary T2NB formation similar to full length Tll misexpression.(E) Images showing phenotype observed upon Tll^{244}::Vp16 misexpression in NB lineages with pan NB driver (*Wor-Gal4*).(G-H) Quantification of number of INPs ($Dpn^{+}Ase^{+}$) or T2NBs ($Dpn^{+}Ase^{-}$) upon Tll^{244}::Vp16 misexpression in NB lineages with pan NB driver (*Wor-Gal4*). Loss of NBs and INPs suggests that Tll^{244}::Vp16 may activate Tll targets that causes premature differentiation of the NBs.(I) Proposed model for regulation of T2NB identity. Trx activates Tll and Tll likely represses some target genes that will in turn repress T2NB genes Sp1, Btd, and Pnt. Tll overexpression can also activate Sp1, Btd, and Pnt in T1NBs through an unknown process. White arrow: T2NB neuroblast; yellow arrowhead: INPs; White dashed line separates central brain from optic lobe; Scale bar: 20 μm. Graphs show mean number ± standard deviation. p-value: ***<0.0005, and ****<0.00005.

Previous studies have shown that overexpression in T2NB lineages of full length Tll results in generation of supernumerary T2NBs (Hakes & Brand, 2020; Quinto-Rives et al., 2020). Overexpressing Tll^{244}::3xMyc alone in T2NB lineages had no notable effect, while overexpression of Tll^{244}::ERD-3xMyc resulted in generation of supernumerary T2NBs as indicated by the presence of many large $Dpn^{+}Ase^{-}$ cells (Fig. 3.2 B-C, F). Overexpression of Tll^{244}::Vp16-3xMyc in T2NBs resulted in a modest decrease in the number of T2NBs and showed less cells marked with Myc (Fig. 3.2 C,F). We hypothesized that this weak phenotype and Myc signal may be a from the driver being shut down by the transgene expression. We utilized *Wor-Gal4* to drive expression in all NBs while Ase-Gal80 was utilized to shut down expression in NBs were Ase is active (T1NBs). Tll appears to repress *ase*, and as such it would seem the activator form of Tll results in activation of *ase*. This activation could result in AseGal80 turning on in T2NBs. To establish what phenotype misexpression of Tll^{244}::Vp16-3xMyc

results in we instead used pan-NB driver *Wor-Gal4* alone. We could observe that overexpression of Tll^{244}::Vp16-3xMyc resulted in significantly less INPs and T2NBs compared to control (Fig. 3.2E, G-H). This suggests that Tll^{244}::Vp16-3xMyc expression results in premature differentiation of NBs, potentially through activation of Tll targets that are typically kept repressed in NBs. From these data we conclude that Tll is likely functioning as a repressor to promote T2NB function. Future work should be done using MARCM to label a single NB lineage clone and induce a *tll* knockout in combination with Tll^{244}::Vp16-3xMyc vs Tll^{244}::ERD-3xMyc misexpression to clearly show the rescue of T2NB identity with repressor form of Tll. Validation should include looking at expression or transcription of genes like *btd*, *pnt*, and *sp1* to assess T2NB identity.

We showed in Fig. 3.1 that Tll is necessary to maintain T2NB gene activity, and the finding that Tll acts as a repressor suggests that Tll may be repressing unknown targets that in turn result in shutdown of T2NB related genes (Fig. 3.2I). But what are these potential targets? Furthermore, previous work shows that Tll misexpression in T1NBs can cause a lineage conversion into T2NBs (Hakes & Brand, 2020; Quinto-Rives et al., 2020). So how does expression of a transcriptional repressor result in activation of genes that are typically repressed in T1NBs, or even have inaccessible enhancers in T1NBs as indicated in Chapter 2 Fig. 2.2. As demonstrated in chapter 2, when looking at genes that are specific to T1NBs, or T1NBs and INPs, only Ase and Pros were specifically expressed. But repressing these genes alone is not sufficient to result in activation of T2NB gene identity. This necessitates a better means of elucidating how Tll is regulating T2NB identity.

Method to identify Tll targets

To understand how Tll is functioning to promote T2NB identity, it is necessary to find what genes Tll is directly acting on. To do this we have designed an approach where we preferentially enrich larval brains with T2NBs through blocking differentiation using *brat* mutants as described in Chapter 2. The next step is to establish conditions to find the shortest time frame to in which *tll* can be effectively knocked down. This would be confirmed through sm-FISH to look at changes in *tll* transcript abundance. We would then perform bulk RNA-seq on brains where *tll* knockdown has been induced vs no induction. The next step would be to identify what genes are upregulated upon loss of Tll and to look at which of these upregulated genes are bound by Tll by using Cut&Run against Tll on T2NB enriched brains. We would put preference towards genes which are bound by Tll at neurogenic enhancers, identified in chapter 2. The expectation would be that targets of Tll should repress T2NB identity when misexpressed in T2NBs. This overall workflow is shown in Fig. 3.3A. Depending on results, expanding the approach to look at genes in gene rich regions from which neurogenic enhancers cannot be clearly distinguished may prove necessary to find key factors.

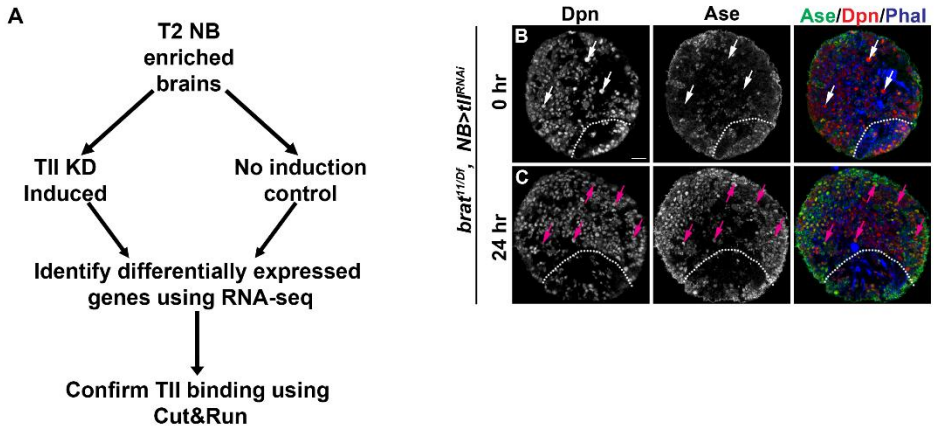


Figure 3.3 Experimental design to identify Tll targets

(A) Scheme to identify genes that Tll regulates in T2NBs.(B) Images showing Ase upregulation in T2NBs upon Tll knockdown using a pan NB driver (*Wor-Gal4*). This confirms that Tll knockdown can be effectively induced in a T2NB enriched brain generated from Brat loss of function background. White arrow: T2NB neuroblast; magenta arrow: T1NB; White dashed line separates central brain from optic lobe; Scale bar: 20 μm.

We validated the approach listed in Fig. 3.3A by testing a 24 hour induction compared to no induction control. We could see that after incubating for 120 hours, the no induction samples were primarily composed of large $Dpn^{+}Ase^{-}$ cells consistent with enrichment of T2NBs (Fig. 3.3B). Upon knocking down *tll* for 24 hours, it could be seen that Ase was upregulated in a large number of cells (Fig. 3.3B). This is consistent with the observation that *tll* knockdown results in Ase upregulation when converting to a T1NB identity. These observations confirm that the established system is capable of being used to enrich for T2NBs, and that *tll* can still be effectively knocked down after NB enrichment has occurred. The next steps will be to conduct a time course and look at changes in *tll* transcript to establish the optimal timing for induction of *tll* knockdown.

Identification of genes that promote T2NB lineage progression

Outside of maintaining T2NB cell identity, one other potential function of Tll is to promote NBs to remain undifferentiated. This role is supported by the observation that Tll is rapidly inactivated in immature INPs and is kept off in INPs. Overexpression of Tll in the T2NB lineage results in progeny cells reverting back to a NB state (Hakes & Brand, 2020; Quinto-Rives et al., 2020). Additionally, the observation that overexpressing an activated form of Tll results in premature differentiation suggests that genes bound by Tll can promote differentiation (Fig. 3.2E)

We sought to identify genes that may be involved in promoting proper T2NB lineage progression. Beyond considering Tll as a potential suppressor of differentiation,

once Tll shuts down, immature INPs are not fully committed to an INP identity. Young INPs but not old INPs can respond to high levels of Notch signaling and revert back to a NB, indicating that the process of INP commitment to differentiation involves multiple steps of maturation that are not activated immediately after Tll is shut down (Farnsworth et al., 2015). Another gene that likely works to keep these factors off until needed for the late maturation steps is Erm. Erm serves as a master regulator of immature INP commitment becoming expressed in immature INPs and shutting down when INPs reactivate Dpn expression (Janssens et al., 2017; Janssens et al., 2014; Weng et al., 2010). Erm is known to function to promote commitment via gene repression and is also thought to suppress *tll* activity (Janssens et al., 2014; Quinto-Rives et al., 2020). We considered binding by both Tll and Erm when identifying genes that are likely to promote proper T2NB lineage progression.

We utilized the neurogenic enhancers identified in chapter 2 and found which of these enhancers were bound by both Tll in T2NBs and Erm in immature INPs. We looked at if mRNA was enriched in INPs from the genes associated with these enhancers, and after filtering for TFs found 35 candidate genes (Fig. 3.5 A).

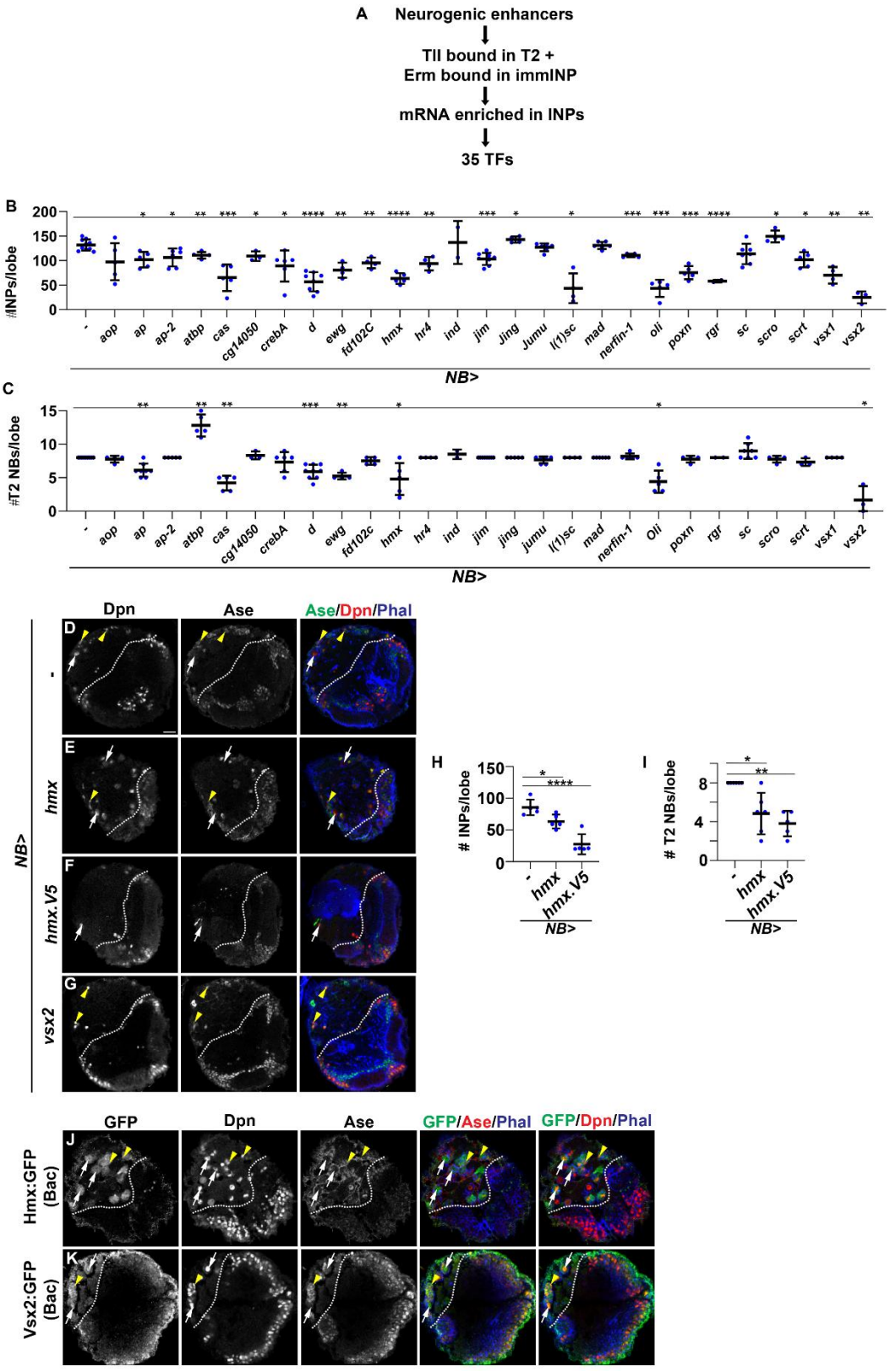

A
Neurogenic enhancers
TII bound in T2 +
Erm bound in immINP
mRNA enriched in INPs
35 TFs
B
#INPs/lobe
NB>
C
#T2 NBs/lobe
NB>
Dpn
Ase
Ase/Dpn/Phal
NB>
hmx
hmx.V5
vsx2
H
INPs/lobe
I
T2 NBs/lobe
GFP
Dpn
Ase
GFP/Ase/Phal
GFP/Dpn/Phal
Hmx:GFP (Bac)
Vsx2:GFP (Bac)

Figure 3.4 Identification of genes that promote T2NB lineage progression

(A) Scheme to identify genes that regulate lineage progression (B) Quantification of number of INPs (small $Dpn^{+}Ase^{+}$ cells) per brain lobe upon transgene expression with pan NB driver (*Wor-Gal4*).(C) Quantification of number of T2NBs (large $Dpn^{+}Ase^{-}$ cells) per brain lobe upon transgene expression with pan NB driver (*Wor-Gal4*).(D-G) Images of INPs and T2NBs upon Hmx or Vsx2 overexpression with pan-NB driver (*Wor-Gal4*).(H) Quantification of number of INPs (small $Dpn^{+}Ase^{+}$ cells) per brain lobe upon Hmx and Hmx.V5 over expression with pan NB driver (*Wor-Gal4*).(I) Quantification of number of T2NBs (large $Dpn^{+}Ase^{-}$ cells) per brain lobe upon Hmx or Hmx.V5 overexpression with pan NB driver (*Wor-Gal4*).(J-K) Images of Hmx or Vsx2 GFP reporter expression in larval brains. Hmx and Vsx2 appear to promote differentiation in T2NB lineages in previously unidentified roles. White arrow: T2NB neuroblast; yellow arrowhead: INP; White dashed line separates central brain from optic lobe. Scale bar: 20 μm. Graphs show mean number ± standard deviation .p-value: *<.05, **<.005, ***<0.0005, and ****<0.00005.

If a candidate gene was involved in promoting differentiation we would expect that overexpression in NBs would result in a premature differentiation of the NB. This would appear to result in a reduced number of INPs due to differentiating NBs no longer proliferating. Furthermore, we would expect to see a reduction in the number of T2NBs as T2NBs would either be lost to differentiation or would turn on Ase and shrink in size as a consequence of differentiation. Either way, the typical read out of larger size and $Dpn^{+}Ase^{-}$ marker profile would be lost. We assayed 29 of the 35 candidate TFs by misexpressing in NBs. We excluded previously investigated genes (*ham, opa, ey,* and *erm*) and *esg* which has been previously defined to function in differentiation of neurons (Abdusselamoglu et al., 2019; Farnsworth et al., 2015; Quinto-Rives et al., 2020; Symonenko et al., 2018). The resulting phenotypes from the candidate misexpression are shown in Fig. 3.5 B-C. Two genes that were misexpressed but not included on the graph are *onecut* and *creb B*. Misexpression of Onecut resulted in cell death and significant defects in morphology, while Creb B misexpression appeared to produce increased number of INP-like cells but with no observable NBs. These phenotypes were

inconsistent with premature differentiation but were not able to properly quantified for INP and NB number and were excluded for that reason.

Seven genes (*ap ,d, cas, ewg, hmx, oli,* and *vsx2*) were found to show decreased number of INPs and T2NBs upon misexpression (Fig. 3.5B-C, D-G). D is known to specify early INP temporal identity while Cas has been previously shown to specify temporal identity of NBs and INPs (Bayraktar & Doe, 2013; Dillon & Doe, 2024; Li et al., 2013). Considering these defined roles may be producing the observed phenotype, we did not investigate these genes further. We looked at the expression pattern of the remaining genes using reporters and found that Ap was expressed only in a subset of GMCs and neurons, but not INPs. Ewg was expressed in neurons but not in NBs or INPs, while Oli was only expressed in a subset of NBs. Because these genes were not found to be expressed in most INPs lineages, we did not investigate further at this time.

We looked at the remaining genes *hmx* and *vsx2*. Hmx is known as H6-like-homeobox, and was found to be expressed in T2NBs with expression increasing in INP progeny (Fig. 3.5J). A small subset of T1NB also expressed Hmx, but considering Opa which is needed for INP function can also be found in a subset of T1NBs, this observation was not used to exclude Hmx from further investigation. Similar to Hmx, Vsx2 is another homeobox gene known as Visual system homeobox 2. Vsx2 was also found to be expressed in a subset of T1NBs and in T2NBs with increased expression in the progeny (Fig. 3.5K). Vsx2 is also highly similar to Visual system homeobox 1 (Vsx1), but as shown in Fig. 3.5B-C, Vsx1 misexpression could not recapitulate the phenotype observed upon Vsx2 misexpression. Furthermore, Vsx1 was only found to be expressed

in a subset of neurons. We conclude that Vsx1 is unlikely to function redundantly with Vsx2 in the T2NB lineage.

Due to there being two available misexpression lines for Hmx, we decided to assess if the same phenotype could be observed upon misexpression with either line. We found both lines were sufficient to result in loss of INPs and T2NBs, but that the UAS-Hmx.V5 line produced a stronger phenotype (Fig. 3.5 D-F, H-I). From these data we conclude that Hmx and Vsx2 are likely to play roles in promoting T2NB lineage progression.

Ase alone is not responsible for loss of INPs upon loss of Tll or Trx

In Chapter 2 it was shown that misexpressing Ase in T2NBs was able to promote generation of GMCs instead of NBs. It has also been observed that loss of Tll expression results in Ase upregulation in T2NBs, while Tll misexpression causes down regulation of Ase (Hakes & Brand, 2020; Quinto-Rives et al., 2020). Similarly, loss of Trx in T2NBs results in Ase upregulation upon conversion to T1NBidentity (Komori et al., 2014). This would suggest that Ase may be a key target that is repressed to promote T2NB function. But it has been previously shown that *ase* mutant NBs have no apparent phenotype (Carney et al., 2012). If loss of Trx and Tll is resulting in a true lineage conversion into T1NBs, these converted NBs would similarly not be affected by loss of Ase expression. We sought to test these possibilities.

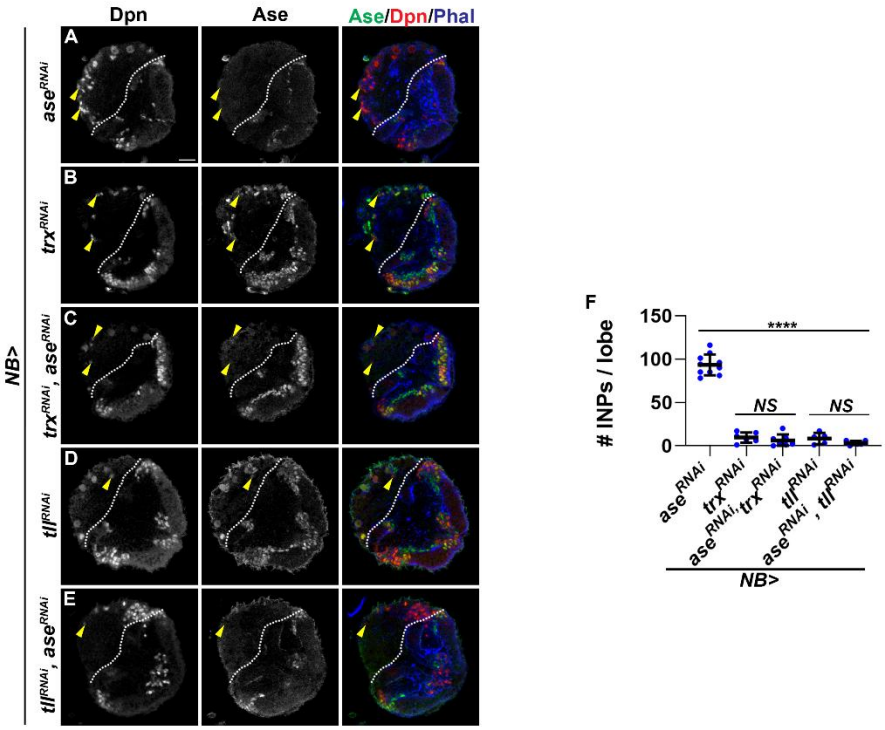


Figure 3.5 Ase knockdown does not restore generation of INPs upon loss of Tll or Trx

(A-E) Images of INPs upon *ase*, *trx*, or *tll* knockdown with pan-NB driver (*Wor-Gal4*).(F) Quantification of number of INPs (small Dpn$^+$ cells) upon *ase*, *trx*, or *tll* knockdown with pan-NB driver (*Wor-Gal4*). Loss of Ase does not increase the number of INPs in Tll or Trx loss of function experiments. Yellow arrowhead: INP; White dashed line separates central brain from optic lobe; Scale bar: 20 μm. Graphs show mean number ± standard deviation p-value: ****<0.00005.

We first knocked down expression of Ase and looked at the number of INPs generated by counting the number of small Dpn$^+$ cells found on the dorsal side of the brain. While controlling driver dilution, we looked at the number of INPs observed when driving *trx*^{RNAi} compared with *trx*^{RNAi} and *ase*^{RNAi}. We saw a significant reduction in the number of INPs when driving *trx*^{RNAi} compared to driving *ase*^{RNAi}, but there was not a significant change in the number of INPs between driving *trx*^{RNAi} vs driving both *trx*^{RNAi} and *ase*^{RNAi} (Fig. 3.4 A-C,F). We then tested driving *tll*^{RNAi} compared against driving both *tll*^{RNAi} and *ase*^{RNAi}. We also observed a significant loss in the number of INPs when

driving *tll*^{RNAi} compared to *ase*^{RNAi} alone (Fig. 3.4A,D,F). Knocking down Ase expression in a *tll*^{RNAi} background did not appear to alter the number of INPs compared to *tll*^{RNAi} alone (Fig. 3.4D-F). When looking at the location of the dorsal lateral T2NB lineages, no small Dpn^{+} cells could be observed, confirming the apparent loss of INPs (Fig. 3.4 D-E). These data further confirm that loss of Tll and Trx results in a conversion of T2NBs into T1NB which do not respond to loss of Ase expression. This data also proves that upregulation of Ase alone is not sufficient to restore generation of INPs upon Tll or Trx loss, consistent with the fact that Ase misexpression does not suppress T2NB related gene expression shown in Chapter 2.

Interestingly, the combination of driving *tll*^{RNAi} and *ase*^{NAi} showed a large cluster of Dpn^{+} cells near the dorsal surface of the brain. The identity and origin of the cluster cells is unknown, but this dense clustering pattern is not consistent with INPs. These cluster of Dpn^{+} cells could be observed where the mushroom body NBs are typically located, a subset of T1NBs which express Tll higher levels than most other T1NBs (Kurusu et al., 2009). With the knockdown being driven by a pan-NB driver, T1NB lineages would also be affected. The combined loss of *ase* and *tll* could potentially result in defects in mushroom body NB division. It is also feasible that these cluster of Dpn^{+} cells arise from the dorsal most T2NBs through a lineage specific mechanism. Future work would be needed to determine how this particular phenotype arose.

Identifying the role of Vsx2 and Hmx in T2NB lineages

The next step was to assess the exact roles Vsx2 and Hmx may play. To do so, we performed loss of function experiments to look for potential alterations to T2NB lineages progression. We drove two different RNAi lines to try knocking down Hmx and

found neither line resulted in a change to T2NB number, but that there was altered INP number (Fig. 3.6A-D). Strangely, knock down with one RNAi line resulted in an increase in the number of INPs while another line caused a reduction (Fig. 3.6A-D). Driving *hmx*$^{RNA\#1}$ showed an increase in the number of INPs and this transgene has been reported to have no off-target effects unlike *hmx*$^{RNA\#2}$ but that assessment cannot necessarily be considered accurate. To better understand what Hmx is doing will necessitate use of a mutant allele to specifically assess phenotype without unpredictable off target effects that can occur when utilizing RNAi. Currently, no known amorphic alleles specific to only *hmx* exist, but a line where GFP is inserted in the endogenous *hmx* locus could potentially show a loss of function phenotype. Alternatively, this line could be used to develop a mutant through imprecise excision of the GFP in hopes of deleting a necessary portion of *hmx*. Another option is to utilize Crispr-cas9 to create a targeted mutant of *hmx*.

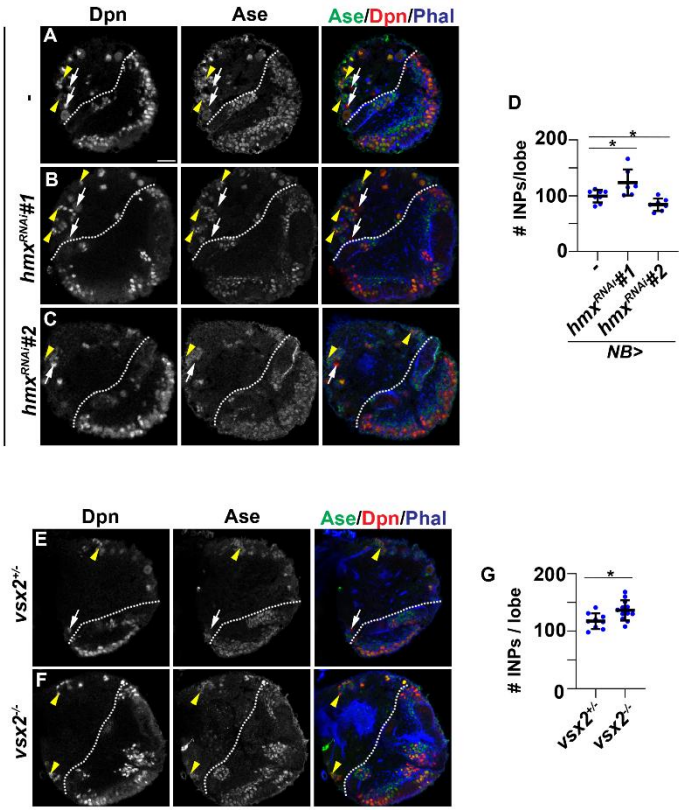


Figure 3.6 Identifying the role of Hmx and Vsx2 in T2NB lineages

(A-C) Images of INPs and T2NBs upon *hmx* knockdown with T2NB driver (*Tll-Gal4*).(D) Quantification of number of INPs (small $Dpn^{+}Ase^{+}$ cells) per brain lobe upon Hmx knockdown with pan NB driver (*Wor-Gal4*).(E-F) Images of INPs and T2NBs in v*sx2* heterozygous ($vsx2^{DF571/+}$) and homozygous ($vsx2^{DF571/DF6235}$) mutant brains.(G) Quantification of number of INPs (small $Dpn^{+}Ase^{+}$ cells) per brain lobe in *vsx2* heterozygous mutant and homozygous mutant brains. Hmx and Vsx2 appear to promote proper INP differentiation. White arrow: T2NB neuroblast; yellow arrowhead: INP; White dashed line separates central brain from optic lobe. Scale bar: 20 μm. Graphs show mean number ± standard deviation. p-value: *<.05

To investigate Vsx2 function, we utilized two available deficiency lines where portions of the genome were deleted such that the combination of both lines resulted in only the *vsx2* gene being removed. We compared the heterozygous mutants to homozygous mutants and found that the number of T2NBs was not affected, but that the complete loss of *vsx2* showed an increase in the number of INPs. This data

suggests that Vsx2 may play a role in promoting proper differentiation of INPs into GMCs. Further work will be needed to establish how Vsx2 and Hmx work mechanistically, and if Hmx and Vsx2 may potentially work redundantly considering the have similar expression patterns, similar misexpression phenotype, and that both are homeobox family TFs.

Approach to visualize enhancer activity

One limitation in terms of looking at the regulation of genes that function to promote stemness, and the decommissioning of these genes during differentiation is that current assays for enhancer activity are limited in resolution to show inactivation of enhancers. For example, Tll is highly expressed in T2NBs and is shut down quickly in the immature INP progeny (Hakes & Brand, 2020; Quinto-Rives et al., 2020). Visualization of Tll expression with a GFP reporter can demonstrate the high expression in the NB, but signal persists in the INPs largely due to GFP stability (Fig. 3.7A). An enhancer identified for *tll* is specific to T2NBs and quickly becomes in accessible in the progeny after NB division (Larson et al., 2021). When looking at activity of this enhancer using a GFP reporter, it can be observed that the GFP signal persists well into the lineage (Fig. 3.7B-C). Using sm-FISH to look at *gfp* transcript instead of GFP protein expression helps show reduced *gfp* enrichment later in the T2NB lineage, but *gfp* is still well enriched in the immature INPs. This could be due to *gfp* not being degraded properly as an artificial transcript. To correct for this lack of timely degradation one option would be utilize an intron as a reporter readout. Introns are spliced out of messenger mRNA and as such are extremely short lived. Designing a construct where

an enhancer drives transcription of an intron could be utilized to show enhancer activity with better specificity.

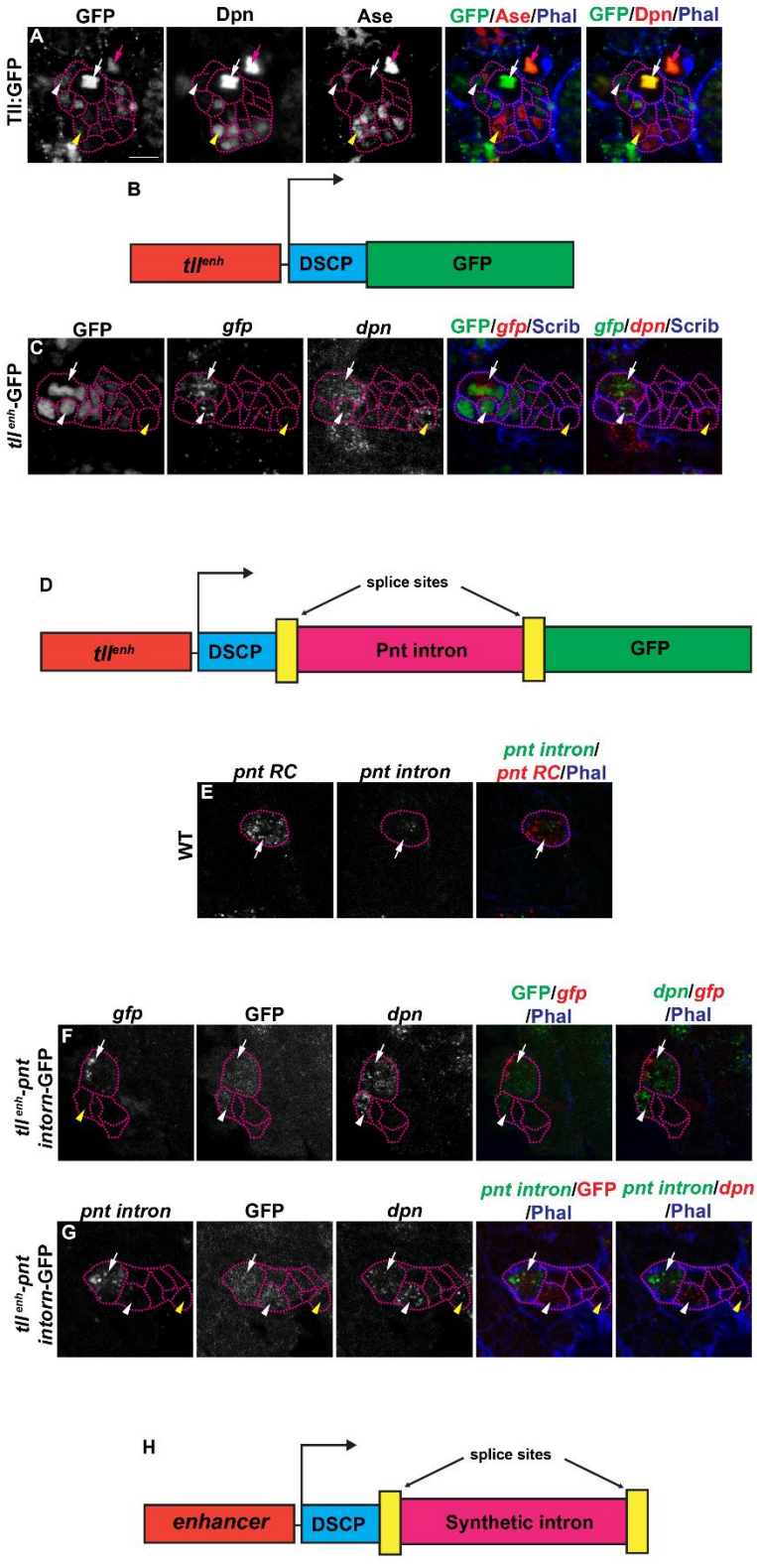

GFP
Dpn
Ase
GFP/Ase/Phal
GFP/Dpn/Phal
A
Tll:GFP
B
tll enh
DSCP
GFP
GFP
gfp
dpn
GFP/gfp/Scrib
gfp/dpn/Scrib
C
tll enh-GFP
D
splice sites
tll enh
DSCP
Pnt intron
GFP
pnt RC
pnt intron
pnt intron/
pnt RC/Phal
E
WT
gfp
GFP
dpn
GFP/gfp
/Phal
dpn/gfp
/Phal
F
tll enh-pnt intorn-GFP
pnt intron
GFP
dpn
pnt intron/GFP
/Phal
pnt intron/dpn
/Phal
G
tll enh-pnt intorn-GFP
H
splice sites
enhancer
DSCP
Synthetic intron

Figure 3.7 Method to improve enhancer activity detection

(A) Images of Tll:GFP reporter expression in larval brains. Tll GFP expression persists into the T2NB lineage being detectable in INPs.(B) Diagram for design of *tll*^{enh}-GFP.(C) Images of *tll*^{enh}-GFP co-stained with GFP antibody, *gfp* mRNA probe, and *dpn* mRNA probe. Transcripts of *gfp* do not persist as long as GFP protein but are still well detected in immature INPs.(D) Diagram for design of *tll*^{enh}*-pnt intron*-GFP.(E) Images of T2NB showing transcript of *pnt RC* is detected in T2NBs and *pnt intron* mRNA is also detected at much lower levels.(F) Images showing of *tll*^{enh}*-pnt intron*-GFP transcript and protein are present in T2NBs where GFP expression appears destabilized. The construct appears to localize correctly and functions to specify GFP (G) Images showing of *tll*^{enh}*-pnt intron*-GFP showing *pnt intron* mRNA is detected in T2NBs at higher levels than observed without reporter expression. The *pnt intron* mRNA appears to be constrained to the T2NB with limited to no persistence into the lineage.(H) Diagram for design of enhancer reporters that could utilize a synthetic intron. White arrow: T2NB neuroblast; white arrowhead: immature INP; yellow arrowhead: INP; Magenta dashed line outlines T2NB lineage cell boundaries. Scale bar: 10 μm.

To test this approach, we inserted a *pnt* intron sequence including splice sites downstream of the drosophila synthetic core promoter (DSCP) and upstream of GFP. The *tll* enhancer would then be used to drive expression (Fig. 3.7D). We utilized *pnt* for testing purposes as it is endogenously transcribed in T2NBs and would have no potential issues with incompatible splicing machinery. We tested first that we could detect the *pnt* intron transcripts in type NBs without the reporter inserted. Transcripts of the *pnt* intron was detected in sparse amounts in the T2NB where *pnt RC* isoform transcripts were well enriched (Fig. 3.7E). This indicates that the detection of the *pnt* intron was working correctly.

We looked at the brains where the intron reporter construct was inserted. We could detect GFP signal in the T2NBs, but it was quite weak compared to lines without the intron (Fig. 3.7F,C). This could be due to destabilization of *gfp* transcription from the presence of the intron directly upstream of GFP as opposed to the promoter sequence. We saw the GFP transcript abundance appeared to be much lower in the lines containing an intron, supporting the idea that the *gfp* could not be well transcribed (Fig. 3.7F,C). Since we could

detect *gfp* specifically in T2NBs, we could confirm the construct was properly inserted and is functional.

We looked at the *pnt* intron in samples were the intron reporter was present. We could detect the *pnt* intron in the T2NB at levels that looked to be better enriched than the endogenous *pnt* intron alone (Fig. 3.7G,E). Little of the *pnt* intron could be detected in the immature INPs, consistent with suggested timing of *tll* enhancer activity (Fig. 3.7G). This confirms that use of an intron reporter can be used to assay enhancer activity. The next step would then be to design a new reporter where a synthetic intron is inserted using endogenous splice sites (Fig. 3.7H). Unlike the *pnt* intron, a synthetic intron would not be detected endogenously and could produce a signal only indicative of enhancer activity. This approach could be used to better elucidate the process of enhancers shutting down during differentiation and whether factors like Vsx2 and Hmx are involved in that process.

Identification of Btd targets

Tll may be a master regulator of T2NB gene identity, but Btd has been shown to be necessary and sufficient for promoting the generation of INPs from NBs. The loss of *btd* observed in Trx or Tll loss of function backgrounds is likely a key factor in the observed loss of immature INP generation (Fig. 3.1K-M, Fig. 3.4F). Sp family TFs like Btd are generally suggested to play roles as transcriptional activators (Emili et al., 1994). This leads to the question of what Btd might be activating to promote immature INP and INP generation.

We sought to identify potential Btd targets by first taking the neurogenic enhancers identified in Chapter 2 and looked at which of these sites were bound by Btd using Cut&Run against Btd performed on T2NB enriched brains. Next we looked at

which of these genes had mRNA that was enriched T2NBs or T2NBs and INPs. From that criteria we were able to pull out 19 TFs (Fig. 3.7A). The next step was to test if misexpressing any of these factors in T1NBs would be able to induce generation of INPs, recapitulating Btd function. We excluded genes that were previously misexpressed in T1NBs (*pnt, six4, optix*) or genes from which no misexpression transgenes were available (*Kr-h1, zfh2, atos, lilli*) (Chen et al., 2021; Komori et al., 2014). Of these lines, reporters were available for *lilli* and *zfh2* which showed Lilli is expressed ubiquitously in the larval brain while Zfh2 is only detected in neurons. This pattern is not consistent with Btd activity suggesting these genes are not likely to be activated by Btd.

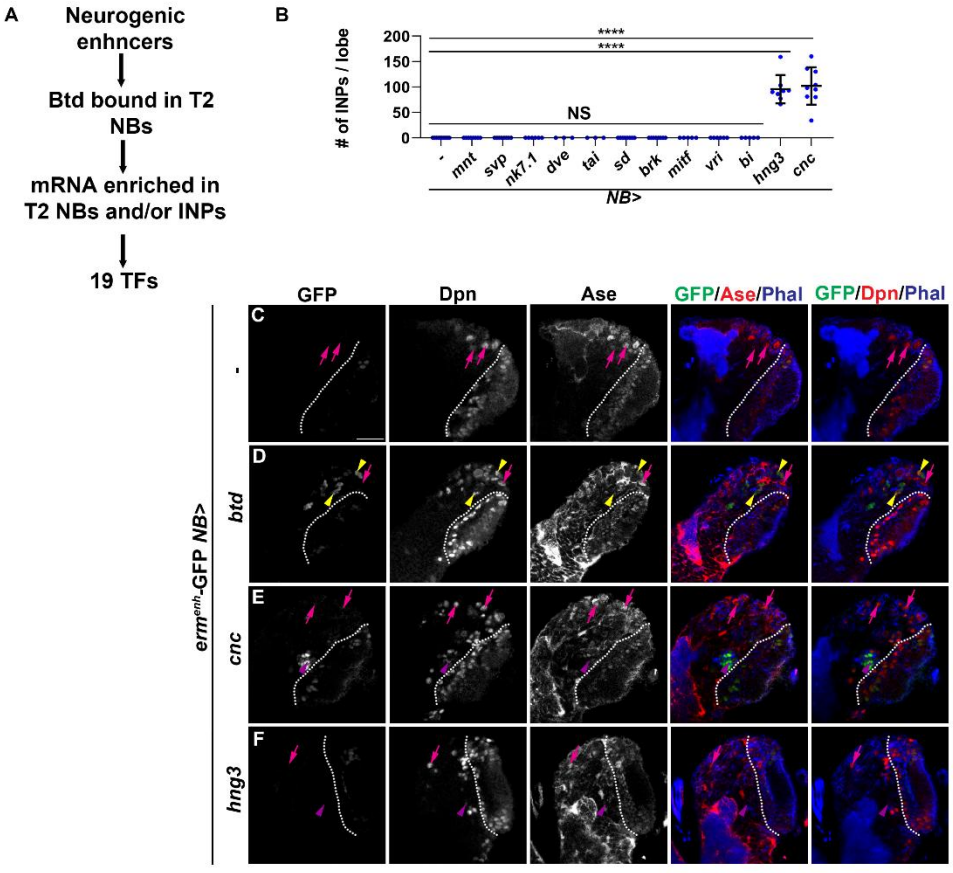


Figure 3.8 Candidate Btd targets could not recapitulate Btd function

(A) Flowchart to identify candidate Btd target genes.(B) Quantification of number of INPs (small Dpn^{+}Ase^{+} cells) found on the ventral side of the brain upon transcription factor misexpression in T1NB lineages with pan NB driver (*Wor-Gal4*).(C-E) Images of *erm*^{enh}-GFP expression in T1NB lineages upon Btd, Cnc, or Hng3 misexpression with pan-NB driver (*Wor-Gal4*). Btd misexpression turns on immature INP specific *erm* enhancer in NB progeny while the candidate Btd targets could not recapitulate this pattern. Magenta arrow: T1NBneuroblast; yellow arrowhead: INPs; White dashed line separates central brain from optic lobe; Scale bar: 20 μm. Graphs show mean number ± standard deviation. p-value: ***<0.0005, and ****<0.00005.

We misexpressed the candidate genes and looked for if T1NBs could be induced to generate INPs, similar to Btd. We assayed samples by looking at the ventral side of the brain, where only T1NBs are present, and checked for the presence of small cells (<5 um) that were Dpn^{+}Ase^{+}. From this criteria, only two genes showed a phenotype, *cnc* and *hng3*. The next step was to validate if misexpression of these factors was actually inducing generation of INPs as small Dpn^{+}Ase^{+} cells could also be produced from cells reverting to a T1NB state. Btd misexpression is capable of inducing T1NBs to generate immature INPs which activate an immature INP specific *erm* enhancer that is otherwise not active in the ventral brain (Fig. 3.7C-D)(Janssens et al., 2017). We looked at activity of this enhancer upon misexpression of Cnc or Hng3. We saw Hng3 misexpression was not sufficient to turn on this enhancer, indicating that Hng3 is not sufficient to induce generation of immature INPs (Fig. 3.8F). Cnc misexpression did show a cluster of cells that turned on the *erm* enhancer, but this clustered pattern is not similar to the expression of the enhancer in a lineage specific fashion seen upon Btd misexpression (Fig. 3.8D-E). Furthermore, misexpression of other available Cnc transgenic lines were not able to induce any phenotype, suggesting that the generation of small Dpn^{+}Ase^{+} cells was a non-physiological phenotype induced through especially strong misexpression of the Cnc transgene.

Upon eliminating these genes from consideration, we found then that no candidate Btd targets were able to recapitulate Btd function. To better understand what Btd is regulating will require a different approach. Previously, it was determined that Btd is expressed in T2NBs lineages, but the pattern was unknown. Through use of sm-FISH, we were able to look at the pattern of *btd* transcription in T2NB lineages. Rather than being detected only in the NB and newly born immature INPs like *tll*, *btd* was found to be transcribed in multiple immature INPs and may be detected in the early INPs (Fig. 3.9A). This leads to the idea that Btd may not be promoting gene activity that is needed in NBs but actually functions in the immature NB progeny to specify immature INP identity. Btd expression is necessary and sufficient to result in Erm expression in the immature INP progeny, but loss of Btd does not result in supernumerary NB formation that is observed from Erm loss alone, or loss of Pnt which is known to activate *erm* (Janssens et al., 2017; Komori et al., 2014; Zhu et al., 2011). Btd loss did not appear to affect Pnt expression, nor is Ase upregulated indicating that T2NB identity is retained (Komori et al., 2014). This suggests that Btd may be needed to specify immature INP

identity in NB progeny in a parallel mechanism to Pnt mediated activation of *erm* (Fig. 3.9E).

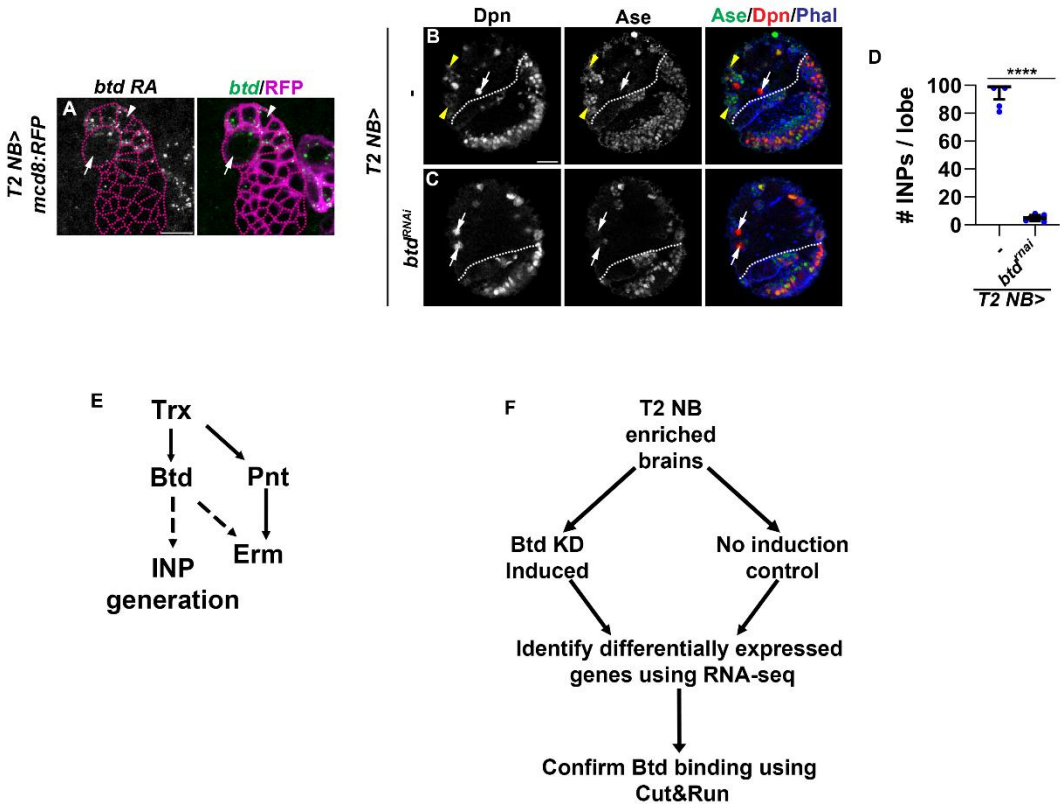


Figure 3.9 Experimental design to identify Btd targets

(A) Images of *btd* transcripts in T2NB lineages marked with mcd8:RFP driven by T2NB driver (*Tll-Gal4*) ; Scale bar: 10 μm (B-C) Images showing phenotype upon *btd* knockdown with T2NB driver (*Tll-Gal4*). Scale bar: 20 μm (D) Quantification of number of INPs (small $Dpn^{+}Ase^{+}$ cells) found on the per brain lobe upon btd knockdown with T2NB driver (*Tll-Gal4*).(E) Proposed model for regulation of INP generation via Btd, Trx, and Pnt.(F) Scheme to identify genes that Btd regulates in T2NBs. White arrow: T2NB neuroblast; white arrowhead: immature INP; yellow arrowhead INP; Magenta dashed line marks T2NB lineage; White dashed line separates central brain from optic lobe. Graphs show mean number ± standard deviation . p-value: ****<0.00005.

To understand exactly how Btd may activate immature INP identity in NB progeny, we need to be able to better elucidate what genes are regulated by Btd. One approach to do this would be to knock down *btd* in T2NBs and look at changes in RNA expression, but previous attempts to knockdown *btd* using the Pan-NB driver *Wor-Gal4*

only produced a mild phenotype, indicating inefficient knockdown. Homozygous mutants for *btd* are embryonic lethal so that approach cannot be used either. Recently though, we found a specific driver in T2NBs (*Tll-Gal4*) that Is quite strong with ability to drive multiple lines and remain effective. We tested driving btd^{RNAi} using this line and could observe a dramatic loss in the number of INPs, indicating that this knockdown is effective (Fig. 3.9B-D).

Using a similar approach to that outlined in Fig. 3.3, brains would be enriched for T2NBs and then *btd* would be knocked down. RNA-seq on these samples would be performed comparing against a no induction control set. Genes that show changes in mRNA enrichment would be checked for Btd binding from acquired Cut&Run data (Fig. 3.9F). One potential pitfall of this approach could be that if Btd regulated genes are primarily active in immature INPs and INPs, then detection using NB enriched brains may prove difficult. Single cell sequencing of T2NB lineages and filtering for immature NB progeny could provide an alternative approach. Additionally, available Btd Cut&Run data has weak binding compared to other available TFs which may provide poor insight into Btd Binding. Producing a new Btd antibody or attempting to create a Btd construct that contains tag may be necessary to acquire robust binding data.

Discussion

Even though TFs Tll and Btd have been known to play key roles for T2NB function for a number of years, little insight has been gained in terms of how these genes function. The finding that Tll maintains T2NB functional identity through acting as a repressor is notable for a number of reasons. The human homolog of Tll;Tlx appears to play a conserved role in promoting neurogenesis and neural stem cell maintenance

and as such understanding of how Tll functions could provide insight into the how Tlx is working during neurogenesis (Islam & Zhang, 2015; Roy et al., 2004; Sobhan & Funa, 2017; Sun et al., 2017; Sun et al., 2008). Tlx has also been implicated in tumorigenesis of subsets of high grade glioblastomas (Sobhan & Funa, 2017; Sun et al., 2017). Knowledge of how Tll functions could potentially be utilized to better understand how Tlx can drive glioblastoma formation and how to best target Tlx for therapeutic potential. Importantly, the knowledge that Tll is likely functioning as a repressor, and the outlined experiments to uncover what the major targets are of Tll would provide better knowledge into how stem cell identity is maintained and what factors turn on upon *tll* knockdown that can promote T1NB identity as the major T1NB factors Ase and Pros are not sufficient to explain the phenotype seen from Tll misexpression. The findings that *tll* is likely downstream of Trx in addition to the likely role of Tll as a repressor strongly suggest that Tll is not likely to function in complex with Trx. This still leaves the question open as to what genes are working with Trx to maintain T2NB identity.

No candidates for Btd targets were able to recapitulate the ability of Btd to induce generation of INPs. This could be a matter of multiple targets needing to be expressed to promote INP generation, but it is also feasible that Btd is promoting gene activity that turns of immature INP specification in the newly born progeny as opposed to GMC specification. Erm is one gene necessary for immature INP function, and activation of Erm in newly born progeny could be sufficient to explain how Pnt misexpression can induce generation of INPs from a small subset of T1NBs. Understanding how Btd promotes immature INPs to be generated could provide better insight into how progeny fates are determined. It is also possible Btd is functioning as a repressor similar to Tll,

but in such we could expect many of the genes Btd targets would likely overlap with Tll targets. Further work to specifically test if Btd functions as an activator or repressor in T2NBs may be needed, but previous attempts to generate Btd^{ZF} chimeras with ERD or Vp16 attached were not sufficient to induce any phenotype upon misexpression. Work is in progress to generate a full length UAS Btd transgene with ERD or Vp16 attached to see which can enhance or suppress the generation of INPs.

The identification Hmx and Vsx2 as novel TFs involved in T2NB lineage progression has interesting potential. The observation that both Hmx and Vsx2 are expressed throughout the T2NB lineage, but become more highly upregulated in INPs would suggest that these are not regulators of temporal identity like D or Opa which are not expressed sequentially in INPs (Abdusselamoglu et al., 2019). Further work is needed to understand the exact roles of Hmx and Vsx2, but these genes could provide insight into how INPs are directed to divide a limited number of times. A new means of testing if genes like Hmx and Vsx2 play roles in shutting down of enhancer activity was shown where use an intron as a reporter in combination with sm-FISH allows for higher resolution in terms of visualizing where an enhancer is active in a NB lineage. This new technique could help provide better insight into when a given enhancer is turned on or off and could show subtle changes in enhancer activity through regulation via TFs or histone modifiers.

References

Abdusselamoglu, M. D., Eroglu, E., Burkard, T. R., & Knoblich, J. A.(2019). The transcription factor odd-paired regulates temporal identity in transit-amplifying neural progenitors via an incoherent feed-forward loop. *eLife*, *8*. https://doi.org/10.7554/eLife.46566

Álvarez, J. A. D.-B., F.J.(2018). Origin and specification of T2NB neuroblasts in the Drosophila embryo. *Development*, *145*(7), dev158394.

Bayraktar, O. A., & Doe, C. Q.(2013). Combinatorial temporal patterning in progenitors expands neural diversity. *Nature*, *498*(7455), 449-455.

Bischof, J., Maeda, R. K., Hediger, M., Karch, F., & Basler, K.(2007). An optimized transgenesis system for Drosophila using germ-line-specific φC31 integrases. *Proceedings of the National Academy of Sciences*, *104*(9), 3312-3317. https://doi.org/doi:10.1073/pnas.0611511104

Carney, T. D., Miller, M. R., Robinson, K. J., Bayraktar, O. A., Osterhout, J. A., & Doe, C. Q.(2012). Functional genomics identifies neural stem cell sub-type expression profiles and genes regulating neuroblast homeostasis. *Dev Biol*, *361*(1), 137-146.

Chen, R., Hou, Y., Connell, M., & Zhu, S.(2021). Homeodomain protein Six4 prevents the generation of supernumerary Drosophila T2NB neuroblasts and premature differentiation of intermediate neural progenitors. *PLoS Genet*, *17*(2), e1009371. https://doi.org/10.1371/journal.pgen.1009371

Dillon, N. R., & Doe, C. Q.(2024). Castor is a temporal transcription factor that specifies early born central complex neuron identity. *Development*, *151*(24). https://doi.org/10.1242/dev.204318

Emili, A., Greenblatt, J., & Ingles, C. J.(1994). Species-specific interaction of the glutamine-rich activation domains of Sp1 with the TATA box-binding protein. *Mol Cell Biol*, *14*(3), 1582-1593. https://doi.org/10.1128/mcb.14.3.1582-1593.1994

Farnsworth, D. R., Bayraktar, O. A., & Doe, C. Q.(2015). Aging Neural Progenitors Lose Competence to Respond to Mitogenic Notch Signaling. *Curr Biol*, *25*(23), 3058-3068.

Gibson, T. J., Larson, E. D., & Harrison, M. M.(2024). Protein-intrinsic properties and context-dependent effects regulate pioneer factor binding and function. *Nature Structural & Molecular Biology*, *31*(3), 548-558. https://doi.org/10.1038/s41594-024-01231-8

Hakes, A. E., & Brand, A. H.(2020). Tailless/TLX reverts intermediate neural progenitors to stem cells driving tumourigenesis via repression of asense/ASCL1. *eLife*, *9*, e53377. .

Islam, M. M., & Zhang, C. L.(2015). TLX: A master regulator for neural stem cell maintenance and neurogenesis. *Biochim Biophys Acta*, *1849*(2), 210-216.

Janssens, D. H., Hammn, D. C., Anhezini, L., Xiao, X., Siller, K. H., Siegrist, S. E., Harrison, M. M., & Lee, C.-Y.(2017). A Hdac1/Rpd3-poised circuit balances continual self-renewal and rapid restriction of developmental potential during asymmetric stem cell division. *Dev Cell*, *40*(4), 367-380.

Janssens, D. H., Komori, H., Grbac, D., Chen, K., Koe, C. T., Wang, H., & Lee, C. Y.(2014). Earmuff restricts progenitor cell potential by attenuating the competence to respond to self-renewal factors. *Development*, *141*(5), 1036-1046.

Komori, H., Xiao, Q., Janssens, D. H., Dou, Y., & Lee, C. Y.(2014). Trithorax maintains the functional heterogeneity of neural stem cells through the transcription factor Buttonhead. *eLife*, *10.7554/eLife.03502*.

Krogan, N. J., Dover, J., Khorrami, S., Greenblatt, J. F., Schneider, J., Johnston, M., & Shilatifard, A.(2002). COMPASS, a histone H3 (Lysine 4) methyltransferase required for telomeric silencing of gene expression. *J Biol Chem*, *277*, 10753-10755.

Kurusu, M., Maruyama, Y., Adachi, Y., Okabe, M., Suzuki, E., & Furukubo-Tokunaga, K.(2009). A conserved nuclear receptor, Tailless, is required for efficient proliferation and prolonged maintenance of mushroom body progenitors in the Drosophila brain. *Dev Biol*, *326*(1), 224-236.

Larson, E. D., Komori, H., Gibson, T. J., Ostgaard, C. M., Hamm, D. C., Schnell, J. M., Lee, C. Y., & Harrison, M. M.(2021). Cell-type-specific chromatin occupancy by the pioneer factor Zelda drives key developmental transitions in Drosophila *Nat Commun*, *12*, 7153.

Li, X., Chen, Z., & Desplan, C.(2013). Temporal patterning of neural progenitors in Drosophila. *Curr Top Dev Biol*, *105*, 69-96.

Miller, T., Krogan, N. J., Dover, J., Erdjument-Bromage, H., Tempst, P., Johnston, M., Greenblatt, J. F., & Shilatifard, A.(2001). COMPASS: a complex of proteins associated with a trithorax-related SET domain protein. *Proc Natl Acad Sci U S A*, *98*, 12902-12907.

Quinto-Rives, N., Komori, H., Janssens, D. H., Kondo, S., Dai, Q., Moore, A. W., & Lee, C.-Y.(2020). Sequential activation of transcriptional repressors promotes progenitor commitment by silencing stem cell identity genes. *eLife*(9), e56187.

Rajan, A., Anhezini, L., Rives-Quinto, N., Chhabra, J. Y., Neville, M. C., Larson, E. D., Goodwin, S. F., Harrison, M. M., & Lee, C.-Y.(2023). Low-level repressive histone marks fine-tune gene transcription in neural stem cells. *eLife*, *12*, e86127. https://doi.org/10.7554/eLife.86127

Roy, K., Kuznicki, K., Wu, Q., Sun, Z., Bock, D., Schutz, G., Vranich, N., & Monaghan, A. P.(2004). The Tlx gene regulates the timing of neurogenesis in the cortex. *J Neurosci*, *24*(38), 8333-8345. https://doi.org/10.1523/jneurosci.1148-04.2004

Sobhan, P. K., & Funa, K.(2017). TLX-Its Emerging Role for Neurogenesis in Health and Disease. *Mol Neurobiol*, *54*(1), 272-280.

Sun, G., Cui, Q., & Shi, Y.(2017). Nuclear Receptor TLX in Development and Diseases. *Curr Top Dev Biol*, *125*, 257-273.

Sun, G., Yu, R. T., Evans, R. M., & Shi, Y.(2008). Orphan nuclear receptor TLX recruits histone deacetylases to repress transcription and regulate neural stem cell proliferation. *Proc Natl Acad Sci U S A*, *104*(39), 15282-15287.

Symonenko, A. V., Roshina, N. V., Krementsova, A. V., & Pasyukova, E. G.(2018). Reduced Neuronal Transcription of Escargot, the Drosophila Gene Encoding a Snail-Type Transcription Factor, Promotes Longevity. *Front Genet*, *9*, 151. https://doi.org/10.3389/fgene.2018.00151

Weng, M., Golden, K. L., & Lee, C. Y.(2010). dFezf/Earmuff maintains the restricted developmental potential of intermediate neural progenitors in Drosophila. *Dev Cell*, *18*(1), 126-135.

Zacharioudaki, E., Housden, B. E., Garinis, G., Stojnic, R., Delidakis, C., & Bray, S. J.(2016). Genes implicated in stem cell identity and temporal programme are directly targeted by Notch in neuroblast tumours. *Development*, *143*(2), 219-231. https://doi.org/10.1242/dev.126326

Zhu, S., Barshow, S., Wildonger, J., Jan, L. Y., & Jan, Y. N.(2011). Ets transcription factor Pointed promotes the generation of intermediate neural progenitors in Drosophila larval brains. *Proc Natl Acad Sci U S A.*, *108*(51), 20615-20620.

Material and Methods

Table 3.1 Key Resources for Chapter 3

Reagent type (species) or resource	Designation	Source or reference	Identifiers	Additional information
Antibody	anti-GFP (Chicken polyclonal)	Aves Labs, INC.	Cat#GFP-1020, RRID:AB_2307313	IF(1:2000)
Antibody	anti-RFP (Rabbit polyclonal)	Rockland	Cat.#600-401-379, Lot#31089	IF(1:200)
Antibody	anti-Ase (Rabbit polyclonal)	Weng et al., 2010 doi: 10.1016/j.devcel.2009.12.007.		IF(1:400),
Antibody	anti-Dpn (Rat monoclonal)	Lee et al., 2006a doi: 10.1038/nature04299.	clone 11D1BC7.14	IF(1:1000)
Antibody	anti-cMyc (Mouse Monoclonal)	Roche, Basel, Switzerland	Cat.# 11 667 149 001	IF(1:100)
Antibody	anti-Scrib (Rabbit Polyclonal)	Albertson & Doe 2003 doi.org/10.1038/ncb922		IF(1:500)
Antibody	anti-Tll (Rabbit polyclonal)	Asian Distribution Center for Segmentation Antibodies	Code#812	Cut&Run (1ul)
Antibody	anti-Btd (Rabbit Polyclonal)	Lifeome	RB7981	Cut&Run (1ul)
Antibody	anti-Erm (Rb Polyclonal)	Hildebrandt et al., 2021 doi.org/10.1186/s41065-021-00209-6		Cut&Run (1ul)

Antibody	Alexa Fluor 488 AffiniPure Anti-Chicken IgY (IgG) (H+L) (Donkey polyclonal)	Jackson Immuno Research Laboratories, INC.	Cat#703-545-155, RRID:AB_2340375	IF(1:500)
Antibody	AlexaFluor 488 AffiniPure anti-Rat IgG (H+L) (Goat polyclonal)	Jackson Immuno Research Laboratories, INC.	Cat#112-605-167 RRID:AB_2338404	IF(1:500)
Antibody	anti-Mouse IgG (H+L) Highly Cross-Adsorbed Secondary Antibody, Alexa Fluor 488 (Goat polyclonal)	ThermoFisher Scientific	Cat#A-11029, RRID:AB_2534088	IF(1:500)
Antibody	anti-Rabbit IgG (H+L) Highly Cross-Adsorbed Secondary Antibody, Alexa Fluor 488 (Goat polyclonal)	ThermoFisher Scientific	Cat#A-11034, RRID:AB_2576217	IF(1:500)
Antibody	anti-Rabbit IgG (H+L) Highly Cross-Adsorbed Secondary Antibody, Alexa Fluor 546 (Goat polyclonal)	ThermoFisher Scientific	Cat#A-11035, RRID:AB_2534093	IF(1:500)
Antibody	anti-Guinea Pig IgG (H+L) Highly Cross-Adsorbed Secondary Antibody) Alexa Fluor 488 (Goat polyclonal)	Invitrogen	Cat#A-11073	IF(1:500)
Chemical compound	Alexa Fluor Plus 405 Phalloidin	Invitrogen	Cat#: A30104	IF(1:100)
Chemical compound	Alexa Fluor 488 phalloidin	Invitrogen	Cat#: A12379	IF(1:100)
Chemical compound	Rhodamine Phalloidin	ThermoFisher Scientific	Cat#R415	IF(1:100)

Genetic reagent (D. melanogaster)+A36:C60B37AA36:C160	y1; M{vas-int.Dm}ZH-2A w*;M{UAS-Tll$^{244:}$:Vp16-3xMyc}VK20	This paper		Transgene expressing Tll 1-244 with C-terminusl zinc fused with VP16 transcriptional activation domain and 3xMyc epitote tag
Genetic reagent (D. melanogaster)	y1; M{vas-int.Dm}ZH-2A w*;M{UAS-Tll^{244}::ERD-3xMyc}VK21	This paper		Transgene expressing Tll 1-244 with C-terminusl zinc fused with ERD transcriptional repressor domain and 3xMyc epitote tag
Genetic reagent (D. melanogaster)	y1; M{vas-int.Dm}ZH-2A w*;M{UAS-Tll^{244-}3xMyc}VK21	This paper		Transgene expressing Tll 1-244 with C-terminusl zinc fused with 3xMyc epitote tag
Genetic reagent (D. melanogaster)	*brat11/CyO, Actin-GFP*	Lee et al., 2006b doi: 10.1016/j.devcel.2006.01.017.		
Genetic reagent (D. melanogaster)	*bratKO06028/CyO, Actin-GFP*	Lee et al., 2006b doi: 10.1016/j.devcel.2006.01.017.		
Genetic reagent (D. melanogaster)	*tll^{RNAi}* UAS-tll-miRNAs	Lin et al., 2009 doi:10.1371/journal.pone.0008392		
Genetic reagent (D. melanogaster)	*rbbp5^{EXL16}/Tm6B*	Komori et al. 2014 doi:10.7554/eLife.03502		
Genetic reagent (D. melanogaster)	*y1, M{vas-int.Dm}ZH-2A w*; M{UAS-insbFL-myc}ZH-86Fb*	Komori et al., 2018 doi: 10.1101/gad.320333.118.		
Genetic reagent (D. melanogaster)	*Wor-Gal4(II)*	Lee et al., 2006a doi: 10.1038/nature04299.		
Genetic reagent (D. melanogaster)	*Wor-Gal4(III)*	Weng et al., 2010 doi: 10.1016/j.devcel.2009.12.007.		
Genetic reagent (D. melanogaster)	*Ase-Gal4(II)*	Zhu et al., 2006 doi: 10.1016/j.cell.2006.08.045.		

Genetic reagent (D. melanogaster)	*UAS-apkcCaax*	Sotillos et al., 2004 doi: 10.1083/jcb.200311031		
Genetic reagent (D. melanogaster)	*UAS-MITF*	Gift from Francesca Pignoni		
Genetic reagent (D. melanogaster)	*UAS-Hmx*	Gift from Jens Rister		
Genetic reagent (D. melanogaster)	*UAS-Hmx.V5*	Gift from Jens Rister		
Genetic reagent (D. melanogaster)	*UAS-Vsx1*	Erclik et al.(2017) doi: 10.1038/nature20794		
Genetic reagent (D. melanogaster)	D. melanogaster: VanGlow reporter fly: PBac{tll enh-GFP::Luc(nls)}VK31	Larson et al. 2021 doi:10.1038/s41467-021-27506-y		
Genetic reagent (D. melanogaster)	*w1118; Df(2L)Exel8040/CyO*	Bloomington Drosophila Stock Center	BDSC: 7847 FlyBase: FBst0007847; RRID:BDSC_7847	
Genetic reagent (D. melanogaster)	*y1 w*; PBac{y+mDint2 w+mC=tll-EGFP.S}VK00037*	Bloomington Drosophila Stock Center	BDSC: 30874 FlyBase: FBst0030874; RRID:BDSC_30874	
Genetic reagent (D. melanogaster)	*w1118; PBac{Sp1-EGFP.S}VK00033*	Bloomington Drosophila Stock Center	BDSC: 38669 FlyBase: FBst0038669; RRID:BDSC_38669	
Genetic reagent (D. melanogaster)	*y1 w*; PBac{y+mDint2 w+mC=ap-GFP.FPTB}VK00031*	Bloomington Drosophila Stock Center	BDSC: 83378 FlyBase: FBst0083378 RRID:BDSC_83378	

Genetic reagent (D. melanogaster)	*y1 w*; PBac{y+mDint2 w+mC=Oli-GFP.FPTB}VK00033*	Bloomington Drosophila Stock Center	BDSC: 68192 FlyBase: FBst0068192 RRID:BDSC_68192	
Genetic reagent (D. melanogaster)	*w1118; PBac{y+mDint2 w+mC=ewg-GFP.FPTB}VK00033*	Bloomington Drosophila Stock Center	BDSC: 66752 FlyBase:FBti0185273 RRID:BDSC_66752	
Genetic reagent (D. melanogaster)	*w1118; PBac{y+mDint2 w+mC=ewg-GFP.FPTB}VK00033*	Bloomington Drosophila Stock Center	BDSC: 66752 FlyBase:FBti0185273 RRID:BDSC_66752	
Genetic reagent (D. melanogaster)	*w1118; PBac{y+mDint2 w+mC=ewg-GFP.FPTB}VK00033*	Bloomington Drosophila Stock Center	BDSC: 66752 FlyBase:FBti0185273 RRID:BDSC_66752	
Genetic reagent (D. melanogaster)	*w1118; P{y+t7.7 w+mC=GMR31F04-GAL4}attP2 (Tll-Gal4)*	Bloomington Drosophila Stock Center	BDSC: 46187 FlyBase: FBst0046187; RRID:BDSC_46187	
Genetic reagent (D. melanogaster)	*w*; P{y+t7.7 w+mC=10XUAS-IVS-mCD8::RFP}attP40*	Bloomington Drosophila Stock Center	BDSC: 32219 FlyBase: FBti0131967; RRID:BDSC_32219	

Genetic reagent (D. melanogaster)	*y1 w*; P{w+mC=UAS-mCD8::GFP.L}LL5, P{UAS-mCD8::GFP.L}2*	Bloomington Drosophila Stock Center	BDSC: 5137 FlyBase: FBti0012685; RRID:BDSC_5137	
Genetic reagent (D. melanogaster)	*w*; P{w+mC=UAS-Dcr-2.D}2, P{w+mC=UAS-mCherry.CAAX.S}2; TM2/TM6B, Tb1*	Bloomington Drosophila Stock Center	BDSC: 59022 FlyBase: FBti0012685; RRID:BDSC_59022	
Genetic reagent (D. melanogaster)	*Oregon-R-C*	Bloomington Drosophila Stock Center	BDSC: 5 FlyBase: FBst0000005; RRID:BDSC_5	
Genetic reagent (D. melanogaster)	*y1 v1; P{y+t7.7 v+t1.8=UAS-LUC.VALIUM10}attP2*	Bloomington Drosophila Stock Center	BDSC: 35788 FlyBase: FBti0143388; RRID:BDSC_35788	
Genetic reagent (D. melanogaster)	*eGFP^{RNAi} y1 sc* v1 sev21; P{y+t7.7 v+t1.8=VALIUM22-EGFP.RNAi.4}attP40*	Bloomington Drosophila Stock Center	BDSC: 41550 FlyBase: FBti0148871; RRID:BDSC_41550	
Genetic reagent (D. melanogaster)	*P{UAS-lacZ.B}Bg4-1-2*	Bloomington Drosophila Stock Center	BDSC: 1776 FlyBase: FBti0013988; RRID:BDSC_5430	
Genetic reagent (D. melanogaster)	*Ase^{RNAi} w1118; P{GD12444}v28280*	Vienna Drosophila Resource Center	VDRC:v28280	

			Flybase: FBti0082204 RRID:VDRC_v28280	
Genetic reagent (D. melanogaster)	*w1118; P{w+mC=UAS-Dcr-2.D}2*	Bloomington Drosophila Stock Center	BDSC: 24650 FlyBase: FBst0002465 0; RRID:BDSC_24650	
Genetic reagent (D. melanogaster)	*w*; P{w+mC=tubP-GAL80ts}10; TM2/TM6B, Tb1*	Bloomington Drosophila Stock Center	BDSC: 7108 FlyBase: FBti0027799; RRID:BDSC_7017	
Genetic reagent (D. melanogaster)	*w*; P{w+mC=tubP-GAL80ts}20; TM2/TM6B, Tb1*	Bloomington Drosophila Stock Center	BDSC: 7019 FlyBase: FBti0027796; RRID:BDSC_7019	
Genetic reagent (D. melanogaster)	*w*; snaSco/CyO; P{w+mC=tubP-GAL80ts}ncdGAL80ts-7*	Bloomington Drosophila Stock Center	BDSC: 7018 FlyBase: FBti0027798; RRID:BDSC_7018	
Genetic reagent (D. melanogaster)	*w*; P{w+mC=UAS-aop.WT}Ia/CyO*	Bloomington Drosophila Stock Center	BDSC: 5790 FlyBase: FBst0005790 RRID:BDSC_5790	
Genetic reagent (D. melanogaster)	*y1 w*; P{w+mC=UAS-AP-2.M}1*	Bloomington Drosophila Stock Center	BDSC: 23881 FlyBase: FBst0023881 RRID:BDSC_23881	
Genetic reagent (D. melanogaster)	*w*; P{y+t7.7 w+mC=UAS-CrebA.F}attP2*	Bloomington Drosophila Stock Center	BDSC: 79021 FlyBase: FBst0079021	

			RRID:BDSC_79021	
Genetic reagent (D. melanogaster)	*y1 w*; P{w+mC=UAS-ewg.H}3*	Bloomington Drosophila Stock Center	BDSC: 77876 FlyBase: FBti0196670 RRID:BDSC_77876	
Genetic reagent (D. melanogaster)	*w*; P{w+mC=UAS-l(1)sc.LSC}2; P{UAS-l(1)sc.LSC}3*	Bloomington Drosophila Stock Center	BDSC: 51670 FlyBase: FBst0051670 RRID:BDSC_51670	
Genetic reagent (D. melanogaster)	*y1 w*; P{w+mC=UAS-sc.USC}3*	Bloomington Drosophila Stock Center	BDSC: 51672 FlyBase: FBti0154818 RRID:BDSC_51672	
Genetic reagent (D. melanogaster)	*w1118; P{w+mC=UAS-tai.B}JB1*	Bloomington Drosophila Stock Center	BDSC: 6378 FlyBase: FBti0018776 RRID:BDSC_6378	
Genetic reagent (D. melanogaster)	*w*; P{w+mC=UAS-sd.S}V1*	Bloomington Drosophila Stock Center	BDSC: 9373 FlyBase: FBst0009373 RRID:BDSC_9373	
Genetic reagent (D. melanogaster)	*w1118; P{w+mC=UAS-vri.2}1*	Bloomington Drosophila Stock Center	BDSC: 78077 FlyBase: FBti0197953 RRID:BDSC_78077	
Genetic reagent (D. melanogaster)	*y1 w*; P{w+mC=UAS-brk.J}8.1*	Bloomington Drosophila Stock Center	BDSC: 93081 FlyBase: FBst0093081 RRID:BDSC_93081	

Genetic reagent (D. melanogaster)	*w*; P{w+mC=UAS-dve.5.0}3*	Bloomington Drosophila Stock Center	BDSC: 7086 FlyBase: FBst0007086 RRID:BDSC_7086	
Genetic reagent (D. melanogaster)	*y1 w*; M{RFP3xP3.PB w+mC=UAS-onecut.ORF.3xHA.GW}ZH-86Fb/TM3, Sb1 Ser1*	Bloomington Drosophila Stock Center	BDSC: 95326 FlyBase: FBst0095326 RRID:BDSC_95326	
Genetic reagent (D. melanogaster)	*y1 w* P{ry+t7.2=hsFLP}12; P{w+mC=UAS-bi.P}2/CyO; MKRS/TM6B, Tb1*	Bloomington Drosophila Stock Center	BDSC: 80150 FlyBase: FBst0007086 RRID:BDSC_80150	
Genetic reagent (D. melanogaster)	*btd^{RNAi} y1 v1; P{y+t7.7 v+t1.8=TRiP.JF03389}attP2*	Bloomington Drosophila Stock Center	BDSC: 29453 FlyBase: FBst0029453 RRID:BDSC_80150	
Genetic reagent (D. melanogaster)	*rbbp5DF w1118; Df(3L)BSC447/TM6C, Sb1 cu1*	Bloomington Drosophila Stock Center	BDSC: 24951 FlyBase: FBab0045271 RRID:BDSC_24951	
Genetic reagent (D. melanogaster)	*vsx2DF Df(1)BSC571, w1118/FM7h/Dp(2;Y)G, P{w+mC=hs-hid}Y*	Bloomington Drosophila Stock Center	BDSC: 25114 FlyBase: FBab0045466 RRID:BDSC_25114	

Genetic reagent (D. melanogaster)	*vsx2DF Df(1)Exel6235, w1118 P{w+mC=XP-U}Exel6235/FM7c, sn+*	Bloomington Drosophila Stock Center	BDSC: 7709 FlyBase: FBab0037801 RRID:BDSC_7709	
Genetic reagent (D. melanogaster)	*w1118; PBac{y+mDint2 w+mC=Vsx2-GFP.FPTB}VK00033/ TM3, Sb1*	Bloomington Drosophila Stock Center	BDSC: 42292 FlyBase:FBst0042292 RRID:BDSC_4292	
Genetic reagent (D. melanogaster)	*w1118; PBac{y+mDint2 w+mC=Vsx1-GFP.FPTB}VK00033/ TM6C, Sb1*	Bloomington Drosophila Stock Center	BDSC: 465827 FlyBase: FBti0182614 RRID:BDSC_65827	
Genetic reagent (D. melanogaster)	*w1118; PBac{y+mDint2 w+mC=lilli-GFP.FPTB}VK00033*	Bloomington Drosophila Stock Center	BDSC: 42276 FlyBase: FBst0042276 RRID:BDSC_42276	
Genetic reagent (D. melanogaster)	*w1118; PBac{y+mDint2 w+mC=zfh2-GFP.FPTB}VK00033/ TM3, Sb1*	Bloomington Drosophila Stock Center	BDSC: 38674 FlyBase: FBti0147738 RRID:BDSC_38674	
Genetic reagent (D. melanogaster)	*tll^{RNAi} wP{VSH330031}attP40*	Vienna Drosophila Resource Center	VDRC:v330031 Flybase: FBst0490960 RRID:VDRC_v330031	

Genetic reagent (D. melanogaster)	*hmx$^{RNAi\ \#1}$ w1118; P{GD11781}v52505*	Vienna Drosophila Resource Center	VDRC: v52505 FlyBase:FBst0469869 RRID:VDRC_v52505	
Genetic reagent (D. melanogaster)	*hmx $^{RNAi\ \#2}$ w1118; P{GD9519}v40128*	Vienna Drosophila Resource Center	VDRC: v40128 FlyBase:FBst0463399 RRID:VDRC_v40128	
Genetic reagent (D. melanogaster)	*hmx:GFP PBac{fTRG00011.sfGFP-TVPTBF}VK00033*	Vienna Drosophila Resource Center	VDRC: v318004 FlyBase:FBst0491300 RRID:VDRC_v318004	
Genetic reagent (D. melanogaster)	*M{UAS-ATbp.ORF.3xHA.GW}ZH-86Fb*	FlyORF	FlyORF: F001691 FlyBase: FBst0501047	
Genetic reagent (D. melanogaster)	*M{UAS-cas.ORF.3xHA.GW}ZH-86Fb*	FlyORF	FlyORF: F001826 FlyBase: Bst0502905	
Genetic reagent (D. melanogaster)	*M{UAS-CG14050.ORF.3xHA.GW}ZH-86Fb*	FlyORF	FlyORF: F003104 FlyBase: FBst0502438	
Genetic reagent (D. melanogaster)	*M{UAS-D.ORF.3xHA.GW}ZH-86Fb*	FlyORF	FlyORF: F00636 FlyBase: FBst0501289	
Genetic reagent (D. melanogaster)	*M{UAS-fd102C.ORF.3xHA.GW}ZH-86Fb*	FlyORF	FlyORF: F000257	

			FlyBase: FBst0501348	
Genetic reagent (D. melanogaster)	*M{UAS-Hr4.ORF.3xHA.GW}ZH-86Fb*	FlyORF	FlyORF: F002369 FlyBase: FBst0501733	
Genetic reagent (D. melanogaster)	*M{UAS-ind.ORF.3xHA.GW}ZH-86Fb*	FlyORF	FlyORF: F000047 FlyBase: FBst0501408	
Genetic reagent (D. melanogaster)	*M{UAS-jing.ORF-VN}ZH-86Fb*	FlyORF	FlyORF: F004786 FlyBase: FBst0502994	
Genetic reagent (D. melanogaster)	*M{UAS-jumu.ORF.3xHA.GW}ZH-86Fb*	FlyORF	FlyORF: F002208 FlyBase: FBgn0015396	
Genetic reagent (D. melanogaster)	*M{UAS-Mad.ORF.3xHA.GW}ZH-86Fb*	FlyORF	FlyORF: F001716 FlyBase: FBst0501432	
Genetic reagent (D. melanogaster)	*M{UAS-nerfin-1.ORF.3xHA.GW}ZH-86Fb*	FlyORF	FlyORF: F000461 FlyBase: FBst0501453	
Genetic reagent (D. melanogaster)	*M{UAS-Oli.ORF.3xHA.GW}ZH-86Fb*	FlyORF	FlyORF: F000021 FlyBase: FBst0501466	
Genetic reagent (D. melanogaster)	*M{UAS-Poxn.ORF.3xHA.GW}ZH-86Fb*	FlyORF	FlyORF: F000102 FlyBase: FBst0501491	

Genetic reagent (D. melanogaster)	*M{UAS-rgr.ORF-VNshort}ZH-86Fb*	FlyORF	FlyORF: F004870 FlyBase: FBst0503070	
Genetic reagent (D. melanogaster)	*M{UAS-scro.ORF.3xHA.GW}ZH-86Fb*	FlyORF	FlyORF: F000666 FlyBase: FBst0501515	
Genetic reagent (D. melanogaster)	*M{UAS-scrt.ORF.3xHA.GW}ZH-86Fb*	FlyORF	FlyORF: F001921 FlyBase:FBst0501516	
Genetic reagent (D. melanogaster)	*M{UAS-Vsx2.ORF-CC}ZH-21F*	FlyORF	FlyORF:F0003625 FlyBase: FBst0502660	
Genetic reagent (D. melanogaster)	*M{UAS-Mnt.ORF.3xHA}ZH-86Fb*	FlyORF	FlyORF:F001147 FlyBase: FBst0500736	
Genetic reagent (D. melanogaster)	*M{UAS-svp.ORF.3xHA.GW}ZH-86Fb*	FlyORF	FlyORF:F000492 FlyBase: FBst0501553	
Genetic reagent (D. melanogaster)	*M{UAS-NK7.1.ORF.3xHA.GW}ZH-86Fb*	FlyORF	FlyORF:F001842 FlyBase: FBst0501459	
Genetic reagent (D. melanogaster)	*M{UAS-cnc.ORF.3xHA.GW}ZH-86Fb*	FlyORF	FlyORF:F000602 FlyBase: FBst0501270	
Genetic reagent (D. melanogaster)	*M{UAS-tll.ORF.3xHA.GW}ZH-86Fb*	FlyORF	FlyORF:F000061	

			FlyBase: FBst0501563	
Genetic reagent (D. melanogaster)	*M{UAS-hng3.ORF.3xHA.GW} ZH-86Fb*	FlyORF	FlyORF:F000696 FlyBase: FBst0501397	
Genetic reagent (D. melanogaster)	*M{UAS-crebB.ORF.3xHA.GW }ZH-86Fb*	FlyORF	FlyORF: F000425 FlyBase: FBgn0014467	
Genetic reagent (D. melanogaster)	D. melanogaster: VanGlow reporter fly :PBac{erm enh-GFP::Luc(nls)}VK00033	Janssens et al., 2017 doi: 10.1016/j.devcel.2017.01.014		
Recombinant DNA reagent	VanGlow-GL-DSCP Gateway Destination vector	Janssens et al., 2017 doi: 10.1016/j.devcel.2017.01.014	Addgene Plasmid #83338	
Recombinant DNA reagent	*pUAST-Tll244:3Xmyc-attB (plasmid)*	This study		Plasmid DNA of a transgene expressing Tll 1-244 with 3 copies of Myc epitope
Recombinant DNA reagent	*pUAST-Tll244::Vp16-3Xmyc-attB (plasmid)*	This study		Plasmid DNA of a transgene expressing Tll 1-244 with Vp16 and 3 copies of Myc epitope
Recombinant DNA reagent	*pUAST-Tll244::ERD-3Xmyc-attB (plasmid)*	This study		Plasmid DNA of a transgene expressing Tll 1-244 with ERD and 3 copies of Myc epitope
Commercial assay or kit	B5-labeled HCR RNA-FISH iprobe (btd-RA)	Molecular Instruments, Inc	*btd-RA*	
Commercial assay or kit	B5-labeled HCR RNA-FISH iprobe (EGFP)	Molecular Instruments, Inc	*EGFP*	
Commercial assay or kit	B2-labeled HCR RNA-FISH iprobe (dpn)	Molecular Instruments, Inc	*dpn-RA*	

Commercial assay or kit	B2-labeled HCR RNA-FISH iprobe (pnt-RC)	Molecular Instruments, Inc	*pnt-RC*	
Commercial assay or kit	B2-labeled HCR RNA-FISH iprobe (pnt intron)	Molecular Instruments, Inc	*pnt intron*	
Commercial assay or kit	HCR RNA-FISH amplifiers	Molecular Instruments, Inc		
Commercial assay or kit	Click-iT™ EdU Cell Proliferation Kit for Imaging, Alexa Fluor™ 555 dye	ThermoFisher Scientific	C10338	
Commercial assay or kit	RNeasy Micro Kit	Qiagen	Cat#74004	
Commercial assay or kit	CUTANA ChIC/CUT&RUN Kit	Epicypher	SKU: 14–1048	
Commercial assay or kit	Illumina Tagment and DNA enzyme and Buffer	Illumina	20034210	
Commercial assay or kit	IDT for Illumina DNA/RNA UD Indeces	Illumina	20026121	
Commercial assay or kit	NEBNext Ultra II DNA Library Prep Kit for Illumina	New England Biolabs	Cat#: E7645L	
Commercial assay or kit	NEBNext Multiplex Oligos for Illumina (96 Unique Dual Index Primer Pairs)	New England Biolabs	Cat#: E6440L	
Chemical compound	ProLong Gold Antifade Mountant	Invitrogen	Cat#: P36930	
Chemical compound	Agencourt AMPure XP - 5 mL	Beckman Coulter	Cat#: A63880	
Chemical compound	Sodium butyrate	Sigma Aldrich	Cat#: B5887	
Chemical compound	Trizol	ThermoFisher Scientific	Cat#:15596026	

Fly genetics and transgenes

Experiments involving driving UAS-transgenes with Gal4 lines were carried out by setting up crosses in 6 oz plastic bottles. Samples were collected for egg lay over 8-hour intervals. Embryos were allowed to grow 24 hours at 25ºC to larval stage before genotyping and transferring samples to a meal cap. All samples driving a UAS-

transgene were prepared with at least one copy of Tubulin-Gal80^{TS} included to prevent embryonic expression. Most samples were incubated at 33C for 72 hours to induce transgene expression. Samples that were prepared under different conditions include Fig. 3.1J where samples were grown at 25ºC for 72 hours after transferring to meal cap before shifting to 33ºC 24 hours prior to dissection. After transferring to a mealcap samples in Fig. 3.3B were grown at 25ºC for 120 hours prior to dissection, while samples in Fig. 3.3C grown at 25ºC for 96 hours and shifted to 33ºC 24 hours prior to dissection. Samples not driving a UAS-transgene were grown in meal caps for 96 hours at 25ºC prior to dissection. Validation of GFP transgenes was done on wandering third instar larvae. Worniu-Gal4 was used to drive Pan NB expression, while *Worniu-Gal4,AseGal80* or *31F04-Gal4* (*Tll-Gal4*) was used to drive T2NB expression. Experiments using multiple UAS-transgenes were controlled for driver dilution with the same number of UAS-transgenes included.

For generation of UAS-Tll^{244} chimeras, Tll nucleotide sequence corresponding to the first 244 amino acids was fused with 3XMyc epitope and cloned into the pUASt-attB vector through use of standard PCR, restriction digest and ligation procedures. The Transgene were inserted into the pUAST-attB M(3xP3-RFP.attP)VK20 docking site using ΦC31 integrase-mediated transgenesis (Bischof et al., 2007). DNA injections were carried out by Genetivision Inc. Transgenic flies were identified in the F1 generation based on their red eye color and PCR on genomic DNA. To create the pnt intron reporter we ordered gBlocks (Integrated DNA Technologies, Coralville, IA) with pnt intron sequence containing splicing sites and used traditional cloning to clone into VanGlow vector with the DSCP (Addgene#83338) targeting downstream of the DSCP

and upstream of the GFP luciferase. These transgenes were cloned with Gateway LR Clonase (ThermoFisher Scientific, Waltham, MA) to insert previously validated *tll* enhancer (Larson et al., 2021) generated from PCR-amplified genomic region into the VanGlow vector The transgenic reporters were integrated into the VK22 site on chromosome 2 using φC31-mediated integration (Genetivision, Stafford, TX).

Table 3.2 Pnt intron sequence used for enhancer reporter construction

Pnt intron sequence	aacaatctggtgggggcgttgagcagctccacggctgcttcgctgggactgg gctacttcaatgatatggcgccctttgtgggcgatgcgaatgcctactacacg gactcggatgtcaacttctttagttcaggtacaggtcagcaaatatttaccgac atcaaaaacggtgcttttaattacgattgctggggtgtgaaaaggcagcaaa ccagaagaagacgctttgcggtggcataattaaattcgtaatttgtttttaagtgt ttgacacgcaacaagtcggggtggctaaggggaactgactgggatataca cgcagagaaaaaatgttctagtaactaagttctagtaactaatgatattcaac atatactacgtttagttttcactttacaaaataaacaaatttcaatttaattatatttg taaagttacaatatattactataaatacatttttcgctgcgtgcatcagattgcgc tgggtgataagtggcttgttgagcgctagaagatgtggccggcctcagatgta tctggcagatacggatgctcttgcgctctctggaggcggcacctaaagaggc gctgccaactctttggccagccaacgaggggctgtatctgtatctttgtgtctct gtgcctgcgagcgaatgggaatcgaaacgaagcgctggcaaagctttttta tttctttgccgtgcgcgagagggacagctacagggctgcgcgtgtgtatgtggt tatgtgccaacaggttttcgtatcccacagatacacgagtgtacatcgaaatgt gttaaatttcgttgtattcgcaattaatgtagcgtgcacaccattagatcgggttg gttgtgcctgtgtgcgtgggtatctgtgtgctgcggcctgtgcttgtgtgtgcgc gctgtgattttgattggttttcgaagtcttgcgctcgcttgagagacgccccatttc tatgaacaccatttaatagaaattgcgaacaatctgtaatcaccggattttggc gtgtgaaaaatgtatctggggattttagcgatgcgaatttcccacgataaataa atggctttctaagatttgcatatacattttatattatatctttaatttatgacaagact tctgtgaaacagaatttaatagaaatataatttttaatttttattgaaattaaacgtt tcattcataagttgacggccacagattatactctttccatacccatatctataca acaatgtctaatccaattactatctcatatttcgtatcgcttacaggctacaaca ccagcaacacacacgaccgcatcaacaacagcacgcccccgcagcagc agcaatcgcagcagccgactgtcaat

Immunofluorescent staining and antibodies

Larval brains were genotyped before dissecting in phosphate buffered saline (1X PBS). All dissections were done in less than 30 minute time points. Following dissection samples were fixed for 23 minutes at 25°C in a solution of 100 mM PIPES (pH 6.9), 1 mM EGTA, 0.3% Triton X-100 and 1 mM MgSO4 and 4% formaldehyde. Samples were then washed with 1X PBS and 0.3% Triton X-100 (1X PBST) for 30 minutes at 25°C. Samples were incubated with 1X PBST and primary antibody (found in Key Resources

Table) for 3 hours at 25°C. Following primary antibody incubation, samples were washed again with 1X PBST for 30 minutes at 25ºC. After washing, samples were incubated overnight at 4ºC in a solution of 1X PBST and secondary antibodies and/or phalloidin (found in Key Resources Table). The following day samples were washed in 1X PBST for 30 minutes at 25ºC before equilibrating in ProLong Gold antifade mount (ThermoFisher Scientific).

Hybridization Chain Reaction (HCR) and immunofluorescent staining

Samples in which mRNA transcripts in larval brains were detected was done by performing in situ HCR v3.087. HCR probes can be found in the Key Resources Table which were generated using NCBI sequences. DEPC treated water was used in preparation of reagents starting at initial fixation step. Samples were dissected under RNAse free conditions in 1X PBS. Samples fixed for 23 minutes at 25ºC in a solution of 100 mM PIPES (pH 6.9), 1 mM EGTA, 0.3% Triton X-100 and 1 mM $MgSO_4$ with 4% formaldehyde concentration. Samples were washed in a solution 1X PBS and 0.3% Triton X-100 (1X PBST) for 30 minutes at 25ºC. Following washing, samples were incubated in hybridization buffer (10% formamide, 5×SSC, 0.3% Triton X-100 and 10% dextran sulfate) at 37°C for 1 hour. After 1 hour, 5 nM of primary mRNA HCR probes (Molecular Instruments, Los Angeles, CA) were added to each sample and incubated overnight at 37°C. Following the overnight incubations, samples were washed with SSC buffer (10% formamide, 5×SSC, 0.3% Triton X-100) and for 30 minutes at 25ºC. Samples were then incubated with amplification buffer (5×SSC, 0.3% Triton X-100 and 10% dextran sulfate). Secondary hairpins (Molecular Instruments, Los Angeles, CA) were denatured at 95 °C for 2 mins and incubated on ice for 5 minutes before 3 μM (6

μM for Alexa Fluor 546) of each hairpin were added to each sample. Samples were incubated overnight at 25℃. The following day samples were washed in 1X PBST before fixing for 12 minutes to initiate immunofluorescent staining protocol as listed above.

Collection of Brains for CUT&RUN

Collection of T2NB enriched or immature INP enriched brains used for Cut&Run was done according to (Larson et al., 2021; Quinto-Rives et al., 2020). T2NB enriched lysate was collected from brat$^{11/DF}$ brains were collected in 8 hour windows and transferred to a meal cap 24 hours after collection. Samples were then incubated at 25ºC for 120 hours before dissecting. ImmINP enriched brains were acquired as described with *Wor-Gal4* driving UAS-Insb in brat$^{11/DF}$ brains by shifting samples to 33ºC 12 hours prior to dissection to induce synchronous differentiation into immature INPs. All samples were dissected in 1X PBS before further processing.

CUT&RUN on enriched brains

Samples were prepared as described in (Gibson et al., 2024; Rajan et al., 2023). Brains were dissected in under 45 minutes with at least 50 brains per replicate with two replicates acquired per sample. After dissection, samples were kept in 1XPBS and spun down for 3 minutes at 600 g before supernatant was removed. Samples were prepared using CUTANA ChIC/CUT&RUN (Epicypher) per the manufacturer's protocol with the following modifications. Samples were resuspended in 100 μl wash buffer and transferred to a dounce homogenizer. Samples were dounced at least 40 times on ice before transferring to a 1.5 ml tube. Samples were spun for 3 minutes at 600 g. Pellet was processed using CUT&RUN kit. For each sample, 0.5 ng of antibody was used (or

0.5 µl if antibody concentration was unknown). Additionally, 0.5 ng of *Escherichia coli* spike-in DNA was added into every sample as a spike-in control. The following antibodies were used and can be found in key resources table: rabbit anti-Erm, rabbit anti-Btd, and rabbit anti-Tll.

After Cut&Run was completed, DNA was diluted up to 50 µl with 0.1x TE. Library prep was done using NEBNext Ultra II DNA Library Prep Kit for Illumina (E7645) along with NEBNext Multiplex Oligos for Illumina (E6440). Manufacturer's protocol was followed with some modifications. Adaptor was diluted by a ratio of 1:25. The bead clean-up steps were performed with 1.1 x AMPure Beads and without size selection. The PCR cycle were set to match ChIC/CUT&RUN kit. DNA was eluted in 20 µL 0.1 x TE. Agilent TapeStation was used to assess DNA quality and concentration. In samples that had greater than 1% adaptor, additional bead cleanup was done before sequencing on IlluminaNovaSeq-6000 chip (University of Michigan Advanced Genomics Core) with 151-bp end reads.

RNA-seq on NB or INP enriched brains

Samples were prepared as previously described (Quinto-Rives et al., 2020). Samples were dissected in 20-minute intervals and at least 50 brains were collected. All samples were prepared in triplicate. Samples were prepared in RNase-free conditions. RNA was isolated using TRIzol (ThermoFisher Scientific) and mRNA was then purified using the RNeasy Micro Kit (Qiagen) according to the manufacturer's instructions. Libraries were prepped using SMART-Seq Stranded Kit (Takara, 634444) according to

manufacturer's instructions. RNA was sequenced on IlluminaNovaSeq-6000 chip with 150bp end paired reads(University of Michigan Advanced Genomics Core).

Imaging and Quantification of immunofluorescent samples

Images of samples were acquired on a Leica SP5 scanning confocal microscope (Leica Microsystems Inc) using a 63X glycerol immersion objective. Images were taken at 1.5X zoom for whole lobe, or 3X zoom for single neuroblasts. Whole brain lobe images were taken with z-stacks of 1.51 µm thickness, while smFISH images were taken with 0.5 µm thickness.

Quantification was done with observer blinded to genotypes. Analysis shown in graphs was done with two-tailed Student's t-test with p-values <0.05 (*), <0.005(**), <0.0005 (***), and <0.00005 (****). Dot plots were made on GraphPad Prism. Only the central brain was looked at and identified based on morphology. T1NBand T2NB NBs were identified based on size (diameter >9 µm) and expected marker profile or labeling with mcd8:GFP or mcd8:RFP. INPs were identified by small size (diameter<6 um) and expected marker profile. Experiments targeting T1NBs in Fig. 3.8 utilized only the ventral side of the brain, while assays looking at T2NBs were taken on the dorsal side of the brain. Quantifications were done using one brain lobe per brain. Fractions of T2NBs were calculated by counting number of apparent T2NBs compared to the expected eight. INPs were counted every 4.5 um while number of NBs were counted every 7.5 µm.

Chapter 4 Future Directions and Conclusions

In chapter 2, we demonstrated that T1NBand T2NBs share the vast majority of neurogenic enhancers and that both NB types are competent to generate INPs. We demonstrated that by removing Ase, Btd can more effectively act to induce generation of INPs from T1NBs. We were limited in being able to investigate if Pros is also serving as a barrier, but the observation that *pros* is a target of Ase in addition to the fact that T2NBs downregulate Pros suggest that this is likely the case. Even with removal of Ase, less than 60% of T1NBs on the ventral side of the brain could be induced to generate INPs. This suggests that other barriers exist to prevent T1NBs from generating INPs. Possible factors could include the expression of lineage specific transcription factors that might restrict developmental potential. Another possibility is that not all T1NBs have the same inherent capacity to generate INPs. Approaches used throughout this thesis looked at chromatin accessibility using NB enriched brains. This method essentially provides an average of all the T1NBor T2NBs and the chromatin state that exists in these cells. But NB populations are heterogeneous and it is possible that specific T2NB lineages may have a more restricted chromatin state that would prevent Btd from acting. The observation that Tll misexpression can only reprogram ~60% of T1NBs into T2NBs could be due to this same possibility. Future work could use clonal approaches to misexpress Btd or Tll and assess if specific T1NB lineages are more resistant to reprogramming to generate INPs or conversion into T2NBs. Future work utilizing single

cell ATAC-seq could be used to compare these resistant T1NBs to the permissive T1NBs and better establish what that chromatin specific differences are that creates a NB that can be readily reprogrammed. This particular work has implications for inducing reprogramming to promote regeneration in the nervous system.

Tll has remained a tricky gene to define the downstream targets of that maintain T2NB identity. Ase was suggested to be the factor that is repressed to maintain T2NB identity, but in chapter 2 and 3 we showed that misexpression of Ase alone does not alter T2NB specific gene programming and removing Ase is not able to restore the generation of INPs from T2NBs in when *tll* was knocked down. Chapter 3 outlined that Tll likely serves as a repressor and provided a means to identify what the targets of Tll are that need to be kept repressed to maintain T2NB identity. This could also be useful to better understand what the defining differences between T1NB and T2NBs are. Beyond the scheme shown in chapter 2 to knockdown *tll* to identify targets, another approach that is in preparation is to misexpress Tll in T1NB enriched brains. T1NB enriched brains can be produced by using a T1NB specific Gal4 driver to drive $Apkc^{Caax}$ or $pros^{RNAi}$ to block T1NB differentiation. Combining this approach with another binary expression system allows us to look at how Tll can induce conversion of T1NBs. A QUAS-Tll could be driven by elav-QF2 a pan neuronal driver that is active in NBs. By inducing this expression of Tll in T1NB enriched brains, it would be possible to look at both gene expression changes, and also potential changes in chromatin regulation mediated by Tll. Misregulated genes found in both Tll loss of function and Tll misexpression would be prime candidates for Tll targets.

Thus far, only two enhancers that are specific to all T1NBs but not active in T2NBs have been identified as shown in chapter 2. These are enhancers for *ase* and *pros*, but identification of what makes these enhancers specific to T1NBs has remained elusive. Enhancers for both genes exist that are active in T1NB and T2NBs, but what separates the T1NB specific enhancers from the nearby Pan NB enhancers is unclear. Tll appears to bind both sets of enhancers, but it could be that some binding is transient or not facilitating repression. The identification of Tll targets may provide insight into key genes and where to find other T1NB specific enhancers. Finding more of these specific enhancers may help establish if certain binding motifs or other features are present that allows for T1NB specific activity.

The observation that Tll is acting as a repressor and is a target of Trx suggests that Tll is unlikely to function with Trx to promote activation of T2NB specific gene programming. Btd loss does not cause Ase upregulation or loss of Pnt, which is observed upon loss of Trx, so it seems unlikely that Btd alone is functioning with Trx (Komori et al., 2014). It is possible that multiple genes work with Trx to specifically active T2NB related genes and that loss of one factor alone is not sufficient to show a phenotype. When considering this possibility, the Six family transcription factors are promising candidates. Six4 is known to be involved in specification of T2NBs but postembryonic removal has no effect (Chen et al., 2021). Other Six family genes that are expressed in T2NBs include Sine Ocululis (So) and Optix. Previous attempts to create triple mutants of these genes were unsuccessful and because *six4* exists on a different chromosome than *so* and *optix*, the use of techniques like MARCM to create a mutant clone is limited. With the discovery that *Tll-Gal4* can effectively drive 3+ UAS

transgenes specifically in T2NBs, we have a potential means of testing for redundancy in these genes. Unlike *six4*, *so* mutants survive to adulthood. Experiments would be prepared in a s*o* mutant background where *Tll-Gal4* can be used to drive knockdown of *six4* and *optix*. The exact RNAi lines to be used would be determined by looking at which knockdown lines prove most effective by looking for changes in either reporter expression or through looking at transcripts with sm-FISH. A potential pitfall is that if a conversion to a T1NB state occurs, then the *Tll-Gal4* would likely be inactivated. If the conversion is unable to fully manifest before inactivation of the Gal4 happens might cause a weakened phenotype. Misexpression in T1NBs post-embryonically of any of these factors alone does not result in a phenotype, but it cannot be excluded that expressing a combination of these factors might be sufficient to promote conversion to a T2NB identity. It is also possible that Sp1 and Btd may work in tandem with these genes, but removal of both Sp1 and Btd has the same result as removal of Btd alone, indicating that these factors are not the main genes that are needed to promote Trx specificity

We established that none of the Btd candidate targets could recapitulate Btd misexpression phenotype. Two drawbacks exist in terms of identifying Btd targets that may have resulted in an inability to identify the key genes. One is that Btd Cut&Run data shows very weak binding compared to other TFs. Btd is not thought to be highly expressed, so this may not be unusual, but this result may have excluded a number of genes that were only weakly bound. Second, we lack the current knowledge on whether Btd functions as an activator or repressor in T2NBs. Misexpression of Btd zinc fingers, which constitute the DNA binding of Btd, fused with transcriptional activator domain

Vp16 or transcriptional repressor domain ERD was not sufficient to produce any phenotype. Attempts to instead create a UAS-Btd::ERD and UAS-Btd::Vp16 where full length Btd sequence is used instead have been initiated. The goal would be to elucidate if one of these transgenes can suppress or enhance the generation of INPs upon misexpression of Btd in T1NBs. Work to create these transgenes thus far has not successfully produced colonies, but further attempts are being made with hopes that more amplification of the DNA to be ligated into the UAS plasmid will resolve the issue. If Btd only acts to promote immature INP specification in the progeny, it would be important to understand what the processes that are needed to activate immature INP specification are. The data from Chapter 2 suggests that immature NB progeny are relatively plastic, and that the fate of becoming an INP or GMC does can be specified independently of factors inherited by the NB. Better understanding of how immature progeny fate can be determined could be useful to better understand how to induce reprogramming and regeneration.

We were able to identify two genes that have no previously characterized role in T2NB lineages, *hmx* and *vsx2*. Both are homeobox genes that can promote differentiation when misexpressed in T2NBs. Vsx2 loss appears to result in a greater number of INPs being produced, but future work to increase sample number would be needed to feel more confident in this result. Furthermore, how Vsx2 is working mechanistically is unknown. Similar to the idea of generating *UAS-Btd:ERD* and *UAS-Btd::Vp16* lines, *UAS-Vsx2::ERD* and *UAS-Vsx2::Vp16* lines have been made. We would misexpress these lines in T2NBs and find if the premature differentiation phenotype observed upon misexpression of full length Vsx2 can be suppressed or

enhanced. This would provide insight into how Vsx2 might be promoting differentiation of INPs. Knockdown of *hmx* produced conflicting data, and to resolve this will require the use of a mutant allele. Checking whether the endogenous Hmx is still functional in the line in which GFP is inserted into the *hmx* locus will be the first step. Depending on this result, other approaches such as excising a p-element or using Crispr-Cas9 to generate a mutant allele could be done. Hmx may play a similar role to Vsx2 and future work should look into potential redundancy in targets that are acted.

We also established a new way of visualizing enhancer activity. Previous methods of looking at enhancer activity were limited in looking at when an enhancer shuts down due to signal persistence from reporters. The use of an intron as a reporter provides a readout that is extremely short lived. This indicates that when the intron signal is detected, the enhancer must be actively promoting transcription. This technique provides a means to look at more subtle changes in enhancer activity and allow for better resolution of timings for enhancer activity that cannot be resolved with chromatin based approaches like ATAC-seq.

The validation of expression patterns for more than 100 transcription factors in the central brain in addition to compiling a list of enhancer activity patterns in the larval brain for more than 800 enhancers could provide a key resource for future studies that may not be well appreciated at that time. Understanding of what cell types many genes and enhancers are active in has important implications to better uncover gene regulatory networks and being able to better understand what factors play important roles in neurogenesis.

Overall, this work and the proposed experiments will provide important insights into how the competency to regulate INPs is determined. We have shown that immature NB progeny is relatively plastic and can take on an immature INP or GMC fate depending on inputs like Btd or Pros respectively. The fact that T1NB and T2NBs can retain their cell identity while altering the progeny being produced is a useful observation that suggests other stem cells within the same organ system may retain similar sorts of plasticity. The observation that factors like Ase serve as a barrier to the generation of INPs indicates that intrinsic barriers to increased neurogenic output are likely to exist in other neural stem cell populations. This type of information could be important for inducing regeneration from adult neural stem cells in humans, cell types that are positive for the Ase homolog Ascl1 (Roychoudhury et al., 2020; Soares et al., 2022; Soares et al., 2021). Lastly, misexpression of Ase can be used to suppress tumorigenesis without inducing premature differentiation that would be observed upon misexpression of Pros in NBs. This approach to suppress tumorigenesis without ablating the entire stem cell pool could be utilized for cancer therapies, as targeted approaches that do not destroy the entire stem cell pool have significantly less side effects.

References

Chen, R., Hou, Y., Connell, M., & Zhu, S.(2021). Homeodomain protein Six4 prevents the generation of supernumerary Drosophila T2NB neuroblasts and premature differentiation of intermediate neural progenitors. *PLoS Genet*, *17*(2), e1009371. https://doi.org/10.1371/journal.pgen.1009371

Komori, H., Xiao, Q., Janssens, D. H., Dou, Y., & Lee, C. Y.(2014). Trithorax maintains the functional heterogeneity of neural stem cells through the transcription factor Buttonhead. *eLife*, *10.7554/eLife.03502*.

Roychoudhury, K., Salomone, J., Qin, S., Cain, B., Adam, M., Potter, S. S., Nakafuku, M., Gebelein, B., & Campbell, K.(2020). Physical interactions between Gsx2 and Ascl1 balance progenitor expansion versus neurogenesis in the mouse lateral ganglionic eminence. *Development*, *147*(7). https://doi.org/10.1242/dev.185348

Soares, D. S., Homem, C. C. F., & Castro, D. S.(2022). Function of Proneural Genes Ascl1 and Asense in Neurogenesis: How Similar Are They? [Mini Review]. *Frontiers in Cell and Developmental Biology*, *10*. https://doi.org/10.3389/fcell.2022.838431

Soares, M. A. F., Soares, D. S., Teixeira, V., Heskol, A., Bressan, R. B., Pollard, S. M., Oliveira, R. A., & Castro, D. S.(2021). Hierarchical reactivation of transcription during mitosis-to-G1 transition by Brn2 and Ascl1 in neural stem cells. *Genes Dev*, *35*(13-14), 1020-1034. https://doi.org/10.1101/gad.348174.120